Introduction of the Hybrid Tidal System

Thesis submitted for the degree of Doctor of Philosophy

School of Engineering, Cardiff University

2017

Sheng Deng

Declaration

This work has not been submitted in substance for any other degree or award at this or any other university or place of learning, nor is being submitted concurrently in candidature for any degree or other award.

Signed ……(candidate) Date ……

STATEMENT 1

This thesis is being submitted in partial fulfilment of the requirements for the degree of PhD.

Signed ……(candidate) Date ……

STATEMENT 2

This thesis is the result of my own independent work/investigation, except where otherwise stated, and the thesis has not been edited by a third party beyond what is permitted by Cardiff University's Policy on the Use of Third Party Editors by Research Degree Students. Other sources are acknowledged by explicit references. The views expressed are my own.

Signed ……(candidate) Date ……

STATEMENT 3

I hereby give consent for my thesis, if accepted, to be available online in the University's Open Access repository and for inter-library loan, and for the title and summary to be made available to outside organisations.

Signed ……(candidate) Date ……

STATEMENT 4: PREVIOUSLY APPROVED BAR ON ACCESS

I hereby give consent for my thesis, if accepted, to be available online in the University's Open Access Repository and for inter-library loans after expiry of a bar on access previously approved by the Academic Standards & Quality Committee.

Signed ……(candidate) Date ……

Acknowledgements

First and foremost, I would like to thank my primary supervisors, Dr. Carl Byrne and Dr. Allan Mason-Jones, for giving me this opportunity and providing continuous guidance and support. I also wish to thank the staffs and colleagues at Cardiff Marine Energy Research Group (CMERG), for their help and support during my years in the office. Moreover, I wish to thank Prof. Tim O' Doherty for his support and advice during my studies.

Finally, I would like to thank my friends and family for their continuous support, reassurance and inspiration – particularly my parents for the stimulating debates and pragmatic solutions, for providing me with endless support and encouragement to follow my chosen career path when I doubted myself most, getting me to where I am now.

Abstract

One of the major accepted operating challenges with marine turbines is the harsh operating conditions and the resulting difficulties incurred with maintenance and repair.

This thesis initially investigates the conceptual conversion of the conventional tidal stream turbine system, with built-in generator, into a hydraulically driven system. This design allows the generator and gearbox to be relocated on-shore, for a better accessibility for maintenance and repair. This study shows that the proposed hydraulic system would have an overall efficient of 83%. However, the estimated high construction and installation costs, together with the potential for a catastrophic oil leak causing an environmental hazard, led to the conclusion that the proposal is currently infeasible.

Tidal range energy is not a new concept and has been used over the centuries to generate energy. It has the potential to generate power on both ebb and flood tides, with the advantage of temporal predictability. This research investigates the potential of converting architected commercial docks into small-scale tidal energy, electrical generation systems. The electricity generated would be used locally, thereby limiting transmission losses.

This research proposes a solution to convert a conceptual dock, into a tidal lagoon electrical generation site. The proposed “hybrid” system, incorporates a pumping facility, powered by a tidal stream turbine, which enables the head difference between the dock and the local tide, to be increased. A Matlab program simulates the pumping/storage system, and the results are compared with a storage-only system. Results show that there is an increase in power production and generation time, when using the hybrid system. Another advantage of the hybrid system is that it can be used as a power storage facility for peak demands. It is proposed that this methodology could be applied to other tidal energy sites, including docks, to supply energy to the national grids, not just locally.

The results of the hybrid system show that the total power output generated can be increased by 2% compared with a similar tidal lagoon. However, this increase would vary at different sites, under different parameters such as the size of the reservoir, the number and the size of the tidal turbines installed, and the stream velocity.

The simulation model was developed with the use of comprehensive real data from the Jiangxia Tidal Power Station, recorded over one year. A portion of this his data was initially used to further develop and refine the model. The rest of the data was used to validate the model. To facilitate this work, a Matlab programme was developed to help analyse the recorded data, to identify the key stages during the power generation, and to summarise the operating parameters and the power produced for any chosen period.

The hybrid pumped/storage system was applied to two active commercial docks (Avonmouth, and Cardiff Docks), located in the Bristol Channel. These locations provide a significant potential to generate tidal renewable energy due to the large tidal range. Unfortunately, simulations revealed that 39% of the time, the tidal stream speed was below 1m/s during the randomly selected 16 consecutive days used for testing. This stream velocity is too low to effectively drive the large-scale tidal stream turbines which are used in the numerical model for the pumping operation. As a result of these findings, the simulations modelled on Avonmouth, and Cardiff Docks, were not based on the hybrid system, but merely operated as tidal lagoons – the pumping system was removed. Results are presented which demonstrate the power generating potential for these docks.

However, in the real world, a commercial dock must allow for the arrival and departure of ships, a feature that will impact on the water storage capacity in the docks, and the potential for power generation. To explore the consequences of shipping, the model was re applied to Avonmouth, and Cardiff Docks, to incorporate the scheduled shipping for the same 16 day period, where the shipping information was downloaded from www.marinetraffic.com. Two scenarios are investigated. The

first scenario is where the docks are operated to comply with the shipping schedule, with no regard to the effect on power generation. This requires the water level in the dock must be maintained to a depth required for the ship with the largest draught. The second scenario is where the ships are located, where possible, in the smallest dock, which is maintained at the required depth. This removes the requirement to maintain the water level in the largest dock, thereby allowing the head to be used to generate power. The results of these simulations are compared, and it is shown that both scenarios can be used to generate power, although, as expected, the second scenario generates more power. It is suggested that the simulation could be developed as a facility to influence the scheduling of ships, in order to minimise the effect on power generation.

Table of Contents

List of Figures

Chapter 1

Chapter 2

Chapter 3

Chapter 5

Chapter 6

List of Tables

Chapter 3

Chapter 5

Chapter 6

Nomenclature

t = tonne (t)

f = friction factor

A= Swept area of turbine (m^2)

Ah = Cross area section of the flexible hose (m^2)

Cp = Power coefficient

d = diameter for hose/pipe (mm)

D = diameter of the pipe fitting (mm)

g = gravitational acceleration (m/s^2)

h_pump = head setting of the pump (m)

H_sea = Tidal level (m)

H_tank = water level for the reservoir (m)

h_{loss} = head loss (m)

k = pipe roughness factor

K_2 = loss coefficient

K_b = bend loss

Le = equivalent length

N =Motor max speed (rpm)

p = Motor working pressure (bar)

P = Power (kW)

P_pump = power output by the pump (kW)

P_turbine = Power output by the tidal turbine (kW)

Pbend = pressure loss in the hose's bend (bar)

Pc = Motor charge pressure (bar)

p_{gain_pline} = pressure gained by gravity for pressure line (bar)

p_{gain_rline} = pressure gained by gravity for return line (bar)

p_{loss} = pressure loss (bar)

Pr = initial pressure of the flow in the return line (bar)

Pw = Motor max working pressure (bar)

q = flow rate generated by hydraulic motor (L/min)

Q_out = Flow rate (m^3/s)

Q_pump = pumping flow rate (m^3/s)

Rb = bend radius

Re = Reynolds number

T = Motor output torque (N·m)

Ts = Motor Specific torque (N·m)

u2 = exit flow velocity (m/s)

u_{cb} = flow velocity in the 4.87-inch diameter pipe at crossbeam (m/s)

u_h = flow velocity in the 2-inch flexible hose (m/s)

v = flow velocity (m/s)

V_flow = flow velocity of the tidal stream (m/s)

Vi =Motor Displacement (cm^3/rev)

Greek Symbols

ρ = fluid density

η = efficiency

Θ = bend angle

η_m = Motor mechanical efficiency

ΔH = Head difference

Δpl = Motor pressure loss

Δpm = pressure difference to produce power

Acronyms

OBS: Oscillating body system

PTO: Power take off

WEC: Wavestar energy converter

MCT: Marine current turbine

1. Introduction

The ocean contains enormous energy, but so far, access remains limited. Ocean waves, tidal and non-tidal flows are defined as ocean renewable energy. The UK has the largest tidal resources in Europe, the potential power is approximately 10 GW (GreenMatch.co.uk,2017). To replace fossil fuel combustion and to contribute to environmental protection, renewable energy power plants must be developed. To this end, marine power could be expected to make a great contribution to renewable energy. According to the Nuclear Industry Association (NIAUK.org.2017) which published a detailed energy source for 2017 in the UK. (Figure 1-1)

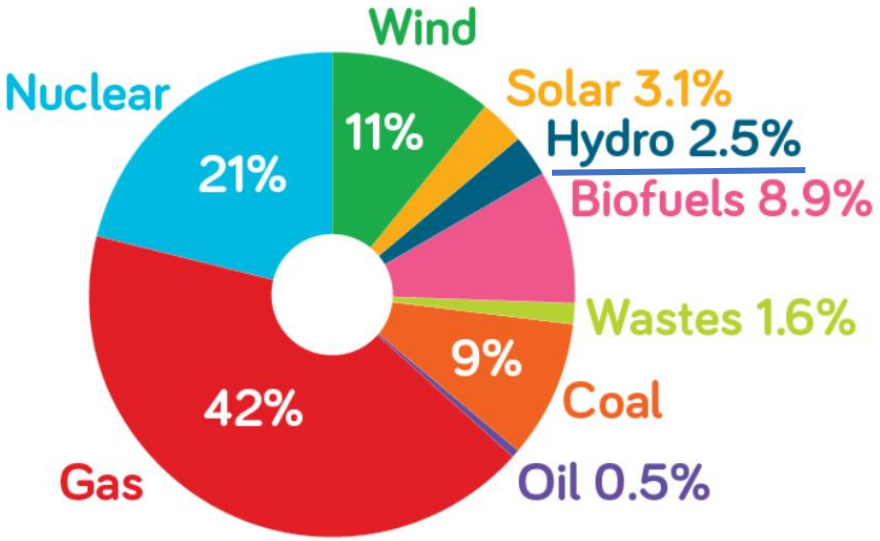

Figure 1-1 Global primary energy consumption by source (NIAUK.org. 2017)

However, despite the significant potential tidal power could provide, the actual installed tidal power system in the UK was still small, according to Figure 1-1, the conventional fuel (Gas and Coal) contributed over 50% of the UK's energy source with 2.5 % for the hydro energy.

There are number of technologies which have been used to generate electric power from the ocean, including wave, tidal range and tidal stream. Each technology has been proven to generate renewable energy, however none are perfect. The research reported in this thesis investigates these technologies, it identifies their weaknesses and strengths, and combines these technologies to propose a new system which could have all the strengths of the existing technologies and which avoiding the weaknesses.

1.1 Structure of the thesis

Chapter 1 introduces that ocean contains significant amount of energy, but the current total installed capacity for the tidal and wave system is small.

Chapter 2 reviews the current renewable energy systems which has a link to the tidal energy industry, these systems include: wave energy devices, tidal stream turbines, hydroelectric station, tidal energy station, pumped hydroelectric storage and wind turbine system.

Chapter 3 proposes a system which features a tidal stream turbine system that uses hydraulic transmission system, the advantage of this system is the accessibility to the key components (generator, pump et al.) which can be located on-shore; the disadvantages are the environmental hazard and cost.

Chapter 4 proposes a hybrid tidal system which would converts the docks into a tidal lagoon with pumped storage, with tidal stream turbine driven pump to adjust water level inside the docks to meet different needs. Newport Docks was used a conceptual site in this chapter.

Chapter 5 discusses the further development of the numerical model of the hybrid system and the validation progress by using recorded data from Jiangxia Tidal Power Station. A Matlab code was developed to analyse the recorded data to highlight the key stages and summaries the information.

Chapter 6 discusses the performance of the hybrid system in Avonmouth, and Cardiff Docks, with Avonmouth Docks has busier shipping traffic and larger size than Cardiff Docks. However, due to the slow stream speed at both sites, the sites were simulated as conventional tidal lagoons with different control methods.

Chapter 7 discusses the results from Chapter 2 to Chapter 6, concludes this thesis and discusses the future works.

1.2 Objectives of the thesis

- To identify the strengths and weakness of tidal turbines, tidal barrage power stations and wave power devices.
- To develop a hybrid tidal technology that combines all technologies, having their advantages whilst overcoming their weaknesses.
- To develop a numerical model for the hybrid system which focuses on small-scale and localized power generation using existing docks.
- To validate the numerical model by using real recorded data from Jiangxia Tidal Power Station
- To apply the hybrid system into active docks, enabling power generation whilst maintaining the shipping schedule.

2. Renewable Technologies Review

There are two sources of ocean renewable energy: waves and tides. These are the sources that generate most of the oceans' energy. In this chapter, current technologies within both areas will be discussed.

2.1 Wave technologies

Ocean waves are generated by wind blown over the ocean surface and tides. The global theoretical energy from ocean waves is estimated at 8 x 10^{15} kWh per year, which is approximately 100 times the total hydroelectricity generated on the planet (Rodrigues. 2008). If this energy could be converted to electricity, this would be a massive contribution to the world's renewable energy issues.

There are various types of wave energy devices; in this section, current wave technologies will be reviewed.

2.1.1 Oscillating Body System (OBS)

Most wave energy devices that operate offshore are oscillating bodies; they either float or are fully submerged and are located in water with depths greater than 40 m where the power generated is greater than at shallower levels. Mooring systems, accessibility of maintenance and the application of long underwater transmission cables are current challenges of this system (Ruol. Zanuttigh. et al. 2010).

2.1.1.1 Floating (OBS)

OPT Powerbuoy

The Powerbuoy is a floating OBS located offshore in water with a minimum depth of 55 metres. The fundamental method of energy converter is hydraulic power take-off (PTO). Two hydraulic cylinders are vertically installed into the body of the device, the design of this system is shown in Figure 2-1.

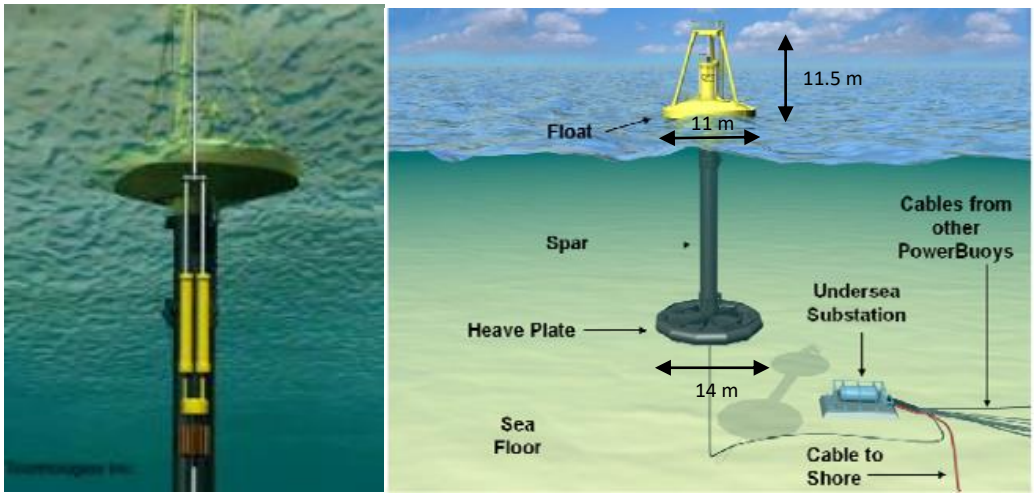

Figure 2-1 The Powerbuoy system (Hossain, J. 2015)

To gain power from oscillating waves, a hydraulic power take-off system has been incorporated into this device. The float oscillates with the movement of the wave; two hydraulic cylinders which are linked to the float, pump fluid to an accumulator for high-pressure fluid storage and to drive an electric generator to produce electricity.

The Mark 3 Powerbuoy, which is the latest testing module deployed in 2011 in Scotland, has a peak power rate of 866 kW, announced by the manufacturer. The rise of pistons is approximately 5 m during peak times. The whole system is 43.5 m tall, the float is 11.5 m above the water surface with a diameter of 11 m, the spar body is 32 m deep under the water and the heave plate has a diameter of 14 m. OPT announced that the ideal working location for the Powerbuoy is about 8 km from shore and with a minimal water depth of 55 m. The Powerbuoy is primarily made of steel, which makes the 180 t body recyclable after 25 years of service life.

The advantage of the Powerbuoy design is it can to generate power at calm sea conditions. The device can produce at least 45 kW with the wave height between 1.6 m and 2 m. OPT claims that the Powerbuoy's mooring system is highly secure and the testing module has survived hurricanes and tsunamis in the Hawaii area. Furthermore, during extreme conditions, the system can automatically lock and pause power

production, and similarly when conditions are normal, the system unlocks back to full working condition. The capacity factor of the Powerbuoy is between 30% - 45% in various situations, with the cost per kWh about £ 0.1- 0.15 which is more expensive compared with the traditional power plant with gas and coal combustion £ 0.05 - 0.1 per kWh. Moreover, sensors and signal transmitting devices within the Powerbuoy allows for the monitoring of the device. For more than one device, there is an undersea substation connecting nearby devices, allowing the transmission of power to shore via underwater cable. There are two different output voltages regarding the frequency; 600 V, 60 Hz, and the other is 575 V, 50 Hz (Oceanpowertechnolegies.com. 2016).

However, there are disadvantages of the Powerbuoy system; firstly, there was a risk of leakage of fluid from the hydraulic system. There is a lack information on the hydraulic cylinder and the hydraulic fluid used by Powerbuoys, for the most common application, the oil is the popular fluid for the hydraulic operation. If there were a leakage, oil would be discharged into the ocean, thereby harming the environment. The other drawback is the visual impact of the Powerbuoy. Even though most of the body is submerged, there is still 11.5 m above the water. However, this design allows access for Powerbuoy maintenance.

2.1.1.2 Submerged OBS

Archimedes Wave Swing (AWS)

The AWS is a fully-submerged off-shore wave energy converter, in 43 m of water (Valerio. Beirao et al. 2007). It has two main parts, the silo which is a bottom restrained, air-filled cylindrical chamber, and the floater which is a moveable upper cylinder. Wave movement generates oscillation of the device which produces electricity.

As shown in Figure 2-2, wave movement generates pressure in the device, when the wave is above the AWS, the volume is compressed by the pressure. When the wave trough is above the AWS, the compressed volume is returned to normal, because of the air stored inside the device. By this linear movement, it is possible to extract energy from the wave motion and convert it into electricity. The key design is the fully submerged body which prevents damage during storm conditions. Similarly, visual impact is kept to a minimum.

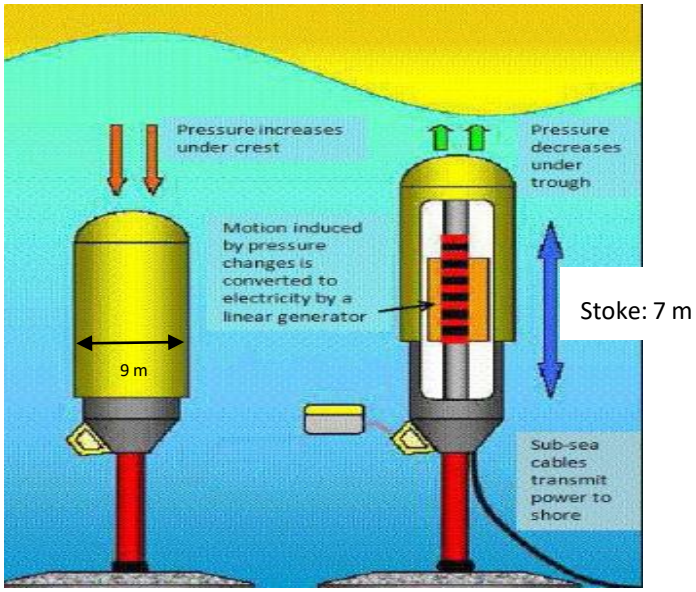

Figure 2-2 AWS wave swing (Valerio, D. Beirao, P. et al 2007)

The 2,000 kW prototype was tested on the north Portuguese coast in 2004. After the test, the whole system was removed. Based in the 2004 test, the stoke was 7 m and the rated flow velocity was 2.2 m/s. To convert the linear motion to electricity, there is one electric linear generator inside the cylinder.

Theoretically, the linear movement of the upper piston drives the linear generator and produces electrical power. The diameter of the cylinder is 9.5 m, with a total height of 43 m from the sea bed. A minimum distance, from the ocean surface to the top of the AWS of 6.5 m, is required for operation. The electrical energy produced by the generator is transferred on-shore to the grid, about 6 km away via underwater cables.

A brake system locks the cylinder from moving to protect it from dangerous water conditions (e.g. storms). Even with the capacity factor of 25%, the company claims a single AWS device produces 5.1 x 10^3 kWh electricity per year.

The maintenance cycle for the AWS is long; minor maintenance occurs every 3 years and every decade a major maintenance must be done. However, even with a long-term maintenance cycle, access for maintenance is not convenient. Like all wave energy devices, a specialist ship is essential. Equally, the fully submerged body is another challenge, the company does not provide any information on how maintenance is implemented. However, it is reasonable to assume that trained technicians with diving skills or unmanned underwater vehicles are required to perform installation and maintenance. Importantly, this design contains fewer components which could be argued contribute to a reduced maintenance complexity.

2.1.2 Power take-off wave devices

2.1.2.1 Oyster wave energy converter

Oyster wave energy converters are near-shore submerged flap design marine energy extractors. The first 315 kW prototype was deployed in Orkney, Scotland in 2009, and successfully demonstrated the concept. After the prototype test, the company, Aquamarine Power has launched the second prototype, Oyster 800, in June 2012. As shown in Figure 2-3, there are two main parts to the Oyster wave converter, the flap, which captures the wave, and the base which is piled into the seabed to support the flap.

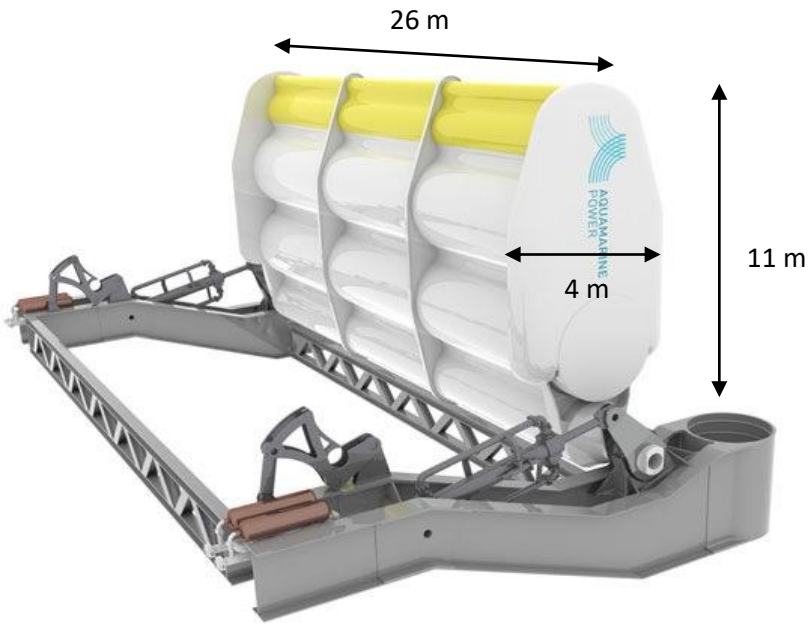

Figure 2-3 Oyster 800 Wave energy converter (Image source: Inhabitat.com)

The testing position of the Oyster is approximately 50 m from shore, with a water depth between 10 and 15 m. The design method pumps water via pipes to an onshore power converter unit, converting to electricity. Waves drive the flaps forwards and backwards, the two hydraulic cylinders which are located on the side of the device are attached to the flap, meaning the motion of the flap pumps fluid by the hydraulic cylinder. Aquamarine Power states the Oyster uses pure water as the hydraulic fluid to reduce the risk of environmental contamination. The energy converter unit, which is located onshore that can be accessed all the time. The water flows to shore via two high pressure pipes and is converted to electricity via a Pelton wheel turbine and a flywheel (Cameron. 2010), which is used to turn the electrical generator. The additional low-pressure pipe is used to return the water back to the Oyster in a closed loop as shown in Figure 2-4.

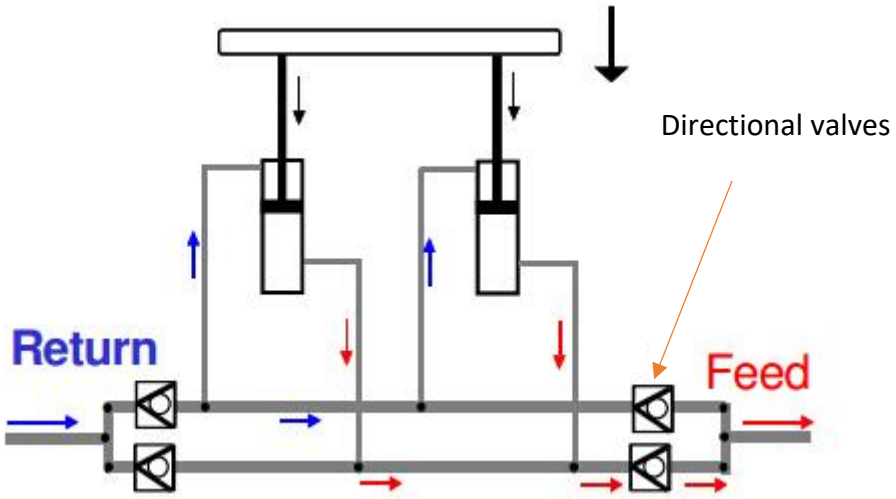

Figure 2-4 The concept drawing of the Oyster pumping device (Ruhlicke. 2013)

The first prototype, Oyster 1 has a flap dimension of 18 m x 14 m x 4 m with a rated power of 315 kW, this device was installed in Orkney in 2009. To capture more power, the Oyster 800 has a larger flap design of 26 m x 11 m x 4 m, which has a rated power output of 800 kW. The fluid pressure in the pipes is up to 160 bar, the high-pressure pipes have a 355 mm diameter and the return pipe has a 400 mm diameter.

It has been claimed by Aquamarine Power that the Oyster 800 generated 10,000 kWh in a 144 hours, suggesting the average output was approximately 70 kW. The system has survived storms during the testing (Cameron. 2010). The key point is the flap designed device can be closed like real oyster which the flap would attach to the base during extreme weather conditions. The Oyster is predicted to have a 15-year service life and can be operated at wave heights of up to 10 m. The device requires maintenance every four months and unlike the offshore submerged devices, the near-shore location and the two side-located cylinders provide good maintenance access. However, maintenance technicians still have to work underwater.

The biggest advantage of the Oyster device is the on-shore energy components, which provide good access and reduce costs. Additionally, the water-based fluid will not damage the environment if leakages occur. The concern with the Oyster is pressure

drops within the system. Because of reduced offshore operations, each maintenance cycle costs about £ 12,700, as claimed by Aquamarine Power. The energy costs £0.09 for every kWh (Bosserelle. Kruger et al. 2015).

2.1.2.2 Pelamis

Pelamis which is shown in Figure 2-5 is an offshore, floating wave energy converter. It contains a set of semi-submerged cylinders linked by hinged joints, it has total length of 180 m with 4 m diameter for each cylinder, the device has a total weight of 1,350 t (Emec.org.uk. 2014). Waves act on the Pelamis by compressing the cylindrical sections relative to each other, across two degrees of freedom. The Pelamis PTO contains hydraulic cylinders that pump fluid. This fluid passes into high-pressure accumulators for energy storage via control manifolds. The fluid is used to drive a hydraulic motor which drives the electric generator to produce electricity, the schematic system is shown in Figure 2-6.

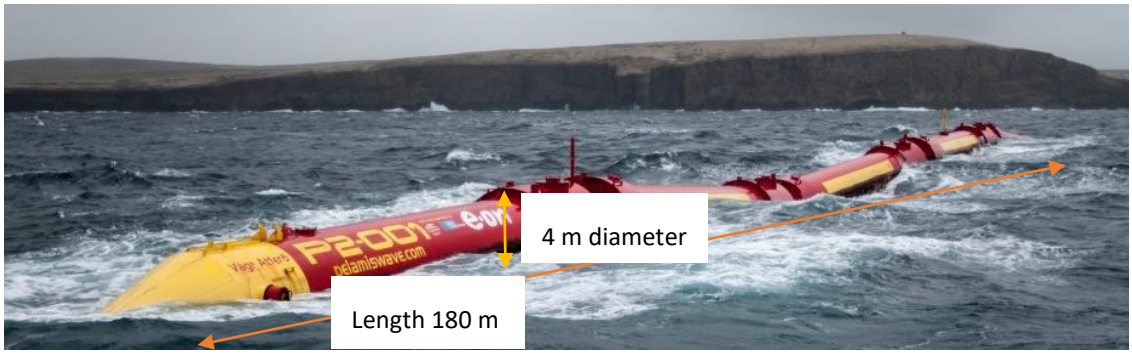

Figure 2-5 Pelamis Wave Energy Converter (Image Source: Emec.org.uk)

A Pelamis unit consists of three units, with a rated power of 750 kW. In 2008, Pelamis launched a second prototype on the northwest coast of Portugal. Pelamis is an offshore device and has a minimum water depth requirement of 50 m and should be located about 2-10 km from the coast. The annual output is expected to be 2.7 million kWh (Emec.org.uk. 2014), with a capacity factor between 25-40 %.

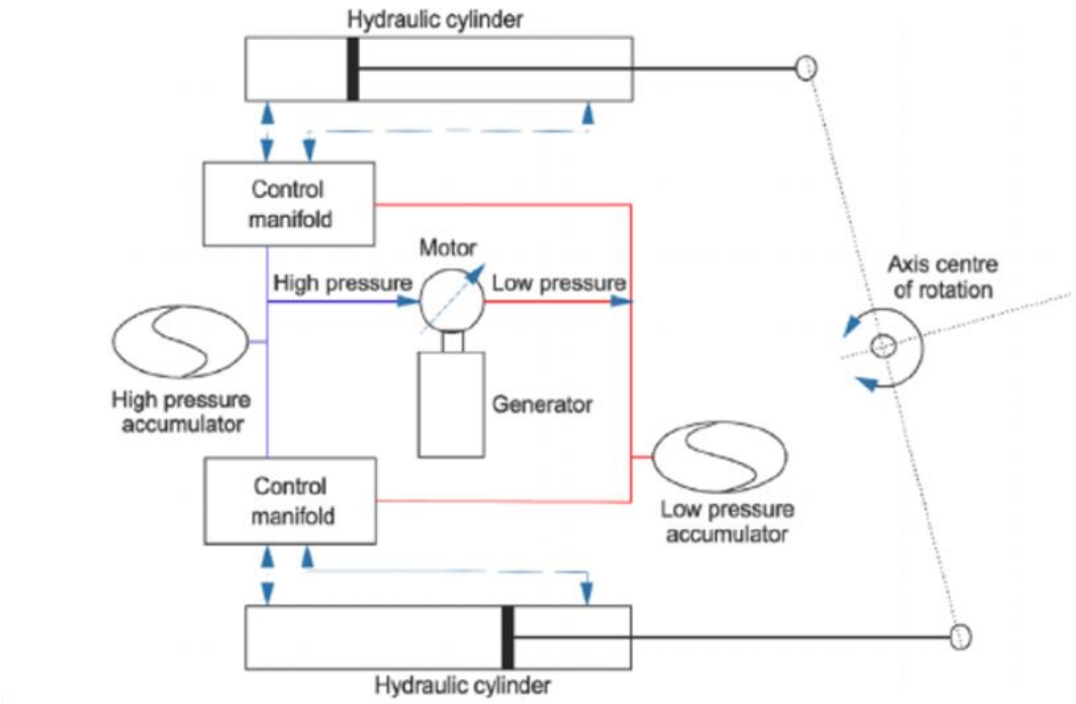

Figure 2-6 Simplified schematic system of Pelamis (Henderson, 2006)

The most important parts in the hydraulic power take-off are two main parts, which can be expressed as the primary and secondary transmissions. The primary transmission consists of hydraulic cylinders and the controls, it directly converts power from the wave to stored energy. The secondary transmission consists of hydraulic motors that connect to the generator. They convert the energy stored in the high-pressure accumulators into electric power, which is transmitted onshore via undersea cables.

The conventional hydraulic devices that use variable displacement pumps to deliver continuous variable pressure and flow, normally have a maximum efficiency of 60%. However, there is a large drop off, if the system is not operating under ideal conditions. However, in the Pelamis PTO, the compressed fluid is directly stored in the accumulators, the drop in the system is only affected by the compressibility, friction in the bearings and seals and the fluid losses along the valves and pipes. The design

could reduce overall losses to under 20%, over a wide range of operating conditions (Henderson. 2006).

Based on a report by Ocean Power Delivery Ltd, the expected cost per kWh will be £0.06, with a predicted service life of 20 years. However, the Pelamis has a short maintenance cycle when compared to other wave devices, requiring service every two months. For maintenance, the company claims it will take 15 minutes to unplug all cables and then towed to shore where maintenance takes place. However, it is still a massive job. Furthermore, the anchor system has proven system safety; the Pelamis has survived several storms in seas around northern Portugal. However, there are doubts that the cables can secure the massive 1,350 t body. The other potential problem is leakage, the oil used inside the system has a working environment of 100-350 bar therefore if there is leakage, the oil will damage the marine environment. To conclude, the Pelamis is claimed to have an overall efficiency as high as 80 % (Emec.co.uk. 2014). Last but not least, the rapid connection anchor system allows fast grid installation.

2.1.2.3 Wavestar

Figure 2-7 shows the Wavestar wave energy converter (WEC), which is a multiple absorber concept, consisting of 20 hemisphere shaped floats attached to a platform. Each hemisphere float is connected to a discrete displacement cylinder which is shown in Figure 2-8. The wave oscillation causes the cylinder to pump fluid, the pressure of the fluid depends on wave conditions. The flow is delivered to an accumulator, then drives a hydraulic motor coupled to the generator, producing power.

Figure 2-7 Concept of the Wavestar (Image Source: Wavestar Energy. 2011)

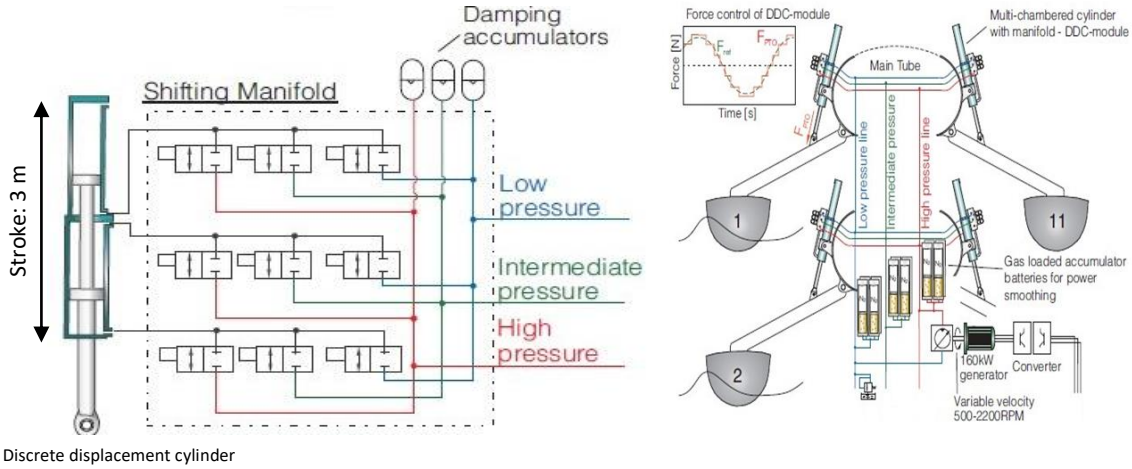

Figure 2-8 Overview of the design of the Wavestar (Hansen. Kramer et al. 2013)

A key point of this design is the discrete displacement cylinder which is shown in Figure 2-8; with 3 m length stroke and three chambers, with the assistance of nine fast on/off valves, the unit can deliver 27 different pressure settings. It is claimed by the company that the overall efficiency is greater than 60%, in all sea states. The commercial size would have 20 of these floats and have a rated power of 600 kW, it has a predicted 20-year service life and would require a single service each year (Marquis. Kramer et

al. 2013).

The Wavestar shows the highest efficiency (94% for each component, 90% for the cylinder), excellent controllability from 9 valves, and a solid structural design against harmful environmental attack.

2.2 Tidal devices

Tidal energy has a great potential in the field of renewable energy. It is an extremely predictable energy resource as the tide is affected by the gravitational force of the moon and the sun and the centrifugal forces generated by the rotation of the earth-moon system. Tidal currents hold significant kinetic energy which can be extracted and converted into electrical power. Tidal turbines are devices which to capture power from tides; however, all current tidal turbine technologies are still under development or prototype testing. In the following sections, the current status of tidal technology will be discussed.

2.2.1 Tidal stream turbines

The technologies behind tidal turbines share similar design features with wind turbines, but with some notable differences. By using tidal streams instead of wind energy to generate electricity, tidal turbines are not as big as wind turbines, for example, a Vergnet GEV HP wind turbine which has a rated power 1,000 kW has a rotor diameter of 62 m (wind-turbine-model.com. 2016), comparing to an Atlantis AR1000 tidal turbine which has 1,000 kW rated power with 18 m rotor diameter, comparing these two models, the wind turbine design required larger rotor to achieve the same power output, which due to the density different between the sea water and air, which the density of sea water (1,030 kg/m^3) is significantly higher than air (1.225 kg/m^3). Due to the higher density of water. Equally, tidal turbines must be designed to protect its component parts from water damage.

2.2.1.1 SeaGen by Marine Current Turbines (MCT) Ltd.

MCT has deployed two prototype tidal turbines, the 300 kW testing module in 2003 and in 2008, the 1,200 kW SeaGen, in Strangford Lough, Northern Ireland. SeaGen is the first large commercial-scale tidal stream generator deployed by MCT.

Figure 2-9 SeaGen by MCT in Strangford Lough (Image Source: MCT)

Figure 2-9 shows the image of SeaGen, which is tidal turbine system that has a twin rotors of 16 m in diameter. The blade is coupled with the gearbox to increase the rotational speed to drive the electric generator. Pitch control is implemented in the system to adjusts the pitch angle of the blade to gain the best performance under different tidal situations. SeaGen is installed at a mean depth of 25 m and is approximately 1.1 km offshore. The 54.6 m tall and 3.5 m diameter steel pillar is piled into the seabed, with a crossbeam length of 29 m. Two 600 kW generators are located on the edge of the crossbeam and comprise 1,200 kW total power.

Maintenance can be carried out on-site, the crossbeam can be lifted above the water to gain access for maintenance. This helps to reduce repair times, improve operational availability and reduces the need for large ships. MCT Ltd. claim the system can be

shut down from full power in less than three seconds during full flow rates.

The installation cost of SeaGen was £3.6 million in 2008 (Plunkett. 2014). MCT stated these costs would be reduced as the technology, manufacturing methods and production volumes were improved. The commercial-scale prototype outputs 5-million kWh with a capacity of 48%, suggesting the cost of a kWh is about £0.07, based on that module. SeaGen is a milestone in tidal technology, it is the world's first commercial-scale tidal turbine generator with well tested prototypes. In terms of upkeep, lifting the blades reduces maintenance difficulties. Furthermore, a three-year environmental monitoring program identified there was no significant impact on marine life around the location of the SeaGen system (Johnson. 2016).

Even though the prototype was tested at Strangford Lough, it was impossible to tell how the system would work under different tidal locations. Although most of the system is submerged, there is still a visual impact which could be a problem for ocean transport. The application of the pitch control method was successful; it allowed the blades to rotate up to 180 degrees, to match the best performance scenario. The blades and hub were protected by antifouling paint which contained copper particles in epoxy to prevent corrosion.

2.2.1.2 Atlantis AR1000

The Atlantis AR1000 which is shown in Figure 2-10 is an offshore, fully submerged conventional tidal turbine with a rated power of 1,000 kW, at a flow rate of 2.65 m/s. The AR1000 is a large-scale tidal turbine with a designed operation depth between 25-60 m. The three-blade turbine has an 18 m diameter and is 22.5 m tall, from the seabed. The hub is 12 m long, and the minimum distance from the tip of the turbine to the ocean surface is 7 m. In 2011, the 1,000 kW prototype was deployed and was successful in producing power in Orkney, Scotland.

Figure 2-10 Atlantis AR1000 installation (Image Source: insider.co.uk)

Unlike the SeaGen, the AR1000 uses fixed-pitch blades in preference to variable pitched blades. The company stated that the benefits of pitched blades for tidal turbine were still unproven. The three blades are believed to provide maximum efficiency for this design. The gearbox and generator are located behind the blade; the shaft speed is 6-15 revolutions per minute (rpm). The turbine can be rotated in slack periods between tides, using a yaw drive, and then fixed in place for the best position, for the next tide.

The gravity base structure weighs in at 1,000 t; it is made of steel with six supporting ballast blocks. The base has no moorings or anchor system, meaning less impact on the seabed. After extensive testing, Atlantis demonstrated the turbine could be removed from the water in less than 60 minutes, and that the installation could be completed in less than 90 minutes. However, due to the large-scale body, a large ship is essential, and the cost is increased when the tidal current is greater than 2 knots. However, turbine removal does not require divers, which significantly reduces costs

and health and safety risks.

The company has suggested that the capital cost of £7 million/1,000 kW by 2013, after a 66,000 kW farm, this price could be reduced by £5 million/1,000 kW, the cost of the produced energy is predicted about £0.30-0.35 per kWh.

However, the gravity base structure does not have moorings and anchors, the survivability during extreme weather conditions is questionable and, additionally, underwater cables could be insecure. The system is expected to have a major service every five years, and the life of the main structure is 20 years, but only 5-10 years for the blades. There is no visual impact of the system because it is fully submerged.

2.2.1.3 Scotrenewable SR250

The Scotrenewable tidal turbine which is shown in Figure 2-11 is an offshore floating tidal stream turbine; the floating design leads to ease of installation, operation and maintenance in offshore environments. The main body consists of two horizontal axis rotors, each rotor having two blades. The turbine extracts kinetic energy from the tidal flow and converts it to electricity, though the PTO system. It is then transmitted onshore. Figure 2-12 shows the two modes of this system: 1. operational mode with the rotors down to produce power; 2. transport/survivability mode with rotors retracted to decrease stream drag, allowing the system to be towed back to shore during storms/maintenance.

Figure 2-11 Scotrenewable turbine ready to be installed (Image Source: renews.biz)

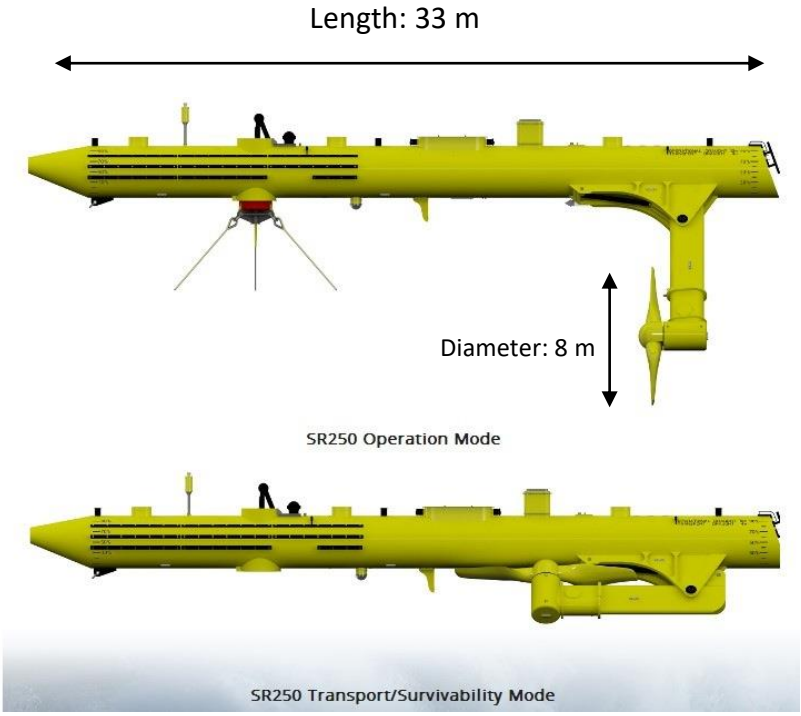

Figure 2-12 Two modes of the Scotrenewable turbine (Shi, W. Atlar, M. et al. 2016)

The full-scale 250 kW prototype has a 33 m long steel tube body, with a diameter of 2.3 m. A fixed-pitch blade has been implemented to this device to reduce costs and increase reliability. Each turbine, with a diameter of 8 m, drives separate gearboxes and variable-speed generators, located within the tube-shaped body. Generated electricity is transmitted via underwater cables to shore. The company states it takes

approximately 30 minutes to connect and disconnect the system. The SR250 prototype was tested in Orkney at a depth of 37 m. The floating body provided good access for maintenance and installation, and because the weight was 100 t, there was no need for a large ship, a small ship can tow the system to shore. The company claims that this device has a long-term cost projection £0.12 per kWh (Hamliton, M. 2012).

The SR250 has shown that tidal devices can be mobile when compared to the two large-scale systems mentioned in the previous sections. However, because of mobility, the size of the device is small when compared to other tidal energy systems which discussed earlier in this Chapter, therefore the big disadvantage is the small rated power output which is 250 kW.

2.2.2 Tidal energy stations

Tidal energy stations have proven to be long-lasting and reliable sources of power generation. However, they require massive investments for infrastructure construction, but as single systems, they provide the largest energy outputs.

2.2.2.1 La Rance Tidal Power Station

La Rance Tidal Power Station which is shown in Figure 2-13 was in operation in 1966 and was the first tidal power station in the world. Twenty-four turbines were fitted across the barrage to maximise power generation. All turbines are capable of operating bi-directionally, with a peak output of 240,000 kW (Edf.fr. 2017), and an average of 57,000 kW. Approximately 0.12% of French power demand is supplied by La Rance. The barrage is 750 m long which creates a tidal basin of 22.5 km^2. In 1963, the power station cost approximately £500 million (value in 2009) (Reuk.co.uk. 2016). The energy cost per kWh was around £0.02 (Reuk.co.uk. 2016).

Figure 2-13 La Rance Tidal Power Station, France (Image Source: tethys.pnnl.gov. 2009)

2.3 Pumped hydroelectric storage

Another renewable energy system which also featuring using water to generate energy is pumped hydroelectric storage system. This type of system is very similar to the conventional hydroelectric system, as the energy is stored as the gravitational potential energy of the water, which is pumped from a lower place to a reservoir which located in the higher elevation (Evans. 2018). The water is pumped during the off-peak period where the electricity price is lower, and in the peak electricity demand times, the stored water will be released through water turbines to produce electricity.

2.3.1 Glyn Rhonwy pumped hydroelectric storage

Glyn Rhonwy is a proposed pumped hydroelectric storage in the UK which the construction will begin in 2019 with £160 million investment (Quarrybattery.com. 2018), which this system could provide 99.9 MW (9.99×10^7 kW) maximum, the reservoir is located 250 m above the turbine and has a volume of 1.3 million m^3, with

the total storage capacity of 700 MWh ($7x10^9$ kWh) (snowdoniapumpedhydro.com. 2018). This proposed storage will use the closed-loop design which utilises two redundant slate quarries as the upper and lower reservoir (Evans. 2018), an example of the close-loop pumped hydroelectric storage system is shown in Figure 2-14.

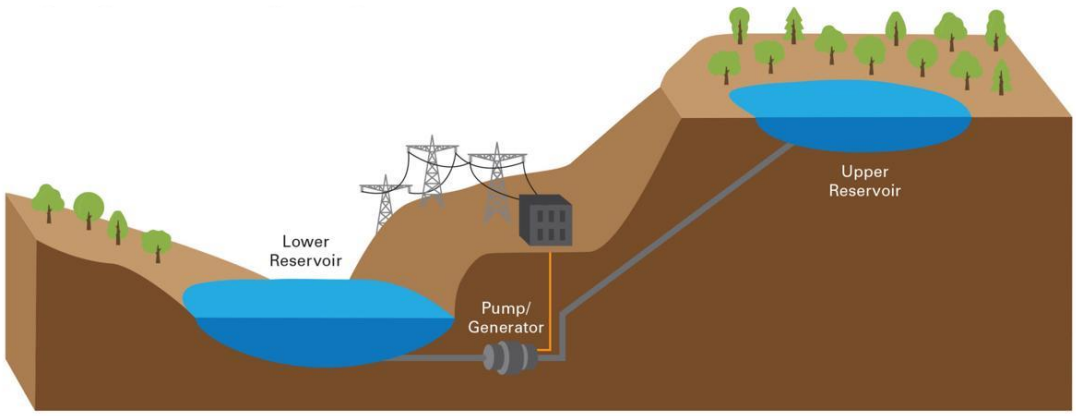

Figure 2-14 Close-loop pumped hydroelectric storage (Image Source: Theengineer.co.uk)

The water will be pumped back to the upper reservoir during the off-peak time where the cost of energy is low, and normally generate power when the demand is high. Hence the price of energy is higher. However, the profit will be determined by the energy price difference between the peak and off-peak time; if the difference is small, then this system would not profit.

2.4 Comparisons between the technologies

Tides and waves are major natural phenomena, which can be enabling the extraction of energy from oceans and seas. Many projects are under development to determine the best methods of energy extraction. Therefore, a general comparison between these two fields is required.

GridWatch.co.uk is a website which displays the real time Nation Grid status in the UK, information like how much energy is produced by which source can be acquired, a detailed discussion of this topic will be in Chapter 4.1 of this thesis.

For wave devices, these can be placed almost anywhere in the ocean; where there is a wave movement, energy will be generated. Wave device designs are various, suggesting a different design for different locations. However, a major weakness is survivability. Given this, all companies cited above, claimed their devices were perfectly safe in the most dangerous of conditions, but without published evidence, these facts are disputed.

For tidal devices, all three systems discussed were designed with turbines. Moreover, all three systems used conventional electrical power generation methods, sharing the same technology with wind turbines.

Comparing the rated power output for the wave and tidal system discussed in Chapter 2.1 and 2.2.1, the La Rance Tidal Power Station and proposed Glyn Rhonwy pump hydroelectric storage were not in this comparison due to their significantly larger scale and power output comparing to these devices. From Figure 2-15, the wave energy device AWS has the largest power output with 2,000 kW, with the rest of the wave devices around 750-800 kW area; and the tidal turbine device with the highest rated power is SeaGen with 1,200 kW, followed by Atlantis which is 1,000 kW and the Scotrenewable 250 has the lowest power with 250 kW.

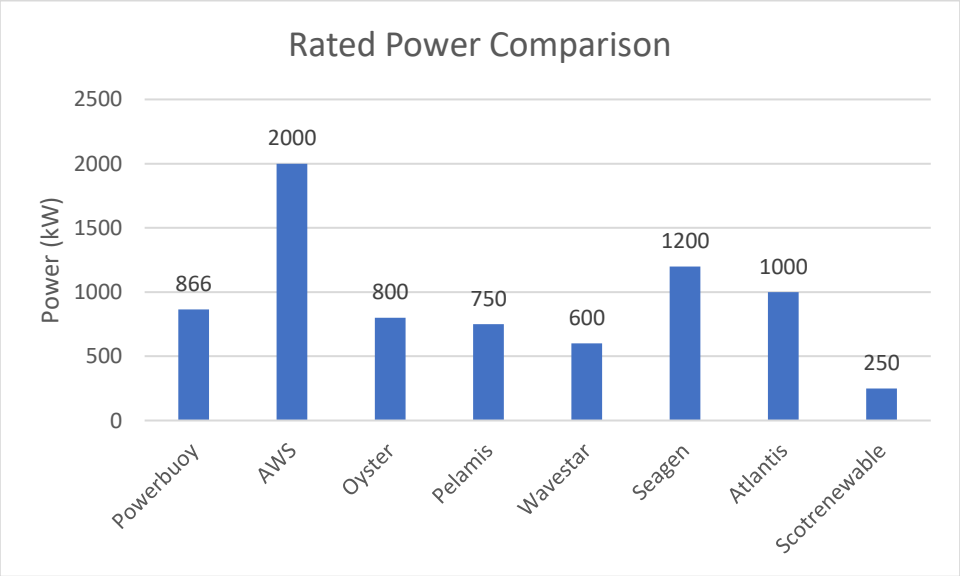

Figure 2-15 Rated Power for a different system

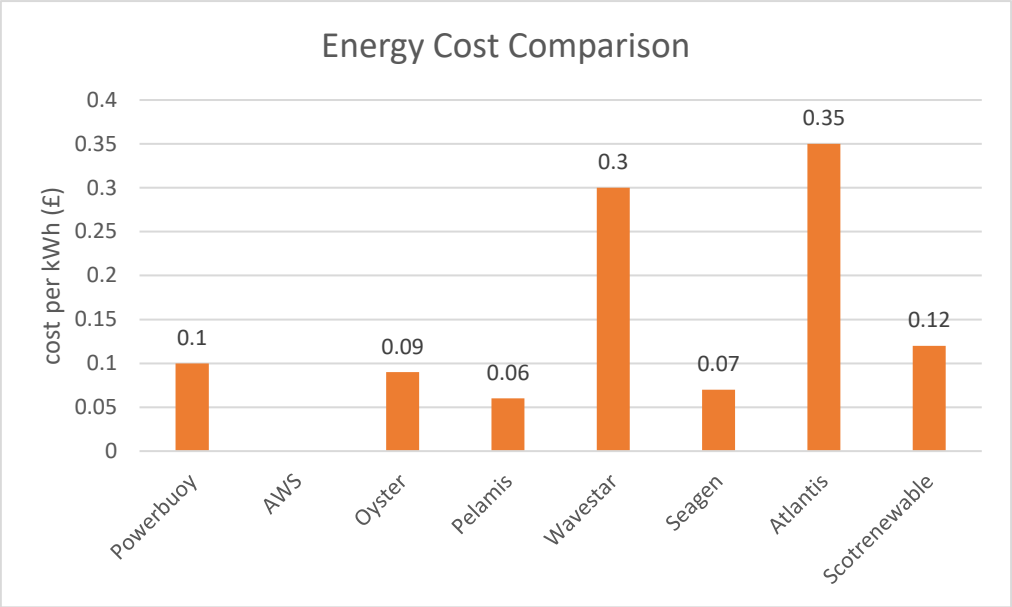

Figure 2-16 Estimated cost GBP per kWh for a different system

Figure 2-16 shows the estimated energy cost for each device that discussed, noted that the information for AWS which has the highest rated power is unavailable. According to the information which shown in Figure 2-16, all systems have an estimated cost value below £ 0.4 and comparing with average kWh unit price in the UK was around £ 0.152 at 2018 (Parliament.uk. 2018). However, the cost would be reduced if more devices are installed.

2.5 On-site review of three renewable energy stations

2.5.1 Introduction

In 2015, the author visited three renewable energy stations in China; hydroelectric, wind and tidal power stations. During the visit, the on-site engineer showed how the systems were run and managed.

2.5.2 Hydroelectric energy station

The first site was a hydroelectric station is Xiaolangdi Hydro Power Station, in central China. The station was constructed between 1994 and 2001 and sits on the yellow river which is the second longest river in China (sixth longest in the world). The dam structure is 1,667 m long and 281 m tall, the reservoir contains 5.1 billion m^3 water (Xiaolangdi.com. 2016), with a maximum height of 275 m. The station has a powerhouse built inside the dam structure; Figure 2-17 shows a schematic design of a hydroelectric plant.

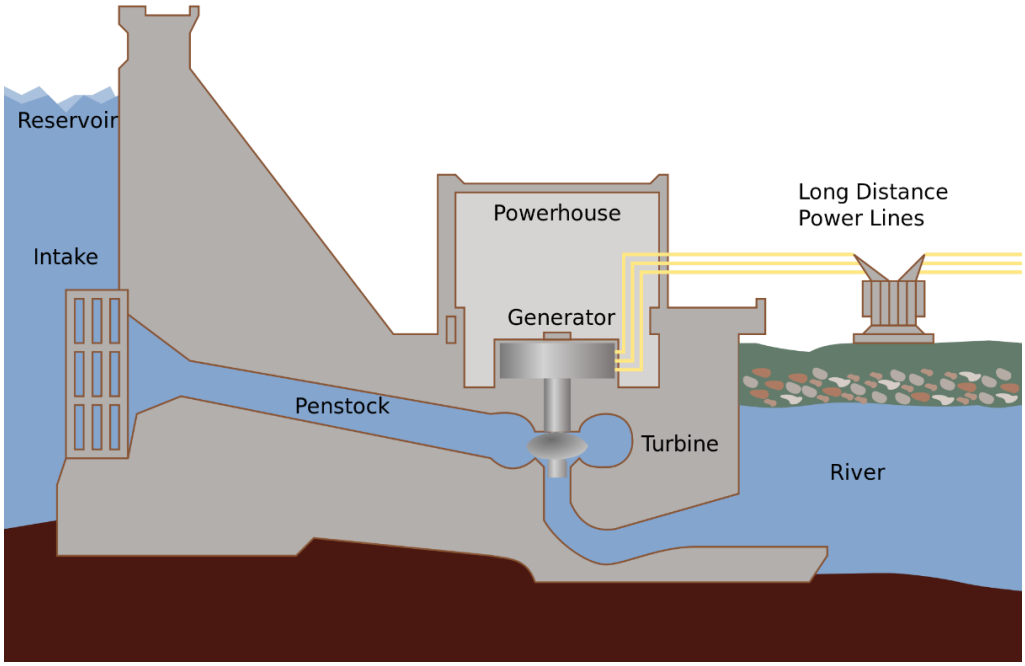

Figure 2-17 Schematic diagram of a Hydroelectric plant. (Image Source: En.wikiversity.org)

The hydro station, which has six rated 300,000 kW Francis turbines installed, has a total energy capacity of 1,800,000 kW. Access to the inside is through a tunnel at the bottom of the dam. The powerhouse is approximately 50 m tall, 30 m wide and 300 m long. The six generators are aligned in the ground, with 5 m between each one. The top casing of the generator is a regular octagon shape which is shown in Figure 2-18.

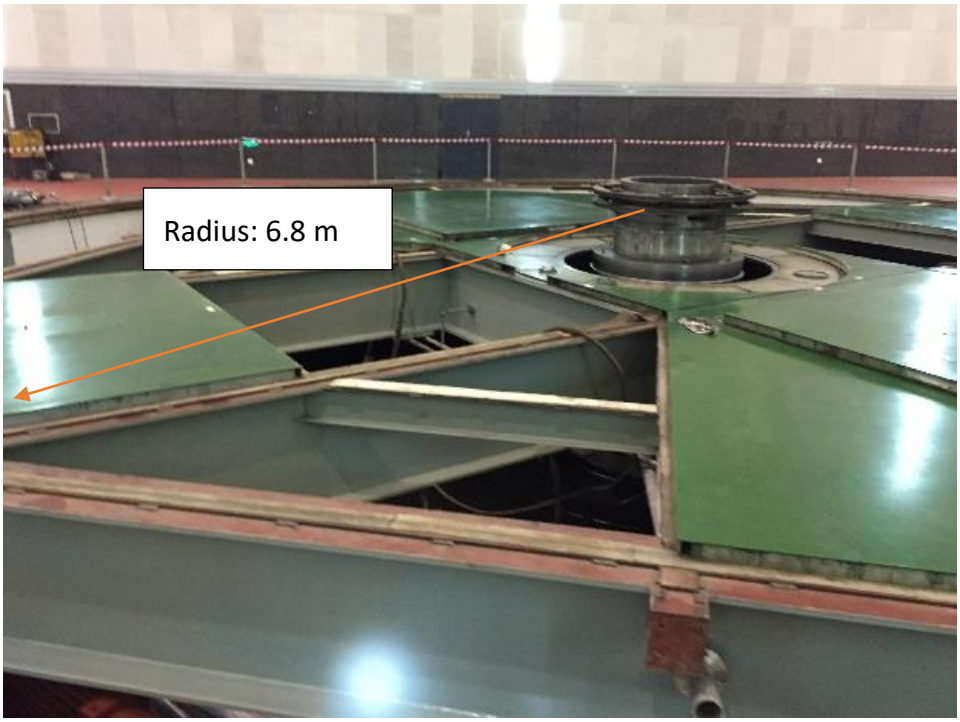

Figure 2-18 Top casing of the hydro station generator

The casing has a radius of 6.8 m. Control and monitoring units are located next to the generator alongside the wall with three boxes containing electronics and gauges for each turbine unit. These display data such as; current power output in megawatts, the speed of the generator, the effective head of the water turbine, the efficiencies and the cost per volume of water per kWh (m^3/kWh).

The lower chamber where the turbine resides can be accessed via a stairway from the powerhouse, about 15 m directly below the generator unit. During the visit, turbine No.4 was undergoing a major service, the first major service since the power plant started operations since 2001. All key components were disassembled and removed from the site using a crane. Once removed, all maintenance and repairs could take place, this was because it was impossible to perform major services if all components were assembled, due to limited space. To perform the maintenance, the intake gate of the turbine unit was shut, and the water pumped out, so personnel could gain access to the chamber. The turbine chamber can be accessed through a tiny window

which has a size approximately 0.7 m x 0.7 m. The American made Francis turbine hung in the centre of the chamber, comprising of at least 30 blades attached to the runner. The diameter of the turbine was 6.36 m, with a height of approximately 3 m. It was made from a composite alloy, to prevent corrosion, the composition of this alloy was not given by the on-site engineer. Due to large water-borne sand grains (avg 35 kg/m^3), some blades were damaged. These marks and scratches were visible on the blade which is shown in Figure 2-19. The damaged blade was repaired and polished with a coating; a special paint was used to prevent corrosion.

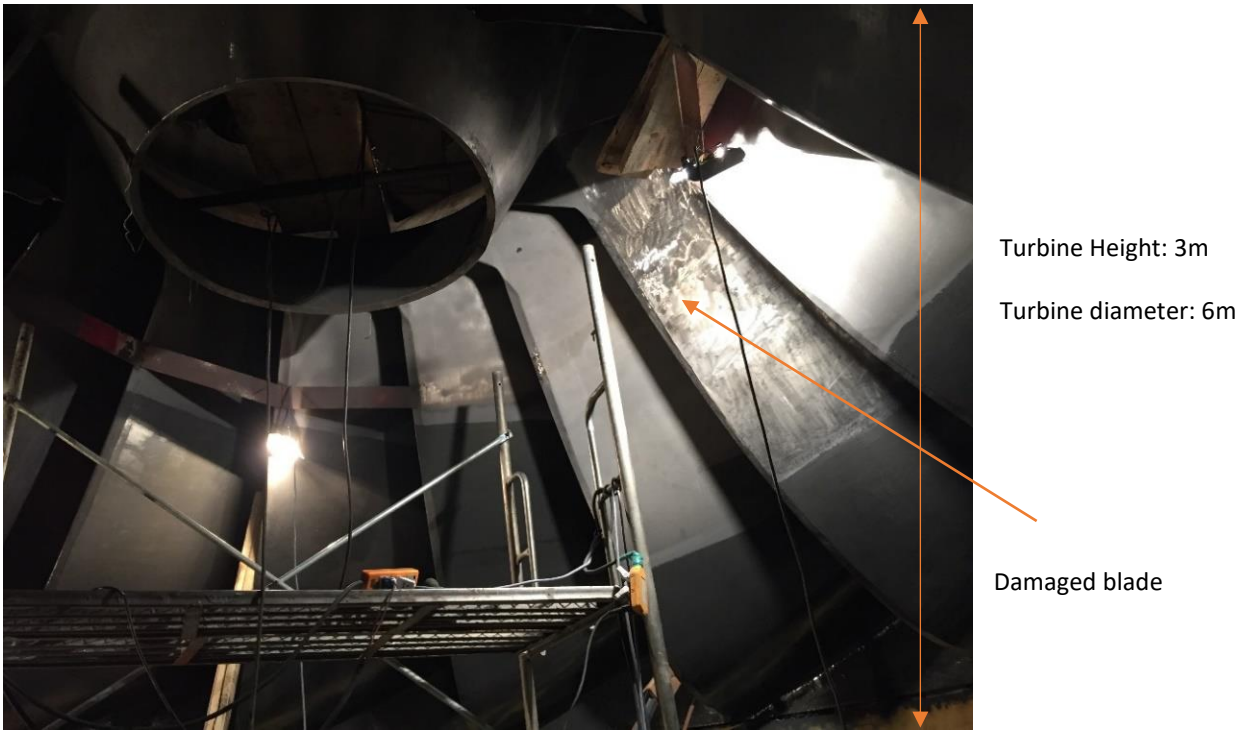

Figure 2-19 Repair of the damaged blades of the No.4 Francis Turbine

Above the turbine chamber was the water chamber, where water from the reservoir enters through a gate and penstock. It then enters a spiral chamber with 9 m diameter. The water enters the guide vane of the turbine which is located in the centre; a hydraulic control operates the open angle of the adjustable guide vane, therefore controlling the amount of water injected into the turbine below. The onsite engineer

stated that the normal working turbine takes a maximum of 300 m^3/s of water to generate at full power, which is rated at 300,000 kW for each turbine unit.

Between the turbine and the generator was a small connecting chamber called the shaft chamber. It was surrounded by ceramic thrust pads which were used to reduce support the vibration of the shaft. The vibration comes from the rotation of the water turbine; this acts as a cooling system. The water was injected directly onto the pads to remove excess heat, to protect the component.

The generator is positioned on the top of these components, the rotor was directly connected to the shaft, and the stator was a regular octagon shape which was the same as the top casing. The stator was covered fully by copper rings, and the cooling system was the same as the ceramic thrust pads, where water is sprayed onto the stator to maintain the system at working temperatures.

All six turbine units shared the same design and structure. It was claimed an overall efficiency above 90% could be achieved which is shown in Figure 2-20. This was due to the large Francis turbine which could reach 95% efficiency, under optimal conditions. According to the data plate of the generator, maximum efficiency of 97% could be reached. To couple all the components and an output frequency of 50 Hz (Chinese standard), the rotational speed of the turbine shaft was set to 107.1 rpm. The rotational speed depends on the speed of the turbine, which was controlled by altering the inlet flow rate, via the guide vane, this control method will be discussed in Chapter 4 of this thesis.

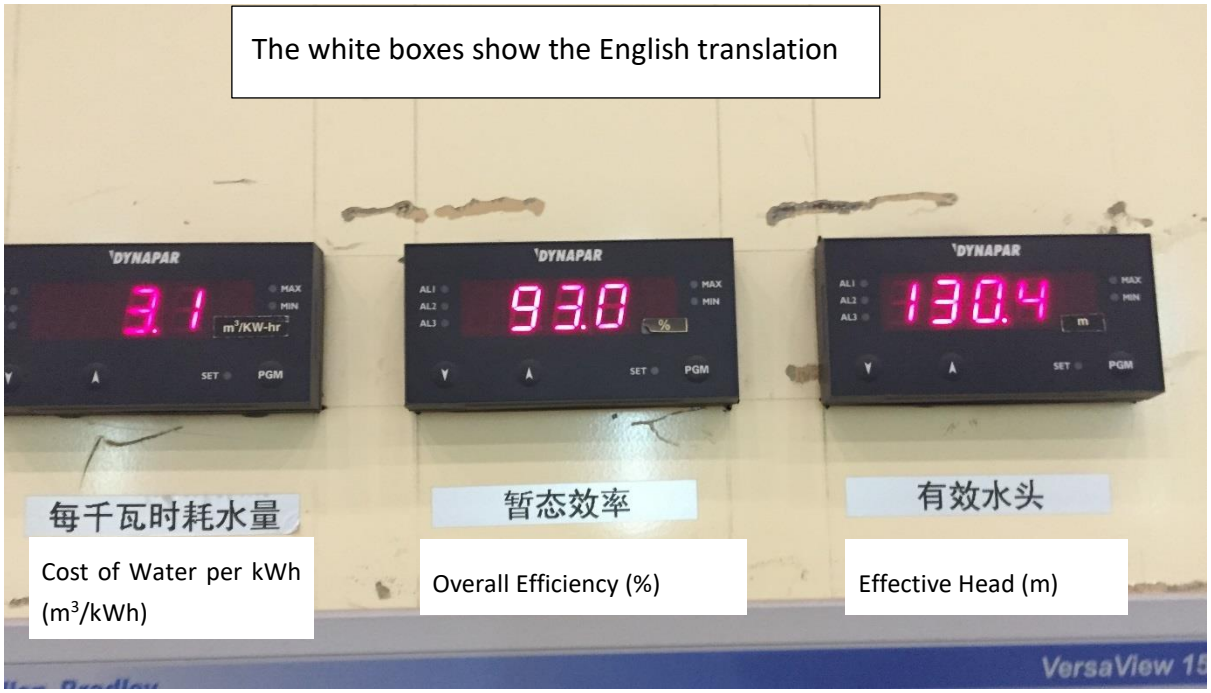

Figure 2-20 Control unit display board

By visiting this site, a reliable working system was observed. The function of each component was explained by onsite technicians, and the vertical axis turbine system of the hydro energy plant was studied.

2.5.3 Tidal energy power station

The second site visited was a tidal energy plant; the Jiangxia Tidal Power Station was built in 1972, in a bay area in eastern China. The 670 m long dam that crosses the bay was originally designed for aquaculture, but it was later converted to a tidal power station. Six 700 kW bulb turbines are installed on site. After a major upgrade in 2007, all six bulb turbines are now operating, generating 4,200 kW, making this the largest tidal power station in Asia, the 3rd largest in the world.

Figure 2-21 shows the Jiangxia Tidal Power Station schematic design. This type of power station does not require a tall dam structure like a hydro power station, but does require a reservoir. The head difference across the two sides of the dam

produces electricity; one of the major advantages of the tidal power system is that tides are more predictable than wind and solar energy.

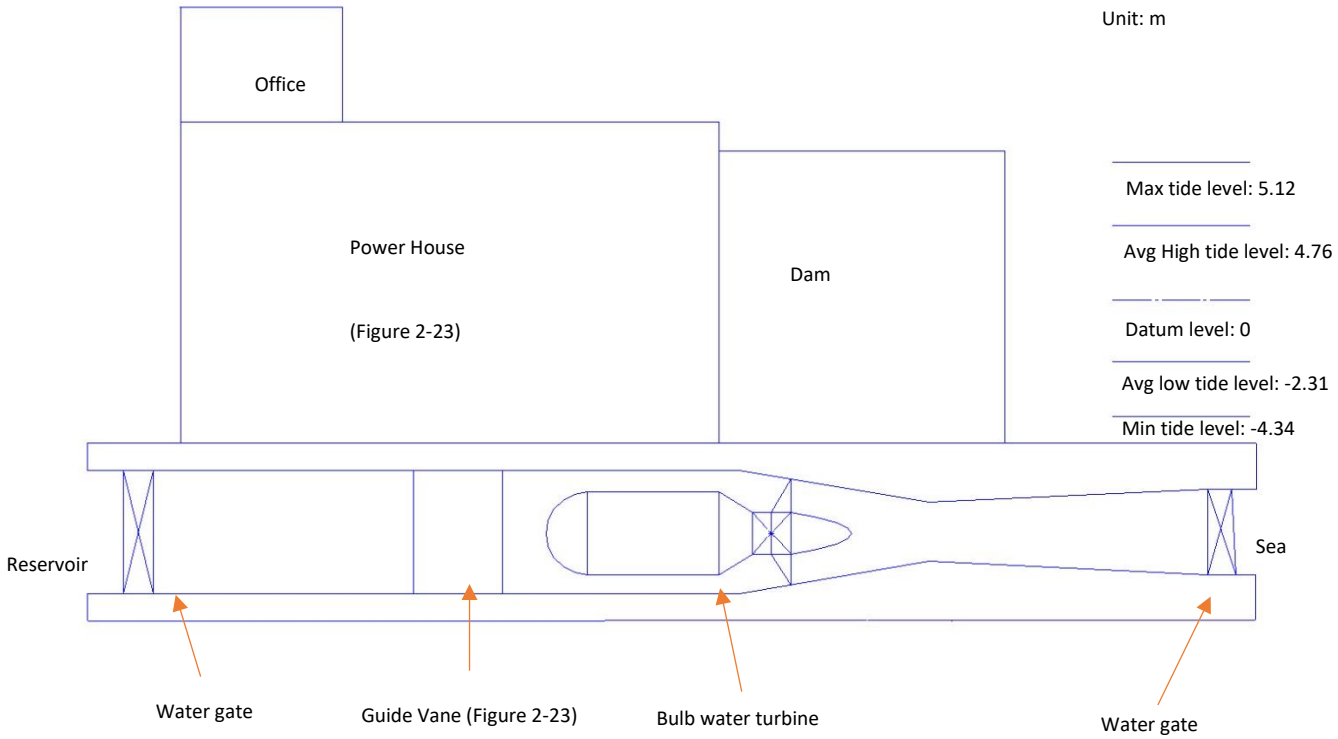

Figure 2-21 Schematic diagram of Jiangxia Tidal Power Station

During the visit, it was stated that the generating time would be at least 14 hours per day. However, due to limitations of the dam structure, originally designed for aquaculture only, it does not hold water for the optimum level of power generation required. The turbines generate power when the head reach 5 m, which normally means the head difference between the two sides of the dam is 1.6 m. According to the chief engineer, during the ebb, more power is generated when compared to the flood situation. This is because the water level drops quicker on the outside the dam, providing bigger head differences for power generation, more of this information will be discussed in Chapter 5.

The powerhouse is located on the south end of the dam; it is approximately 40 m long, 20 m wide and 20 m tall which is shown in Figure 2-22.

Figure 2-22 The powerhouse and the dam at Jiangxia Tidal Power Station (Image source: Chain Guodian Corporation)

When entering the power house, six turbine units located in alignment which is shown in Figure 2-23, the electrical control units are located behind and alongside a wall, behind each turbine unit. The 4-blade 2.5 m diameter bulb turbine is placed ahead of the guide vane; the 16-vane guide is controlled via a hydraulic actuator which is shown in Figure 2-24. An oil tank is placed about 1.5 m above the turbine inlet. During the flood tide, the water enters the turbine via an inlet gate of circular shape with a diameter of 3 m, and during the ebb, this entrance acts as an exit for the water. The bulb turbine is horizontally placed, the shaft is connected to the generator from the turbine directly through the centre of the guide vane. The thrust pad, which tightly encircles the shaft, is made of a type of plastic to save on costs and is cooled by passing

water. The generator shares a similar design to the one used in the hydro power plant, only it is horizontally placed, and is much smaller in size; maximum 3 m in diameter when compared to 18 m. Unlike the huge structure at the hydro station, the entire system is in a condensed package, where the total length from the inlet of the turbine, to the end of the generator is less than 10 m. This is mainly because the rated power for each water turbine system is relatively small comparing to Xiaolangdi Hydro Power Station (700 kW to 300,000 kW). Figure 2-23 does not show the entire layout inside the power house due to camera limitations and accessibility.

Figure 2-23 The layout of the power house

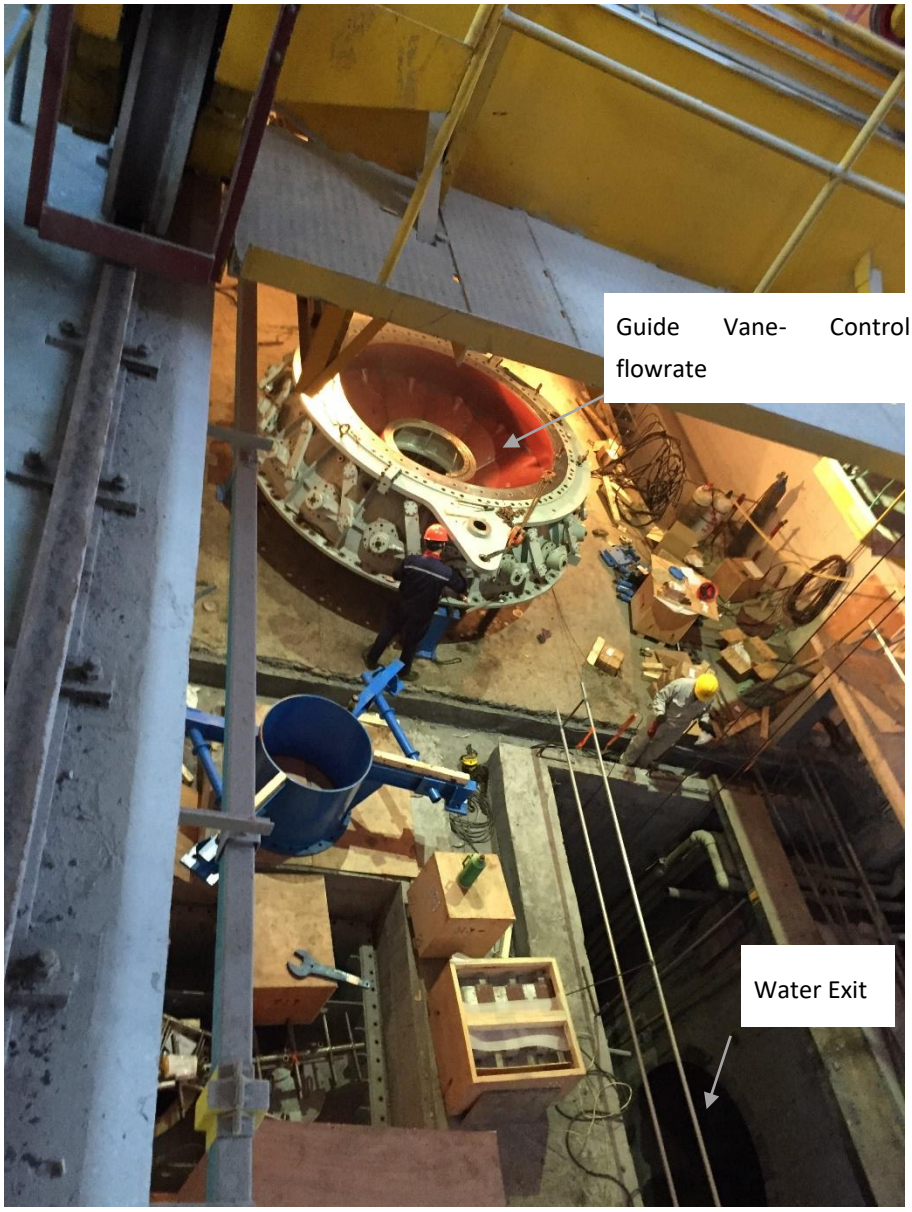

Figure 2-24 The guide vane and the water entrance of the No. 1 unit

To maintain a 50 Hz frequency output to the grid, the system must have a speed of 125 rpm. To accommodate this requirement, excitation of the generator must be altered. By changing the strength of its electromagnetic field, the resistance of the rotor is altered, and therefore the system can be operated under controlled speeds. The minimum overall efficiency is 89%, and with low tide it is slightly higher, at 90%.

2.5.4 Wind turbine farms

The last site visited was a wind farm located in the mountains of central China, about 40 miles west from the hydro station. At the time of the visit, construction had been recently completed. The farm contained China's most advanced wind turbines, consisting of five 2,000 kW turbines and forty 3,000 kW turbines, with a total capacity of 130,000 kW.

The latest and most advanced turbine to date was designed by Huadong Engineering Corporation, China. Figure 2-25 shows the 3,000 kW wind turbine stands 90 m tall from the ground, 3.6 m length glass fibre and resin blades are attached to the hub, which makes the swept area 11,304 m^2 (Zhang. 2011). The nacelle weighs 122 t, plus the 67 t blade, which makes a total of 189 t mass above the tower. The tower has a 5 m base diameter which is tapped towards the top. With the pitch control system installed, the blades adjust automatically to different wind speeds and direction for maximum performance.

Figure 2-25 3,000 kW wind turbine

Additionally, the pitch control system is used as an air brake. When the system requires it, this function changes the blade angle and aligns the blades parallel to the wind, therefore, a reduced lift force acts on the foil. A shaft, connected to a fixed ratio gearbox, is driven by the turbine. The generator is linked to the other end of the gearbox, and the 690 V 50 Hz output electrical current is transmitted to the ground unit via cables and the

voltage is then boosted to 220 kV by a transformer for the grid connection. (Zhang. 2011)

Inside the turbine tower, an electronic control system is located next to the door, where 6 cables connect to the box from the top of the tower. These are the power transmission cables. In the centre of the tower, a ladder provides access to the top of the unit, and is equipped with a climbing aid system. The ladder provides a 50 kg pulling strength for the climber. An electrical motor is inside the blue box on the side of the ladder, driving a steel rope attached to a pulley at the top of the tower.

This type of wind turbine is fully automatic, the pitch control and the yaw control systems adjust the turbine to an optimum position for energy harvest. In the control room, each turbine is monitored; the current wind speed and direction is updated every second, along with the speed of the turbine, the pitch and yaw angle.

Figure 2-26 shows an overview of a single wind turbine unit, where key parameters are monitored: the blade angle for the turbine blade, the Yaw angle for the nacelle, the speed of the generator, the power of the turbine and the current wind speed.

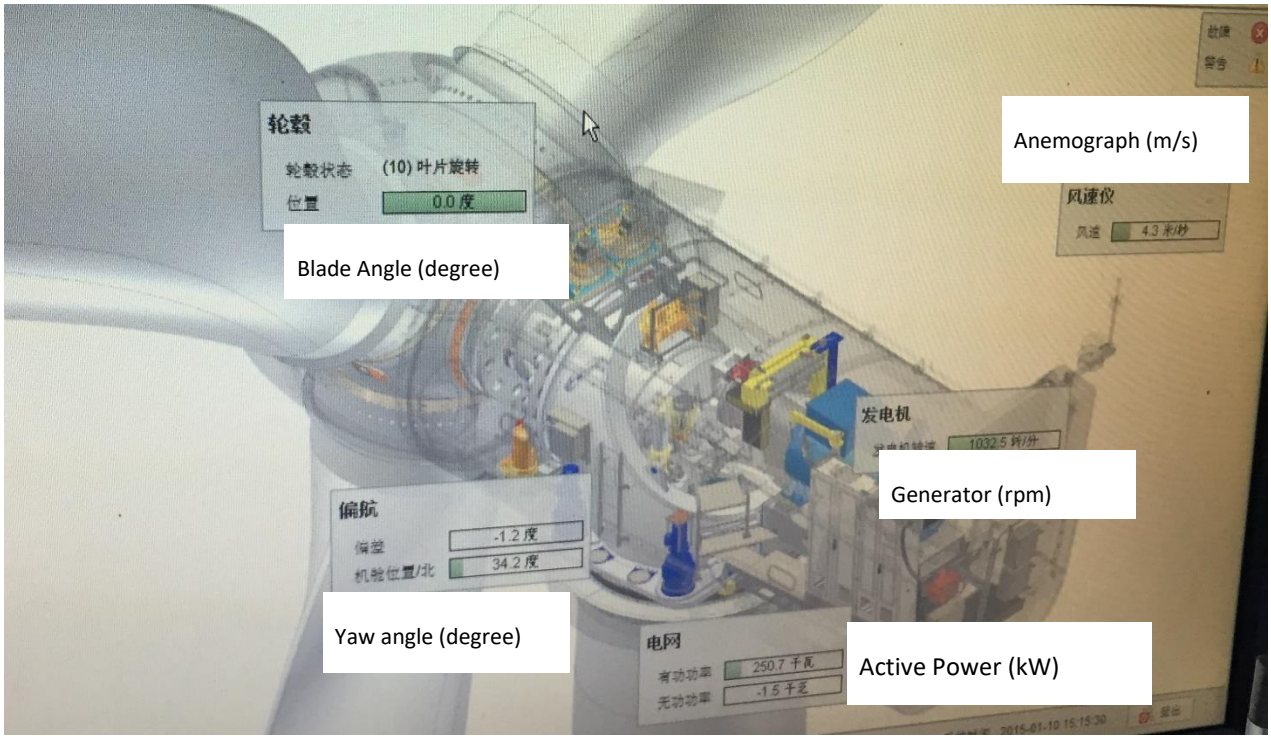

Figure 2-26 Monitoring all the key components of the wind turbine.

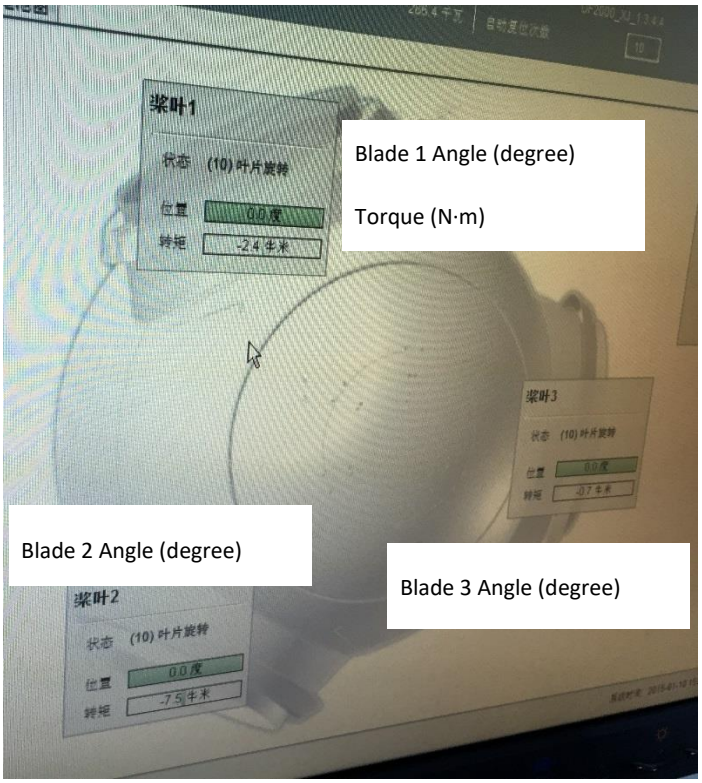

Figure 2-27 Conditional monitoring of the turbine hub

Figure 2-27 shows the hub, where the pitch angles of the three turbine blades can be seen on the screen, along with the torque acting on them.

Figure 2-28 shows the condition of the front of the gearbox, which was connected to the turbine shaft. This system monitors the cooling system of the gearbox, and the oil pressure and temperatures at different parts of the gearbox. This ensured the gearbox was functioning within normal operating temperatures.

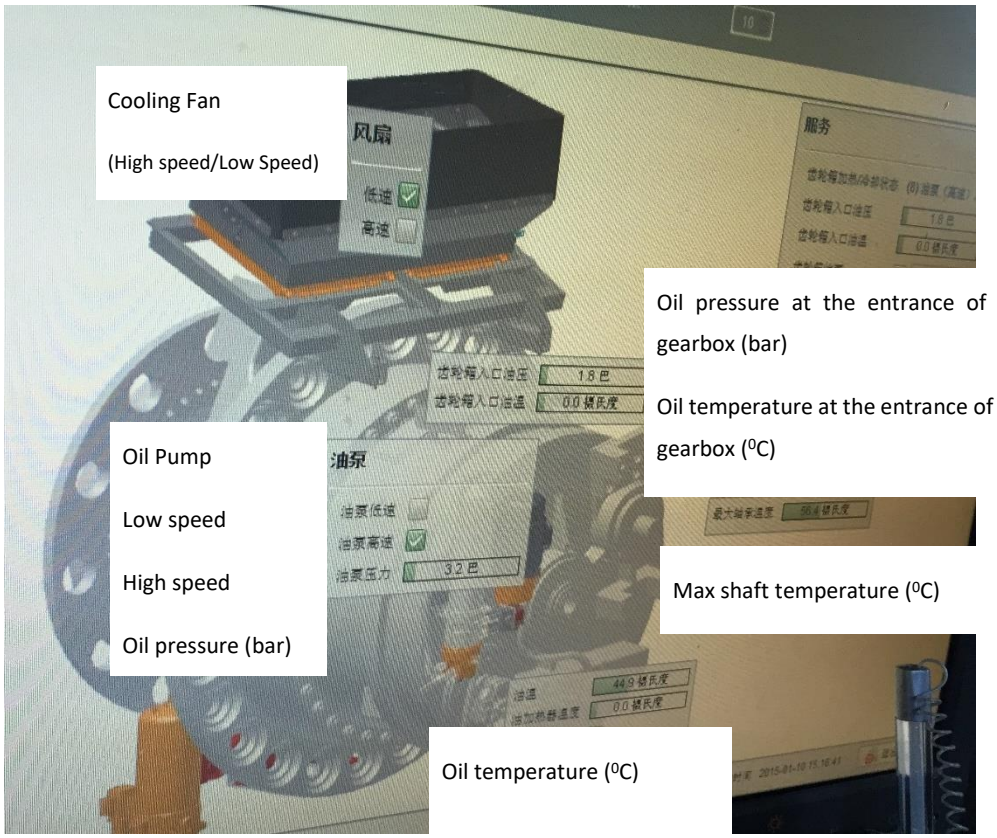

Figure 2-28 Conditional monitoring of the gearbox of the wind turbine

The back of the gearbox, which is used to connect to the gearbox is shown in Figure 2-29, shows the receiving shaft speed and the output speed for the generator connection, the condition of the hydraulic pump and the brake condition. There are two brakes which in red colours are located near the output shaft; these are the emergency brakes for the electrical generator.

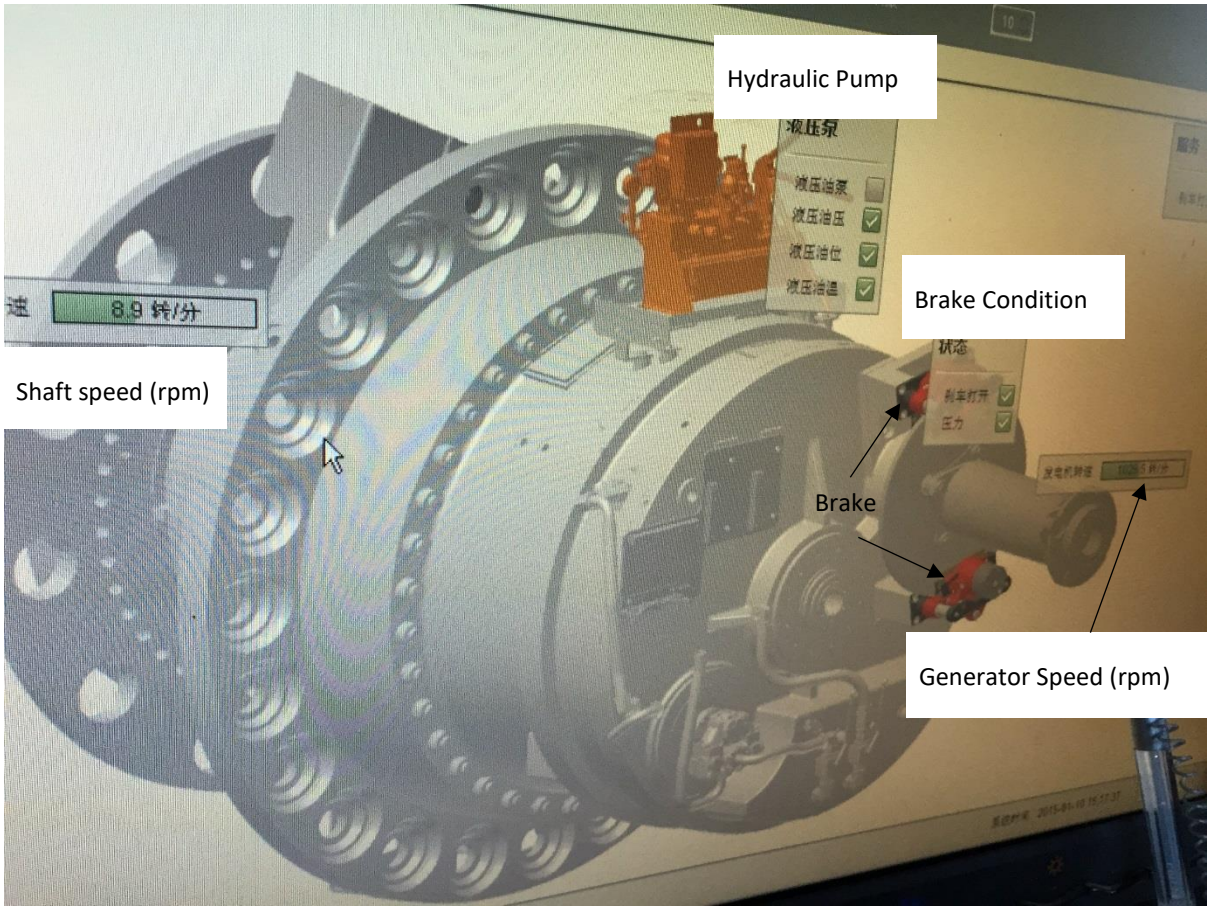

Figure 2-29 The back of the gearbox of the wind turbine

Figure 2-30 shows the condition of the generator, shows the temperatures of the generator, along with the power output and the speed of the generator.

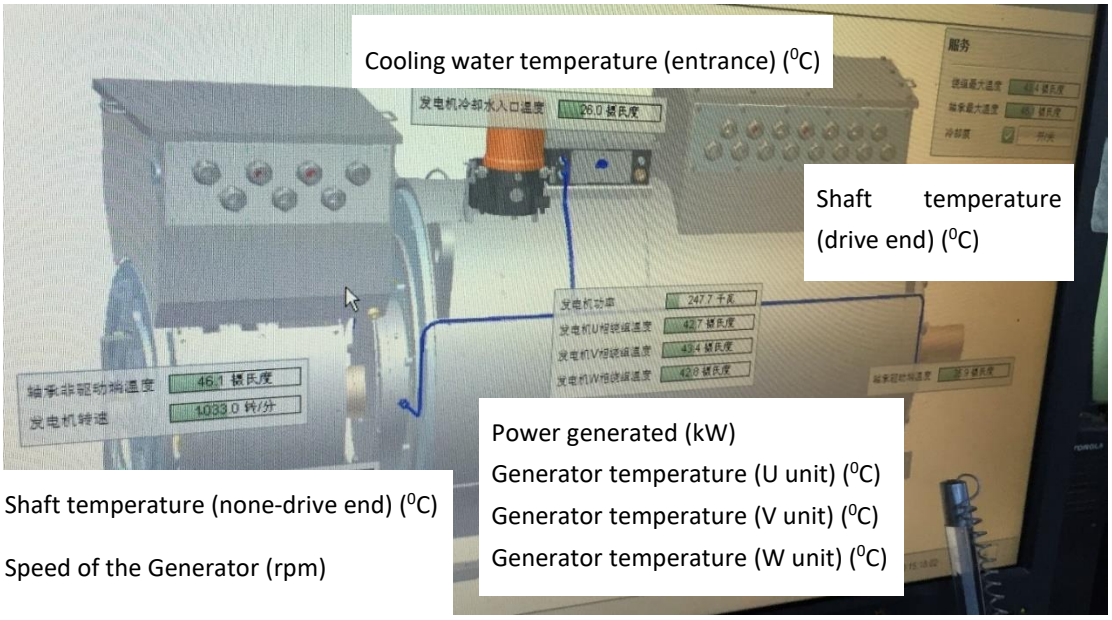

Figure 2-30 Conditional monitoring of the generator of the wind turbine.

The turbine starts generating power when the wind speed is 3.5 m/s. The system is cut off once extreme conditions have been breached, as wind speeds exceed 25 m/s. According to the engineer, the survival wind speed for this type of turbine is 52.5 m/s. The 95.6 ratio gearbox transmitted power from the shaft to the 1,200-rpm generator.

The challenge of building a wind farm in mountainous rather than offshore regions is the unpredictability of wind directions. The wind can change quickly due to mountain topography. Therefore, it requires massive computational analysis to identify optimum sites to locate the turbines (Zhang. 2011).

To conclude, these are three, widely used renewable technologies that are believed to have a similar design to the marine turbine energy system. By studying and observing the mechanics of these systems, their supporting facilities and the control methods, it has provided excellent background knowledge for this system design. What is more, it is understood that most control methods, like changing blade angles, and altering guide vane angles, are automatically controlled by the computer. This provides a quicker and more accurate solution than human controlling. Furthermore, both the hydro and tidal energy plant proved that their designs were reliable and

durable. The components of the hydro plant require major maintenance at 15-year intervals, which is a long period, and the system in the tidal plant has been working for more than 30 years.

2.6 Chapter Summary

These technologies, the hydro and tidal power stations, both use the potential energy of water. They are the most powerful of all discussed technologies due to their large sizes, and as a result, they are the most expensive to construct. The advantages of these systems are reliability; all technologies used in these types of design are well proven in terms of long service life. The main structure of the barrage also has a long life-span and all major components do not require regular servicing. However, these systems are initially costly in terms of construction, and potentially changes in local geography, therefore all systems require detailed investigations and evaluations before construction.

The pumped hydroelectric storage shares similar technology with the hydroelectric systems, the water is stored at a reservoir which located above the turbine, during the off-peak period, when the energy price is cheaper, the water is then pumped back to the upper reservoir, and to be released during the peak period, when the energy price would be higher. By using this system, the power station would generate the power during the peak demand period, but the profit would be determined by the energy price difference between the peak and non-peak times, if the difference is small, then the power station would potentially lose money.

For turbine-type technologies, including tidal stream turbines and wind turbines, the principle was similar; using passing water/wind to generate energy. Due to differences in density between water and air, wind turbines are larger to compensate for deficits in density. For tidal stream turbines, underwater working environments generate extra challenge; the device must be designed to work safely when submerged, and for maintenance, there is less accessibility when compared to wind turbines. However,

the advantage of tidal stream turbines is that tidal streams are well predicted, but the wind is less so.

Last but not least, the visit to Jiangxia Tidal Power Station has provided an insight of how a tidal power station operates between ebb and flood tides, also how to control the flowrate to keep the reservoir level within the design limit, for example, the reservoir at Jiangxia Tidal Power station has a 1.8 m design limit, which during the flood tide, the power station would control how much water flows into the reservoir via the guide vane to ensure the reservoir level is not exceed the 1.8 m design limit. Additionally, a set of recorded data was also acquired during the visit, and it will be discussed in Chapter 5.

3. Hydraulic driven tidal turbines

3.1 Introduction

As discussed in Chapter 2.2.1, the current tidal stream turbine design shares a similar design to the wind turbines, they both using the turbine to drive a generator via a gearbox which all located in the nacelle. With the widely deployment of the wind turbines, there were 9,098 wind turbines in the UK by the end of 2018 (Renewableuk.com. 2018), which indicates this technology is industrially proven. However, there are some problems with the wind turbine system, and by using the similar design, the concern was these problems could also affect the tidal stream turbines.

A research on wind turbine failures which shown in Figure 3-1 & 3-2 shows the causes and downtimes of wind turbines between 2008 and 2012 (Sheng. 2013).

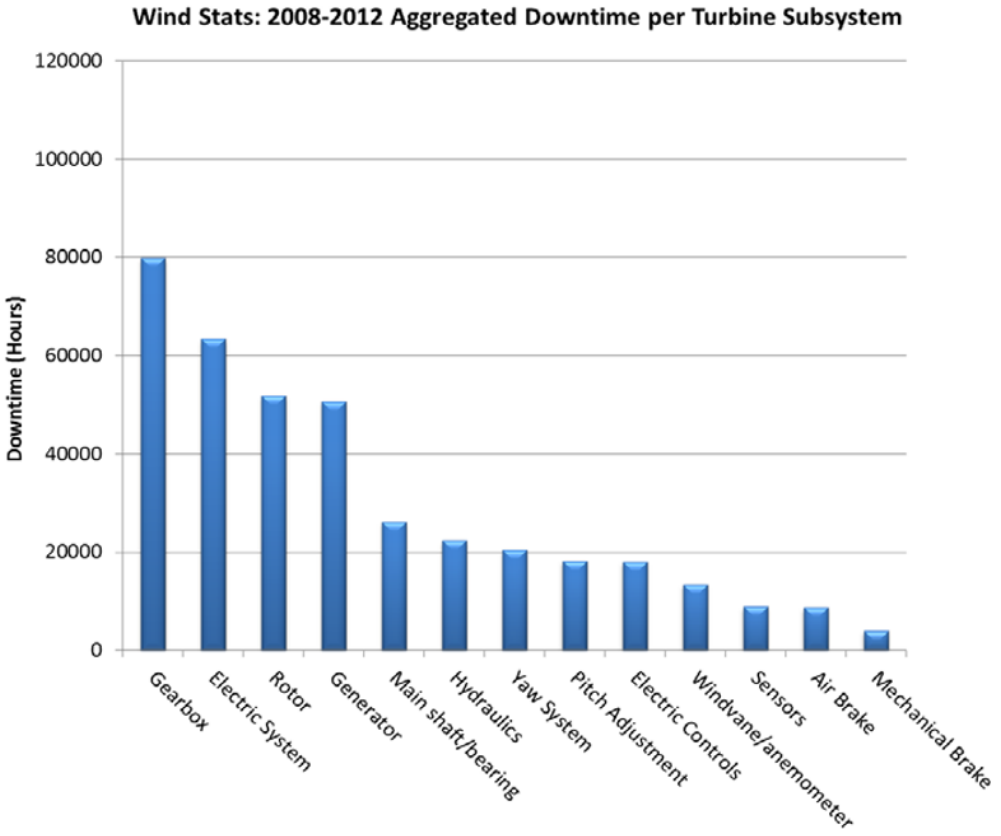

Figure 3-1 Wind turbine component aggregated downtime between 2008-2012 (Sheng. 2013)

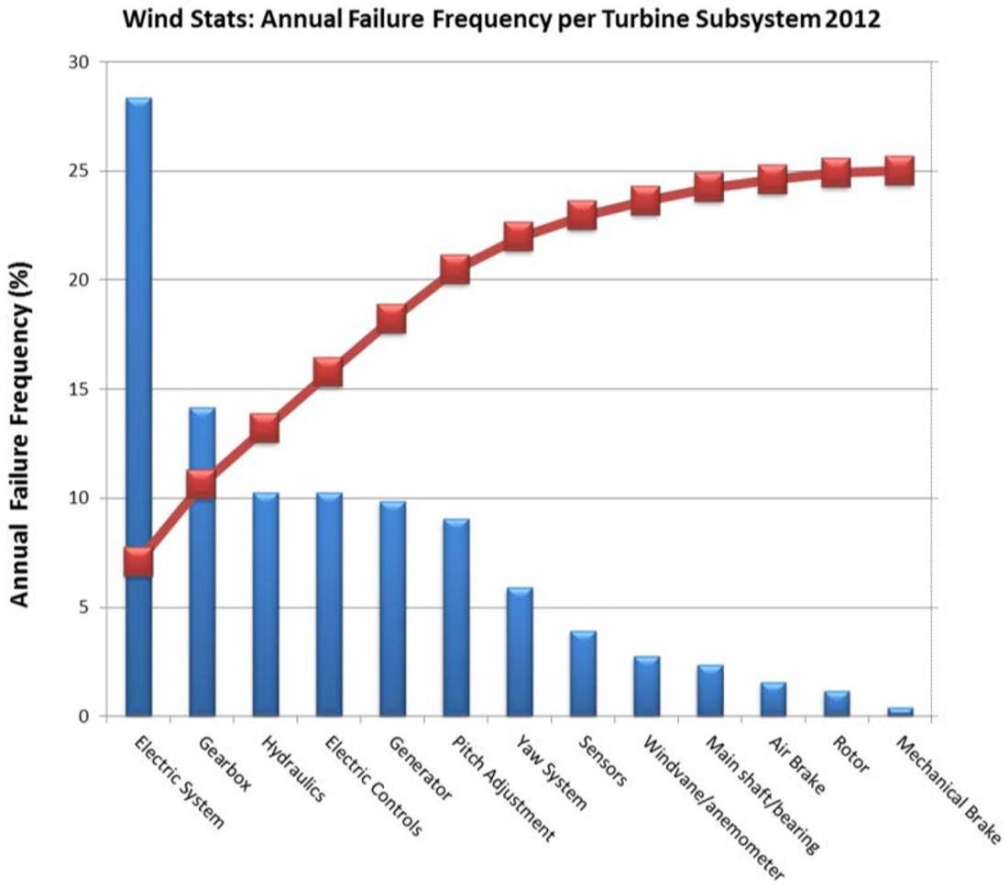

Figure 3-2 Wind turbine component failure frequency (Sheng, 2013)

According to the graphs in Figure 3-1 and 3-2, electrical systems and gearboxes are two major parts that fail, with gearbox failures having the longest downtime rates, when compared to other causes. Therefore, it is necessary to reduce these potential failures in the system. Concerning the underwater environments, it is very difficult to repair these large-scale units, and in many cases, broken parts need to be disassembled and shipped back to shore for repair and maintenance. To reduce the risk of failure, it is suggested that new designs of the power transmission system could be achieved by removing the gearbox unit.

Hydraulic systems are reliable and low-cost solutions for many operations; later in the thesis, hydraulic circuits for power transmission will be discussed as being potentially suitable for tidal turbines.

The initial step of hydraulic turbine design is converting the conventional tidal device, in this Chapter, the MCT's SeaGen will be used as an example, this because it was the first commercial full-scale tidal stream turbine which deployed in 2008, and as discussed in Chapter 2.2.1.1, it featured a twin rotor design, each has a rated power of 600 kW.

The hydraulic transmission system purposed to use hydraulic pump replaces the electrical generator and the gearbox. Each turbine is coupled with this pump, which pressurises the fluid and is transmitted to shore via a pipeline. The onshore unit consists of a hydraulic motor and a generator, the pressurised fluid from the turbine drives the motor and powers the generator to produce electrical energy.

This design eliminates the requirements for underwater gearboxes and generators, which have large failure rates. This approach could provide a more reliable system that may have improved the redundancy and maintenance issues for the current tidal turbine systems. To develop this design further, key parts of the design need to be considered.

3.2 Devices considerations

3.2.1 Pump considerations:

Thorough research was not carried out on the pumps; this was due to the pump specification varying for each case. However, the pump is required to generate a constant pressure with changing tidal velocities. Therefore, a swash plate pump was selected for the design. A swash plate pump is a pressure-compensated variable displacement piston pump, the angle of the swash plate is adjusted by the pressure feedback, which makes this pump to maintain a designated pressure changing flow rates (Fang, X., Ouyang, X. et al. 2018). Because pump information was not yet available for this design, it was assumed the pump could deliver fluid of the required

pressure and flow rate, with an efficiency of 90% at the worst case assumption. The service life for the standard swash plate pump can last around 5 years or more (El-Zahaby. El-Nady. 2006), but the service life of the pump is also related to the cleanness of the hydraulic oil used, the shaft speed of the pump and the pressure output, by using the contaminated hydraulic fluid will significantly reduce the expected service life for the pump. (Casey. 2014)

3.2.2 Motor considerations:

To match the SeaGen's 1,200 kW rated power output, a similar power motor was required. For this design, the Hagglunds Compact CBP motor 400-320 was selected. This motor delivers 1,250 kW on the drive shaft when the speed is 120 rpm, and the torque is at 100 kN·m, more information of the motor will be discussed at Chapter 3.4.1.

For a hydraulic system, it was either closed or open. In this case, a closed loop was selected, this was because comparing to the open loop design, closed loop hydraulic system does not require the fluid goes back to the oil tank, which would potentially reduce the environmental hazards. For the return line, it was designed exactly like the pressure line, so when the flow was in the opposite direction, the pressure characteristics in both lines were the same.

3.3.3 Hydraulic fluid considerations:

Hydraulic oil is widely used as a hydraulic fluid, a value for fluid density was chosen at 870 kg/m^3 in this design.

According to the motor data sheet, this particular motor (the Hagglunds Compact CBP motor 400-320) used hydraulic oil with a viscosity range between 20-10,000 cSt, However, on the motor recommends using 40 cSt for optimal performance (Boschrexroth.com. 2014). Based on this recommendation, a fixed viscosity of 40 cSt

was used for calculations.

3.3.4 Pipe & hose diameter considerations:

From the motor data sheet, the diameter of the input and output ports is 50.8 mm (2 inches), which is the same diameter of the flexible hose required for connection between the motor and the main pipe line. A 2-inch diameter size was chosen for the flexible hose for the pump connection in this design. In this Chapter, the diameter of the hose and pipe are measured in imperial units as it was used by the consulted manufactures, but the SI unit is used in the calculations.

For the main pipe line, the aim was to find a larger diameter pipe that has a working pressure greater than the required pressure for safety. The pipe selected was stainless steel 316 with a diameter of 4.87 inches (123.69 mm) with a maximum working pressure of 344.738 bar (5,000 psi). The larger diameter of hose that is mounted on the central pillar shares the same principle with the pipe, after research in the flexible hose manufacturer, a 5-inch diameter (127 mm) flexible hose was selected for this system.

3.3 Design

As part of the design elements of this design was the conversion from electrical to hydraulic for the SeaGen system, Figure 3-3 shows the draft design of the hydraulic tidal turbine system.

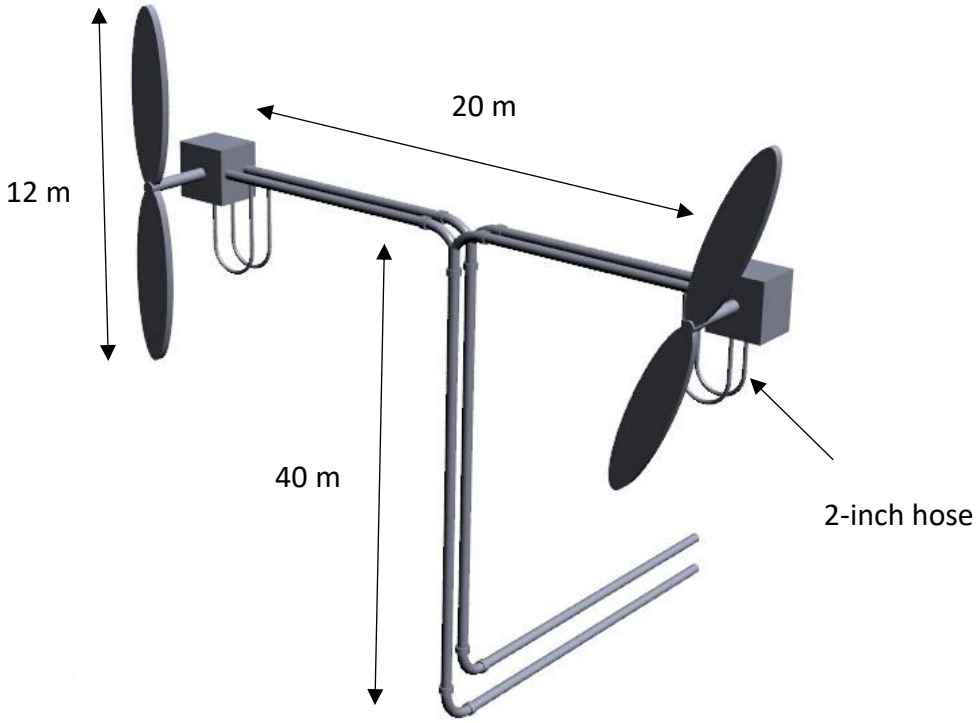

Figure 3-3 Tower structure for the hydraulic marine turbine

As shown in Figure 3-3, the tower structure was based on the SeaGen turbine, which consists a dual two-blade turbine on each side, differing with the original design in that each turbine which droves a pump that pressurises fluid into the pipeline as a way to transfer energy. It shares similar dimensions to the SeaGen turbine, the system is about 40 m tall from the seabed, and the distance between turbines is approximately 20 m. The fluid is delivered to shore via underwater pipeline which is shown in Figure 3-4.

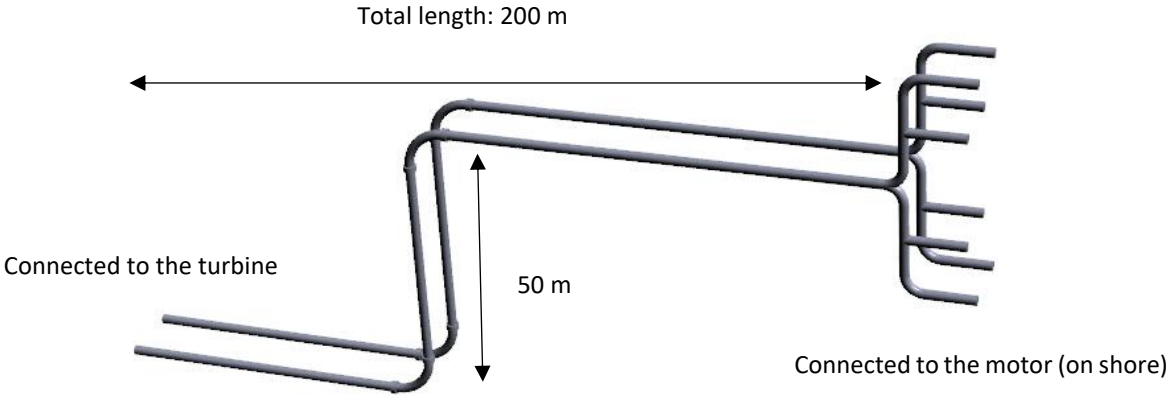

Figure 3-4 Hydraulic pipeline shore end unit

To build a 50,000 kW energy farm with a SeaGen like 1,200 kW devices, 42 individual systems are required, including 42 cables to shore. However, with the application of this hydraulic system, a motor-generator unit can be installed within a short distance, for example Figure 3-5 shows a conceptual farm which contains 10 turbines, the turbines are connected by the main pipeline, which delivers the combined hydraulic fluid to the motor and generator unit which located on shore, the pressure balance valves will be installed to balance the flow pressure. In this design, only one generator will be needed for multiple turbine devices.

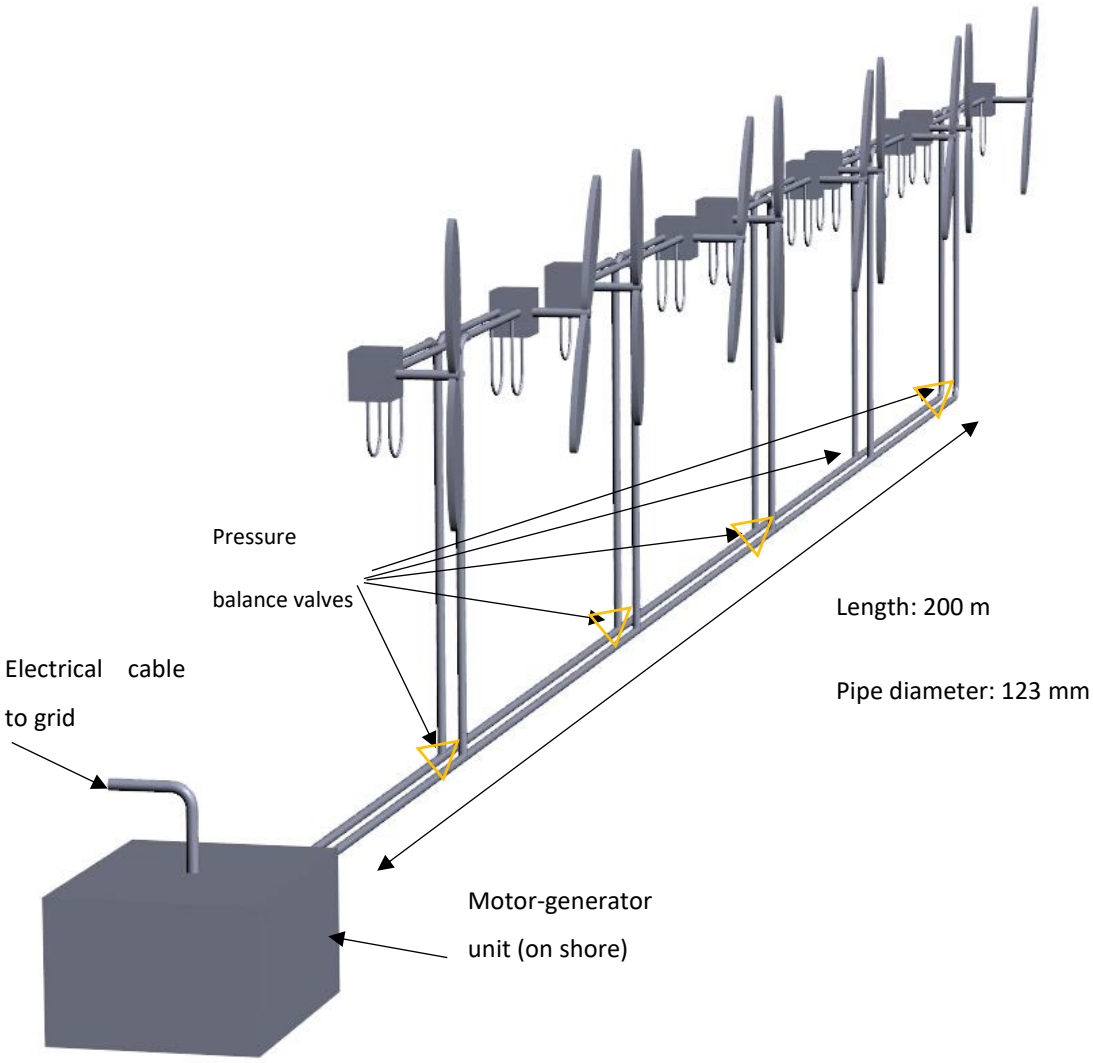

Figure 3-5 Multiple turbines share one motor-generator unit

3.4 Calculation methods

For a hydraulic system, the energy loss is primarily the pressure loss in the system. Therefore, the pressure loss across the system is required to calculate the motor's power and the efficiency of the system.

The primary areas which need to be considered are:

1. Flexible hoses
2. Steel pipes
3. Fittings and couplings
4. Bends in the pipes

There are other areas affecting pressure loss in the hydraulic system. In this design, these are pressure losses due to gravity and pressure loss due to changing fluid viscosity.

3.4.1 Calculations of Motor:

Motor specifications:

From the motor data sheet:

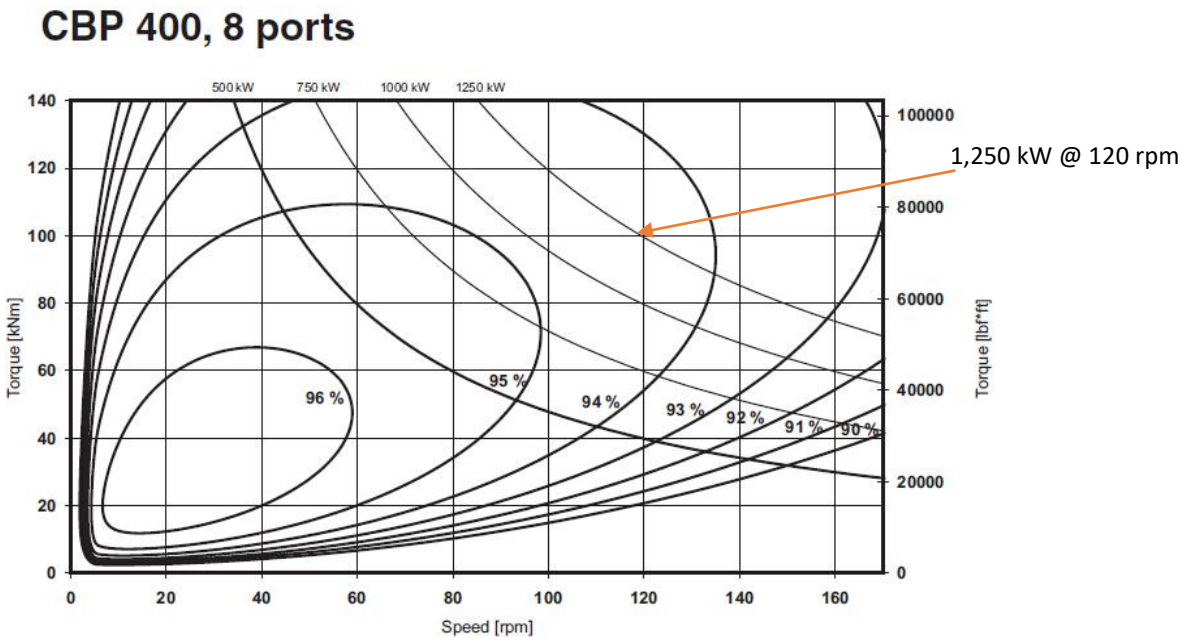

Figure 3-6 Overall motor efficiency (Boschrexroth.com. 2014)

From Figure 3-6, the motor was capable of outputting 1,250 kW at a speed of 120 rpm and a torque of 100 kNm with an efficiency of 94%.

Table 3-1 Motor specifications (Product Manual Compact CBP motor)

CBP 400-320	Displacement $V_i \frac{cm^3}{rev}$	Specific torque $T_s \frac{Nm}{Bar}$	Max Speed n rpm	Max pressure P_w bar
	20,100	320	170	350

Equations used to calculate fundamentals for this motor:

Output power on driven shaft $P = \frac{T \cdot n}{9549} (kW)$ (3-1)

Output torque $T = T_s \cdot (p - \Delta p_l - p_c) \cdot \eta_m \ (N \cdot m)$ (3-2)

Pressure required $p = \frac{T}{T_s \cdot \eta_m} + \Delta p_l + p_c \ (bar)$ (3-3)

Flow rate required $q = \frac{n \cdot V_i}{1000} + q_l \ (l/min)$ (3-4)

Output speed $n = \frac{q - q_l}{V_i} \cdot 1000 \ (rpm)$ (3-5)

Where *P* is the motor output power (kW),

T is the output torque (N·m),

p is the pressure required by the motor (bar),

Δp_l is the pressure loss across the motor (bar),

p_c is the motor charge pressure (bar),

η_m is the motor efficiency,

q is the flow rate required by the motor (l/min),

q_l is the fluid loss across the motor (l/min) and,

n is the motor speed (rpm)

The pressure required for 1,250 kW is (charge pressure is 5 bar):

$$p = \frac{T}{T_s \cdot \eta_m} + \Delta p_l + p_c = \frac{100{,}000}{320 \times 0.94} + 2.7 + 5 = 340.15 \ bar = 4{,}932 \ psi$$

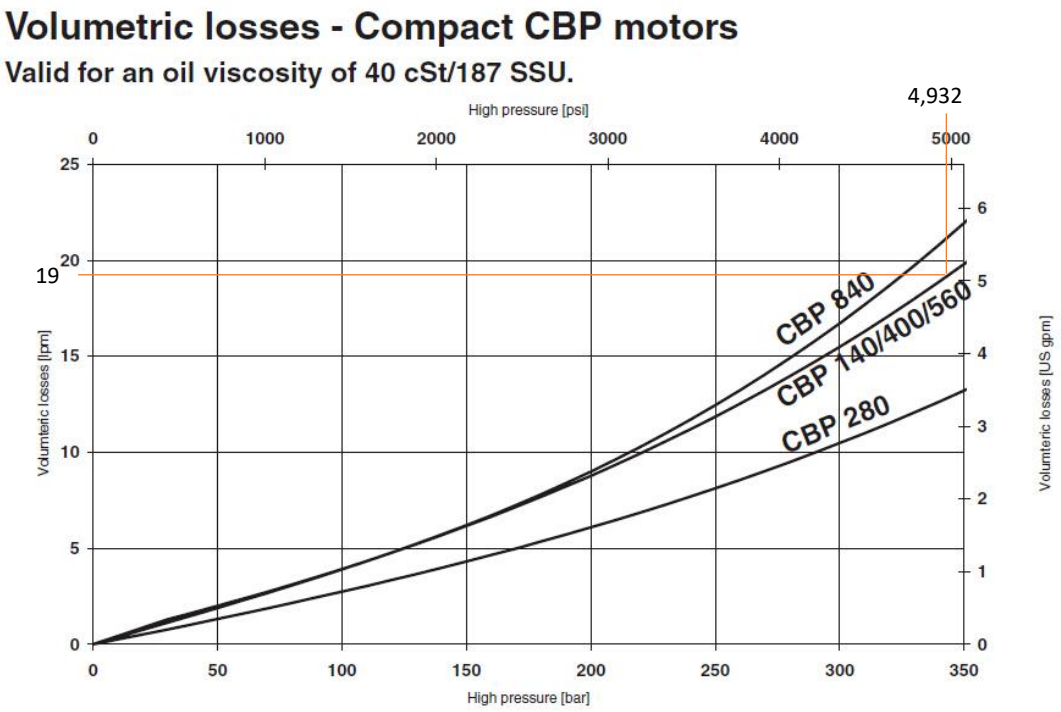

Figure 3-7 Fluid loss profile of the hydraulic motor (Boschrexroth.com. 2014)

From Figure 3-7, the fluid loss of the motor at a required pressure (340 bar) is approximately 19 l/min.

The flow rate required by the motor:

$$q = \frac{n \cdot V_i}{1000} + q_l = \frac{120 \times 20{,}100}{1000} + 19 = 2{,}431\ l/min = 0.04\ m^3/s$$

Because there are two turbine-pump units, the total flow in each division will be half of the total flow rate. The required flow rate for each pump is 0.02 m^3/s

3.4.2 Calculations of Pipes, connection and hoses

A detailed calculation is shown in Appendix I.

3.5 Results

This section will discuss the results from the calculations, a detailed calculation shown in Appendix I.

3.5.1 Pressure losses in the pipelines

a. Pressure loss due to friction

The pressure losses due to friction in the system's pipeline are shown in Figure 3-8 to 3-10.

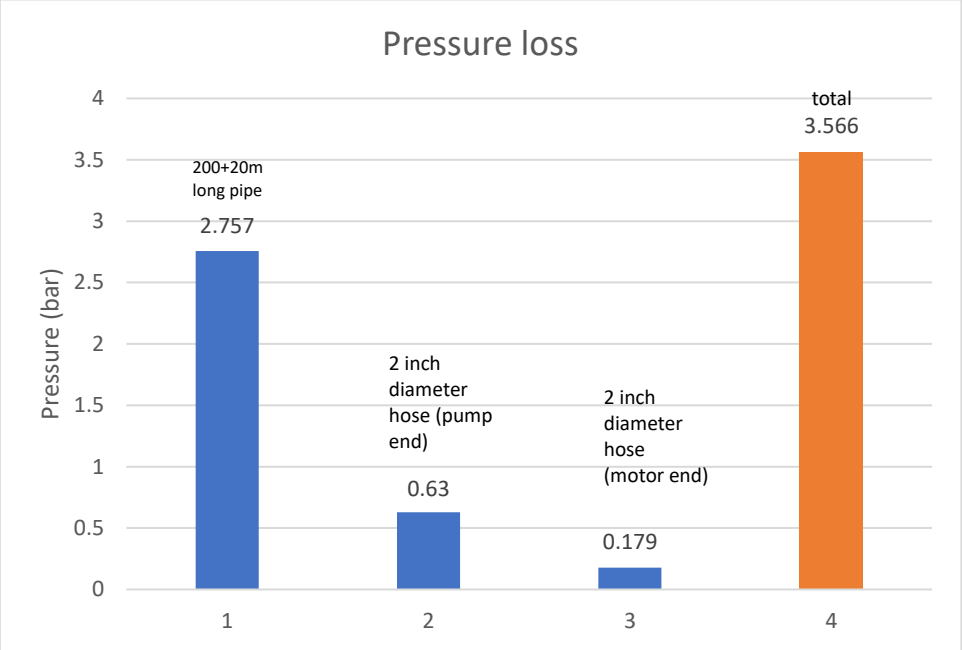

Figure 3-8 Pressure loss in pipes & hoses

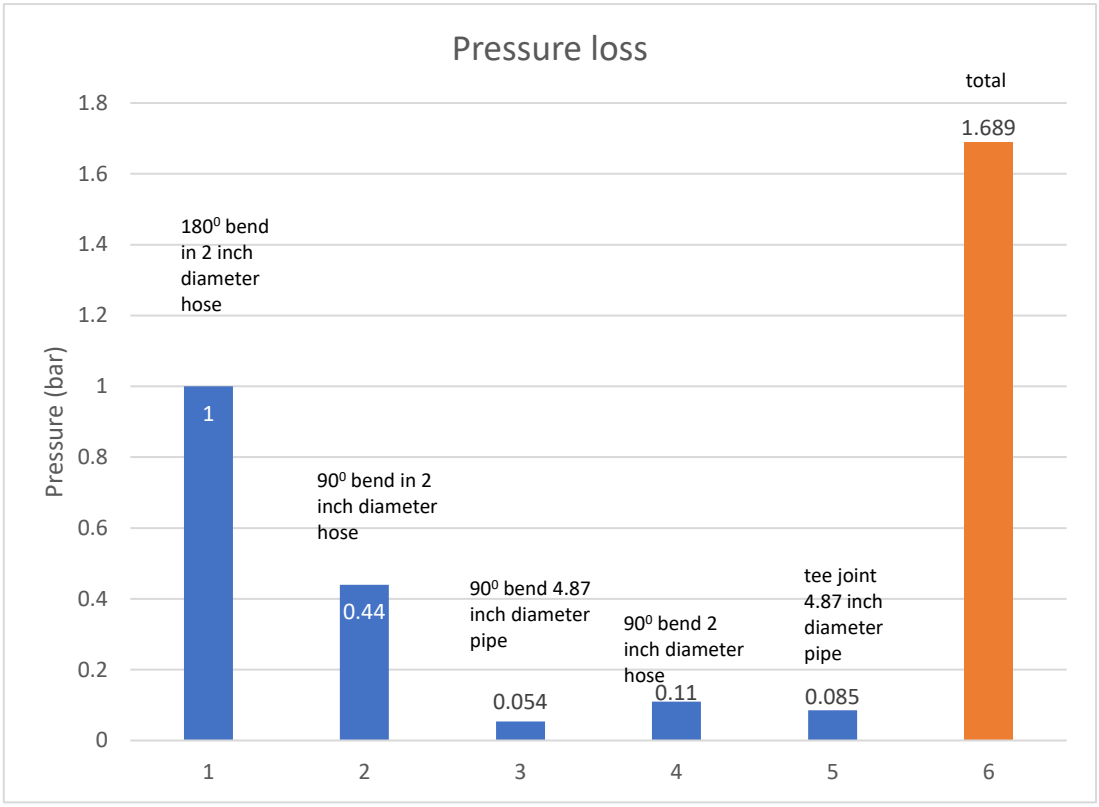

Figure 3-9 Pressure loss in fittings and bends

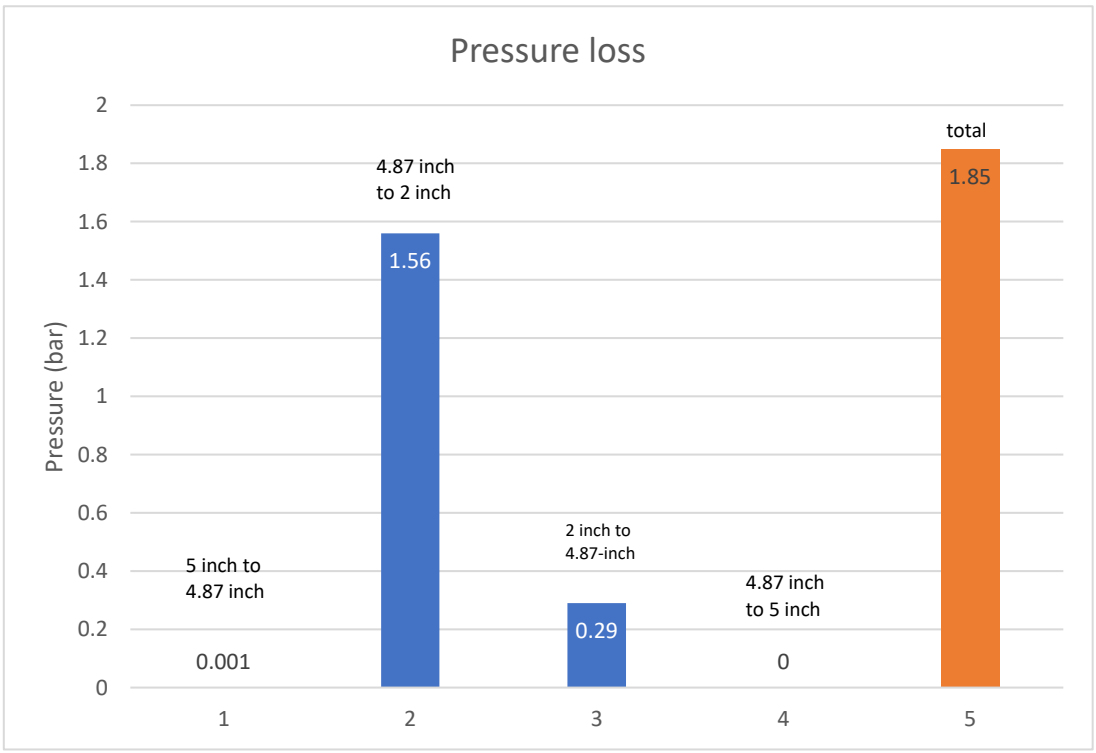

Figure 3-10 Pressure loss during expansion and contraction

b. Pressure loss due to gravity:

As a closed hydraulic loop system is used in this design, the combined pressure changed due to gravity is zero.

Total Pressure loss in the pressure line:

7.965 bar

Total Pressure loss in the return line

6.245 bar

The initial pressure of the return line:

Pressure consumption for power generation:

3.5.2 Hydraulic Motor

From the results in Chapter 3.4.1, the specification of the motor is:

1. Motor output power: 1,250 kW
2. Flow rate required: 2,431 l/min or 0.04 m^3/s
3. Pressure required: 340.15 bar or 4,932 psi

For the hydraulic motor:

$$P = q\Delta p_m \qquad (3\text{-}6)$$

Where P is the motor power, q is the flow rate and Δp_m is the pressure difference to produce power.

Therefore, the pressure difference across the motor is:

$$\Delta p = \frac{P}{q} = \frac{1238.24 \times 1000}{0.04} = 310\ bar$$

The initial pressure p_r at the return line is:

$$p_r = p - \Delta p = 332.1 - 310 = 22.1\ bar$$

The above calculations were made under the assumption of a full power scenario, however, the velocity of the tidal steam changes with time, therefore the motor power for reductions in flow rate must be calculated. Based on these equations, with reduced power output, it has indicated that the initial pressure for the return pipe will increase.

The efficiency of the hydraulic transmission system:

$$\eta_{pressure\_line} = \frac{340 - 7.965}{340} = 97.6\%$$

3.5.3 System efficiency

From the above assumptions, the pump has an efficiency of 90%, the pressure loss in the pipes was given, and the efficiency of the motor can be determined. Therefore, an efficiency distribution of the system can be calculated which is shown in Figure 3-11:

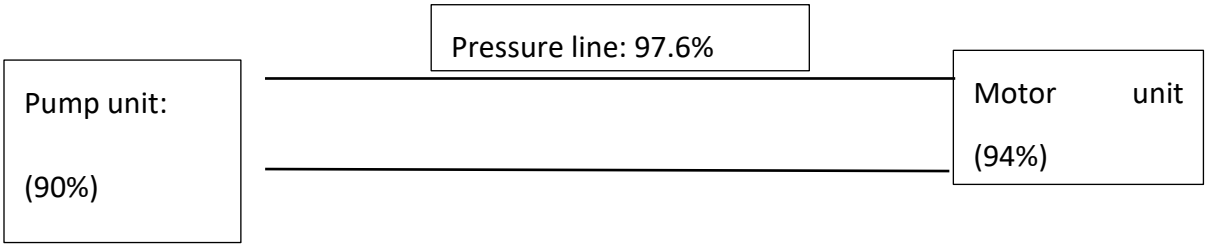

Figure 3-11 Efficiency of the hydraulic system

The total power produced by the hydraulic motor is 1,032.12 kW

The efficiency of the system:

$$\eta = \frac{1032.12}{1250} = 82.57\%$$

Motor power with a reducing flow rate is shown in Figure 3-12.

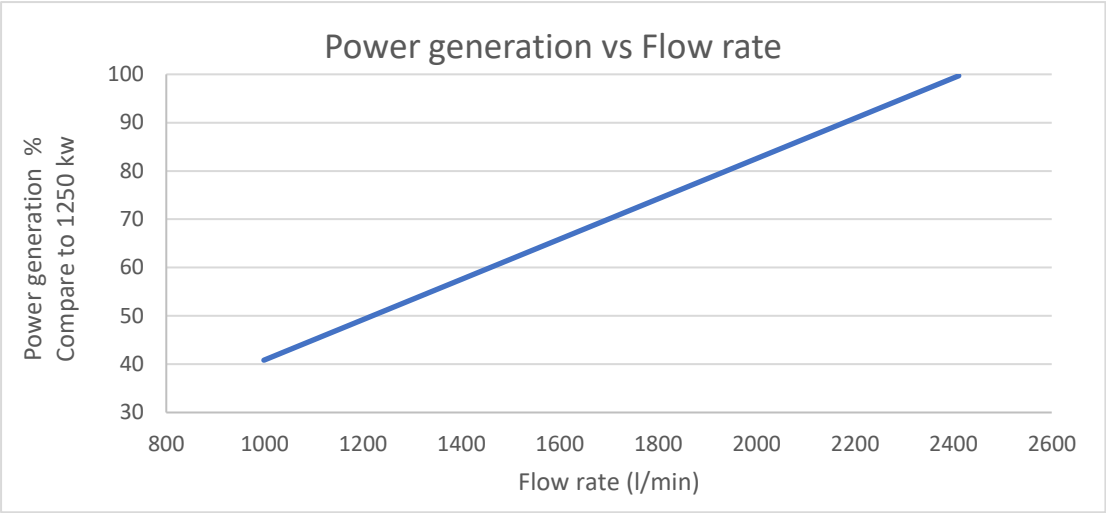

Figure 3-12 The relationship between power generation and flow rate

As shown in Figure 3-12, there is a linear relationship between power generation and flow rate.

A further calculation has been carried out with increased distance to shore, the result shows there is a linear relationship between pressure loss and the pipe distance, with more pressure loss if the length of pipe increases.

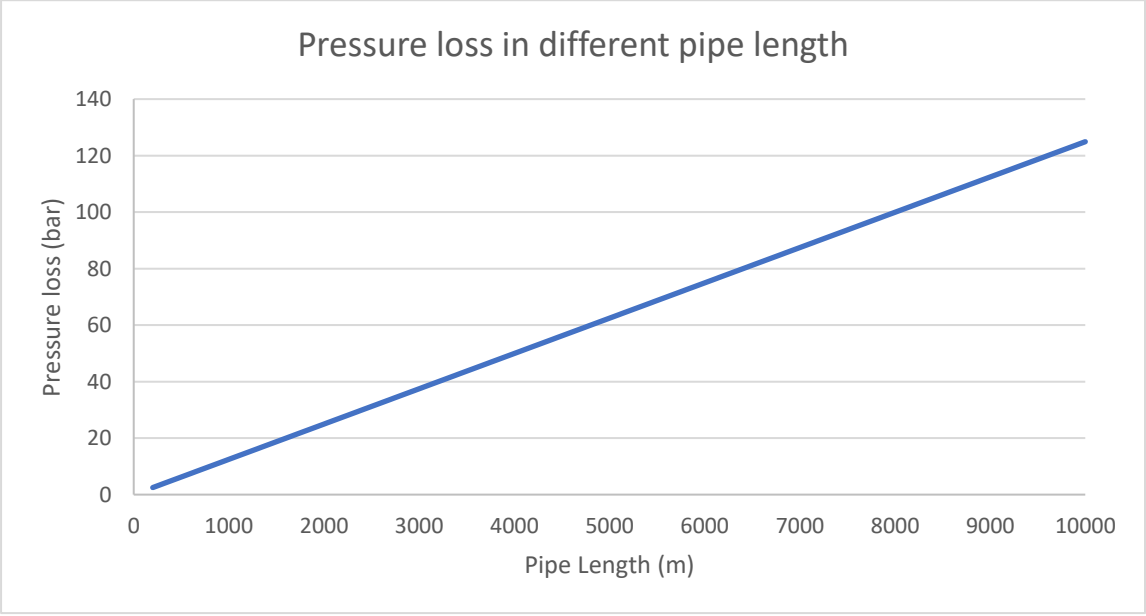

Figure 3-13 Pressure loss vs hydraulic pipe length

From Figure 3-13, it is noted that pressure loss in the pipe is not overly concerning,

due to this system is being deployed under 2000 m from shore. However, the same pressure loss would affect the return line; i.e. to force flow back to the turbine, additional pumps would be used to pressurise the fluid at the shore and to ensure it had enough pressure to overcome the pressure loss in the return pipe.

A study indicated that hydraulic turbines have an overall competitive efficacy against conventional turbines which the results is shown in Figure 3-14.

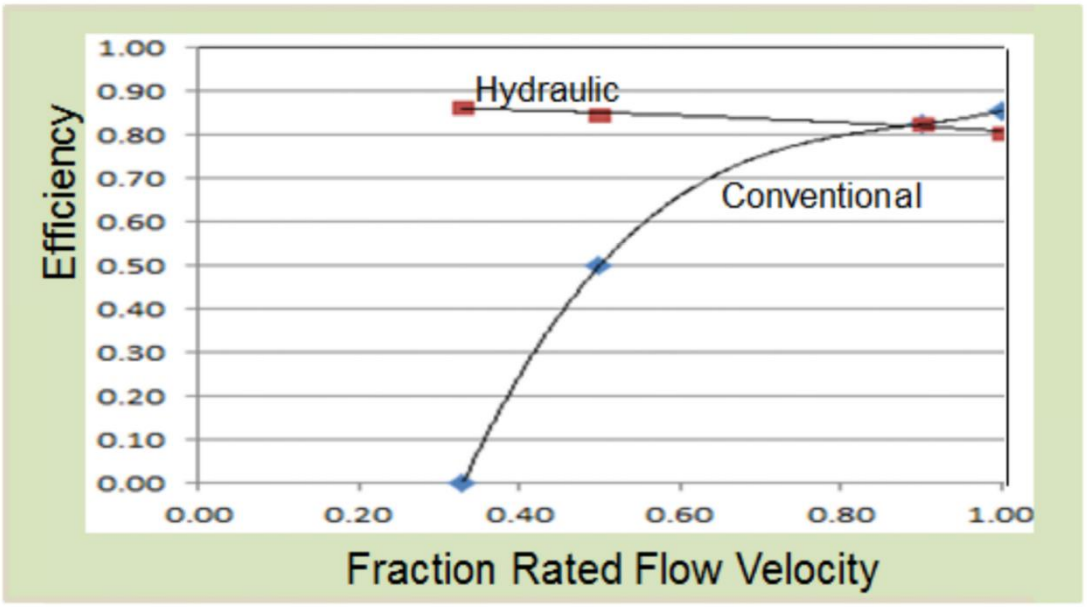

Figure 3-14 Blade to grid efficiency for tidal and wind energy (Jones. 2012)

According to Figure 3-14, at a high rated flow velocity, the conventional electrical unit has a higher efficiency than the hydraulic, but the hydraulic has a consistency in the efficiency range regarding changing flow velocities, particular at lower rated flow velocity in this case. At around 0.35 of rated flow velocity, the hydraulic system can still maintain around 0.86 efficiency, comparing to zero for the conventional system. This is important for tidal devices because tide velocities are not constant. To extract the maximum energy from tides, hydraulic systems would appear to be more advantageous in terms of efficiency.

3.5.4 Hydraulic reliability

The most important factor to increase the reliability of a hydraulic system is the cleanness of the hydraulic oil (Merritt. 1967), if the contaminated oil is used in the system, the service life and performance of the hydraulic components will be reduced significantly. However, in this design, a closed loop hydraulic system is used, and with the oil tank located on shore, which means the accessibility of inspection of the oil cleanness is not a problem.

As there is no specific pump was selected in this design, the detailed information was not available, but from Chapter 3.2, the life of a swash plate pump can last around 5 years, and it is believed with the development of the technology, that life will be expanded with the newer model.

For the hydraulic motor, the Hagglunds Compact CBP motor 400-320 does not specify the service life. However, according to the user manual, the manufacturer suggests a oil filter changes for every six months, as in this design, the motor is located on shore, which means the accessibility will not be a problem.

3.5.5 Total volume of hydraulic oil

From the results, the total amount of hydraulic oil required in the pipeline is: 5.15 m^3 (5,150 l), with the density of 870 kg/m^3, the total weight is 4,480 kg. Furthermore, the on-shore oil reservoir need storage more fluid than the total amount used in the hydraulic system. 8 m^3 (8,000 l) fluid is assumed to be used in total for this hydraulic system.

3.6 Cost Estimates

Modern technology needs to be practical and economical. In previous sections, the practicalities of this system were introduced, in this section, cost estimates will be performed based on available information and facts.

The tower structure of the SeaGen remains the same. Therefore, the main focus of the cost estimate will be on the pipeline.

The pipe manufacturer quoted a price of £142,600 for 400 m in an email in 2014. For most offshore oil and gas pipelines, a protection method called concrete weight coating is used. This technology uses thick concrete to cover the pipeline to prevent damage to the outside. However, after consulting with many concrete coating companies, the answer for coating for the selected pipe was unavailable, due to the size and distance of the pipe. After further research, a protection method called concrete mattress appeared to be suitable for the needs. A concrete mattress is a net with concrete blocks on it which is shown in Figure 3-15.

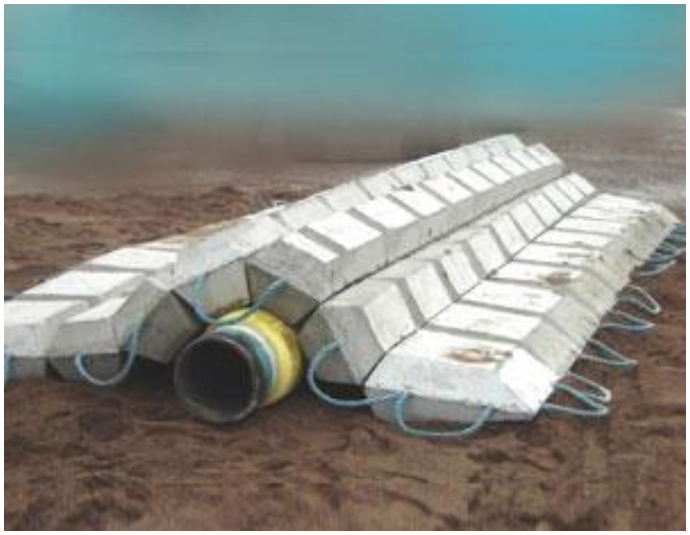

Figure 3-15 Concrete Mattress (Image source: Subseaprotectionsystems.co.uk)

The mattress lies on top of the pipeline, protecting it from outside damage. A British company called SPS provided a quote and indicated the minimum cost would be £750 for a 6 m x 3 m mattress. Based on these figures, to cover 200 m x 3 m would cost £25,500. Furthermore, transportation of the pipeline must be considered; from general logistics, costs would be about £10,00 per lorry (with 44 t capacity) per day (driver inclusive). To deliver the pipeline and mattress to the SeaGen site, costs would come in around £15,300 (fuel & ferry costs inclusive).

The biggest uncertainty for the cost estimates were the construction costs. Due to a lack of information on the Subsea pipeline, the only way to predict costs was based on information from land pipelines.

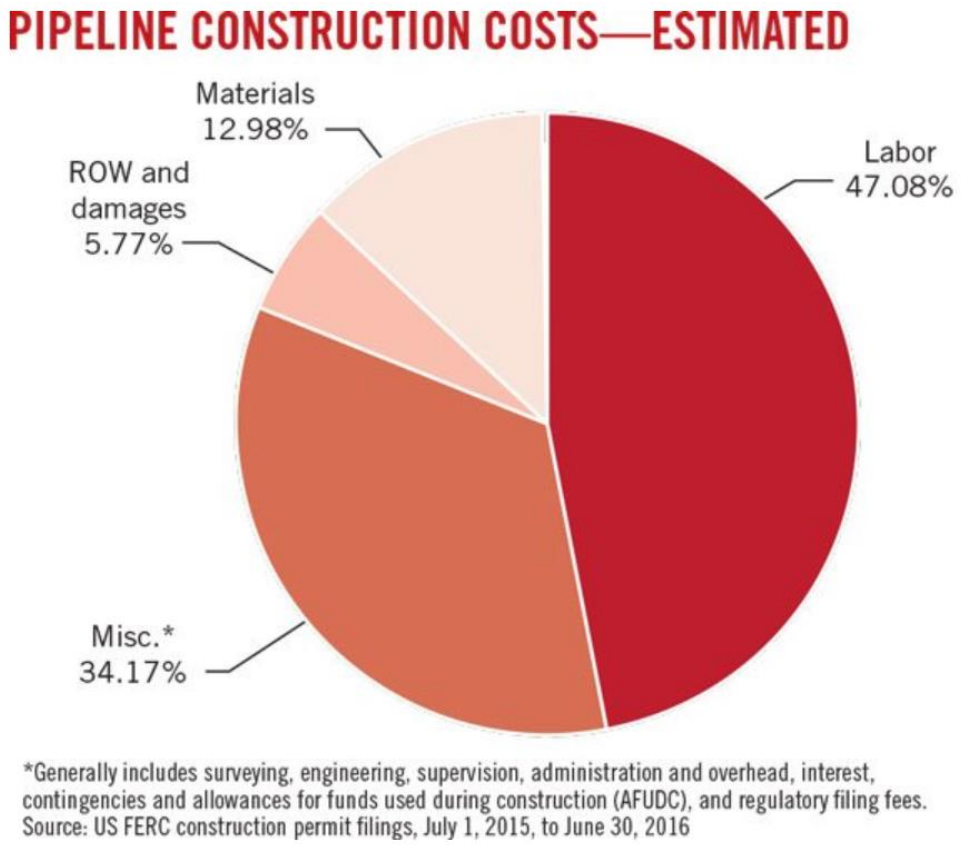

Figure 3-16 Pipeline construction cost drivers (Smith. 2016)

Figures 3-16 shows the cost drivers for onshore oil pipelines which suggests that 47.08 % of the construction costs are Labour, which is the biggest factor in the overall cost. Materials only contributed at 12.98 % of overall cost, and the cost of ROW which means right-of-way, which is a right to make way over a piece of land, which in this case, contributing about 8% of the total cost.

However, for offshore pipelines, the construction costs would be much higher due to harsh working environments, additional specialised tools and environmental protection methods. Therefore, the actual price could be five times more than the onshore pipeline.

The price of shut-down valves was unknown, several valve companies were contacted, but none replied.

To conclude, the initial costs of the Subsea hydraulic pipeline are shown in Table 3-2. These values were using Figure 3-16 as a baseline.

Table 3-2 Cost estimates of the single unit Subsea hydraulic pipeline

Component:	**Price:**
Stainless steel pipe	£ 142,000
Concrete mattress	£ 25,500
Logistics (to SeaGen site)	£ 15,300
Labour	£ 605,600
ROW	£ 743,400
Misc	£ 438,100
Total:	£ 1,969,900

The installation of the pipeline would require specific vessels which would lead to extra costs. For this design, two pipelines would need to be installed to ensure the function of the hydraulic loop. Different strategies for different pipe sizes are also required during installation. For a large-diameter pipe, additional excavation costs might be required for the pipe. This would be difficult to perform for underwater environments, which raises another question, if excavation costs are enormous, would it be more economical to use a single or multiple small diameter pipes that might reduce performance, but would also reduce installation costs. Therefore, calculations were performed to identify a pipe size that would balance costs and performances, in this case, the cost of pipe was assumed to be proportional to its size.

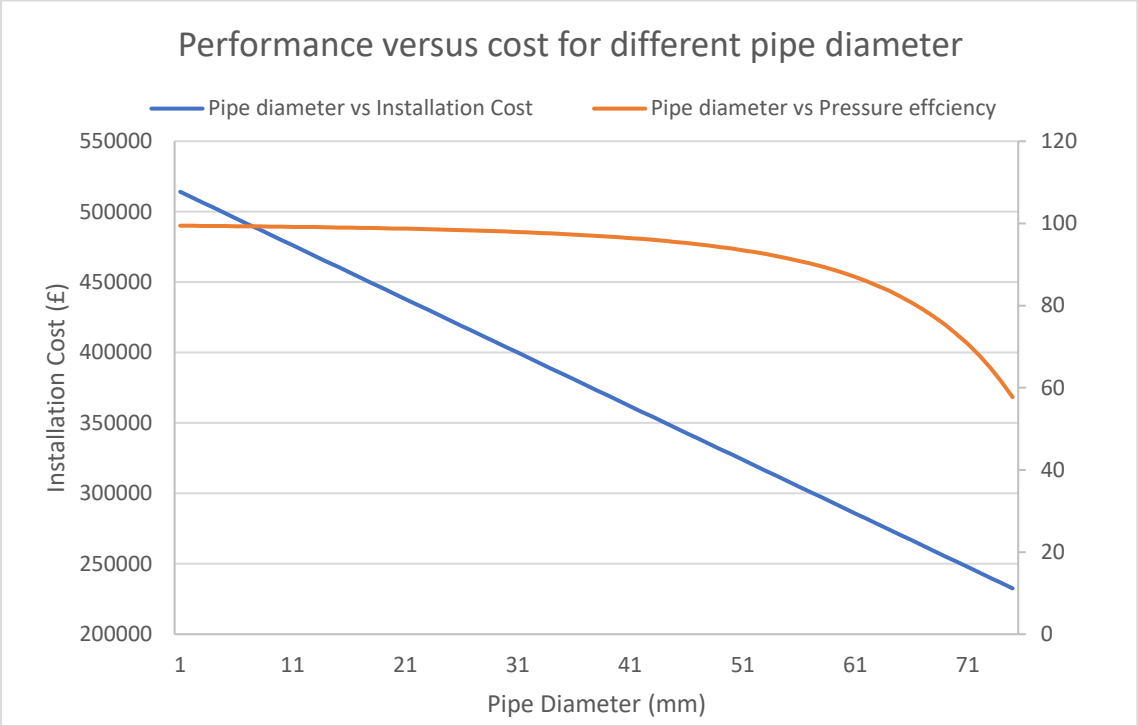

Figure 3-17 Performance vs cost for different pipe diameters

According to Figure 3-17, there was a 10% performance difference for pipe diameters between 68 mm and 124 mm. However, installation costs based on the previous method yielded differences from £515,100 to £300,000, which in percentage terms, equated to an installation price for 68 mm pipe which would cost about 58% of the 124.38 mm pipe with 10% less efficiency. In addition, the pressure efficiency of this figure has not included the pressure loss in the fittings and valves in the rest of the system. The installation cost is carried out based on Figure 3-17, meaning this may not be very accurate, but that indicates that in some circumstances, when it is reasonable to reduce the cost of the system by using a smaller size of pipe, which would not reduce the pressure efficiency in the pipe significantly.

3.7 Discussion

It was noticed that the pressure drop is crucial with the high flow velocity; when compared with the pressure drop across the 200 m main pipeline is 2.5 bar, in the bend of the flexible hose is 1 bar, the largest pressure drop in occurred in the area

contraction where return flow is delivered from pipe back to pump via hose.

However, due to unknown variables in this design, many of the calculations were based on assumed values. The results were not 100% accurate. However, some positive points were noted; pressure drops in the fittings, bends and area changes are key primary designs, especially for a high flow rate system where pressure loss in these areas are considerably larger, when compared with longer distance pipelines.

Some factors used in calculations were assumptions. Due to interconnections in the system, it was difficult to determine the actual data using hand calculations. Like the pressure losses in 1 to 4 split joints, the coupling is not shown in the report. The reason is the joint; it is a special fitting that needed to be customised. There is no information on pressure loss in the similar products due to calculations were not completed. For the coupling, due to a lack of information and background knowledge, the pressure loss was not determined. Further study is required to determine actual losses in each component, to fully investigate this design.

This design suggests using the swash plate pump, the pressure of the pump can remain constant during variable tide velocities; the pump is the only component operating under water, which comparing to the conventional design, which requires both gearbox and generator installed in the tidal turbine, the hydraulic turbine design features fewer components in the water. In addition, by produce flow with a constant pressure, the motor power is linear with the flow rate, and the prediction of the power output is not complicated.

Installation of the pipeline requires specific vessels, leading to extra costs. For this design, two pipelines must be installed to ensure the full functionality of the hydraulic loop. Different strategies for different pipe size are required during the installation, e.g. for a large-diameter pipe, additional excavation may be required, making it difficult to perform in an underwater environment. This raises another question, if the cost of excavation is enormous, would it be more economical to use a single or

multiple small-diameter pipes, reducing the performance, but also reducing installation costs.

Viscosity is another factor that has not yet been considered thoroughly. In the calculations, it was assumed that the viscosity of the fluid is constant, but in real situations, the viscosity can be variable. The fluid has a high temperature in the pump and motor end and has a low temperature in the main pipe line. Moreover, hydraulic oil was the hydraulic fluid in this design and has been widely used as a hydraulic fluid in many hydraulic applications. The potential problems with oil based hydraulic fluids are leakage issues; if there is a leakage problem in the circuit, the surrounding environment will be damaged.

Another problem for this design was the different working condition of the system. Most of the fittings, pipes and hoses are primarily designed for working under normal atmospheric conditions; the underwater environment is totally unlike this atmosphere, all components would have to operate under high water pressure and be rust-resistant. These parts would need to be specially designed for this purpose. The layout of pipe connections must also be considered, as turbulence will occur at each connection. Similarly, the distance between connections needs to be considered also.

3.8 Chapter Summary

The main reason for using a hydraulic transmission is to provide a reliable system that does not require maintenance as regular as the electrical system due to its simpler design at the turbine end. Another reason is that the energy production system is located on-shore, which would provide good access for inspection and maintenance. From calculations, the hydraulic energy transmission line has a total efficacy of 82.9 %. However, pressure losses were significantly larger in bends, fittings and area changes, when compared to 1 bar in a single bend. For a 200 m pipeline, the pressure loss is 2.5 bar. In a straight line pipe, the diameter of the pipe is considerably larger than the

flexible hoses due to the flow velocity is much slower than the one in the flexible hoses. Furthermore, roughness in the stainless steel pipe (the main pipeline) is smaller than the rubber based wire reinforced flexible hose, these factors explain the reasons for pressure loss differences. Moreover, calculations have shown that in hydraulic system design, to reduce the pressure loss in the system, it is necessary to reduce the number of bends and flexible hoses. There is also a need to reduce contraction and expansion areas.

The other issue for this design is the installation of the pipeline. The laying of 200 m of pipes, under the sea, is a massive job. However, considering cables of the electrical have a similar diameter to the stainless-steel pipe, they must be restrained on the seabed. The difference here is that the electrical cable can bend and twist but the steel pipe cannot, and there is an additional pipeline needing to be installed for the return flow.

A major concern of this design is environmental issues. With 4,480 kg of hydraulic fluid inside the pipeline, if there were a system leakage, the surrounding environment is damaged, as oil is toxic and polluting. Another concern is related to the operating temperature; the viscosity is directly related to the temperature, and for a long transmission distance, the flow in the pipe will be cooled by low sea water temperatures. The lower the temperature, the higher the viscosity and the slower the flow. Such a state would lead to greater drag and greater pressure drop.

To conclude, hydraulics has the potential to transmit energy to replace the electrical cables. In this design, the gearbox of the conventional electrical system was replaced by a hydraulic pump, which enables to move other key components like generator and oil reservoir on shore, to gain a better access for inspection and maintenance. However, further research is required to determine the unknowns (e.g. pressure loss in couplings and customised parts).

The future of this design is not based on an individual device like the current

conventional device, the aim of this design is to create an energy farm, consisting of many turbines, using hydraulic power, so turbines can be connected to a single Subsea hydraulic motor-generator unit, thereby transmitting power to shore, comparing for the tidal stream turbine devices (discussed in Chapter 2.2.1) are designed to work individually, for example, 100 conventional tidal stream turbines would need 100 gearboxes, generators and cables, but the hydraulic system has the potential to be integrated, using one main pipeline and single generator if required. However, there are many challenges in this system design; the greatest is environmental concerns. To prevent leakage into the ocean, additional devices and valves are required by law for installation into the pipeline. This may increase costs and decrease this system's performances.

This design has demonstrated some positive points by using hydraulic power. Initial calculations have shown this design was potentially economical. However, by using the hydraulic system, it raises the concerns of environmental issues. Unlike the conventional cable system, if the cable were damaged in the water, it would not cost too much environmental damage, but if a hydraulic pipe was damaged, there would be issues regards to the hydraulic fluids. Therefore, although this design has shown some positives by using hydraulic systems, the potential problem of the hydraulic fluid damages the environment is too high.

4. Hybrid tidal systems

4.1 Introduction

Tidal energy is generated using the level difference between the two water surfaces; when water passes between a barrage between two surfaces, it drives the water into a turbine, generating electrical energy. However, energy generation is entirely dependent on tidal conditions; a big advantage of tidal energy systems is that tides are highly predictable. This means energy output can be predicted to a degree, for example, Figure 4-1 shows a screenshot of GridWatch, which is a website which shows the on-time status of the UK's grid; the tidal cycle is different each day meaning energy generation times can also vary each day. Therefore, to maximise the potential of current standard tidal systems, an innovative design was proposed. The idea was to use current tidal energy plant structures as a base model. Alone this structure could be used as a power source, but this base model also involved another technology, the marine current turbine. However, unlike many tidal turbine designs, this design featured a pump which replaced the generator. The pump controlled the water levels in the reservoir to achieve an optimum head.

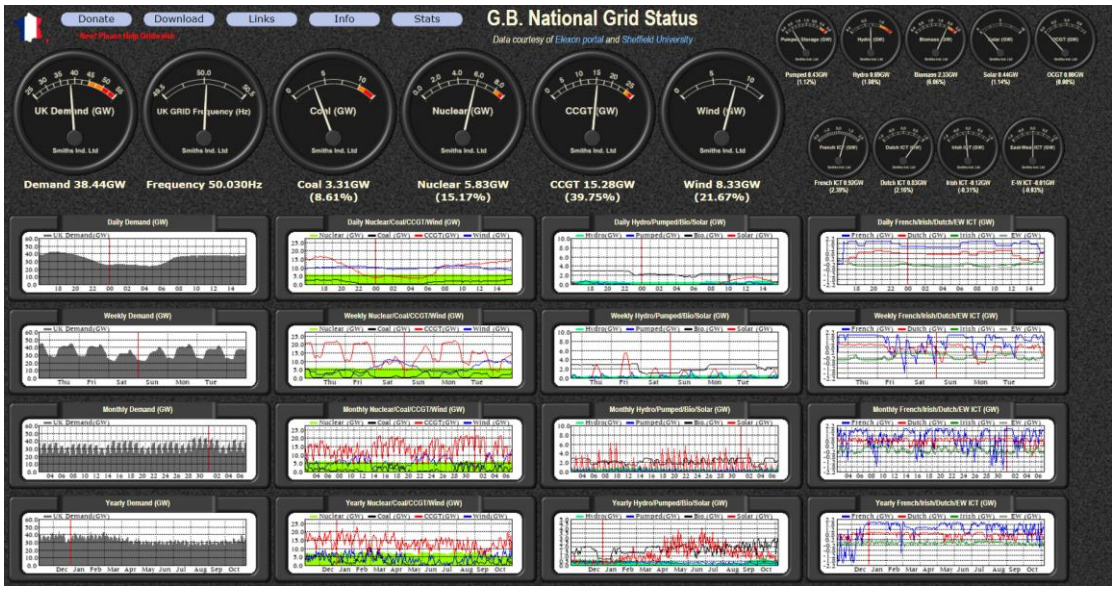

Figure 4-1 UK's national grid status (Image source: GridWatch.co.uk)

4.2 Method

The aim of this research reported in this thesis was to develop a tidal energy system, maximising the extraction of energy from the ocean. The concept was to establish a system which generated electrical energy during tides. However, there was a possibility that generated power could be wasted, because of low power demands in the grid. To focus on this, the thesis introduced a hybrid tidal power concept, consisting of a conventional storage facility, which would harvest excess energy for storage, and release it when required.

Based on current technologies, one method of storing energy from water is to build a reservoir. These systems contain large amounts of water at certain heights. A good example of the application of this method is at hydroelectric power plants, where large dams and reservoirs store a significant amount of potential energy from water.

The design concept was to establish a reservoir which could hold large amounts of water. By placing water turbines at the entrance, energy would be generated during the inward and outward flow of water, similar to technology used in bidirectional tidal power stations. Furthermore, to extract the full potential of the stored power, the head differences between the tide levels and the reservoir levels should achieve design maximum. For this scenario, another technology is required.

In Chapter 2, the benefits and drawbacks of tidal current turbines were discussed. It was stated that the biggest potential problem of the marine turbine was the application of the gearbox, which potentially had high failure possibilities. However, it was possible to bring the concept of tidal current turbines into this system, but not for direct power generation, but to drive seawater pumps. By pumping water from or into the reservoir to maximise the head difference, the benefit would be no electrical power to be consumed for pumping water. Because the marine current turbine was to be driven by tidal currents, it could be operational as long as conditions were met. If potential power needed to be stored, the gates of the reservoir entrance would

close. Therefore, no water would come in or out of the reservoir. This meant the only way to adjust water levels in the reservoir was through the tidal stream turbine-pump unit. Pumping water into the reservoir for a higher level if the tidal level were low, or extracting water from the reservoir for a low level if tidal levels were high. These were the basic design concepts of this design; to build a hybrid tidal energy power system, generating power continuously during the tides, and storing reserved energy, on demand.

After the initial design, like most design procedures, computational analyses were essential. This was to understand the capability of the system, such as maximum power outputs, the operating time of day, the mean power output for a long period, etc. For this proposed system, a numerical model was constructed using Matlab, to provide a first view of the design performance. Matlab was selected because the author had skills in using the software.

The first approach was to build a large lagoon at an optimum location in the sea, to experience the best tidal effects. However, after discussion with supervisors, it was decided to start with an existing construction and to modify it to meet the design criteria. Therefore, docks were chosen for the modifications. This was because the docks could be operated as reservoirs, as the design required. Fortunately, docks were available which could be converted to a power station. As a starting point, Newport Dcoks was used for modelling. Importantly, data were available for the dock, i.e. dock size and tidal profiles near the dock, which could be used for calculations.

The first part of the program was created based on the natural flow basis, without the marine turbine-pump enhancement. The tidal level data was acquired by using a software called Tidal Plotter as shown in Figure 4-2, which provides the accurate tidal level at the desired location.

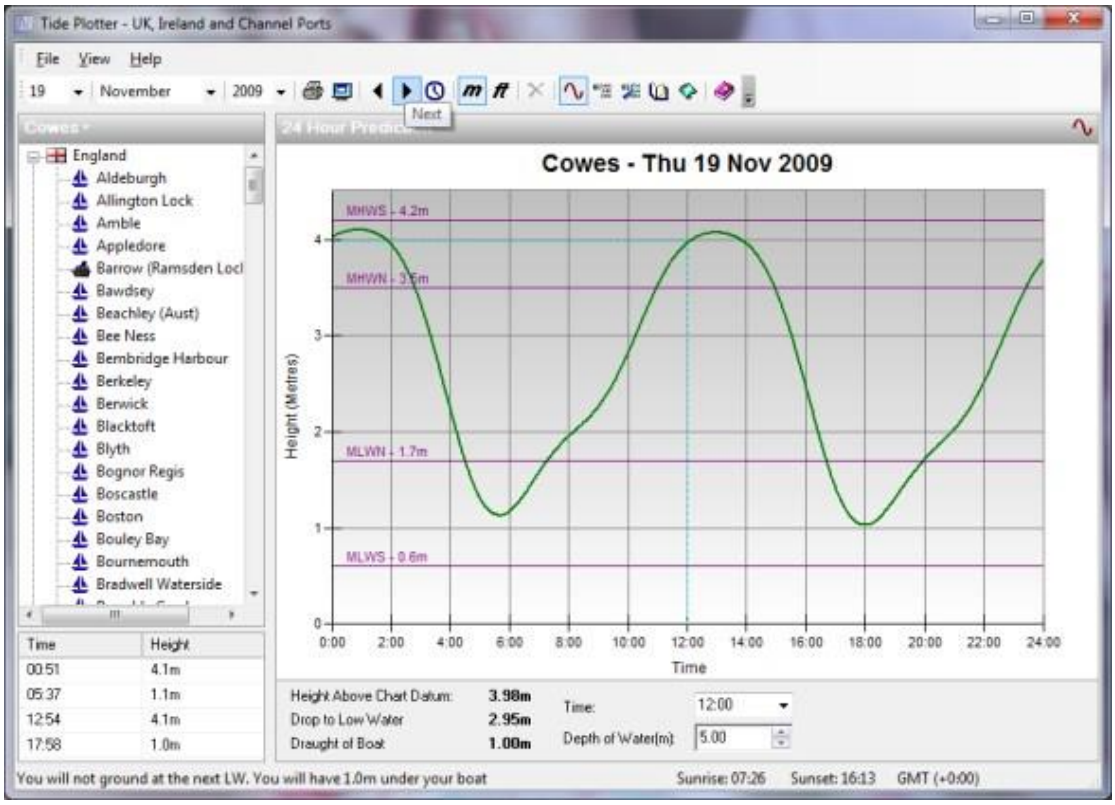

Figure 4-2 Tidal Plotter (Image Source: Chartsandtides.co.uk)

By reading input files, the software generates a tidal level for every second were stored in Microsoft Excel files; the program would calculate the generated power, the dock level. Furthermore, the information for some components used was difficult to get, for example, the characterises of a water turbine, guide vane and generators, therefore, some values used in this software were set to a chosen value, but could be replaced if a realistic value is provided.

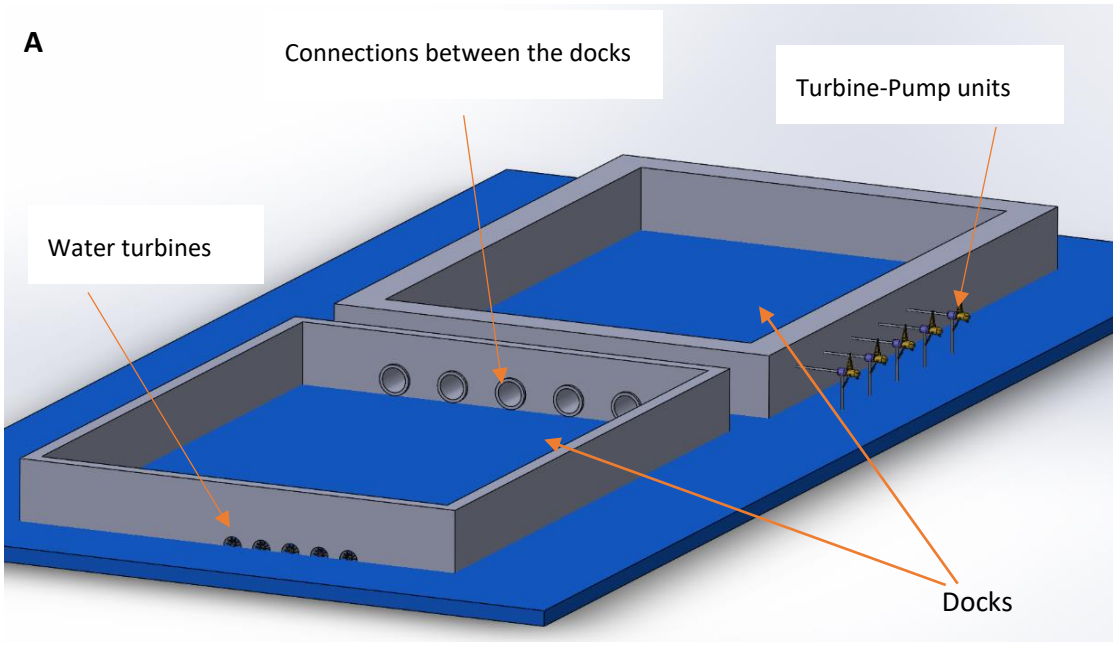
A
Connections between the docks
Turbine-Pump units
Water turbines
Docks

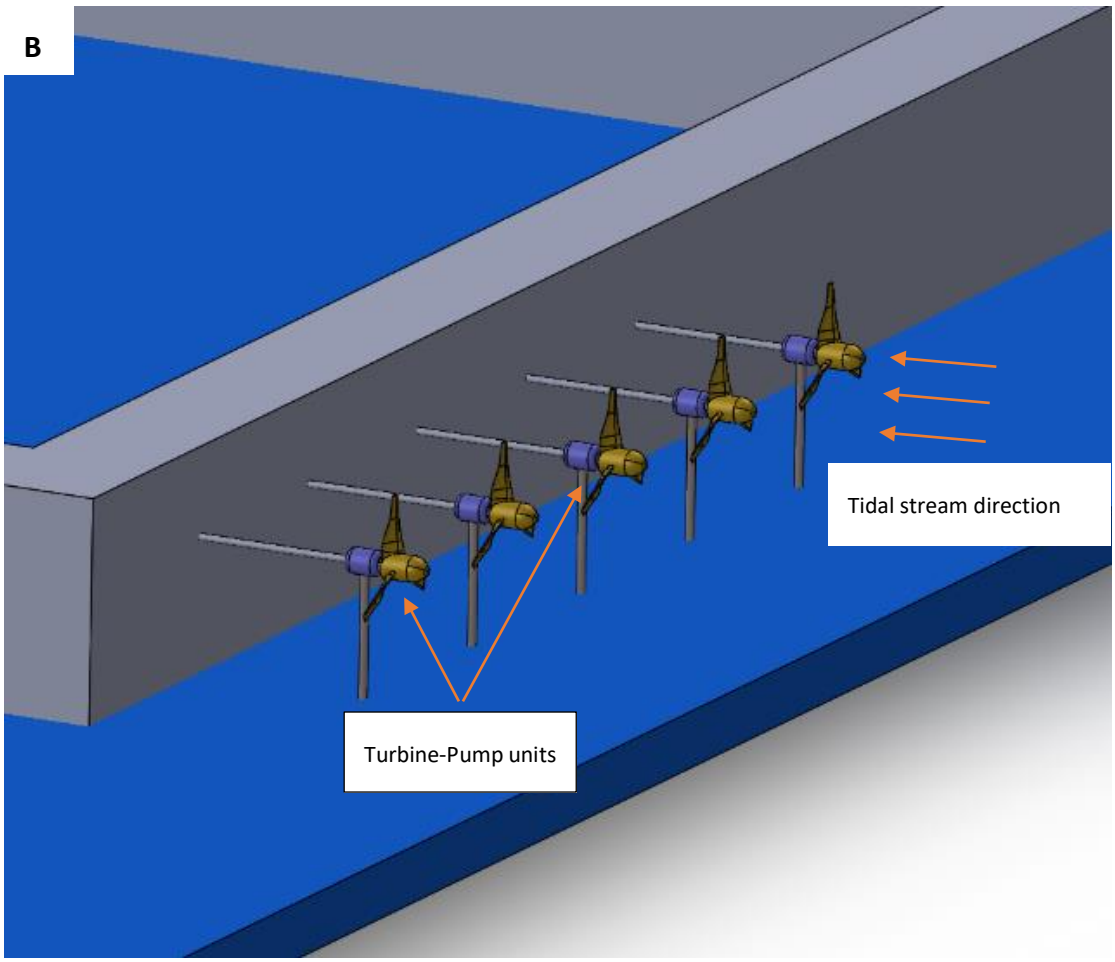
B
Tidal stream direction
Turbine-Pump units

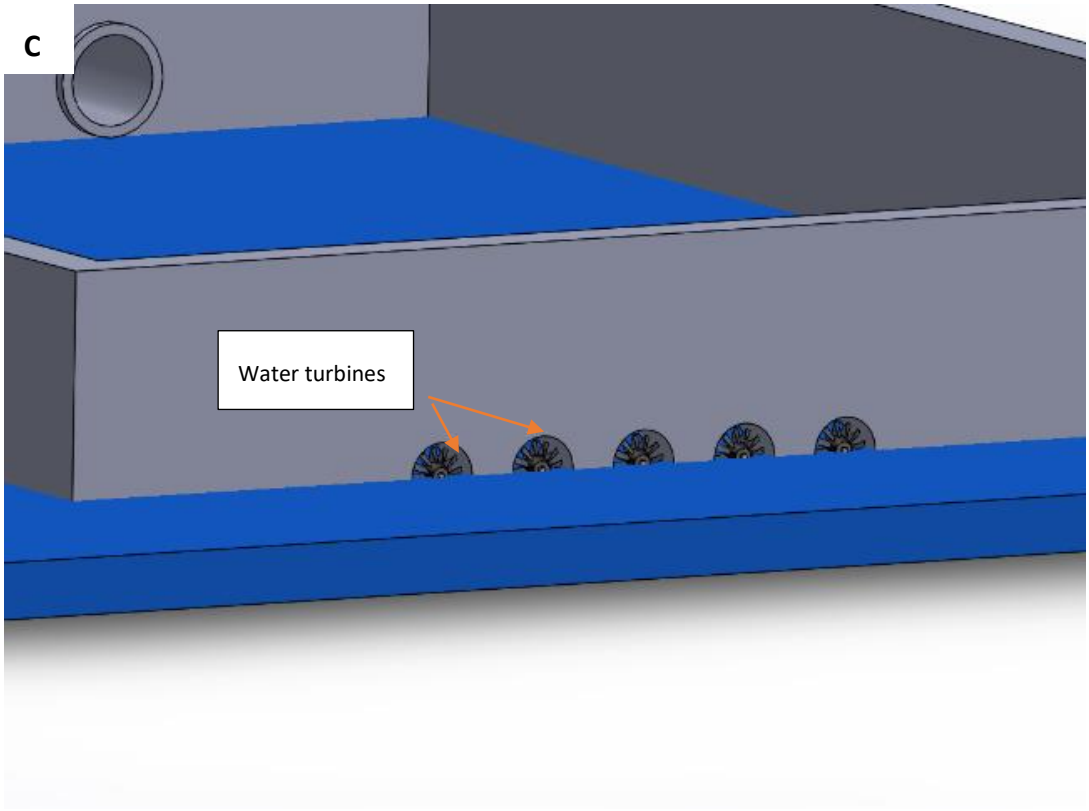

Figure 4-3 Design of the hybrid Tidal system

The conceptual design of this hybrid Tidal system is shown in Figure 4-3. In this example, there are two docks which are connected via pipes, the docks would be used as the reservoir of the conventional tidal energy system. The water turbines are installed to generate electric energy during both ebb and flood tides as shown in Figure 4-3 C. The additional hybrid part which consists of a design that involves using pumps which are powered by tidal stream turbines that connected to the reservoir which is shown in Figure 4-3 B, allowing adjusting water level inside the reservoir. Furthermore, the location of the turbine-pump components in Figure 4-3B is for illustration, the actual location of the unit will be determined varies at different locations.

The program uses a function which can update the dock level; it calculates the power more accurately. During the ebb, when the dock level is greater than the tidal level, the water in the dock will flow into the sea naturally. This enables the water turbine

to generate power. By using the difference in water levels between these two values, an effective head can be calculated, which will be used to calculate the power generated during the ebb. This is generally how this system was designed, by producing power at two different tidal scenarios, with seawater passing through to the dock and leaving the dock naturally.

The flow diagram in Figure 4-4 shows how this concept works under flood and ebb tides, during the power generation stages. As the head decreases with the changing tidal level, the pump which is driven by the tidal stream turbine will start adjusting water level in the docks, by pumping water out from the dock in the flood tide and pumping water into the dock in the ebb tide, this action would reduce the decrease rate of the head, and potentially increase the power output.

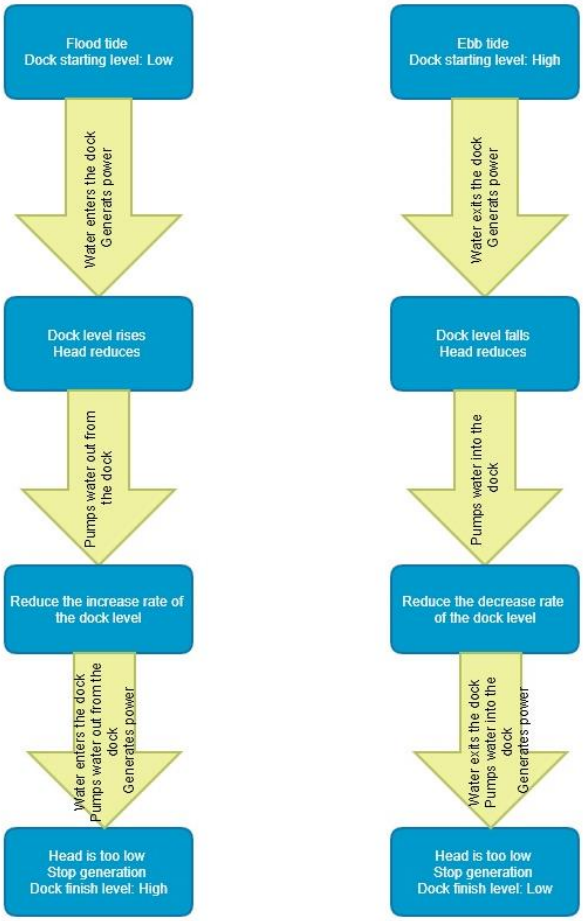

Figure 4-4 Concept of the hybrid system working in the flood tide

For the first stage of modelling, Newport Docks were chosen. This was because the relative tidal information could be accessed and used. However, the following values were assumed: the efficiency of the water turbine, the efficiency of the generator and the size of the inlet gate. Moreover, the head loss across the turbine and the inlet gate have been neglected. Last but not least, as discussed in Chapter 2.4.3, the Jiangxia Tidal Power Station in China features a flow control mechanism, which allows to use guide vane to control the amount of water passing through the turbine, this system is also included in the numerical model.

Figure 4-5 shows Newport Docks which is a combination of two docks which are connected. The water fills the north dock (size 111,075 m^2) and then passes to the south dock (size 420,944 m^2). Which will be specially treated in the modelling. This is because the two docks have different depths; the south dock, filled by water first, has a depth of 10.8 m, whereas the north dock is shallower, with a depth of 8.36 m, a side view of Newport Docks is shown in Figure 4-6. Therefore, the water fills the south dock first. When the dock level reaches 2.44 m (which is the level difference between the two docks), the two docks are filled simultaneously.

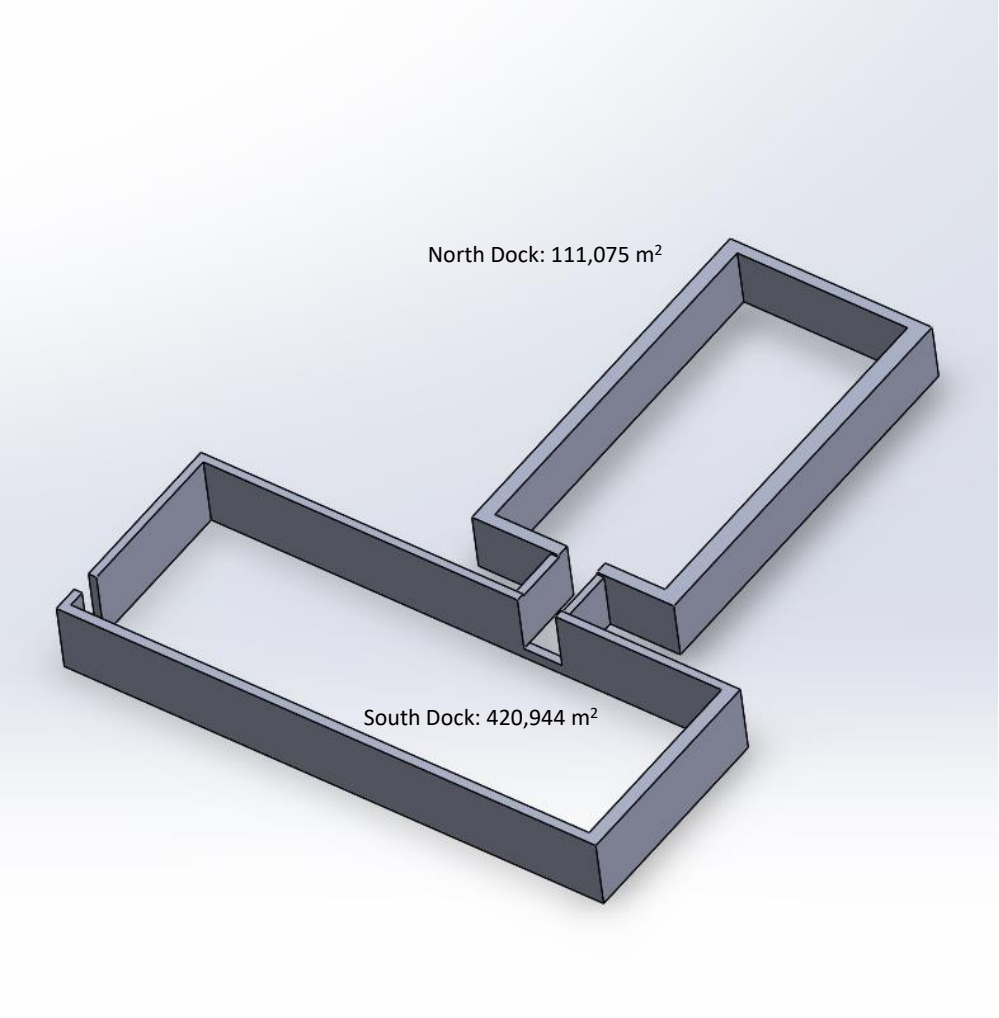

Figure 4-5 Layout and size of Newport Docks

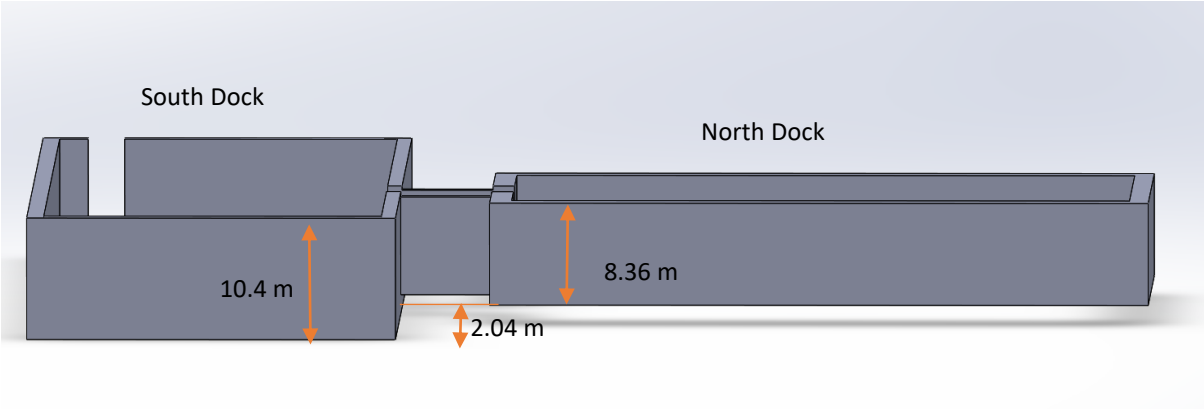

Figure 4-6 Side view of Newport Docks

4.3 Create a model for standard tidal energy system

A numerical model would use Newport Docks as an example to be the reservoir. There are two inputs required, tidal level and tidal stream speed at the site. In this section, a conventional model which does not feature the hybrid part will be discussed first, which would be used as a base line reference, and followed by the hybrid system, the results will be compared and discussed, in addition, the input tidal data and the restraint will be the same for both cases.

4.3.1 Modelling conventional tidal energy system

4.3.1.1 Concept of the numerical model for the conventional system

For a conventional tidal energy system, which is like Jiangxia Tidal Power Station that discussed in Chapter 2.4.3, uses flowing water to spin a water turbine to generate energy. Which can be calculated:

$$P = \rho g \Delta H Q \qquad (4\text{-}1)$$

Where P is the theoretical hydro power in kW, ρ is the fluid density, which in this case, the value for sea water (1,030 kg/m3) is used. ΔH is the head difference between the tidal and dock level, and Q (m^3/s) is the inlet or outlet flow rate depends on the tidal scenario, and g is the gravitational acceleration in m/s^2.

From equation 4-1, the flowrate Q can be calculated:

$$Q = AV \qquad (4\text{-}2)$$

Where A (m^2) is the cross-section area in the penstock in the tidal energy station, and V is the flow speed in m/s.

Where V can be calculated by altering Bernoulli's equation:

$$V = \sqrt{2g\Delta H} \qquad (4\text{-}3)$$

Where flowrate Q can be calculated by using equation 4-2 & 4-3:

$$Q = A \cdot \sqrt{2g\Delta H} \qquad (4\text{-}4)$$

For both cases, the reservoir would have a volume of the total combined volume of both North and South Docks. In addition, a flowrate control was also used in this model with 100 m^3/s limit for both flood and ebb generation.

4.3.1.2 Results from conventional numerical model

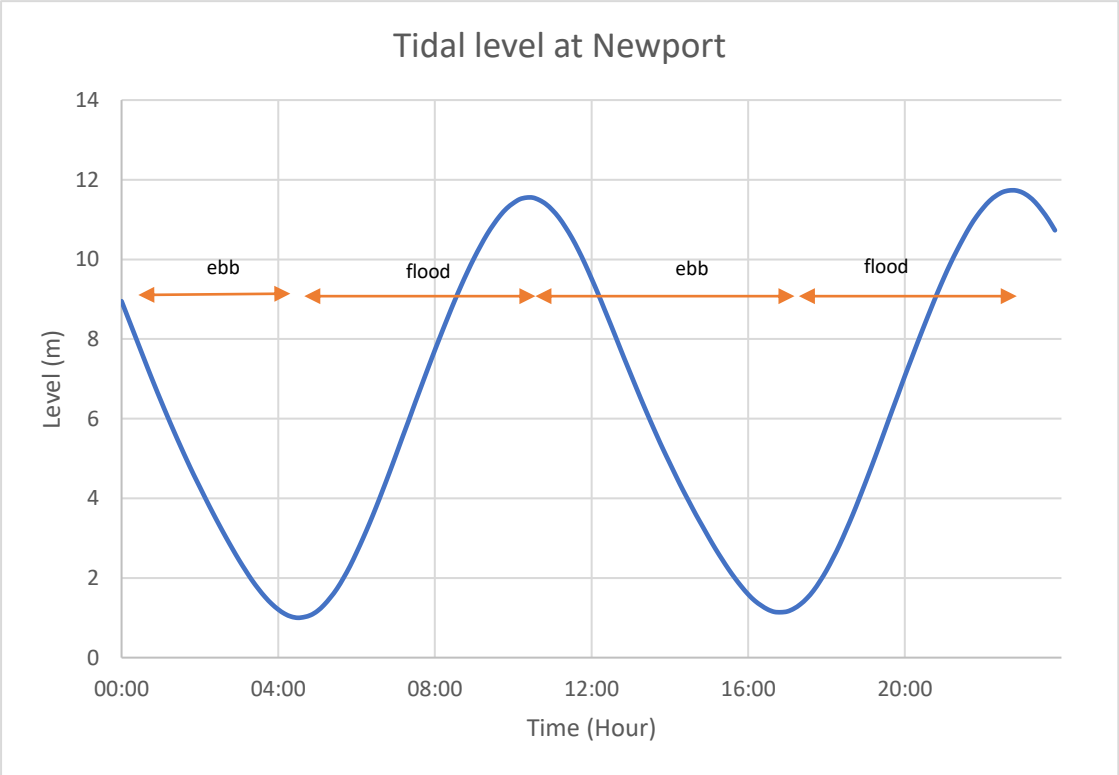

Figure 4-7 Tidal profiles over one day

Figure 4-7 shows a tidal profile for Newport Docks over one day. For this model, the tidal level is the only input file that required.

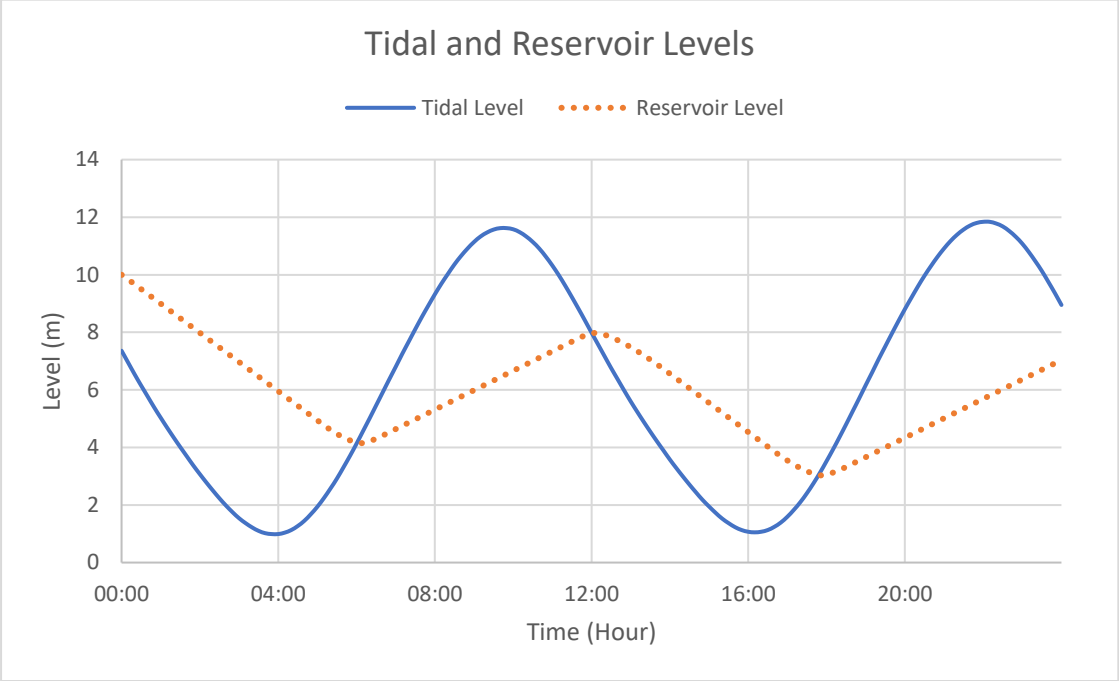

Figure 4-8 Tidal levels and dock levels

Figure 4-8 shows two curves, the solid blue curve uses the same data from Figure 4-7, the tidal level. The dotted curve indicates water levels in the dock during operations. It starts from 10 m because it was set that the dock was full before the operation. Dock levels increase if it is lower than the tide, and it decreases when it is higher than the tide. This indicates that the fill in and fill out method was functioning correctly for this program. Moreover, from Figure 4-8, the changes of the reservoir level look like a liner function, it was due to the flowrate limit of 100 m^3/s setting in the software, the unrestricted values are shown in Figure 4-9, which indicates without the flowrate control, the reservoir would be potentially flooded, and the generation time would be reduced significantly.

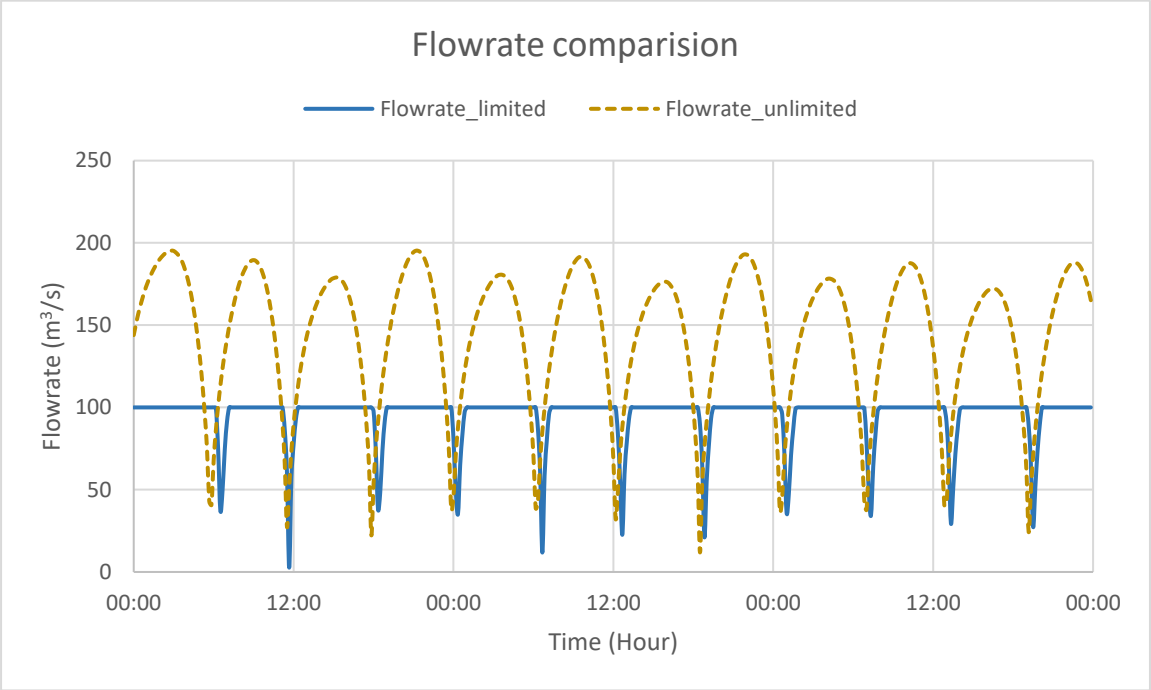

Figure 4-9 Flowrate comparison between two settings (with & without control)

From Figure 4-10, the red dash curve represents the level difference between the tide and the dock. It can be seen that at the points of intersection between the tidal and reservoir level, the level difference was zero, which indicated the concept was correct.

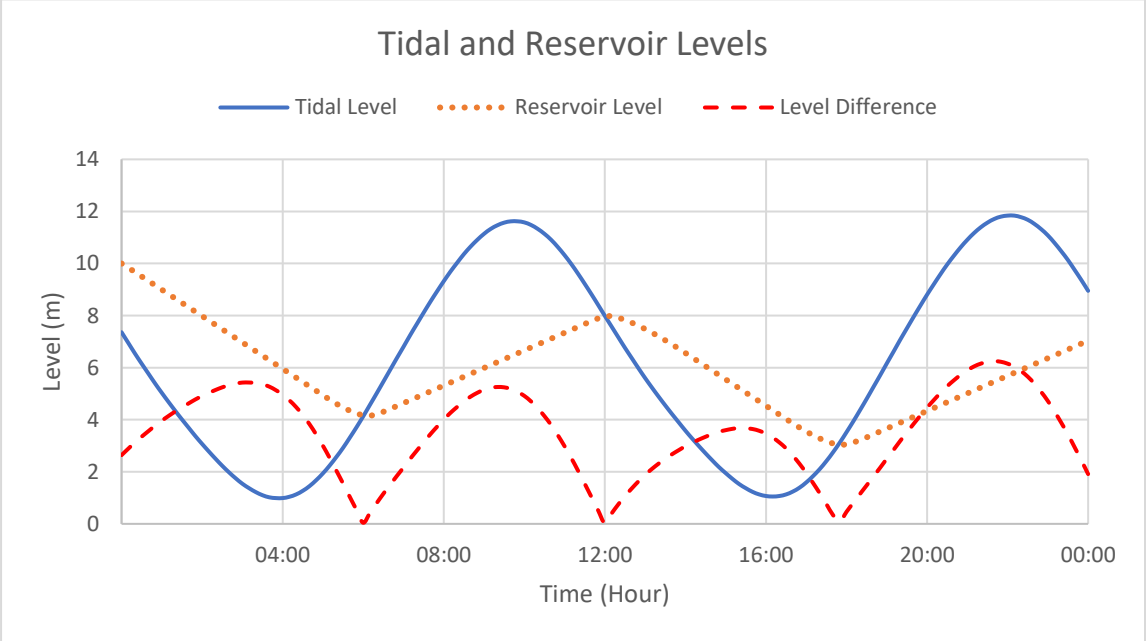

Figure 4-10 Level results

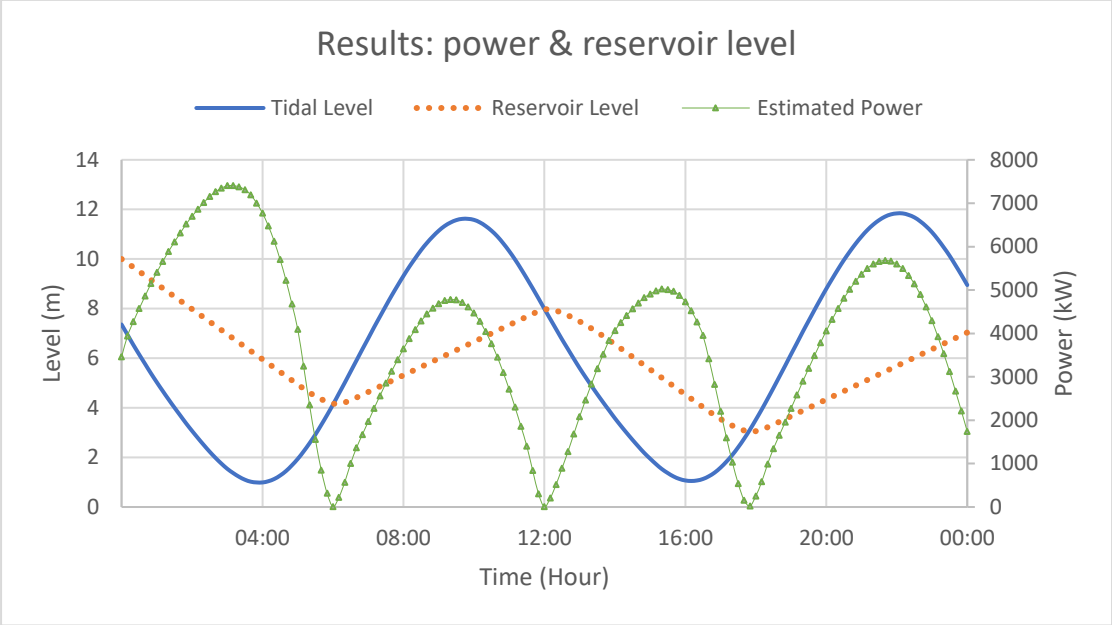

Figure 4-11 The modelling results of the first stage

The final stage the development of this numerical modal is to add power data from the previous calculations. From Figure 4-11, the green curve with triangle markers represents the electrical power output generated by the water turbine. The source of the calculation was the value from the red curve which was the level difference. The highest power output occurred at the biggest level difference, and similarly, no power was generated when the level difference was zero.

The results from this test confirmed the method and concept were behaving correctly. Therefore, the next development would proceed based on this program platform.

4.3.2 Modelling the hybrid tidal energy system

4.3.2.1 Concept of the numerical model for the hybrid tidal system

The next stage of this simulation software was to create the proposed hybrid system with the added pumping component to the conventional system, to enhance the performance of the result from Figure 4-11. The purpose was to use a tidal turbine driven water pump, pumping water to the dock or extracting water to maintain a

reasonable dock level. However, due to missing information on how many turbines can be placed into Newport Docks area, and the actual size of the turbines and pumps, initial values were artificially arrived at. Turbine information was based on MCT's SeaGen as an example. The power of the pump was based on the power of the tidal turbine; as the turbine is used to drive the pump, a similar power output is assumed from the pump, and according to this power, research in the pump manufacturers to seek if this seawater pump is available in the market. By determining the right pump for the design, it was possible to write the code for the additional parts of the modelling program.

The tidal stream speed data was also provided by Tidal Plotter software, which this information would be used to calculate the power output by the tidal stream turbine. As introduced earlier in this chapter, unlike the conventional design to generate electricity directly, a hydraulic pump would be powered which is used to adjust the water level in the dock via a pipe. The turbine-pump system was designed to pump water out of the dock during the flood tide to slow the decrease of head difference, and to pump water into the dock during the ebb tide, for the same purposes. In simplifying this part of the program, the efficiency values for the tidal turbine and the water pump were set at fixed values at 90 %. These values are changed later in the development of the program to improve the accuracy.

The input velocity file read by the program was used to calculate the power of the tidal turbine using the equation 4-5:

$$P_{turbine} = Cp\frac{1}{2}\rho A{V_f}^3 \qquad (4\text{-}5)$$

Where $P_{turbine}$ is the power output from the tidal turbine (kW), ρ is the fluid density in kg/m^3 in this case, the value for sea water at 1030 kg/ m^3 was used, A is the swept area in m^2 of the turbine and V_f is the velocity of the fluid measured in m/s and Cp is the power coefficient which was set to 0.4. Followed by the calculation of the power of the pump, by using the pumping fluid equation 4-6,

$$P_{pump} = \eta Q_{pump} \rho g \Delta H \qquad (4\text{-}6)$$

Where P_{pump} is the pump power (kW), η is the efficiency of the pump which was set to 90%, and Q_{pump} is the pumping flow rate in m^3/s, ρ is the fluid density in kg/m^3, and ΔH is the level difference (m) data which can be accessed from the first part of the program. Because the tidal turbine drives the pump, therefore;

$$P_{turbine} = Cp\frac{1}{2}\rho A {V_f}^3 = \eta Q_{pump} \rho g \Delta H \qquad (4\text{-}7)$$

By altering the equation, the pumping flow rate (Q_pump) (m^3/s) can be calculated:

$$Q_{pump} = \frac{CpA{V_f}^3}{\eta g h} \qquad (4\text{-}8)$$

Then this pump flow rate will attach to the natural flow rate (Q), to form a new flow rate (Q_new). This value will be used to calculate a new dock level and hence, the effective head, shown in the equations below;

$$Q_{new} = Q \pm Q_{pump} \qquad (4\text{-}9)$$

$$H_{Dock_{new}} = \frac{Sum\ (Q_{new}) \cdot Time\ constant}{Dock_{size}} \qquad (4\text{-}10)$$

$$\Delta H_{new} = H - H_{Dock_{new}} \qquad (4\text{-}11)$$

Where *Time constant* is a value based on the data input, $H_{Dock\ new}$ is the new dock level value, and ΔH_{new} is the new effective head (m).

4.3.2.2 Results

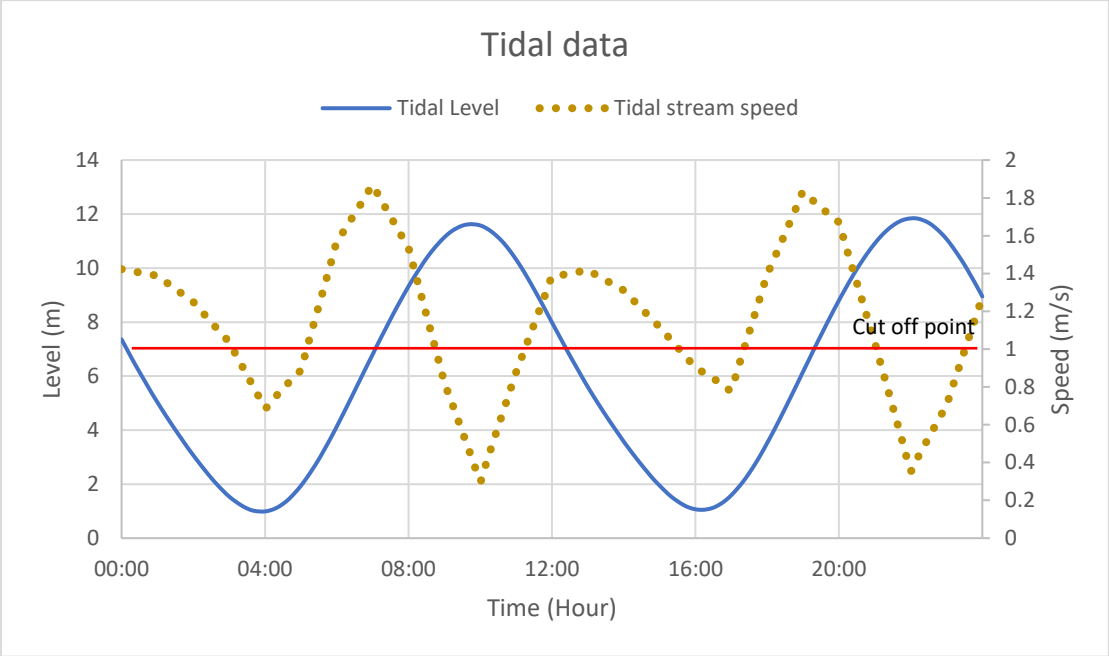

Figure 4-12 Tidal level profile and tidal current profile

Figure 4-12 shows the two input sources, the solid blue line was the same tidal level profile used in the previous test, and the dotted line was the tidal current measured in m/s, used to calculate the power of the marine turbine. Noticeable that the dotted line was not as smooth as the tidal level curve, this was due to the different sample rate provided by Tidal plotter software for tidal level and stream speed, as the rate for tidal level was 144 values per day (one value at 10 mins), but for tidal stream speed was 24 values per day (one value at 1 hour). From Figure 4-12, the highest current speed occurs around in the middle of the flood tide, and when the tides reached the highest level, the current speed was at the slowest. Last but not least, a control method was set for the tidal stream turbine, as shown in Figure 4-12, when tidal stream speed fall below 1 m/s, the tidal stream turbine would be cut off.

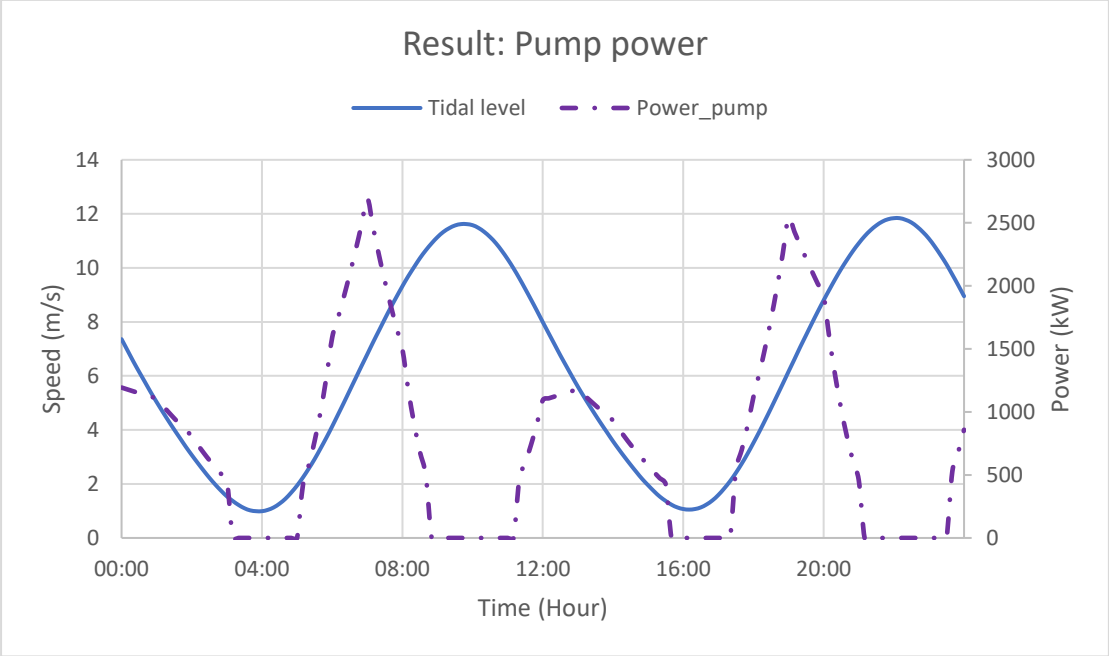

Figure 4-13 Pump power compare with tidal level

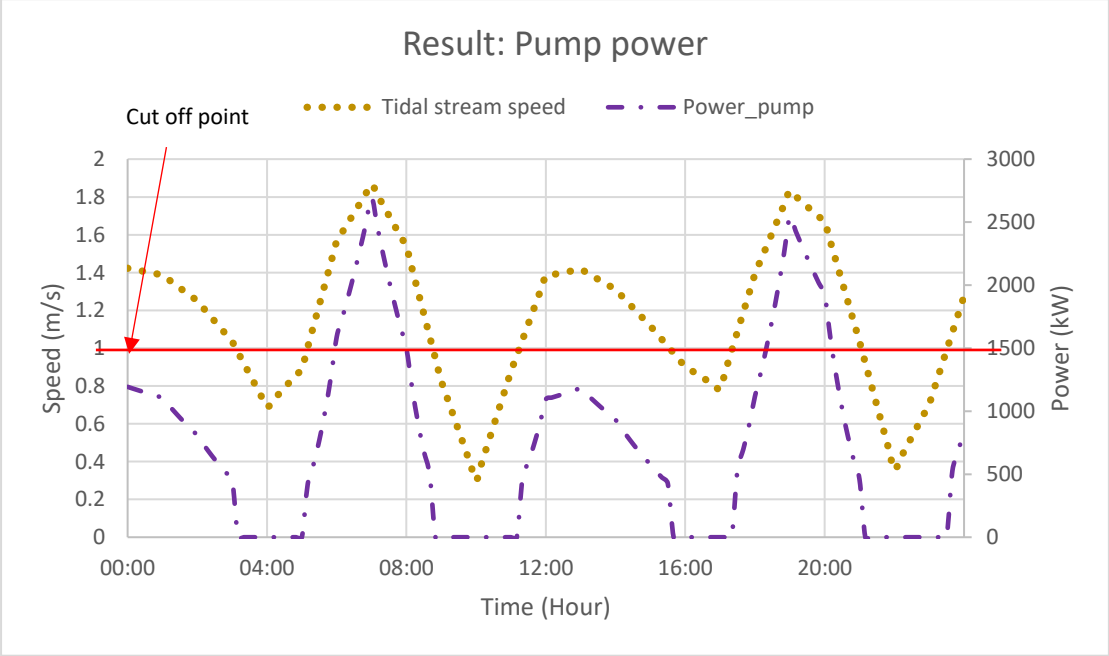

Figure 4-14 Pump power compare with stream speed

Figure 4-13 & 14 shows the power output of the pump which is driven by tidal stream turbine under the tidal condition from Figure 4-12. In this numerical model, a total number of 5 SeaGen liked design of tidal turbines (twin 8-m diameter rotors) are deployed. However, due to the low stream speed, the power output of the tidal

stream turbine was low, with average power of 1,206.5 kW during the operation (does not include down time), with average power of 885 kW during the ebb tide, and 1,527 kW during the flood tide, additionally, the total none-operation time for the tidal stream turbine is 8 hours 10 mins. Furthermore, from the result that shown in Figure 4-14, 39% of the time, the tidal stream speed was below the minimum 1m/s value, which suggests that the tidal condition is not ideal for the tidal stream turbine design like SeaGen.

Figure 4-15 shows the results by using the same 3-day tidal data, the power and energy results were generated from the numerical model for both systems.

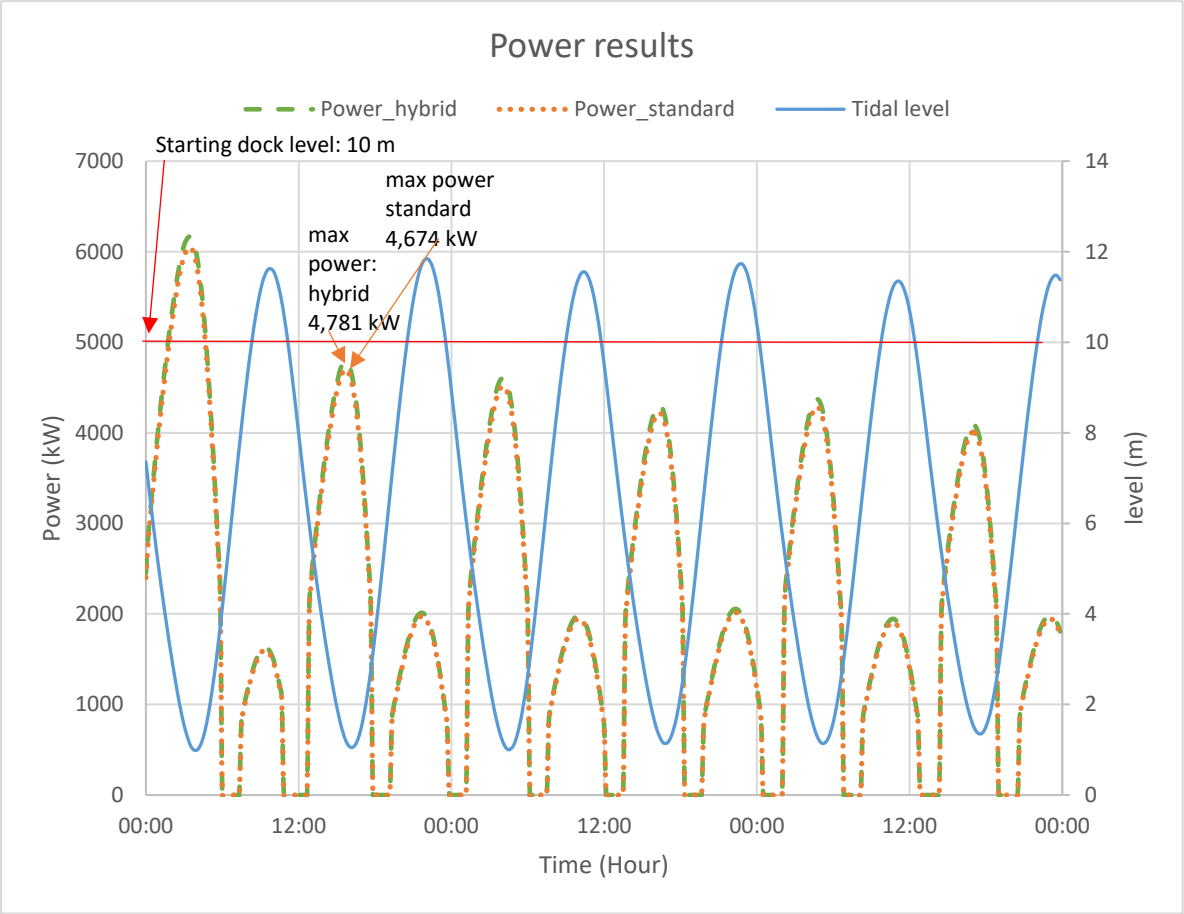

Figure 4-15 Power comparison between these two stages

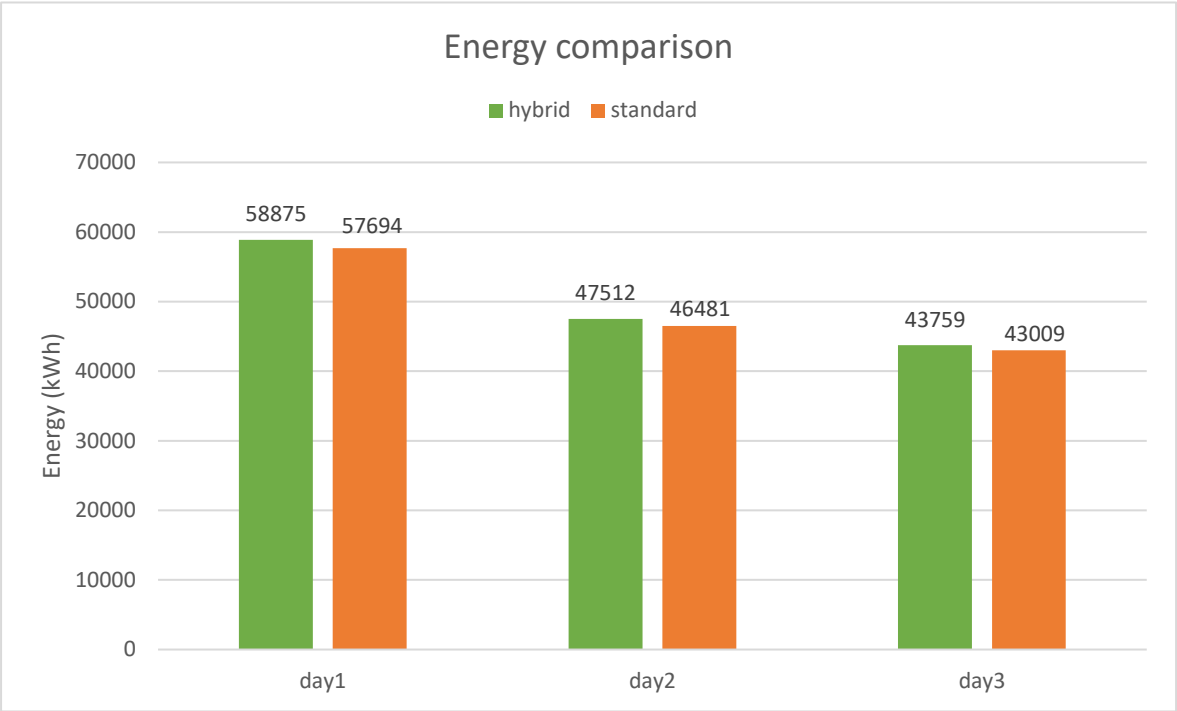

Figure 4-16 Energy comparison between two systems over three days

By comparing the two values from these two stages of modelling, at the starting dock level was set to 10 m as it was assumed that the dock would be full at the start. From Figure 4-15, the power output of the two systems are very similar, with the hybrid system can generate around 2% more peak power than the standard system, this was a result of the low overall power output of the tidal stream turbine. Figure 4-16 shows the total energy generated of the two systems by using the same tidal data from Figure 4-15, the hybrid system could generate around 2% more energy than the standard over the three days (day1: 2.04%, day2: 2.2%, day3: 1.74%). Overall, the amount of extra energy that generated was related to the tidal turbine's power.

4.4 The two-dock interaction method

4.4.1 Aim

The aim was to use one of the docks as the main generation site, and the other to be the power reservoir. In performing this experiment, it was hoped to maximise the power output by shifting tidal conditions. One very fundamental theory related to fluid mechanics is the generation of power requires head differences; when the dock and tidal levels are the same value, there is no head difference and therefore no power output. By using one dock as a power reservoir, when the head difference is below the optimum (the value was set to 4 m in this case), it could be used to adjust water levels in the generation dock to increase or decrease water levels, depending on the tidal conditions.

4.4.2 The design principle

This design proposes a system for marine renewable energy. It uses reliable technologies from tidal-electric systems and tidal turbine systems.

One of the biggest disadvantages of the tidal station is the initial cost, which is too high. To counter this, the idea was to convert these docks into small tidal systems, providing energy to the surrounding areas. However, by introducing this design, another question was raised, how to maximise power generation from a relatively small reservoir (docks) when compared to tidal systems. In the hydroelectric system, power is related to effective head and flow rate passing the turbine. By increasing the head or the flow rate leads to an increase in power output, but a higher flow rate could fill or empty the reservoir quickly, and the system could generate less power in the long term; increased head while maintaining flow rate can increase the power and lengthen the generation time. To achieve this, another feature was introduced into the system. It involved a tidal turbine driven pump to connect to the dock, using power from moving water to adjust water levels inside the reservoir to get an optimum head.

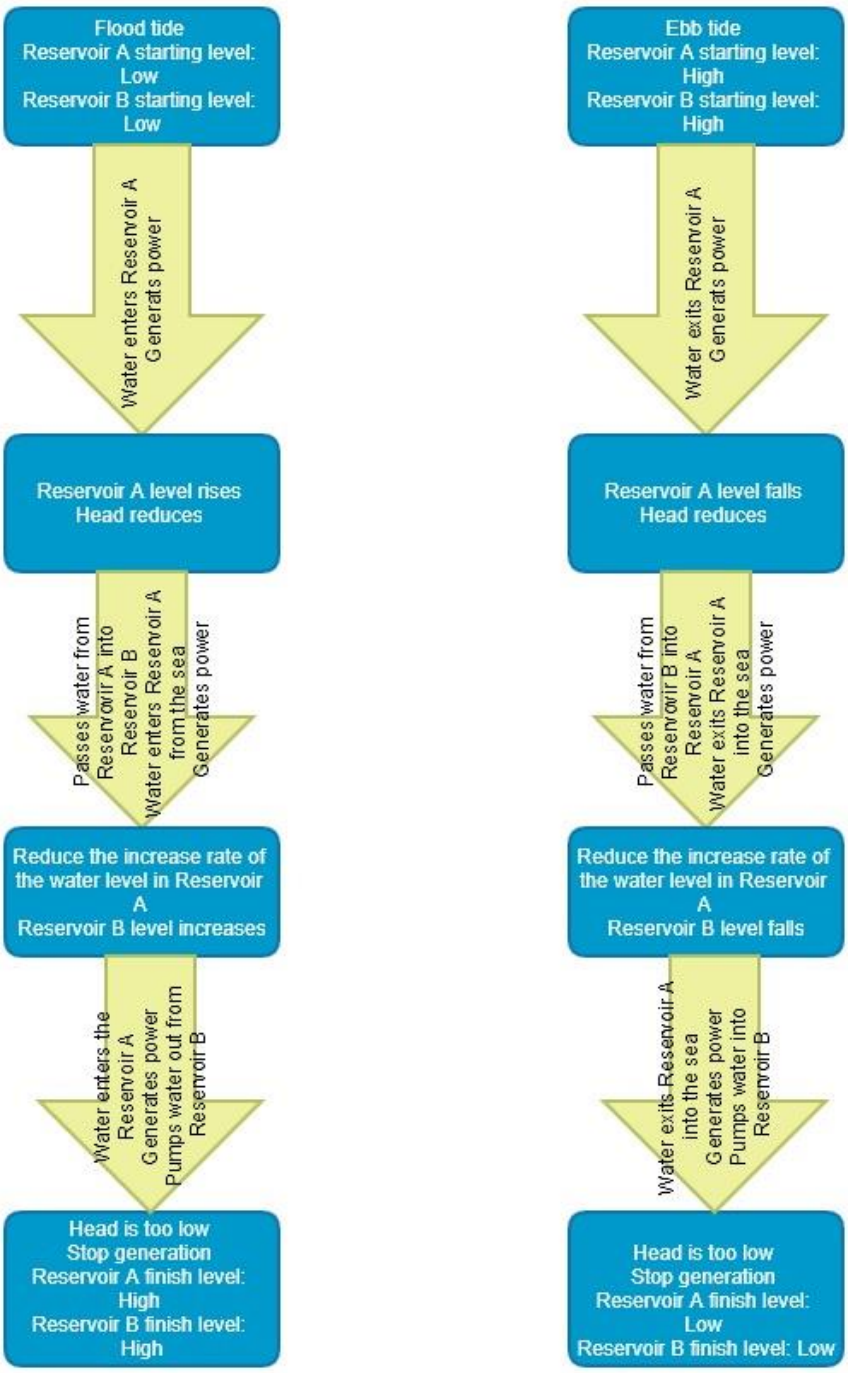

Figure 4-17 Logical flow diagram of the hybrid system in flood and ebb generation

Many sites have more than one dock, and these docks are located close to each other, Newport Docks which used as the example in the previous of this chapter has two docks. According to the flow diagram which shown in Figure 4-17, this design features two reservoirs; Reservoir A is used directly for power generation, and Reservoir B is

used for adjusting water levels for Reservoir A. During the ebb tide, water exits from the reservoir into the open water via water turbines for power generation. When the head difference between the reservoir and the tide is too small, the process is stopped due to the insufficient head. Reservoir B could be used to top up the main reservoir, once its levels are below the optimum. To extend the generation time and maximum power for flood tide generation, water levels for Reservoir B would be low from the ebb generation, and it would accept water from Reservoir A when its head was below the optimum value which was set to 4 m in this case.

4.4.3 The numerical model

Numerical calculations were carried out in Matlab. By altering the core program, the generation dock's information could be changed, for different cases. The threshold head difference for power generation was set at 2 m, which is the minimum head value required for the generation. The additional feature was the power reservoir. When the head difference between the generation dock and the tide was close to the threshold, the system adjusted the water levels in the generation dock by filling with water or letting water out, depending on tidal conditions. During the ebb, the water flowing out from the generation dock, and the water level would be decreased. Once the head difference dropped to a pre-set value, which was 4 m in this case, the large dock would begin to put water into the generation dock, to reduce the decreasing rate of the head. For flood generation, the increasing water levels in the generation dock would have a result in reducing the head, by transferring water from generation dock to the 2nd dock, would have the effect to reduce the decreasing rate of the head during the generation.

The tidal data was the same for both calculations. The generation tanks were set with the initial water level of 5.2 m, which was about half the maximum level. The maximum flow rate for water going in or escaping from the generation dock was set at 100 m^3/s. The larger South dock has a full capacity of 4,546,195 m^3 compared with

the smaller North dock of 928,587 m^3.

4.4.3.1 The smaller dock as the main reservoir

The first attempt was to use the smaller dock as the main generation site, and hence the larger one to be the power reservoir. When the head difference between the dock and the tide was less than the optimum (4 m in this case), the valves connecting these two docks would be opened, allowing the water to move between the docks, therefore adjusting water levels.

4.4.3.2 The larger dock as the main reservoir

The second attempt was to use the large reservoir as the main generation site. Therefore, the smaller reservoir was the power reservoir.

4.4.3.3 Results

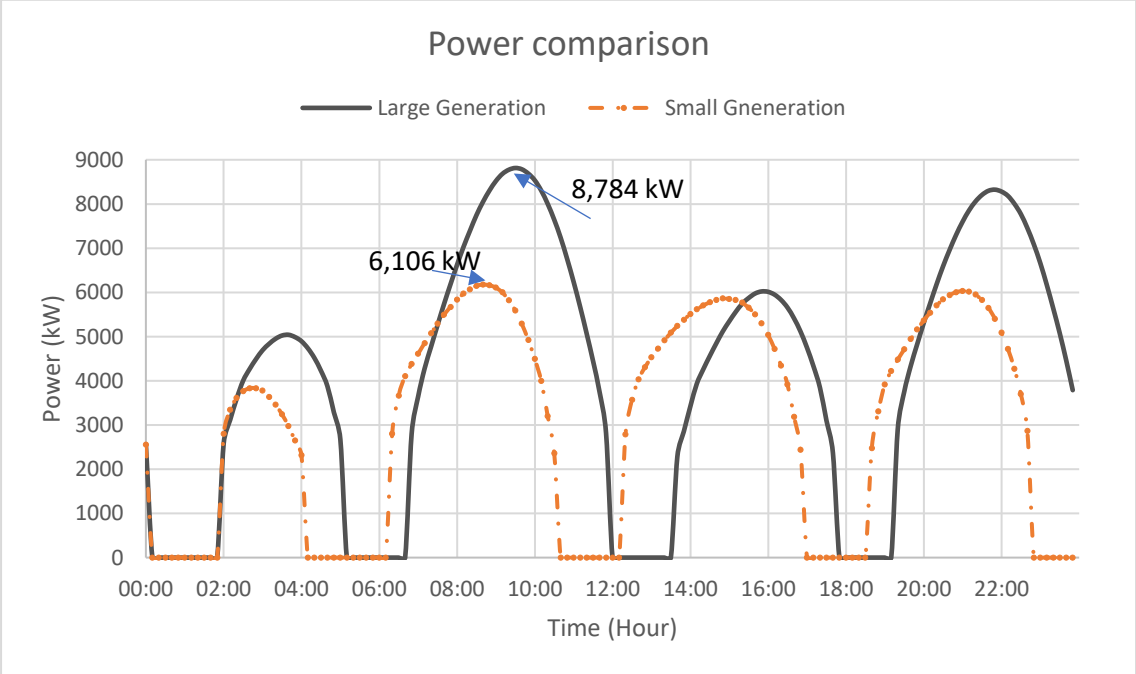

Figure 4-18 Power curves for both generations for 1 day

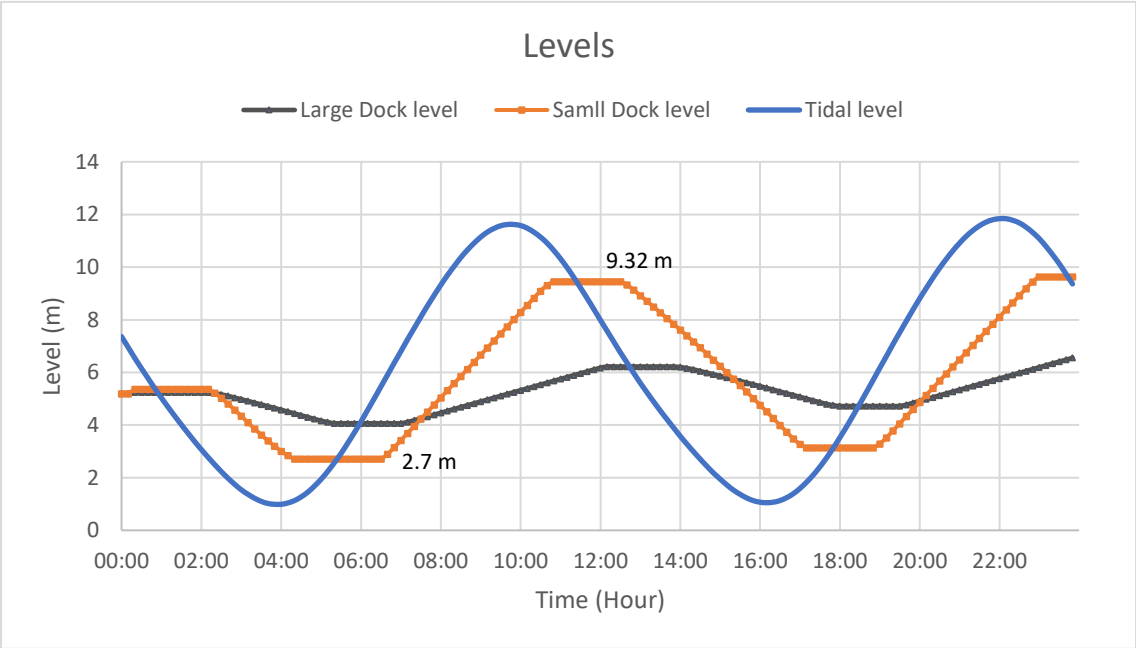

Figure 4-19 Level curves for both generation docks and tides for 1 day

As shown in Figure 4-18, under the same starting water level, the initial power output produced by both docks were identical. However, from 2:00, the large dock had an advantage in terms of maximum power and power generation times. According to Figure 4-19, from 2:00, the water level in the smaller dock dropped much quicker than the larger dock, because the area of the north dock is much smaller than the south dock, therefore under the same amount of flow rate changes, the smaller dock would empty more quickly. As shown in Figure 4-19, the gradient of the level curve for the small dock was similar to the tide, meaning the head difference would not increase much when the tide comes in or goes out. The large dock has a lower slow curve compared to the tidal curve, and when the tide rises or drops, the head difference increased, hence more power was produced. Finally, between 4:00-6:00, the small dock has the lowest level at 2.7 m and the highest level at 12:00 with 9.32 m, both levels are within the dock design limit.

During the second-generation period, the smaller dock started the generation earlier than the large one, due to lower levels, but as noted from Figure 4-19, the smaller dock filled up within about 5 hours, and the level in the large dock increased by 2 m.

This gave the large dock 1.5 hours more generation time than the smaller dock. With the maximum power reaching 8,784 kW compared to the smaller dock 6,106 kW, this yielded a significant 2,678 kW gap difference.

The third power period where the two docks matched each other on maximum power, was about 6,000 kW. The smaller dock generated energy for about 5 hours versus 4 hours 30 mins for the large dock.

For the final generation period of the day, the large dock had the advantage in terms of maximum power; it was more than 8,000 kW compared to 6,000 kW generated by the other dock.

4.4.3.4 Analysis

From Figures 4-18 and 4-19, the power difference was important as a result of the difference in dock sizes; the larger dock held more water and produced energy for longer periods, with better performance. Moreover, from these tests, it is clear that generation times can be shifted by adjusting the water in the generation dock. Importantly, it provides an option for generating power when there is demand, and tidal conditions are not ideal.

Using the smaller dock as a generation site had the advantage of having the quickest response of the system. Due to its small size, it took a short time to reach the optimum level. However, a drawback was the small energy capacity to a short generation period, hence a reduced maximum power.

The area of the larger dock was nearly 5 times that of the smaller dock. It had a large capacity for water, giving it an advantage in terms of generation times, and hence maximum power. But the large size would take longer to prepare to optimum levels.

However, these tests were carried out by feeding using one-day tidal data. To ascertain how the system changes, it must be tested over longer periods.

4.4.4 Testing with more tidal data

4.4.4.1 Results

The second tests were carried out by feeding the system using 3-day tidal data. This ascertained how the system reacted. Other settings remained unchanged.

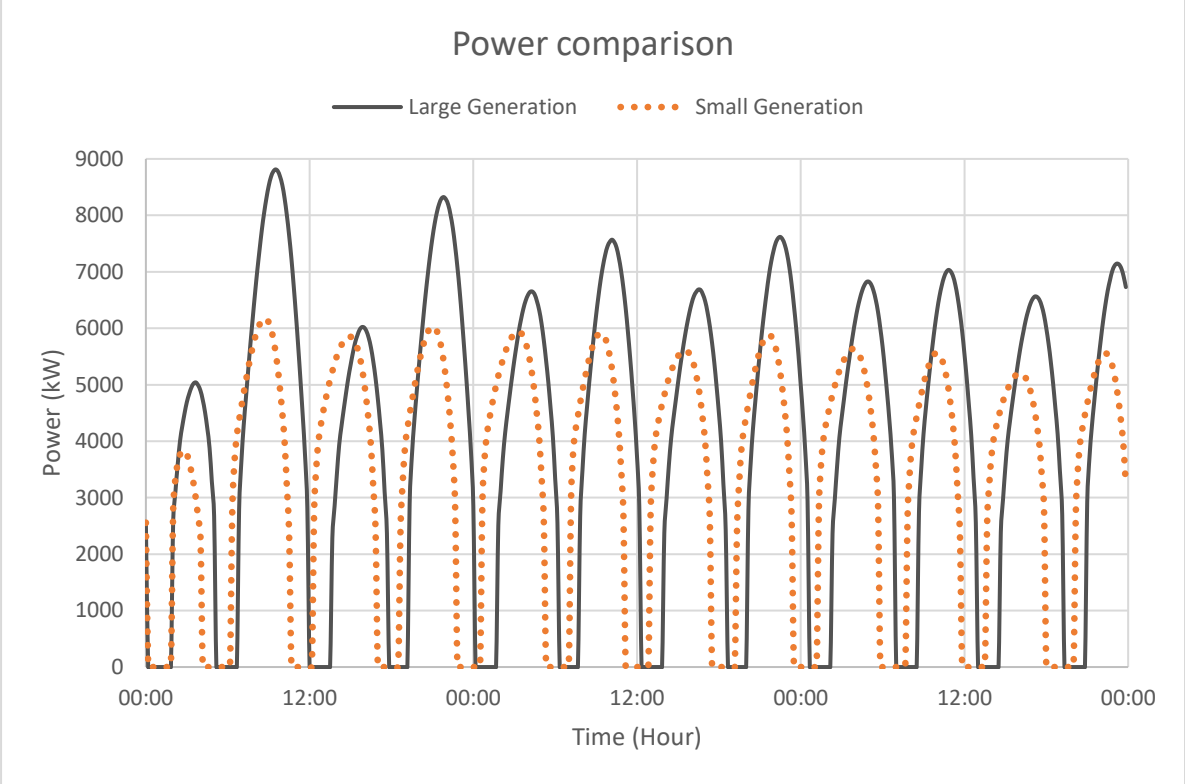

Figure 4-20 Power curves for 3 days

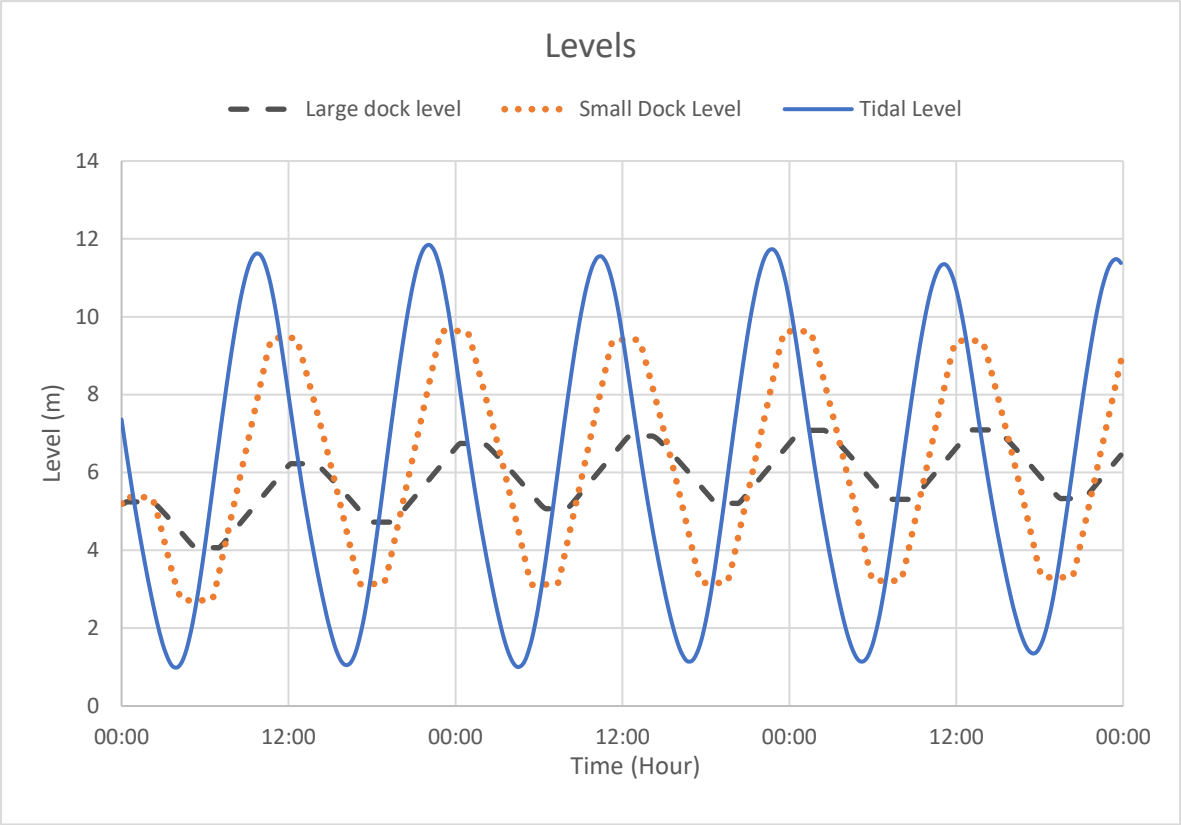

Figure 4-21 Level curves for 3 days

From Figure 4-20, the large dock had advantages in terms of power output over the smaller dock. The power generated during the ebb was generally greater than the flood generation. Also from Figure 4-20, it was noted that power generation by the small dock was consistent in terms of maximum power. The generation time under the flood tide was a fraction more than the ebb period. The average time for flood power generation was 4 hours and 40 minutes, compared with the average time for ebb generation of 4 hours and 10 minutes. Conversely, under the same tidal conditions for large dock generation, the average time for ebb generation was longer when compared to the flood tide, with average times of 5 hours and 20 minutes and 4 hours and 30 minutes, respectively.

Figure 4-21 shows the changing levels of the two systems with tidal profiles. It was noted that the small tank was more sensitive to changes in tidal conditions. From Figure 4-21, there was approximately a half meter difference between the second

crest and the third. The second peak value of the small dock level was approximately 0.2 m different to the third. However, the large dock was less affected by changes; observing the Large Dock Level curves in Figure 4-21, the level difference between the second peak and the third was approximately 0.04 m.

4.4.4.2 Analysis

By performing numerical tests for longer periods, from Figures 4-20 and 4-21, the changes in values with changing tidal conditions were observed. From Figure 4-20, the large dock had a big advantage in maximum power output; this was due to the larger area of the dock, the volume of the large dock is 5,474,782 m^3, whereas it is 928,587 m^3 for the small dock. The potential energy within the large dock is greater than the small dock, at the same level. Additionally, for the same amounts of changing volumes of water, it has a smaller effect for the larger dock size when compared to a smaller dock area.

Therefore, when tidal levels were dropping, if the gate were open, then water inside the dock would flow out due to gravity. For the same flow rate, the decrease rate for the large dock would be much slower than the smaller dock, due to its larger area. As shown in Figure 4-21, it was noted that at every high and low tide position, the head differences of the small dock were less than the those in the large dock. This directly resulted in the difference of the maximum power output of the two systems.

These results have shown that under the same tidal conditions, the two systems performed quite differently in terms of power production and operating times. To use the large dock as the generation reservoir, could provide advantages in terms of the power produced. However, there was a weakness in this system. The additional feature of tidal turbine-pump theory would work less efficiently with this system, because for the same amount of water pumped out of the system, the smaller dock would have more obvious effects than the large dock, due to size differences.

These results were compared with the original results, where no changes were made as indicated in both Figure 4-22 and Figure 4-23. It was noted that although using the whole dock as generation site, it has the largest area of the three systems, but the large dock still had a better performance.

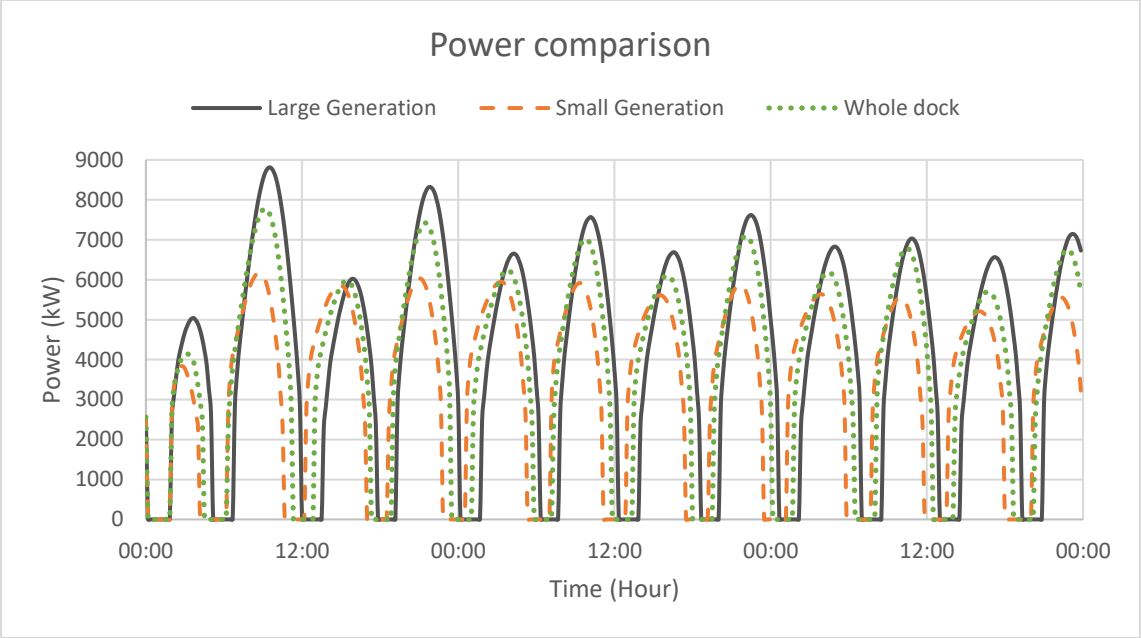

Figure 4-22 Power data of the 3 systems

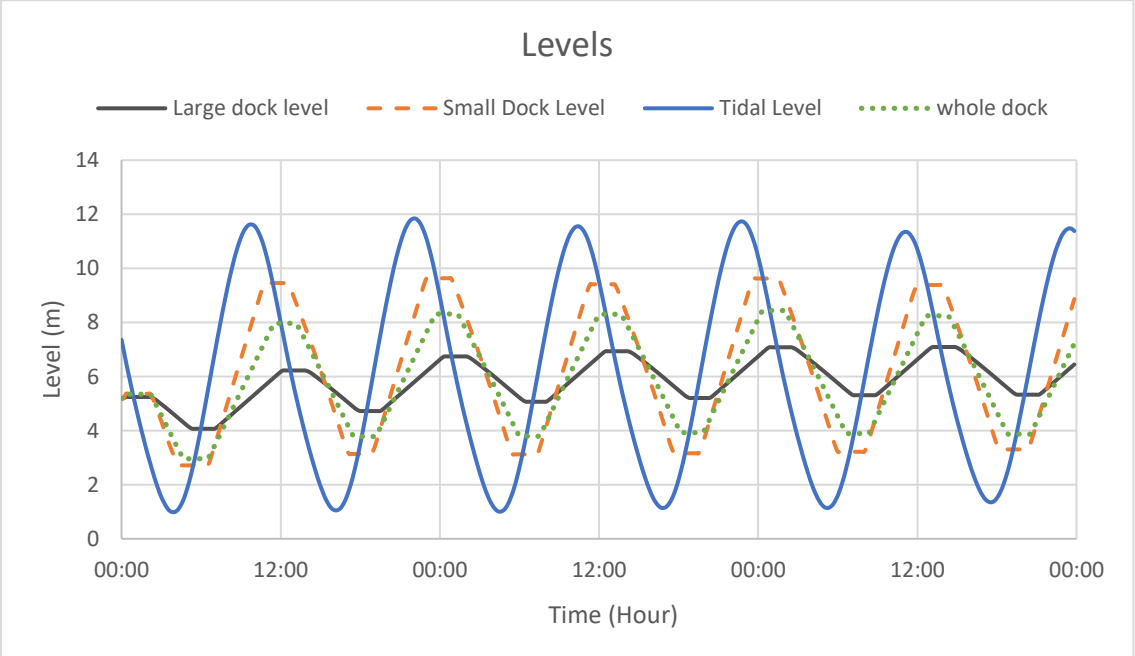

Figure 4-23 Level data of the 3 systems.

4.4.5 Discussion

Based on the results from the numerical models, using the large north dock as the main generation dock was the best option for power production. This option used the other dock as a power reservoir, allowing for adjustments in water levels in the main generation dock. However, by using the same settings for the additional pump-turbine unit for both cases, the effect on the bigger dock would be less than the smaller one due to the size difference. Moreover, this concept did not consider the geography of the docks, and it is likely that for some locations, the tidal stream turbine cannot be installed at the big dock due to its location.

4.5 Tidal power generation versus demand

As tides are constantly shifting, tidal energy can only be generated during the flood and ebb tides, for the best possible performance. Therefore, it is very important to understand how energy is generated from tidal stations, to meet demands.

4.5.1 UK power demand

This case focuses on energy generation during energy peak demand windows, usually between 8:00 and 20:00 which is shown in Figure 4-24.

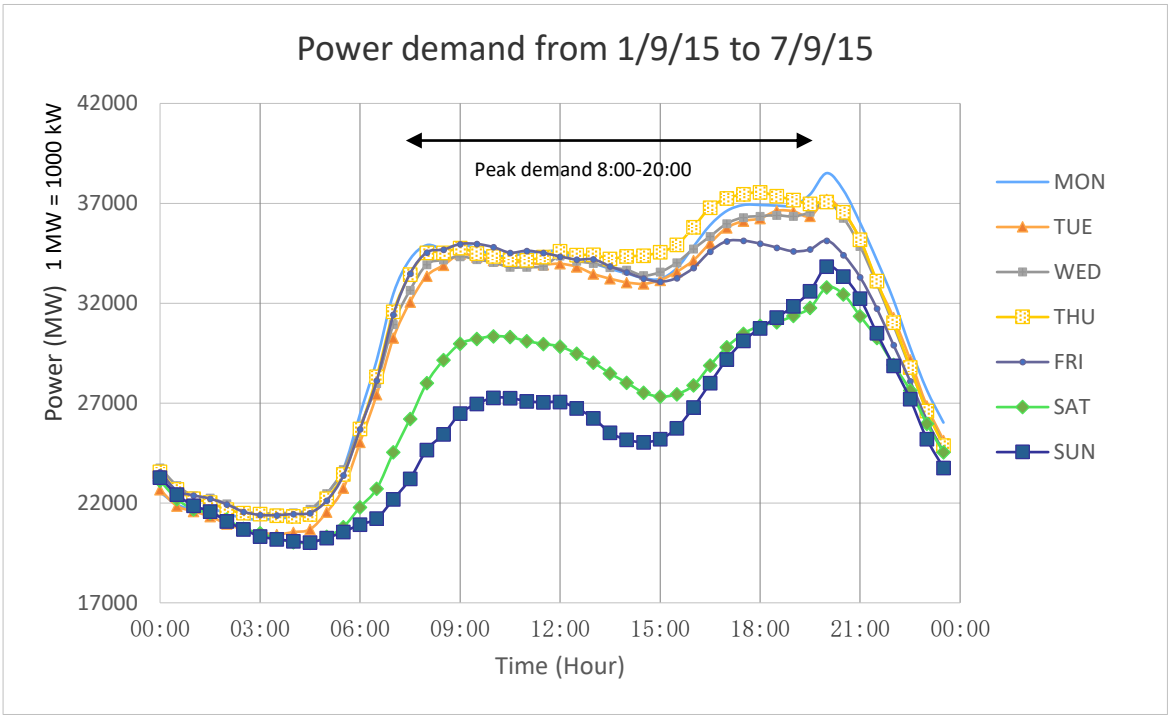

Figure 4-24 Power demand data (National Grid. 2016)

The tides are divided into four different scenarios. The starting point is 8:00.

A. The starting point of the ebb tide;
B. The middle of the ebb tide;
C. At the starting point of the flood tide.
D. In the middle of the flood tide;

These four tidal scenarios represent a tidal cycle, and for each tidal scenario, there are three simulations based on the tidal profile. These three simulations are compared within each tidal case (A-D), with the same tidal range data.

For this case, the system was to set to hold water in the reservoir before the start of the peak window, it would not operate before that time. There were three settings of initial water levels in the reservoir:

1. Full reservoir, where the reservoir level was at the maximum (10.8 m);
2. Half reservoir, where the reservoir level was at half the maximum (5.4 m);
3. Minimum reservoir, where the reservoir level was at the minimum (2 m).

To conclude, a total of 12 different scenarios will be discussed in Chapter 4.5.2.

4.5.2 Case Study

The case study has four tidal scenarios based on the tides at the 8:00, which is the starting time of the grid peak window:

A. Start of the ebb tide: this case focused on power generation at the beginning of the ebb tide. (Chapter 4.5.2.1)
B. During the ebb tide: this case focused on power generation during the ebb tide. (Chapter 4.5.2.2)
C. Start of the flood tide: this case focused on power generation at the beginning of the flood tide. (Chapter 4.5.2.3)
D. During the flood tide: this case focused on power generation during the flood tide. (Chapter 4.5.2.4)

There will be three different starting reservoir levels for each case (A-D), with 1. Full, 2. Half, 3. Minimum starting levels. The hybrid numerical model for Newport Docks will be used to predict the power output and will be compared to the power demand by the Newport City Council, which shows high energy demand during the peak window (8:00-20:00). The aim is to generate power during this peak demand window, so in this case study, the power generation will begin at 8:00.

From this case study, the results would provide insights into how power generation at different stages would compensate for demand on the grid.

4.5.2.1 Case A: Ebb

As shown in Figure 4-25, at the beginning of the peak window, the tidal condition was ebb. The advantage of this scenario was that the stream speed was much faster during the ebb and flood tides. Therefore, the tidal turbine-pump unit would generate more power, due to faster flow speeds. Hence, more water would be pumped into the reservoir and provide a longer power generation window, with a higher head

difference.

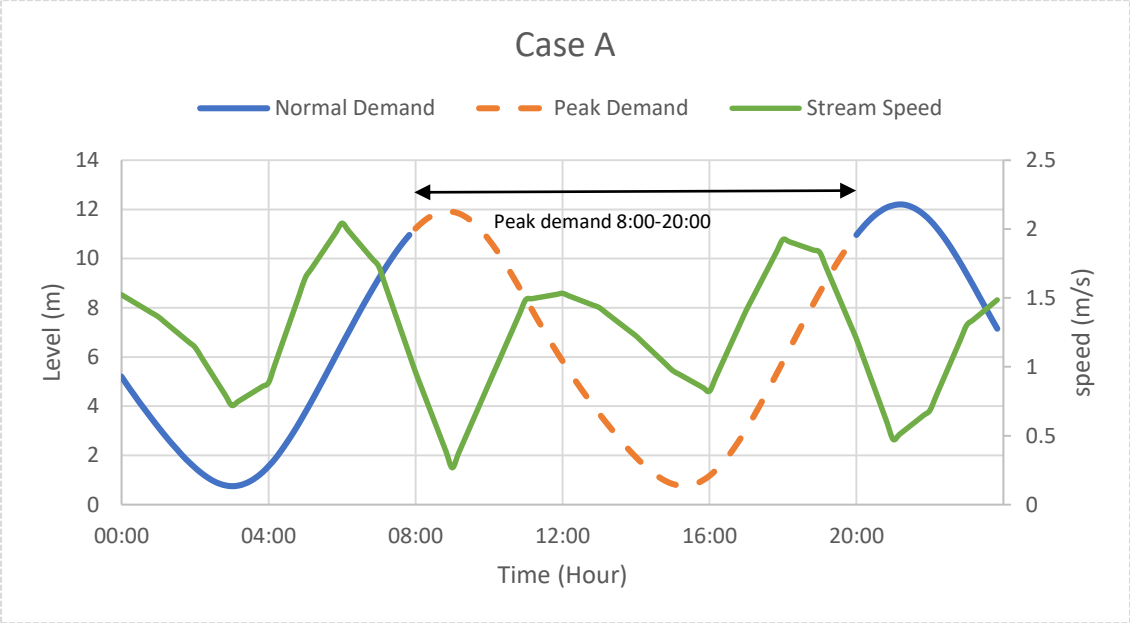

Figure 4-25 Tidal data on 31-07-16 at Newport

Results:

Case: A-1 Full reservoir

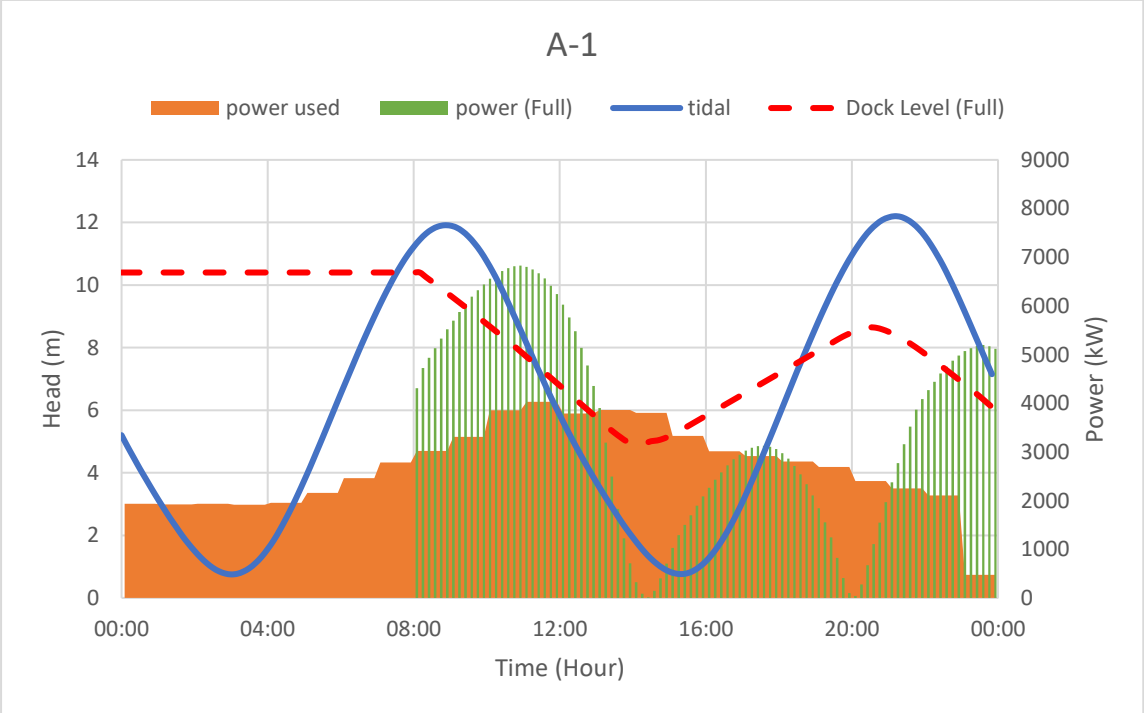

Figure 4-26 Results (full reservoir)

According to Figure 4-26, at the beginning of the peak window at 8:00, with a full tank of water at 10.8 m, the head difference was close to 4 m. This level would provide a power output of approximately 4,000 kW. With a continuously dropping tide, the magnitude of power continues to rise. At 12:00, the tide reached the lowest position; this was where the power generation peaked. When the flood tide began around 14:00, the power generation was cut off due to zero head difference. At around 17:00, the system started to generate power again.

The orange area represents power demands by the Newport City council. At the start of power generation, the simulation expressed in the first cycle (between 8:00 to 14:00) the generated power was more than demand power. However, after the first cycle, there was a gap between 14:00-18:00, where generated power was below demand.

Case A-2: Half reservoir

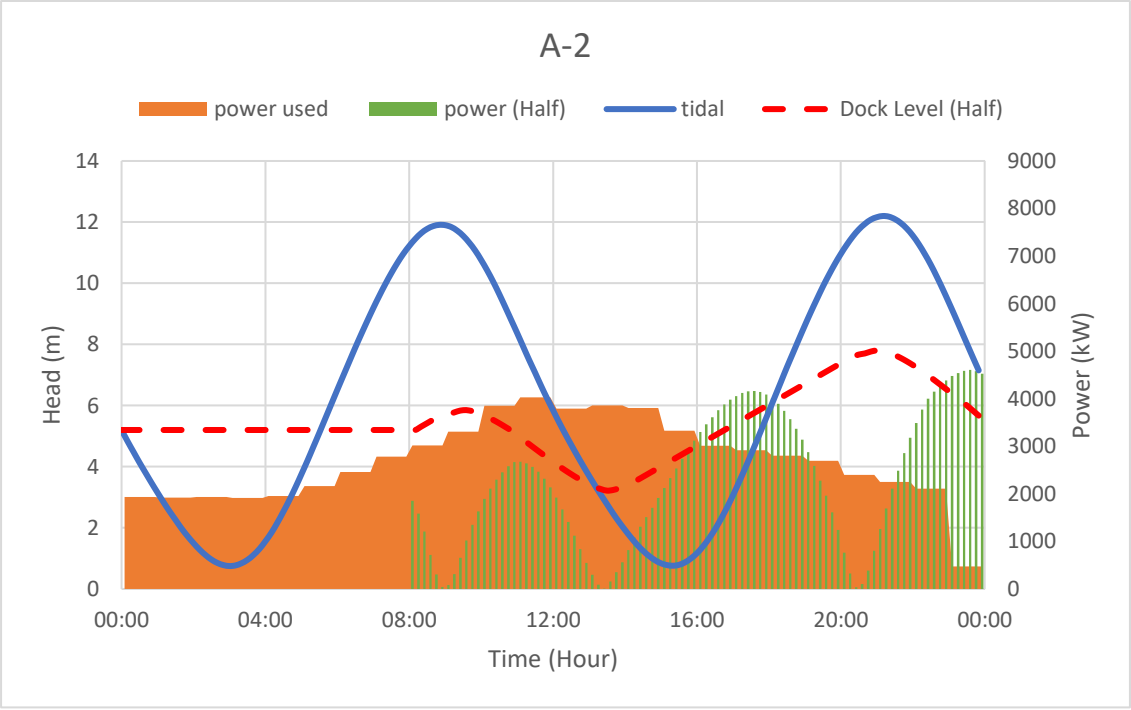

Figure 4-27 Results (half reservoir)

From Figure 4-27, the starting reservoir level of 5.4 m had a low head difference.

Therefore, less power was generated at 8:00 when compared to the same time in Figure 4-26 in the Case A-1. There was a rise in reservoir levels at the start of the operation; this was due to the turbine-pump units. From Figure 4-25, the stream speed at that period was higher than other times, meaning the turbine-pump units could pump more water into the reservoir, to increase the head difference when the tides continued to fall.

In addition, when demand was at its highest between 10:00 and 16:00, the generated power was at its highest, more than 3,000 kW. The system can only generate 2,000 kW for a short period. Furthermore, between 8:00 and 16:00, there were two gaps where the system did not generate any power. This was due to zero head difference. The only period where the system had power coverage was between 17:00 and 20:00. Here, demand was met.

Case A-3: Minimum reservoir

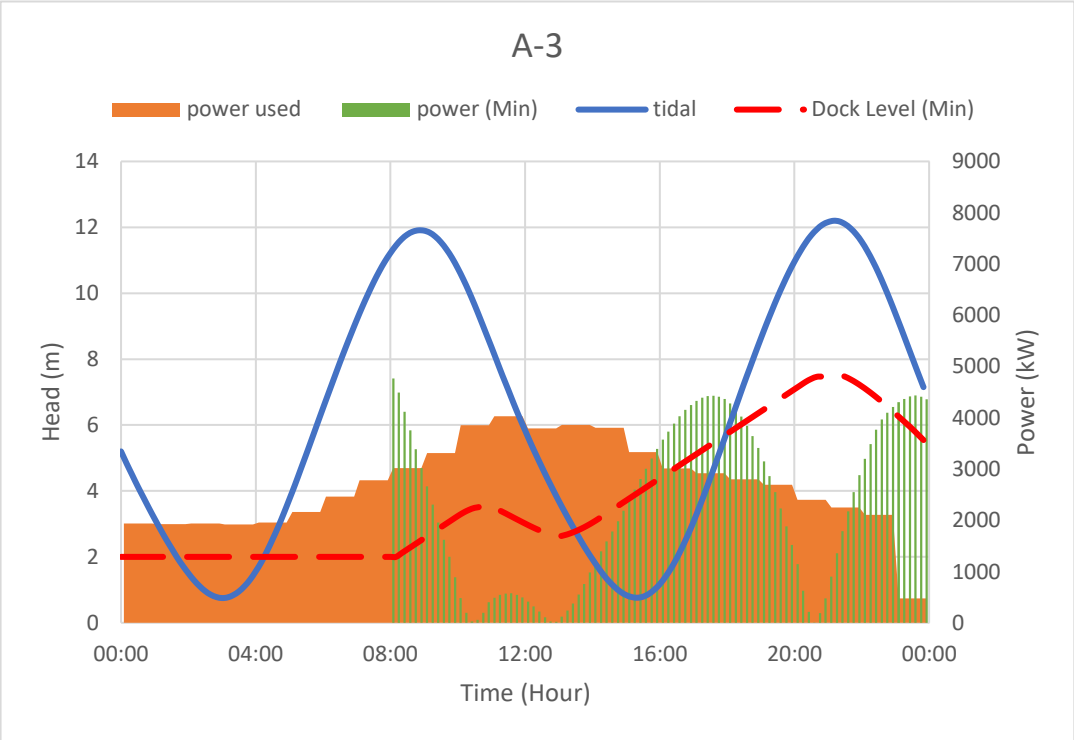

Figure 4-28 Results (min reservoir)

Figure 4-28 shows that the minimum tank level option provided a good head difference at the start of the exercise, generating a high power output. However, due to low reservoir levels and high tidal levels, the magnitude of the head difference fell sharply, because of rising reservoir levels and the falling tide. This meant the power output was not ideal during that period. At around 14:00, the tide started to rise again, and power generation began to increase. At 16:00, the power covered demand and lasted until 20:00.

Discussion:

The average power data between the peak demand window (8:00-20:00) is shown in Figure 4-29.

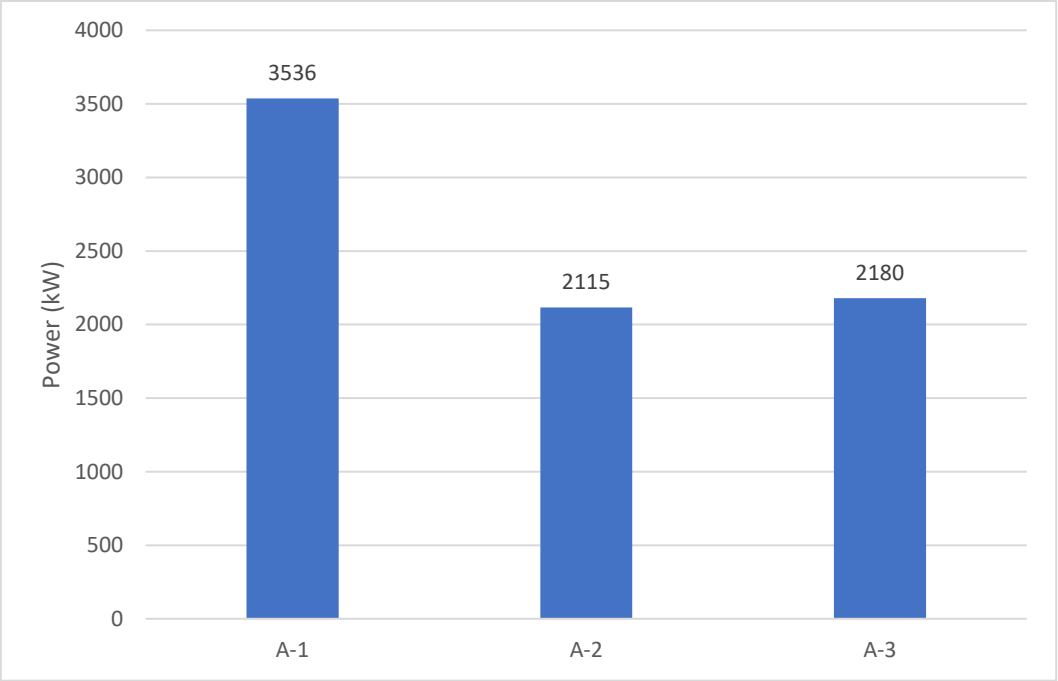

Figure 4-29 Average power output in the peak demand window

From the results shown in Figure 4-27 and Figure 4-29, for Case A-2, the demand was not met until 17:00, and the coverage window was the shortest, around 3 hours. This indicates a suboptimal option; this option has the least average power value with 2,115 kW during the peak demand window.

Case A-3 (minimum tank level), under this tidal scenario, has an average value of 2,180 kW during the peak window, which is about 3% more than Case A-2.

Last but not least, the full tank option Case A-1, under this tidal condition, had the best power output with average value of 3,536 kW. It had the longest coverage window (around 7 hours) and had the shortest gap (around 2 hours). Between 8:00 and 14:00, the system generated more energy than demand. Therefore, this was the best option for this tidal scenario.

4.5.2.2: Case B: Beginning of ebb

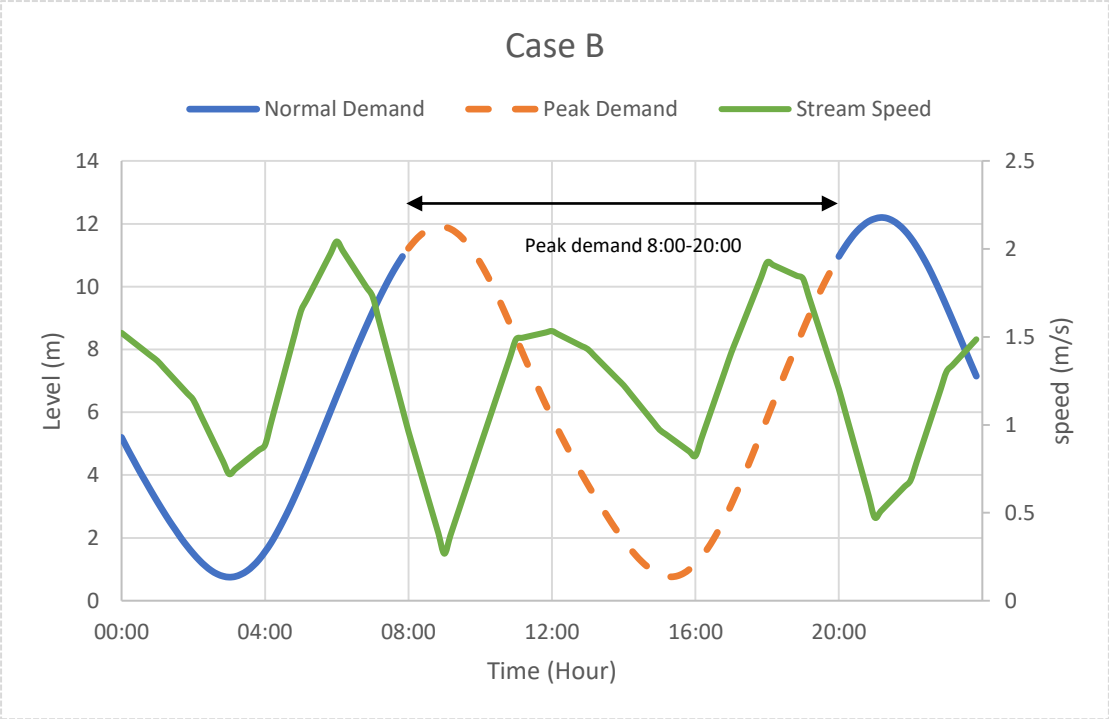

Figure 4-30 Tidal levels with tidal stream speeds on 04-08-16 at Newport

In this case, the tidal scenario at the beginning of the peak window was the early stage of the ebb tide. Here, the tidal level reached the highest point and was about to drop. However, due to the characteristics of the tide, the stream speed was low at the starting point which is shown in Figure 4-30. Therefore, the power output for the tidal turbine-pump unit was low and the water pumped into the reservoir was less.

Case B-1: Full reservoir

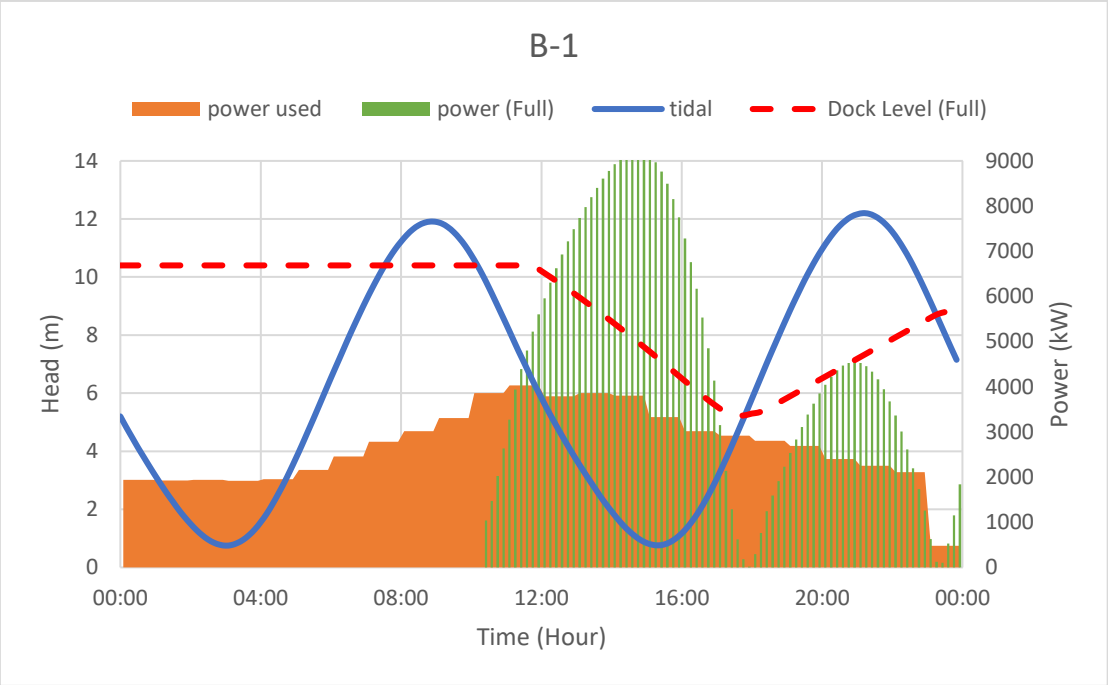

Figure 4-31 Results (full reservoir)

As shown in Figure 4-31, the tide at 8:00 was higher than the reservoir level, but at this point, the reservoir was already full and could not take any more water. Power production began at approximately 10:30, when the tide fell below the reservoir level. During the ebb tide between 10:30 and 15:20, there is a steady increase in the output power, mainly was because the head difference between the tidal level and reservoir level was increased, also during the ebb tide, the stream speed was high, it powered up the turbine-pump units, which were used to pump water back to the reservoir, to maintain a good head difference for power generation. At 12:00, the system started to provide coverage until 18:00. The results showed that peak performance of tidal systems reached more than 9,000 kW, which was approximately 5,000 kW more than the highest demand. The tide started to rise around 16:00, at which time point, the reservoir was still higher than the tide. Therefore, the gap between the two levels closed quickly, and led to a sharper fall in energy production.

Case B-2: Half reservoir

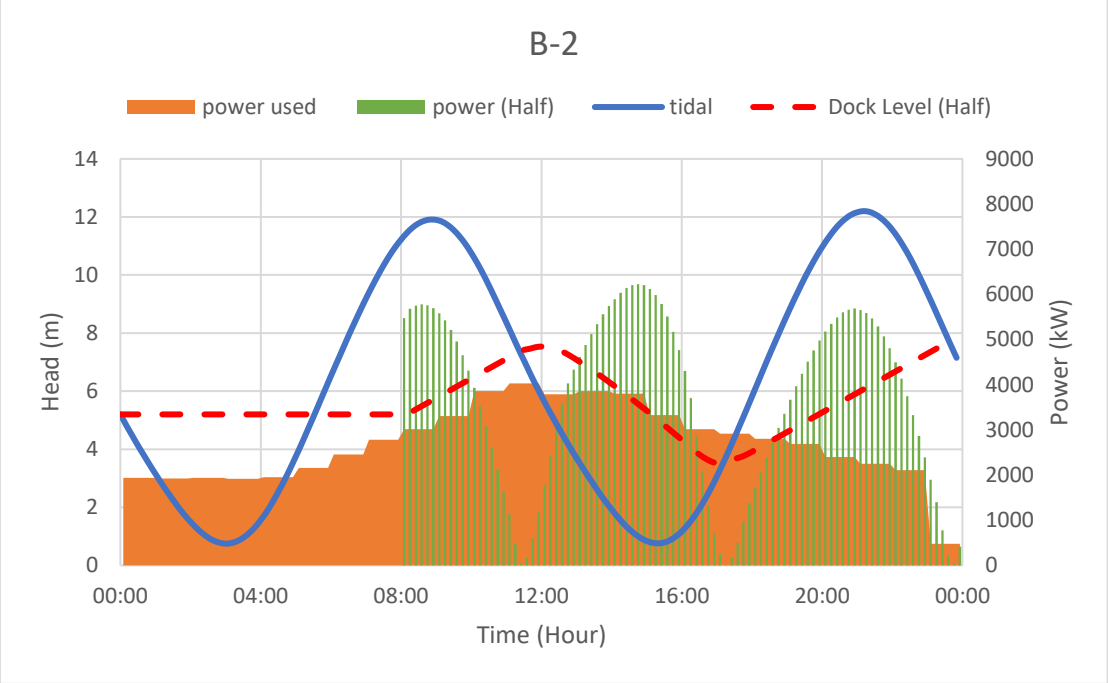

Figure 4-32 Results (half reservoir)

For this option as shown in Figure 4-32, the system provided coverage at the beginning of peak demand window for approximately 3 hours. The high tidal level and half reservoir provided about 5 m head difference for power production. However, the two levels intersected at 12:00, with no power output. Then there was a 2-hour gap where the power output did not match the demand. Finally, another coverage occurred from 14:00 to 18:00 with the ebb, but the beginning of the flood tide resulted in a rapid drop in the energy production as the rising tide quickly matched the falling reservoir, and another between 17:00 to 19:00, there was no generation due to the head was too low (below 2 m setting value).

Case B-3: Minimum reservoir

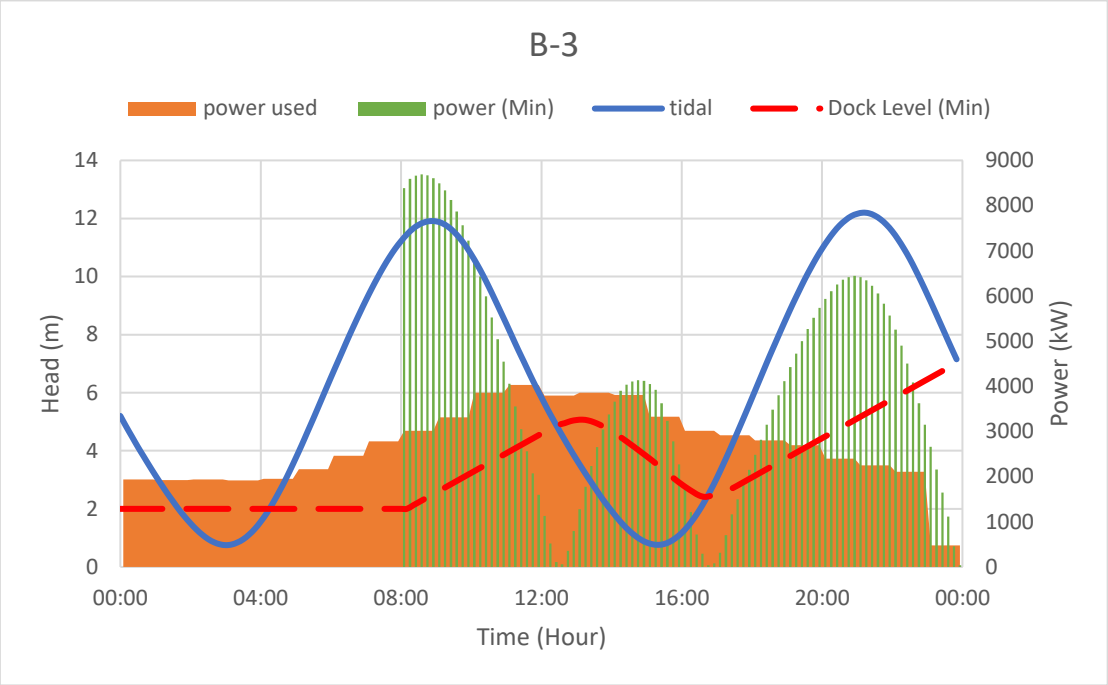

Figure 4-33 Results (min reservoir)

According to Figure 4-33, which shows the power output versus demand, the system provided more than enough power between 8:00 and 12:00. The high starting tide provided an excellent head difference, with the low reservoir levels. The maximum power reached was greater than 8,000 kW for about 2 hours, this was almost 4,000 kW more than demand. The heights levelled off at about 13:00, and power production was on hold for about 1 hour due to the insufficient head, and a short power coverage between 14:00 to 16:00. Furthermore, power production just missed a period where demand was highest; between 10:30 and 14:00, the highest demands occurred, reaching more than 3,500 kW. However, the system could not provide enough energy for this period.

Discussion:

Generally, all three cases had reasonable power outputs during the peak demand window, the average power values are shown in Figure 4-34

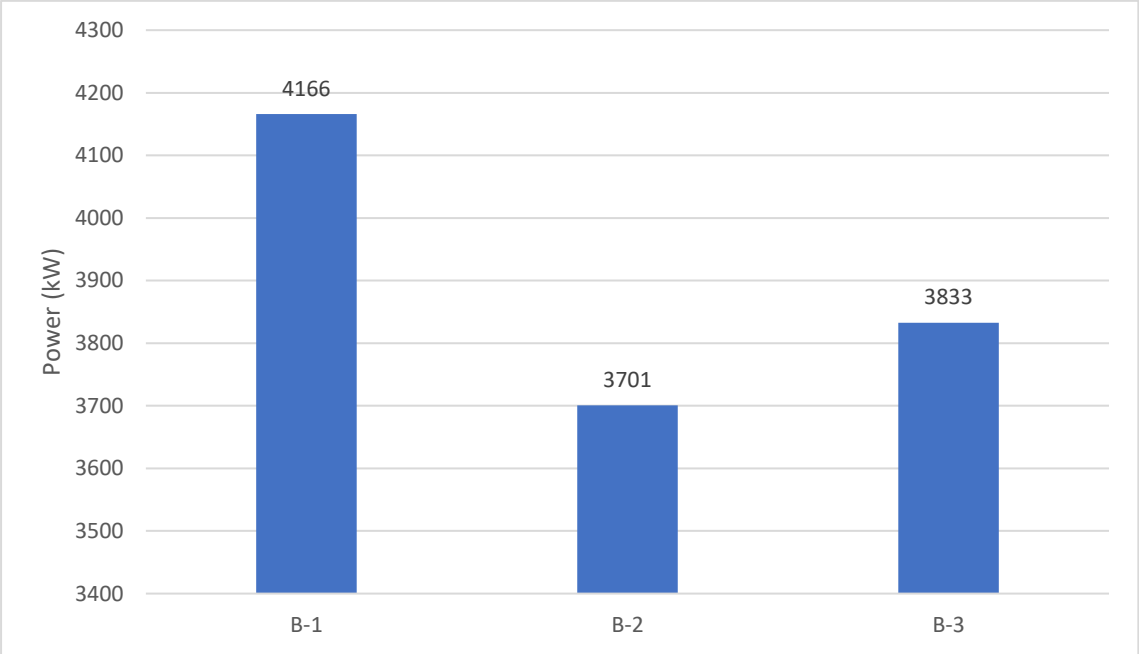

Figure 4-34 Average power output in the peak demand window

For Case B-1, where the reservoir was full, there was an initial 4-hour gap, but the energy produced satisfied demands for most of the remaining time, and it has the highest average power during the peak window with 4,166 kW.

For the second case which is B-2, where the reservoir was half full, this was the best option of three. The peak power performances were almost the same, the coverage time was good, the underperforming time was about 5 hours, when compared to more than 6 hours for the other two cases. However, the average power during the peak demand in this case is the smallest with 3,701 kW, which is around 12% fewer than B-1. Additionally, Case B-3, where the reservoir was at minimum levels, energy generation was good for the first 4 hours, it has an average power value of 3,833 kW, which is around 3.5 % more than B-2. To conclude, Case B-1 which is the ideal case for optimisation, under these tidal conditions.

4.5.2.3 Case C: Flood tide

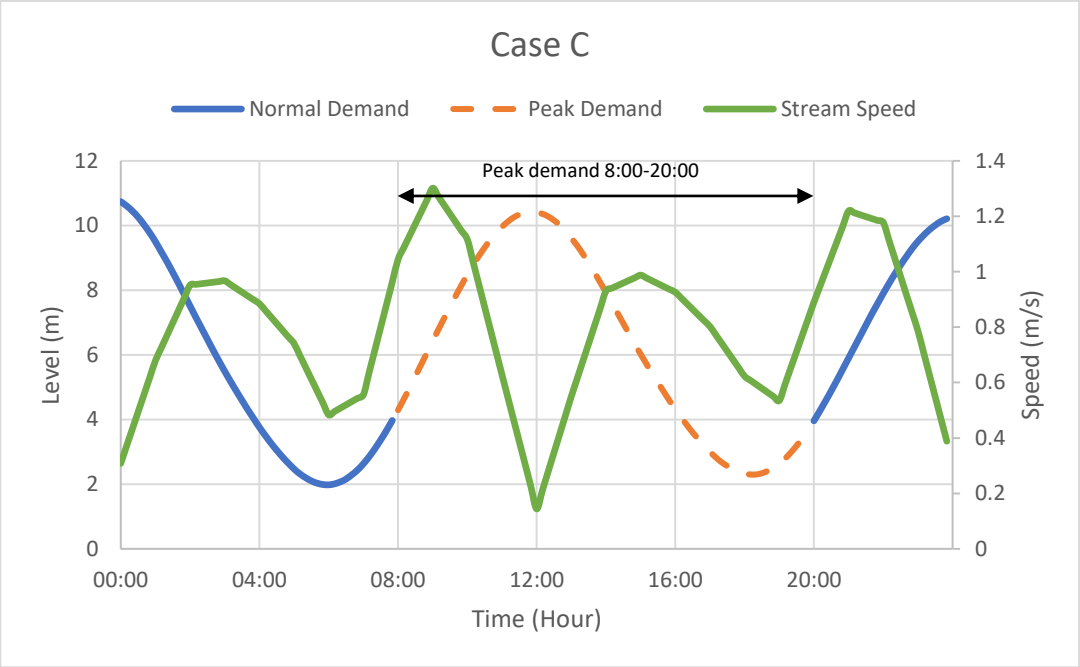

Figure 4-35 Tidal and stream data on 09-08-16 at Newport

In this case, tidal conditions at the starting point, was in the middle of the flood tide. The tides started to rise at the beginning of peak demand, at 8:00. The tidal level and stream speed data is shown in Figure 4-35.

Case C-1: Full reservoir

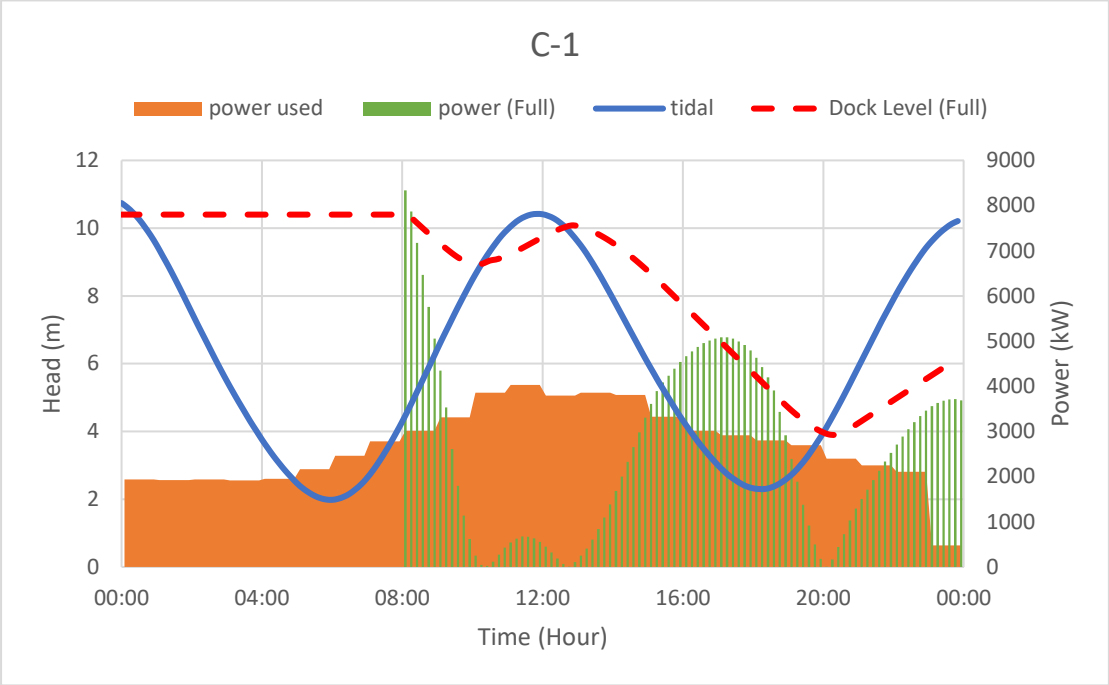

Figure 4-36 Results (full reservoir)

The high reservoir levels provided a good head difference at the beginning, but during flood tides, tidal levels rose quickly, and the head difference dropped in a short time. Therefore, as shown in Figure 4-36, there was a peak at the beginning, followed by a long gap where energy generation was at a minimum. Moreover, the system, under these conditions, could only provide power coverage from 15:00 to 19:00 to satisfy energy demands. However, the demands for this period were lower, about 2,500 kW when compared to high demands of 3,500 kW.

Case C-2: Half reservoir

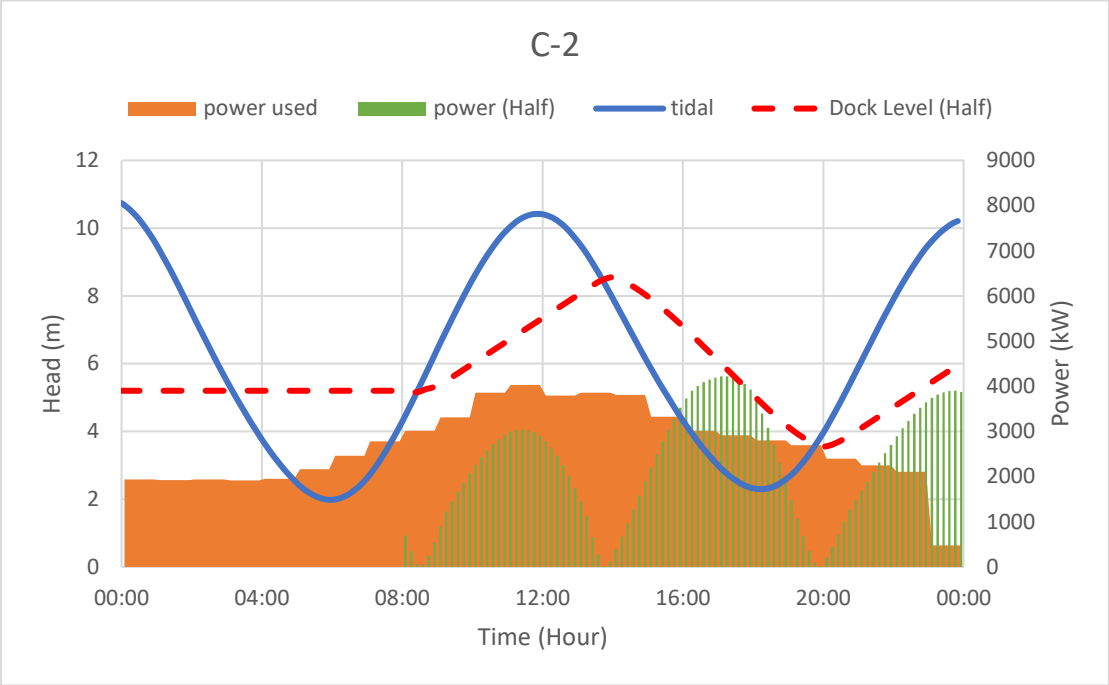

Figure 4-37 Results (half reservoir)

For the half tank option which is shown in Figure 4-37, the two levels practically matched each other, but power generation was low. Following the flood tide, energy outputs begun to increase, but as the head difference was not ideal, the generated power did not meet grid requirements until 16:00. In the end, the energy produced between 16:00 and 18:30 satisfied demand.

Case C-3: Minimum reservoir

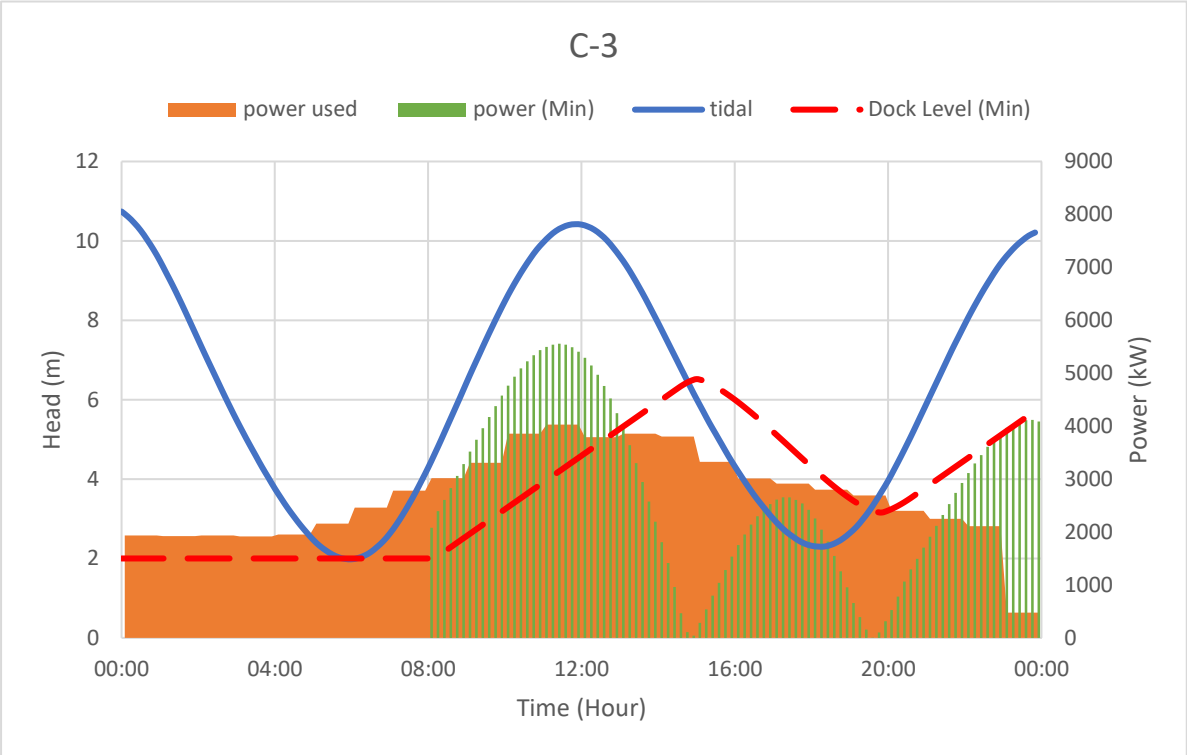

Figure 4-38 Results (min reservoir)

The minimum reservoir level had a low head difference at the start. While tidal levels increased, power generation increased due to low initial levels. The first power generation cycle covered the demand for the first 6 hours. Power generation then began to drop after 14:00, due to changes in tidal characteristics. For the rest of the time, the system did not provide enough power to feed demand.

Discussion:

Figure 4-39 shows the average power values for all three cases in the peak demand window. With case C-3 with the highest value with 2,779 kW over the three.

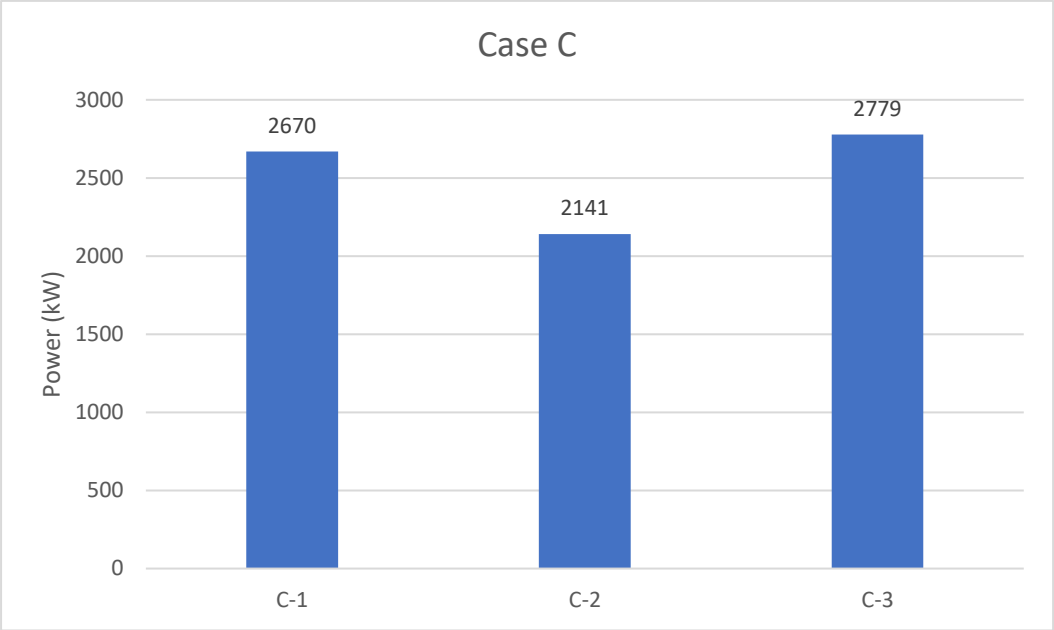

Figure 4-39 Average power output in the peak demand window

By comparing energy outputs, within demand windows, C-1 and C-2 had long periods where demand was not satisfied. C-2 has the lowest value over the three with 2,141 kW, with the difference between C-1 and C-3 is small with 109 kW between them. In the end, the minimum tank option C-3 was the best of these three options with the highest average power value, under these conditions. Coverage times and energy production were reasonable, but unlike previous cases, power over-generation was not high.

4.5.2.4 Case D: Beginning of the flood tide

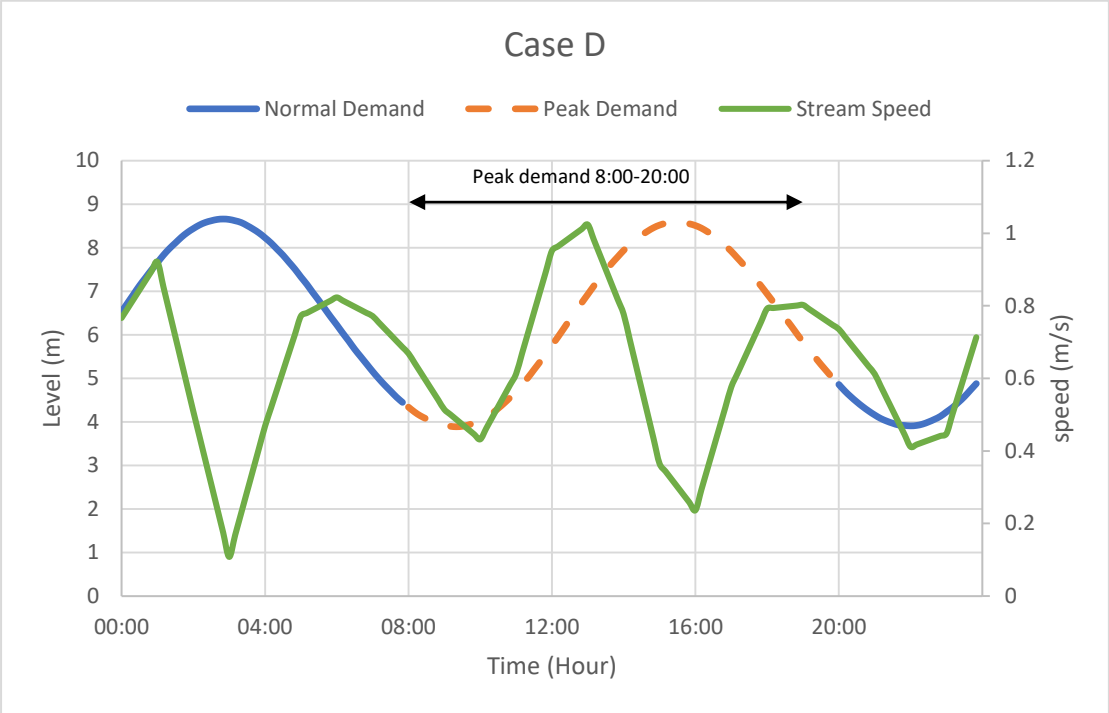

Figure 4-40 Tidal and stream data on 09-08-16 at Newport

In this case, tidal conditions at the beginning of peak demand were about to switch to the flood tide. Under these conditions, the initial tidal level was at its lowest. As shown in Figure 4-40, the stream speed was also at a minimum. The tidal level reached its highest at 16:00 and then the ebb began, which just about reached the end of the ebb at the end of the peak demand window at the time of 20:00. However, the tidal conditions in this case were not ideal. The difference between the highest and lowest tidal level was less than previous cases, being 5 m when compared to 8 m for previous cases. This meant the energy of this tide was considerably less than previous cases, this scenario led to a low performing energy generation for this tidal system.

The tidal range in Case D is noticeably less than the other cases (A, B & C) which were discussed previously. However, the aim of this case study is to find the best starting reservoir level for each tidal scenario (A, B, C & D), the same tidal condition will be used for the three different reservoir-level models value (Full, Half and Min). The

estimated power resulting from these three models are compared with each other. Therefore, the magnitude of the tide is not relevant.

Case D-1: Full reservoir

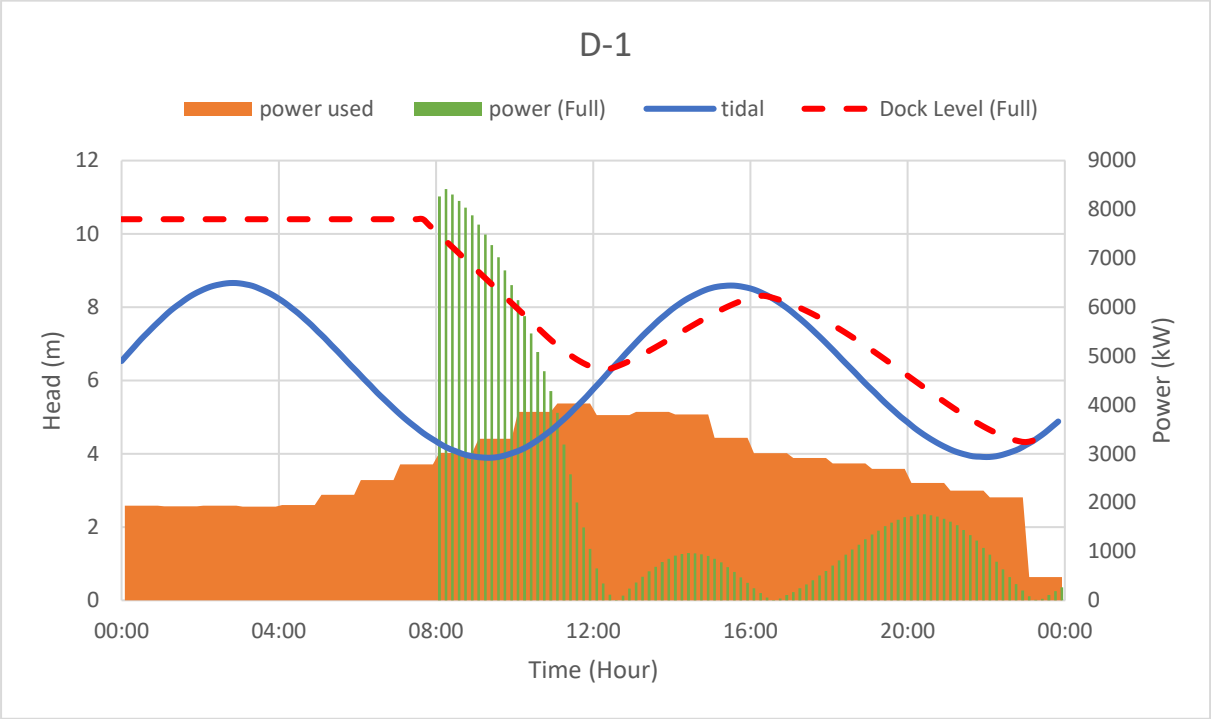

Figure 4-41 Results (full reservoir)

For this scenario, the low tidal level and high reservoir level resulted in an initial high power output, reaching a maximum of 8,000 kW. However, this number dropped quickly when the tide kept rising. At this time, reservoir levels were still higher than tidal levels, so water in the reservoir continued to exit to the sea while the tide increased. Therefore, according to Figure 4-41, after reaching the maximum level, power generation began to fall sharply and dipped below demand at 11:00. When the two levels intersected at 12:00, power generation was significantly below the demand requirements and did not satisfy demands for the rest of the day.

Case D-2: Half reservoir

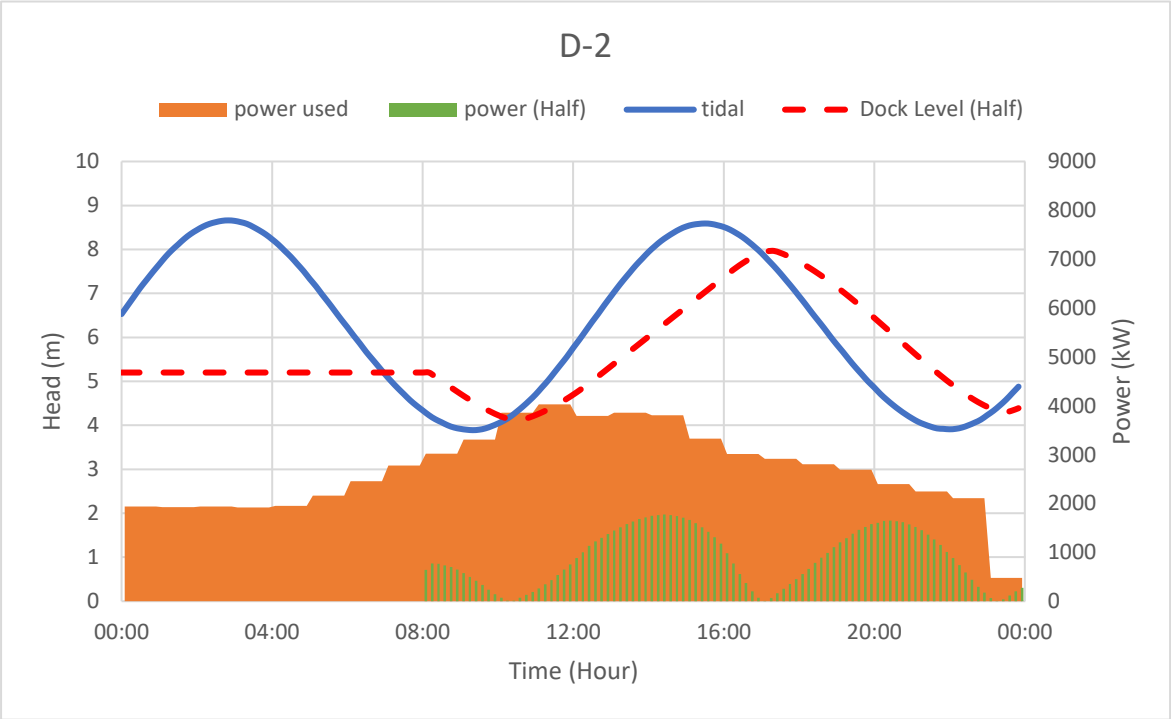

Figure 4-42 Results (half reservoir)

From Figure 4-42, the system did not meet the demand requirements in the time window, under this tidal condition. The maximum power (2,000 kW) was below the minimum demand (2,200 kW). The reason for this outcome was that starting reservoir levels were similar to tidal levels, generating a low power output.

Case D-3: Minimum reservoir

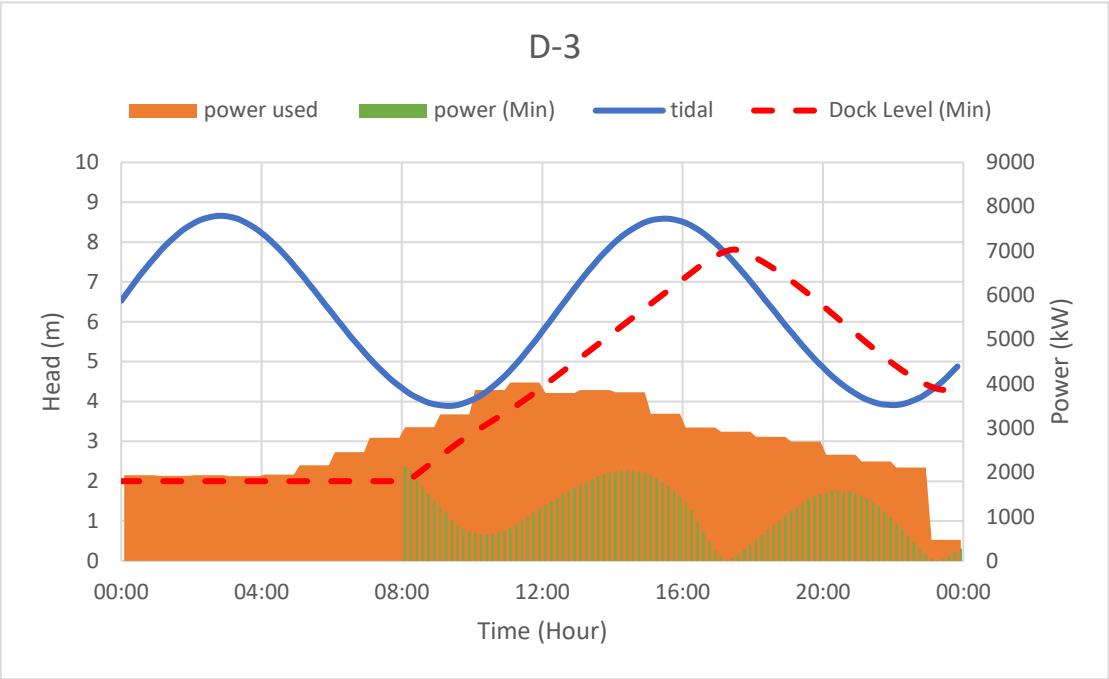

Figure 4-43 Results (min reservoir)

The energy performance in this case was not ideal. Overall, power outputs were below demand requirements. The highest power was about 2,000 kW, which was about 1,500 kW short for that time demand. From Figure 4-43, the head differences were low during power generation, which led to low energy generation.

Discussion:

Figure 4-44 shows the average power values from D-1 to D-3.

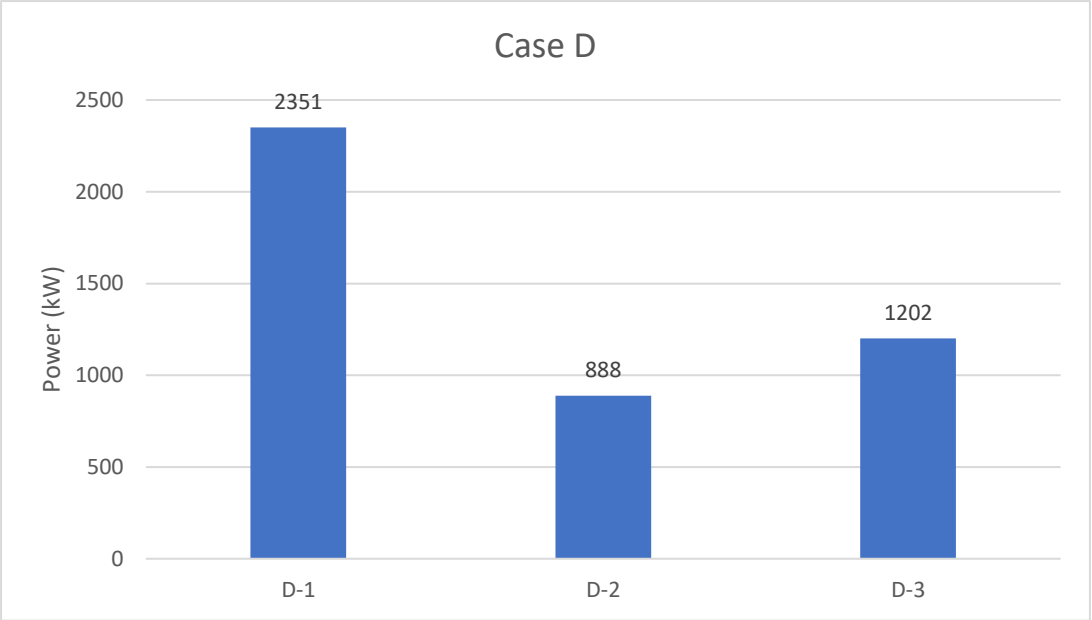

Figure 4-44 Average power output in the peak demand window

These three options did not provide reasonable coverage times for energy demands, under these tidal conditions. This was due to low potential energy from the tide. However, Case D-1 was the best option out of the three with the highest average power value within the peak demand window with 2,351 kW. Initially, while the reservoir level was full, it was the only case that generated more power than was required by demand. The other two cases did not have the same potential.

4.5.3 Conclusions

By running simulations for these four-tidal conditions, with three different reservoir settings, a total of 12 individual cases were analysed, an optimum setting for different tides can be selected for each tidal condition. However, a drawback was that the system focused on generating ebb tides. Ebb tides generally produce more electricity than conventional tidal systems. However, from the results, for some cases, more energy was generated during flood tides (Case C). Therefore, system settings can be changed to accommodate flood tides, and not ebb tides.

The goal of optimisation was to provide coverage in the peak demand energy window,

where power outputs meet demand, and maintaining a low overshoot energy. To optimise this, the system must provide enough energy for the grid. By adjusting settings for tidal systems, i.e. inlet gates, turbine-pump units, it is possible to shift the overshoot energy to gaps where demand is not satisfied. However, due to limitations of the tidal system, the system cannot generate energy where the two levels are the same. During the optimisation of the system, it is important to shift that time to a period when demand is not high.

4.6 Chapter Summary

The results from Matlab numerical simulation for Newport Docks has shown the potential of converting a sea dock into a local tidal energy system, which could provide predictable energy to the surrounding arears. By using the existing docks, the initial construction cost would be reduced significantly, both financially and time wise.

The hybrid tidal system concept features an additional pumping component powered by tidal stream turbines. Although the tidal energy can be highly predicted due to the shifting of tides, it is less controllable. There could be a situation that the generation time would occur within a non-peak energy demand window, which the price for energy would be less than in the peak window. To overcome this problem, to make this proposed system controllable, the additional pump-turbine unit could adjust the water level in the dock while not consuming additional energy, and from 4.5.2 Case studies, there would be an optimum case for the different demand, which would make sure the hybrid tidal system performs at maximum. Moreover, while under standard operation with no demand requirement, the hybrid system would only engage the turbine-pump unit during the ebb tide, by pumping water into the docks to provide additional head, which from the numeral result, there was a 2% increase in power production. Furthermore, for a site with multiple docks (e.g. Newport Docks), the case study in 4.4 identified that using the larger dock as the main reservoir would provide an advantage in power generation, both in maximum power and generation time.

This numerical model was created based on the theoretical equations, with some of the variables could be sourced from somewhere else, but still some of the key variables were unavailable, as the efficiency profile for the components. This numerical model would need to be validated to prove it can provide accurate and reliable results.

5. Data analysis for Jiangxia Tidal Power Station and further development of the numerical model

5.1 Introduction

Recorded data from the Jiangxia Tidal Power Station was kindly donated to the author to develop the proposed hybrid power system further. As noted in the previous chapter, many parameters in the Matlab program were based on hypothetical theoretical values, due to a lack of real, validated information. However, with the help of technicians at the Jiangxia Tidal Power Station, a set of real recorded data will provide valuable information to this design. Importantly, those hypothetical values previously worked with in the Matlab program will be replaced with real data.

5.2 Real data analysis

By comparing the real data with the results from the Matlab simulations, they provide information on the accuracy of the program. By inputting tidal data into the program, and using the results to compare the given data, this would help to improve the program to provide simulations that are closer to reality.

The first step of the validation was to set the basic parameters. The known parameters are the number of water turbines, the area of the inlet gate, the rated power of the bulb turbines, the maximum level of the reservoir and the minimum and maximum head for power generation. However, some parameters were difficult to identify, e.g. the size of the reservoir. In this case, an approximate value from geographical maps was used. Another issue was the actual site; there was a small water gate allowing water to flow across the lagoon. Information about the dimension of such features is unknown. Table 5-1 lists the known parameters and their values.

Table 5-1 Known parameters for Jiangxia Tidal Power Station

Number of Bulb turbines	6
Area of inlet gate	20 m^2
Rated power of bulb turbines	700 kW
Maximum reservoir level	1.8 m
Minimum head for power generation	0.8 m
Maximum head for power generation	5.08 m

Table 5-2 Unconfirmed parameters for Jiangxia Tidal Power Station

Surface area of the reservoir	1,370,000 m^2
Combined mechanical efficiency of the turbine and generator	90% on the ebb 85% on the flood

5.2.1 Unverified parameters

In studying the data, it was noted that the starting and ending times of all six units were not simultaneous, but for this test, all six turbines start and finish generation at the same time. There will be three examples of how these data were analysed.

Figure 5-1 shows an example that recorded data of reservoir level with the tide on 01/08/2011. The data shows the power output by one of the six turbines, noted that X-axis is the time in minutes, which on this set of data, the data is recorded at each minuet, and for 24 hours, there are 1,440 minutes.

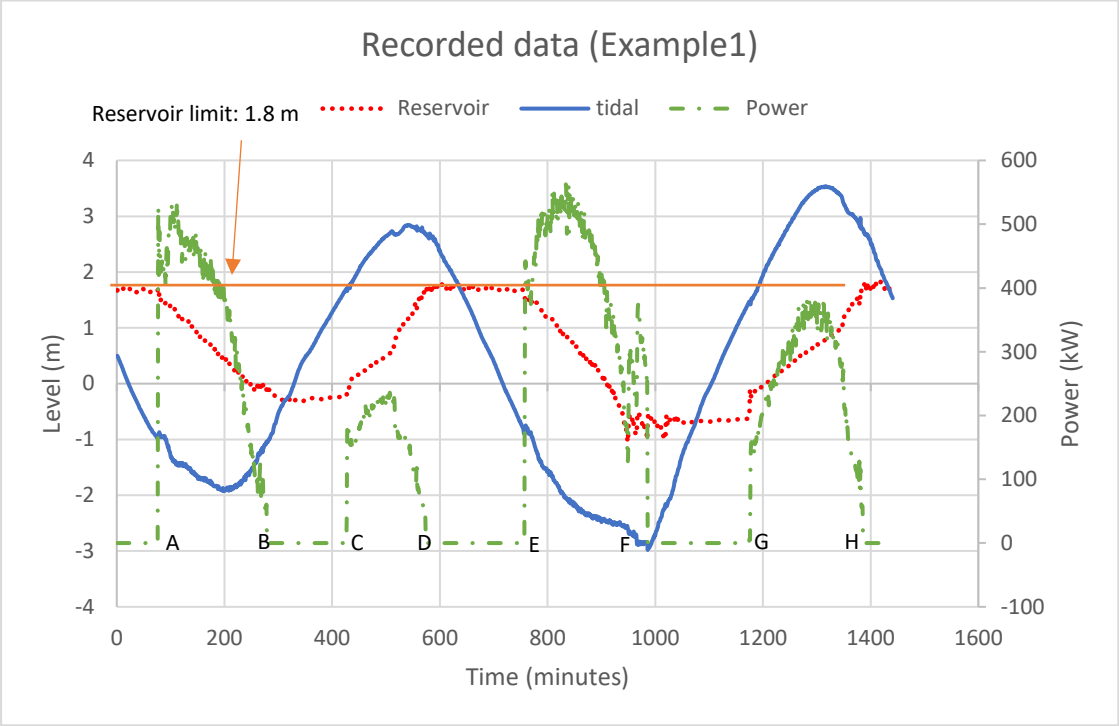

Figure 5-1 Reservoir and tidal levels on 01/08/2011

5.2.1.1 Head value analysis

Power generation requires head. Power is arguably the most important factor in considering a power system. However, the power is also decided by other factors (losses, limits and other user interfaces). Therefore, to understand the power, it was important to understand how the heads were changing. and with that, plus the other profiles, the actual power data can be predicted.

In Figure 5-1, three sets of data are shown; tidal levels (blue solid line), reservoir levels (red dotted line) and power (second Y axis, green dash line), with the different stage marks as shown in Table 5-3.

Table 5-3 Marking of different stages of Figure 5-1

Stage:	Start of the 1st ebb generation	End of the 1st ebb generation	Start of the 1st flood generation	End of the 1st flood generation	Start of the 2nd ebb generation	End of the 2nd ebb generation	Start of the 2nd flood generation	End of the 2nd flood generation
Mark:	A	B	C	D	E	F	G	H

Furthermore, near the starting and ending point of the power generation process, there were some fluctuations, with the most dramatic is occurring near stage F. According to the chief technician at Jiangxia, during these times, the six turbines begin operation in sequence, and that lead to the cause of the fluctuations in reservoir levels.

Test 1:

This test was carried out using tidal data from 01/08/2011, to simulate the operation of the tidal station, using parameters from Table 5-1 and 5-2. The system predicts the level of the reservoir and the total power output. However, due to the missing inlet flow rate (the tidal station used a dynamically controlled guide vane to control the flow), and the efficiency profiles for all mechanical components, the program could not precisely predict power outputs. However, the main objective of this test was to determine how water level in the reservoir change. The results are shown in Figure 5-2.

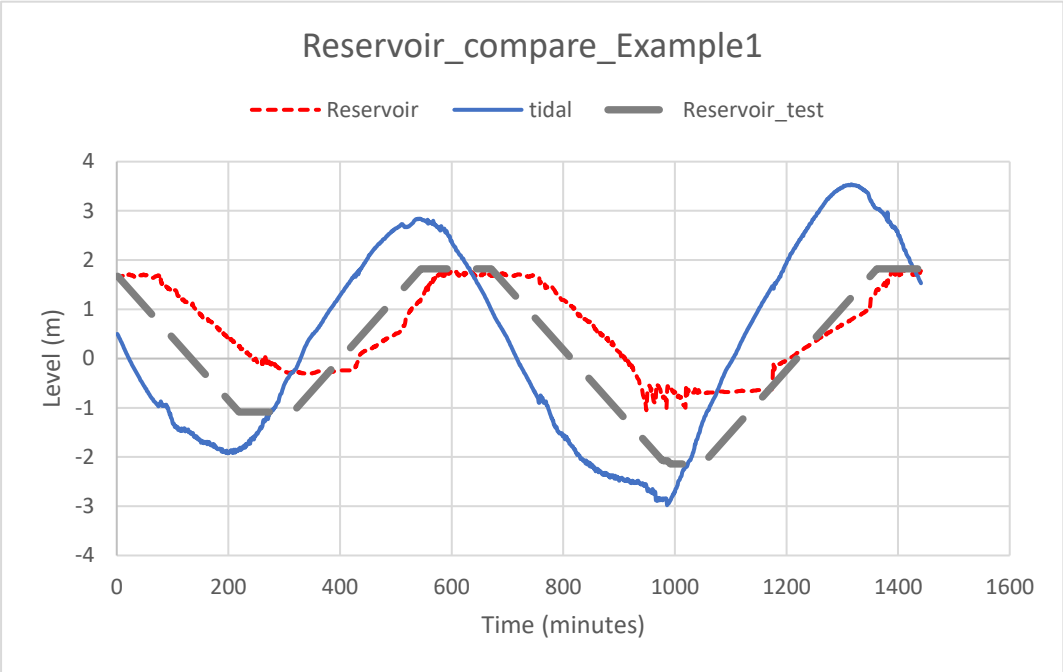

Figure 5-2 Reservoir level comparisons

From Figure 5-2, it was noted that reservoir levels from the simulation (grey dash curve) did not match the real data (red dotted curve). There was also a time shift between these two curves.

Studying the original data once again, what was noticed that from original data, which is shown in Figure 5-3.

According to Figure 5-3, the head values for the starting and ending for Example 1 were highlighted and shown in Table 5-4.

Furthermore, by using the raw data from Figure 5-3, the relationship between the reservoir level and tidal level can also be plotted which is shown in Figure 5-4.

Table 5-4 Level data from key points of Example 1

	Stage	**Time**	**Tidal level (m)**	**Reservoir level (m)**	**Head (m)**
A	Start ebb generation 1	1:16	-0.92	1.6	2.52
B	End ebb generation 1	4:30	-1.23	-0.3	0.93
C	Start flood generation 1	7:05	1.69	-0.24	1.93
D	End flood generation 1	9:32	2.68	1.67	1.08
E	Start ebb generation 2	12:35	-0.89	1.66	2.53
F	End ebb generation 2	16:19	-2.86	-0.77	2.1
G	Start flood generation 2	19:32	1.42	-0.6	2.02
H	End flood generation 2	23:02	2.81	1.7	1.11

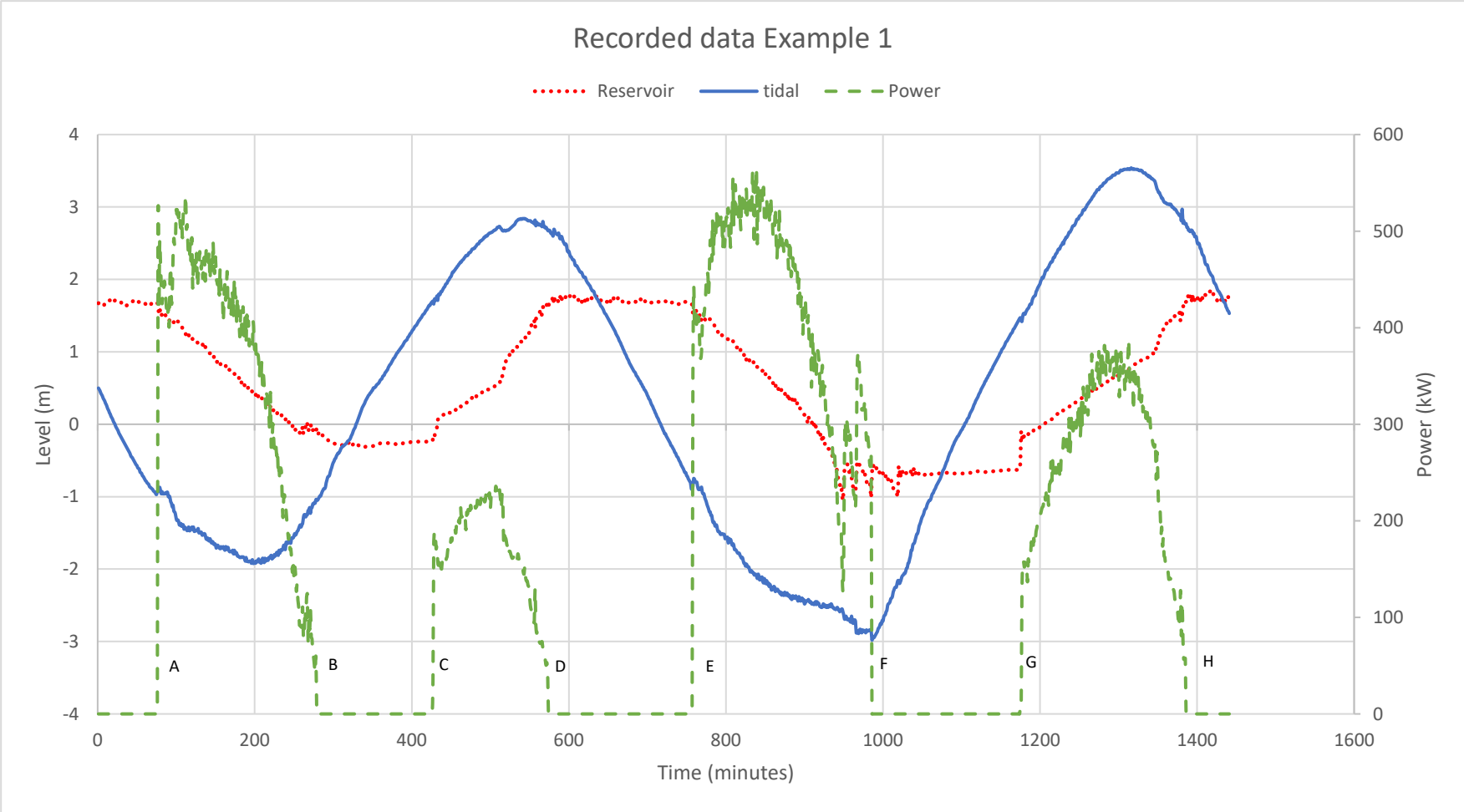

Figure 5-3 Original data on 01/08/2011 with explanations

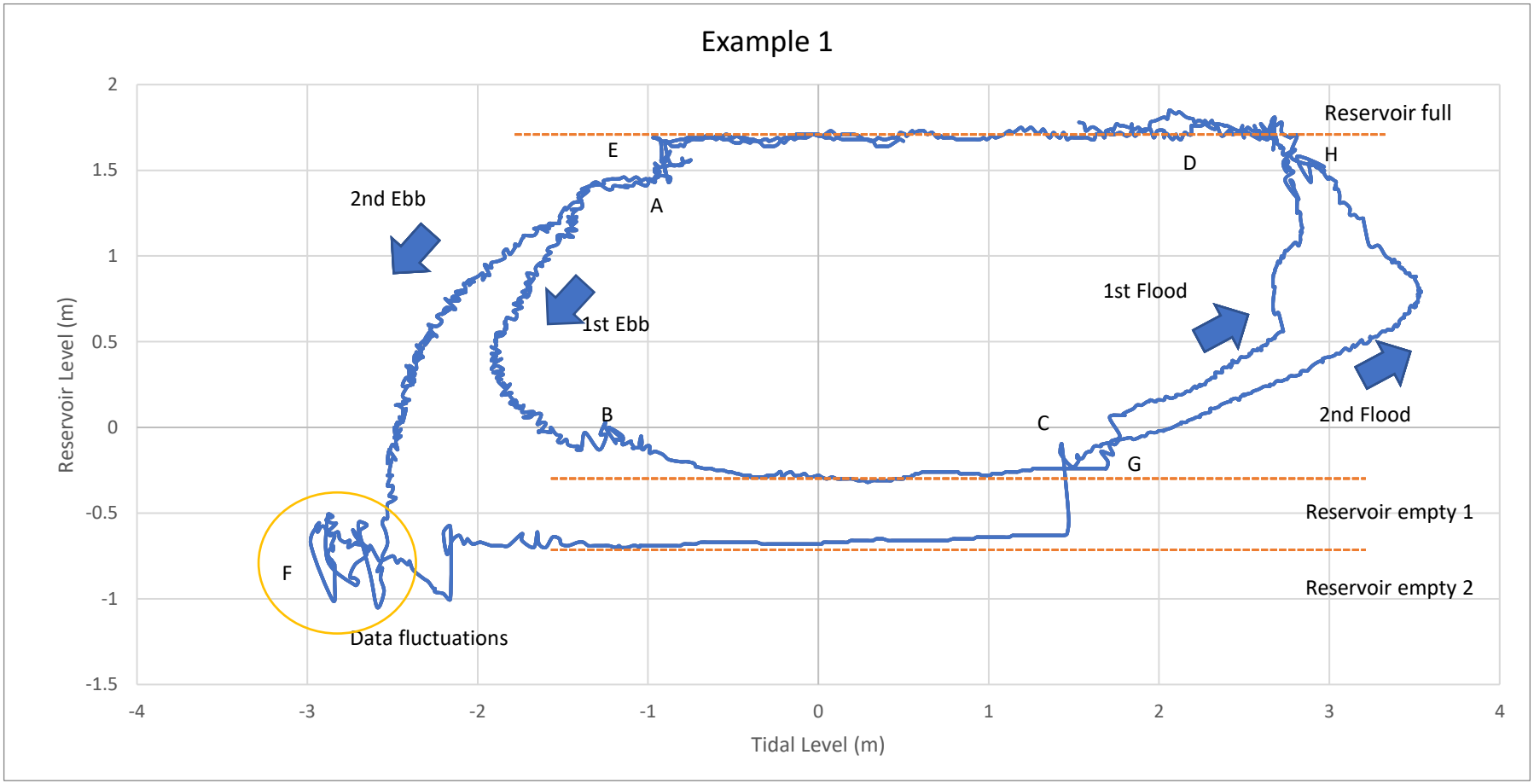

Figure 5-4 Relationship between tidal and reservoir level (Example 1)

Figure 5-4 shows the tidal and reservoir level at each stage, for both flood generations, the generation stopped when the reservoir level reached 1.7 m. Furthermore, there were two different reservoir levels at the end of both ebb generations, -0.3 m for the 1st one and -0.77 m for the 2nd. According to Table 5-3, it was also noticed that for the 1st ebb generation, the Head value was 0.93 m, and 2.1 m for the 2nd, it was assumed that the minimum head requirement for generation was 1 m, and the lower reservoir limit was -0.77 m. Finally, the yellow cycle which highlighted on the left bottom of the Figure 5-4 represents the reservoir level fluctuations at the end of the 2nd ebb generation.

From the given information by the site engineer, the system can be operated if the head was between 0.8-5.08 m. But based on the data, the minimum head in starting power generation was 1.93 m. It was also seen that the conditions for the end flood generation period were the level of the reservoir. From Table 5-3, at both ending points from the two flood generations, the reservoir level was 1.6 and 1.67 m respectively, given the maximum level for the reservoir is 1.8 m. However, for the end of the ebb generation, the first assumption was reservoir level related, because the head from both end points were 1.23 m and 2.1 m respectively. This was a big difference, but by looking at the reservoir level, the first was -0.3 m, and the second was -0.77 m, which were not as close as the flood ones.

From these data, the reasonable assumption was that the starting head for an ebb generation was 2.5 m, and for flood generation, it was 2 m. The end of the generation was reservoir level related for an ebb generation, with generation stopped when reservoir level reached 1.6 m; for flood generation, the assumption was the generation would be stopped under two circumstances, when head less than 1 m or reservoir level below -0.77 m.

To confirm these assumptions, more data was needed for study and analysis.

Data Study 02/08/2011 (Example 2)

To verify the assumptions based on the 01/08/2011 data, data from the next day 02/08/2011 was analysed.

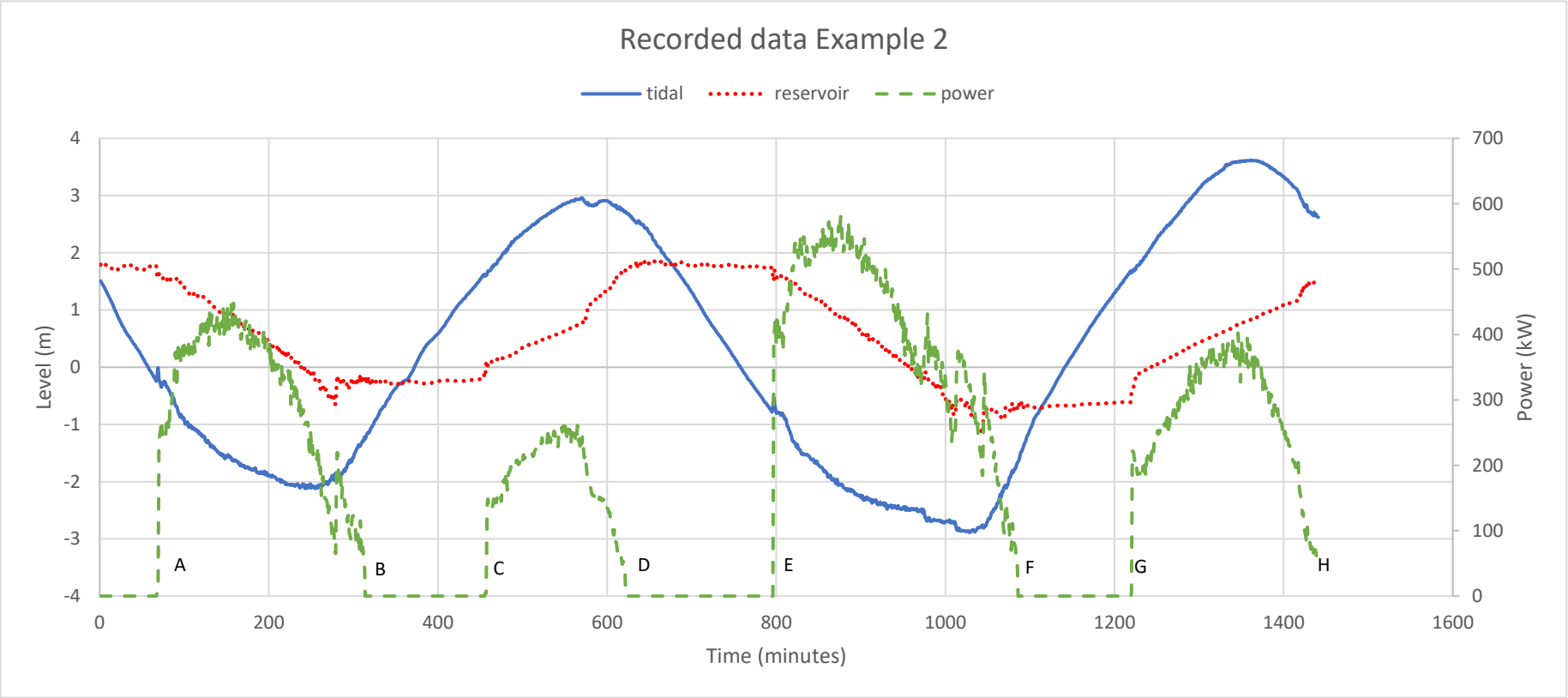

Figure 5-5 Data from 02/08/2011

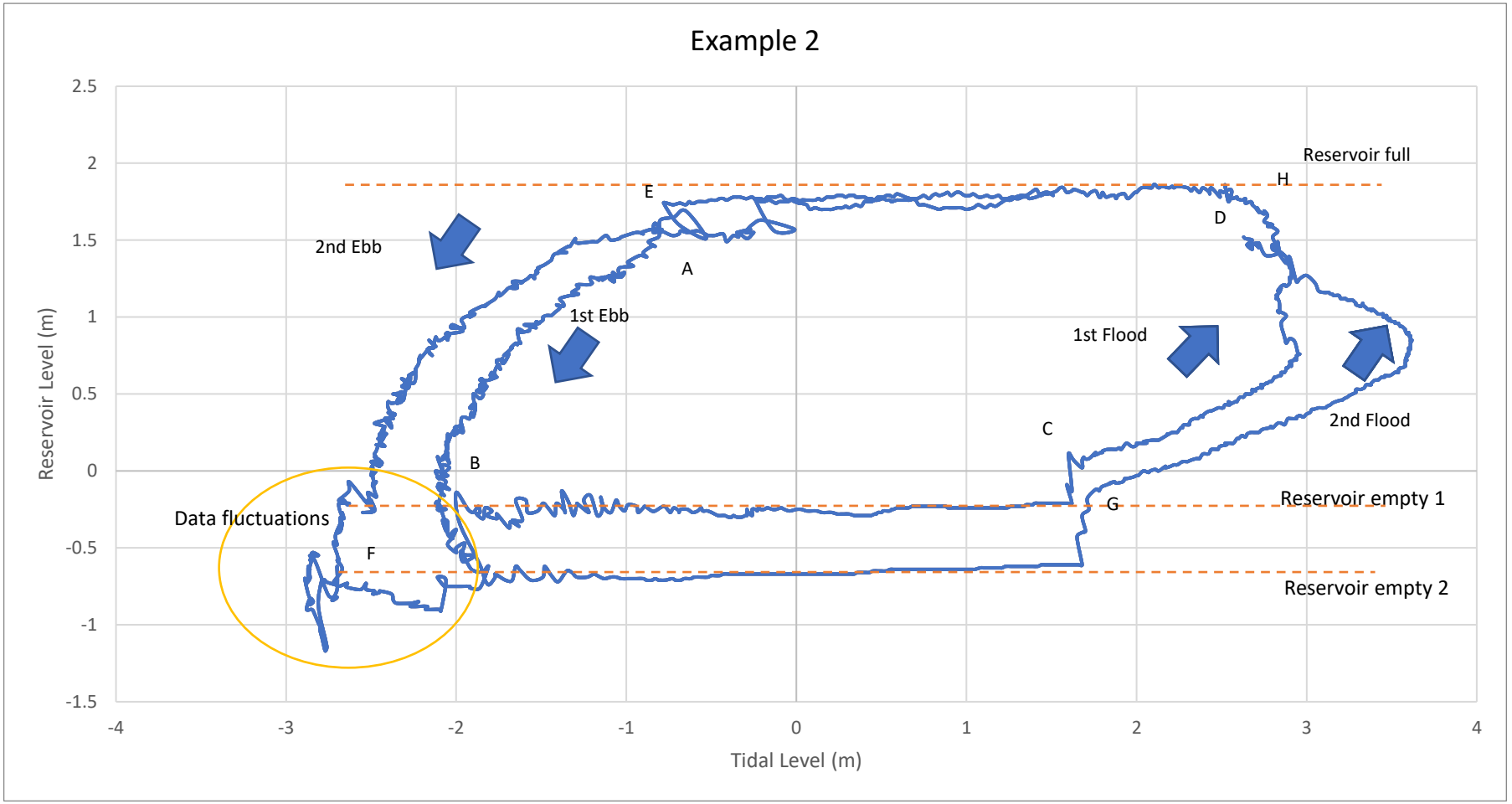

Figure 5-6 Relationship between tidal and reservoir level (Example 2)

To compare with data from Example 1, the same analysis was carried out. Table 5-5 lists the level data from the key points. From Figure 5-5 & 5-6, the tidal range was similar to Example 1, with a maximum height of 3 m and 3.5 m from the two flood tides and -2 m and -2.9 m from the ebb tides. This was compared to day 1; the two maximum values were 2.8 m and 3.5 m, and the minimum were -2 m and -3 m. These similar tidal profiles were very important for analysing the data from two different days. They would be used to verify the assumptions made from Day 1 data analysis.

Table 5-5 Level data from key points of Example 2

	Stage	**Time**	**Tidal level (m)**	**Reservoir level (m)**	**Head (m)**
A	Start ebb generation	1:07	-0.24	1.76	2.0
B	End ebb generation	5:13	-1.22	-0.27	0.95
C	Start flood generation	7:35	1.59	-0.09	1.68
D	End flood generation	10:21	2.71	1.71	1.0
E	Start ebb generation	13:14	-0.78	1.74	2.52
F	End ebb generation	18:04	-1.67	-0.71	0.96
G	Start flood generation	20:18	1.68	-0.61	2.29
H	End flood generation	23:58	2.53	1.55	0.99

From Table 5-5, at the two ebb generations, the reservoir levels were 1.76 m and 1.74 m, which were very close to the claimed 1.8 m maximum at the two starting points. The two lower reservoir levels at the end of both ebb generations were -0.27 m and -0.71 m. Finally, both ebb generations stopped when head value below 1 m, with the 2nd flood generation has reservoir level of -0.71 m, which was higher than the -0.77 m in Example 1. To compare with the values from Table 5-4:

Table 5-6 Head values comparison between Example 1 and Example 2

	Head (m)			
Stage	1st Example 1	2nd Example 1	1St Example 2	2nd Example 2
Start ebb generation	2.52	2.53	2.0	2.52
End ebb generation	1.23	2.1	1.27	0.95

Table 5-7 Reservoir levels comparison between Example 1 and Example 2

	Reservoir Level (m)			
Stage	1st Example 1	2nd Example 1	1St Example 2	2nd Example 2
Start ebb generation	1.6	1.66	1.76	1.74
End ebb generation	0	-0.77	-0.13	-0.61

From Example 1, the assumption for trigger ebb generation was that the head was greater than 2.5 m, and from Example 2, the first ebb generation started with a 2 m head, which was less than the assumed value, but the second value 2.52 m was greater than the assumption. From the reservoir levels, the values were all below the

maximum designed value 1.8 m, but from the 1st Example 2 value in Table 5-6, which was close to the limit 1.8 m, and the head value at that point was 2 m which is below the assumed 2.5 m. This leads to another assumption, which is the reason why the first ebb generation started with a non-ideal head was to prevent the reservoir getting flooded, because the reservoir level was close to the limit, and that was why the generation started with the non-ideal head.

Furthermore, the ending stages for ebb generation provided interesting findings. The head values were different, ranging from a maximum 2.1 m to 0.95 m. But the reservoir level from -0.27 m and -0.30 m from the first generation, to -0.77 m and -0.71 m on the second generation, the findings are from first generation, based on the analysis which discussed in the earlier of this section, it was assumed that there were two conditions that will determine the end of the ebb generation, when head value below 1 m or reservoir level below -0.77 m.

Additionally, From Figure 5-3 to 5-5, it was noted that the range from the first tidal cycle was obviously smaller than the second, with Example 1's range from -2 m to 2.8 m, and the second cycle -3 m to 3.5 m, and from Example 2's -2 m to 3 m from first tidal cycle and -2.9 m to 3.6 m. From these tidal values, the ranges from the second cycle were much higher than the first, but the relationship with reservoir levels cannot be confirmed from these analyses.

For flood generation, the comparison is shown in Tables 5-8 and 5-9.

Table 5-8 Head values comparison between Example 1 and Example 2

	Head (m)			
Stage	1st Example 1	2nd Example 1	1st Example 2	2nd Example 2
Start flood generation	1.93	2.02	1.75	2.29
End flood Generation	1.01	1.11	1.20	0.99

Table 5-9 Reservoir levels comparison between Example 1 and Example 2

	Reservoir Level (m)			
Stage	1st Example 1	2nd Example 1	1St Example 2	2nd Example 2
Start flood generation	-0.24	-0.6	-0.13	-0.61
End flood generation	1.67	1.7	1.6	1.55

From Table 5-8 & 5-9, at the start of flood generation, the average head value was close to 2 m, but there was a 0.54 m gap between Example 2 values. From the reservoir level values, the cut off values were close to the assumed 1.6 m.

Data Study on Example 3:

Figure 5-7 shows Example 3 which is the recorded data on 03/08/2011.

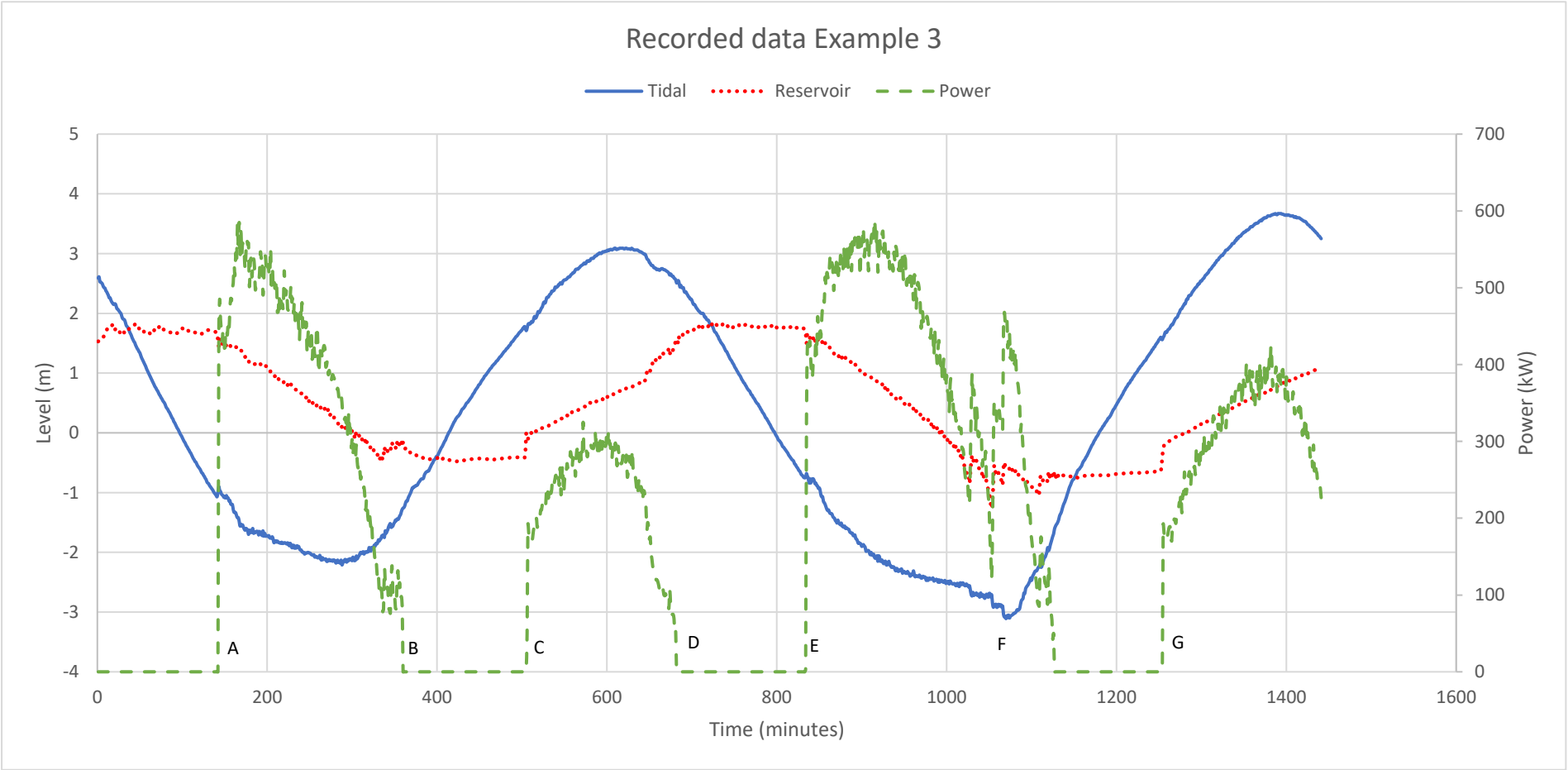

Figure 5-7 Data on 03/08/2011

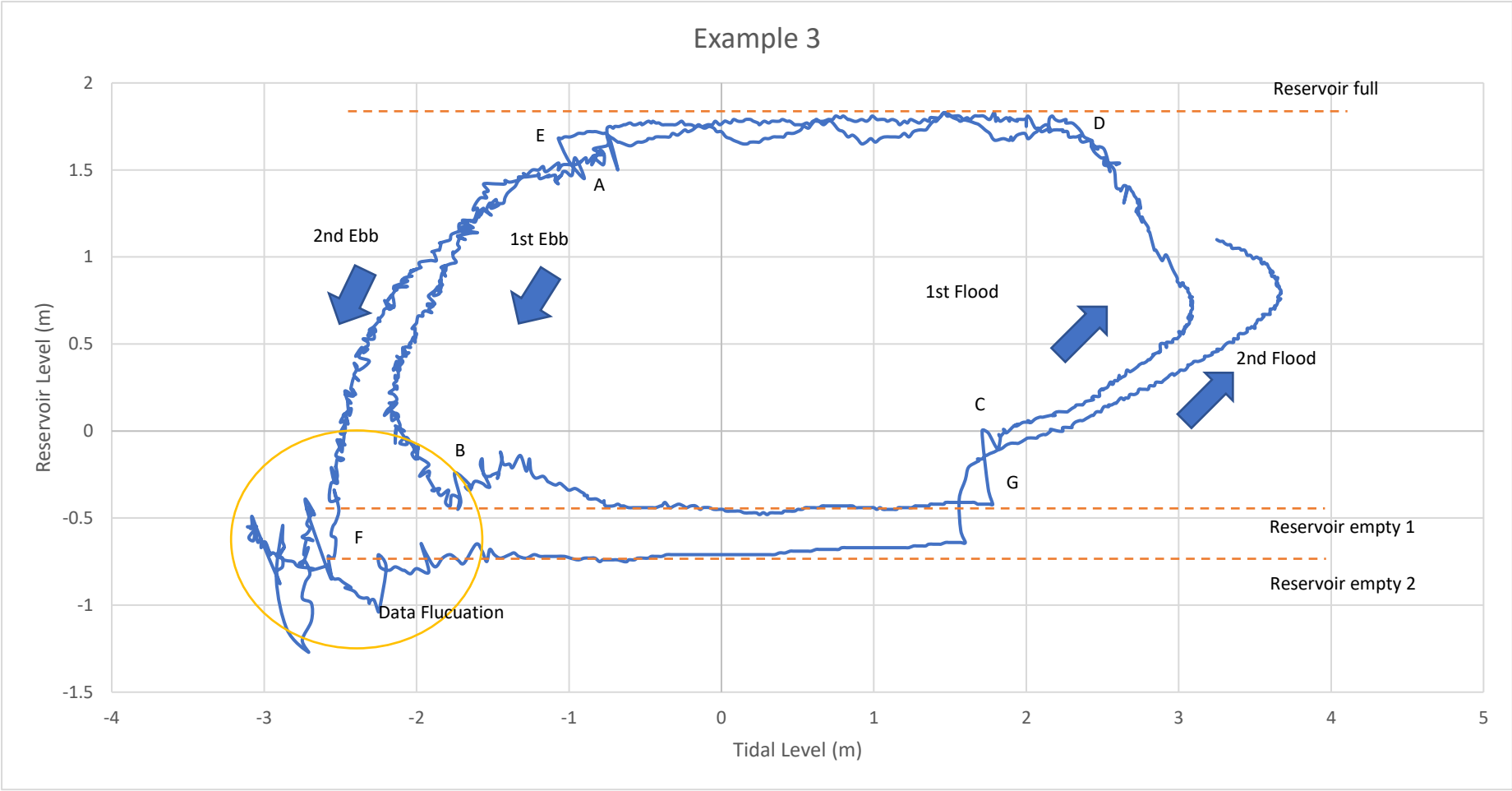

Figure 5-8 Relationship between Tidal and Reservoir level (Example 3)

By performing the same analyses as in the previous studies, the key points are shown in Table 5-10.

Table 5-10 Level data from key points of Example 3

	Stage	**Time**	**Tidal level (m)**	**Reservoir level (m)**	**Head (m)**
A	Start ebb generation	2:20	-1.00	1.55	2.55
B	End ebb generation	5:40	-1.28	-0.23	1.05
C	Start flood generation	8:23	1.78	-0.42	2.2
D	End flood generation	11:20	2.51	1.53	0.98
E	Start ebb generation	13:52	-0.75	1.70	2.45
F	End ebb generation	18:46	-1.69	-0.76	0.93
G	Start flood generation	20:51	1.6	-0.64	2.24
H	End flood generation	00:35*	2.53*	1.55*	0.98*

(* denotes values taken from the following day)

Comparing the data from the two previous examples:

Ebb generation:

Table 5-11 Head values comparison between Examples 1-3

	Head (m)					
Stage	1st Example 1	2nd Example 1	1st Example 2	2nd Example 2	1st Example 3	2nd Example 3
Start ebb generation	2.52	2.53	2	2.52	2.55	2.45
End ebb generation	0.93	2.1	0.95	0.96	1.05	0.93

Table 5-12 Reservoir levels comparison between Examples 1-3

	Reservoir Level (m)					
Stage	1st Example 1	2nd Example 1	1st Example 2	2nd Example 2	1st Example 3	2nd Example 3
Start ebb generation	1.6	1.66	1.76	1.74	1.68	1.66
End ebb generation	0	-0.77	-0.13	-0.61	-0.34	-0.78

From these values, it was believed that the triggering value under normal operations was 2.5 m, and the ending point was based on the reservoir level, where is close to 0 m when the tidal range was low, and -0.7 m for the higher range.

Also, from these six values, only the 1st Example 2 was under 2.5 m, which leads to the assumption, under that scenario, that because the reservoir level was 1.76 m and was

very close to the 1.8 m upper limit, therefore, the system had to release water from the reservoir. However, by looking at other data, it was found that this assumption was wrong. This was due to other data showing that the reservoir held a similar level of 1.78 m for a period, then started to power generation when the head reached 2.5 m, and not 2 m, denying this assumption.

Flood Generation:

Table 5-13 Head values comparison between Examples 1-3

	Head (m)					
Stage	1st Example 1	2nd Example 1	1st Example 2	2nd Example 2	1st Example 3	2nd Example 3
Start flood generation	1.93	2.02	1.68	2.29	2.2	2.24
End flood generation	1.08	1.11	1.0	0.99	0.98	0.98

Table 5-14 Reservoir levels comparison between Examples 1- 3

	Reservoir Level (m)					
Stage	1st Example 1	2nd Example 1	1st Example 2	2nd Example 2	1st Example 3	2nd Example 3
Start flood generation	-0.24	-0.6	-0.13	-0.61	-0.41	-0.64
End flood generation	1.67	1.7	1.6	1.55	1.52	1.55

From Table 5-13 & 5-14, it was believed the head level which triggered flood generation was above 2 m. However, from both head and reservoir levels, there were

two limits for cutting off the flood generation. The first was reservoir level related, which was close to a range between 1.6 m & - 1.7 m (average value 1.65 m taken), and the second limit was head related. From the data from the 2nd Example 2, 1st Example 3 and 2nd Example 3, reservoir levels were 1.55 m, 1.52 m and 1.51 m respectively. There was still a room to reach the 1.65 m value, but the head values dropped from 1.1 m to 1 m, which was the reason why the reservoir did not continue to produce power: the head was too low.

5.2.2 Summary

Based on the analysed data from Chapter 5.2.1, the results which provided a better understanding of how this tidal station works in different tidal scenarios. Some assumptions were made, and then the simulation software was then modified with these assumptions.

For the ebb tide:

Starting conditions: head above 2.5 m.

Ending conditions: reservoir levels dropped to -0.7 m or head is less than 1 m.

For flood tide:

Starting conditions: head above 2 m.

Ending conditions: reservoir levels above 1.65 m or head is less than 1 m.

With the condition settings above, the Matlab software was updated and re-run to check if the results were similar to the recorded data. The input data was again from Example 1 (01/08/2011). By feeding the tidal data from Example 1 into Matlab, and with updated software, the results are shown in Figure 5-9.

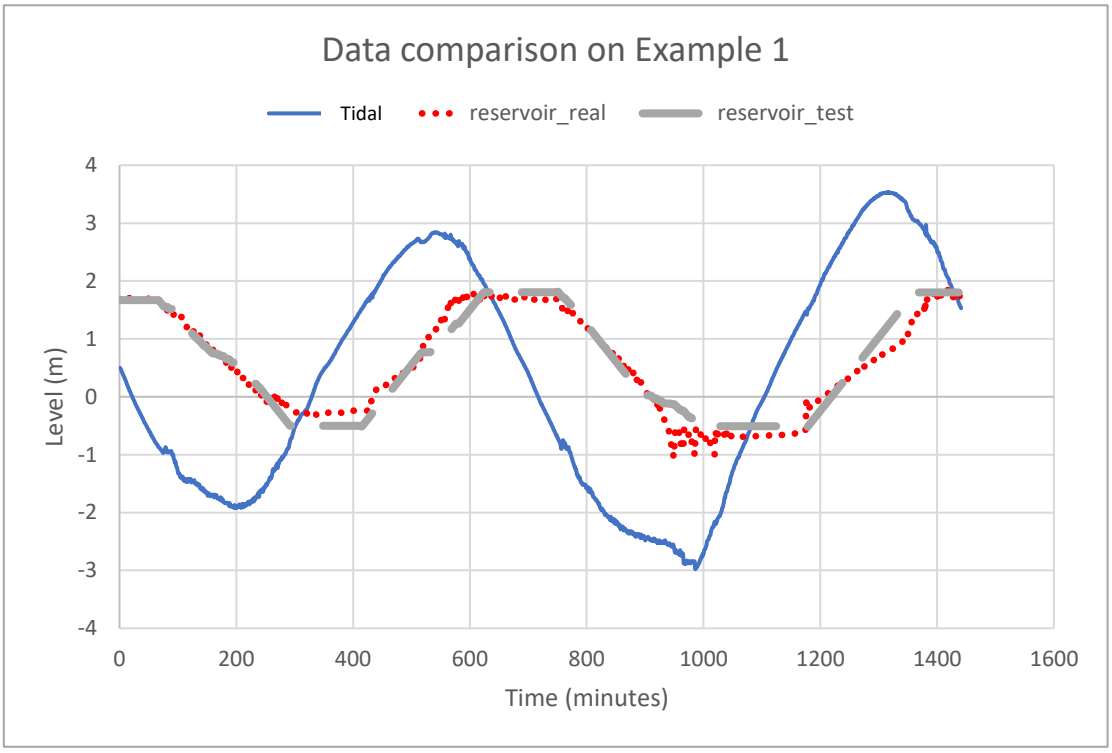

Figure 5-9 Reservoir level comparisons between simulation and real levels

From Figure 5-9, the refined software simulated data matches the real data, although it was not a perfect match. Furthermore, another issue related to reality. When the reservoir shut down after flood generation, reservoir levels continued to rise to levels close to the upper limit; 1.8 m. This was because of a waterway (Figure 5-10) is built inside the barrier, which allowed water to travel freely between the reservoir and the open sea.

Figure 5-10 Overview of the Jiangxia Tidal Power Station (Image source: Xiaoshou.info)

Therefore, after generation, when the water gates for the turbines are closed, reservoir levels were still changing due to the head difference between the tidal and reservoir level, to a small degree. However, the size of this waterway was unknown, but based on the given data, it was possible to calculate the theoretical area of this waterway and update the next development of the software.

5.3 Power data analysis

The previous analysis of data and modification of software predicted the power generation. Because the power output was directly linked to the head, and with the heads correctly predicted, in this section, the power data could be analysed and the results used to improve the software.

From Figure 5-11, which is the same data from Example 1, but this time the concentration is on the power curve.

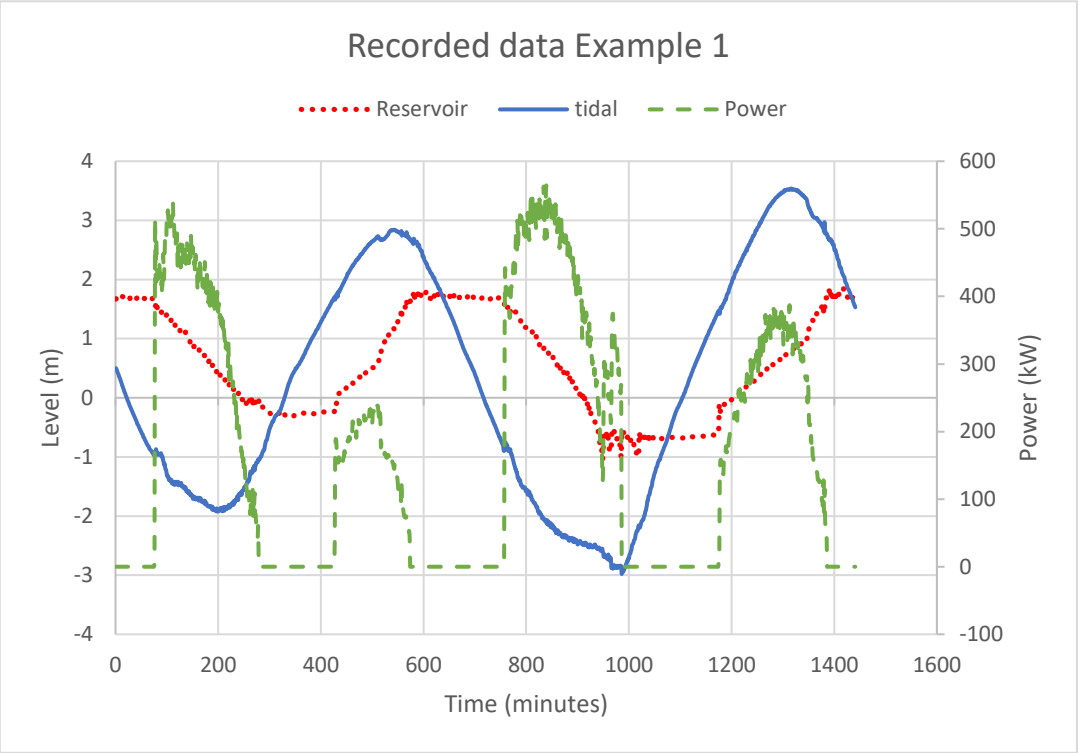

Figure 5-11 Data from 01/08/2011

According to Figure 5-11, it was clear the power generated under ebb tides was greater than the flood tides. It was understood that the under the same settings (flow rate, efficiency, losses), the power generated was directly related to the heads. Therefore, a head-power analysis was important to understand the power outputs, under different heads, under different tidal conditions.

5.3.1 Power-head analysis

The overall efficiency of the tidal system was unavailable. Therefore, to determine this, the power data acquired from Jiangxia Tidal Power Station was used. According to officials from the plant, the inlet flow rate was not measured nor recorded, and the potential hydroelectric power could be calculated by using equation 5-1.

$$P = \eta \rho Q \Delta H \qquad (5\text{-}1)$$

Where P is the potential power in watt, η is the system efficiency, ρ is the density of

the fluid with the value of 1030 kg/m^3. *Q* is the inlet flow rate in m3/s and *ΔH* is the head difference in m.

According to Equation 5-1, the system efficiency *η* can be calculated as:

$$\eta = \frac{P}{\rho Q \Delta H} \qquad (5\text{-}2)$$

However, flow rate *Q* was not recorded by the tidal station. To use equation 5-2, an alternative approach was proposed.

The flow rate *Q* can be calculated by;

$$Q = A\sqrt{2g \cdot \Delta H} \qquad (5\text{-}3)$$

Where *A* is the area of the inlet with a value of 20 m^2, *g* is the gravitational acceleration and *ΔH* is the head defence. Therefore, combining equation 5-1 and 5-3;

$$P = \eta \cdot \rho \cdot \Delta H \cdot A \cdot \sqrt{2g\Delta H} \qquad (5\text{-}4)$$

Overall efficiency is;

$$\eta = \frac{P}{\rho \cdot \Delta H \cdot A\sqrt{2g \cdot \Delta H}} \qquad (5\text{-}5)$$

Where P, and ΔH are both recorded, and *ρ*, *g* and *A* are a constant value. Therefore, the overall efficiency can be calculated using power *P* and head *H*.

5.3.1.1 Analysing power versus head

By separating one day's generation cycles into 4 periods, 1st ebb, 2nd ebb and 1st flood and 2nd flood, to see how power generation changes under different tidal scenario and head, a detailed head-power analysis can be carried out.

Figure 5-12 shows an example which the relationship between the power output and head difference of a turbine, with A marks the starting of the generation and B is the

end.

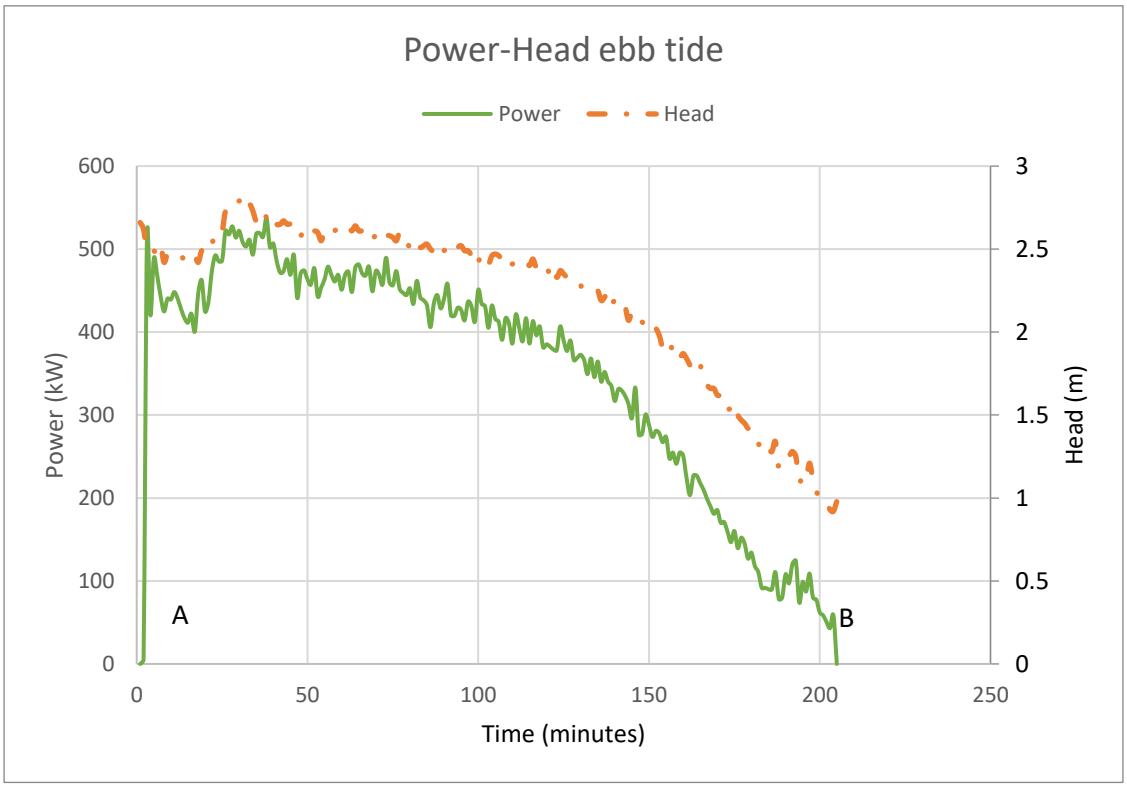

Figure 5-12 Ebb generation head-power data

From Figure 5-12, if only consider where the power generation is above 100 kW (under normal generation conditions with an operative head), the average power for the 1st ebb was 390 kW with an average head 2.34 m;

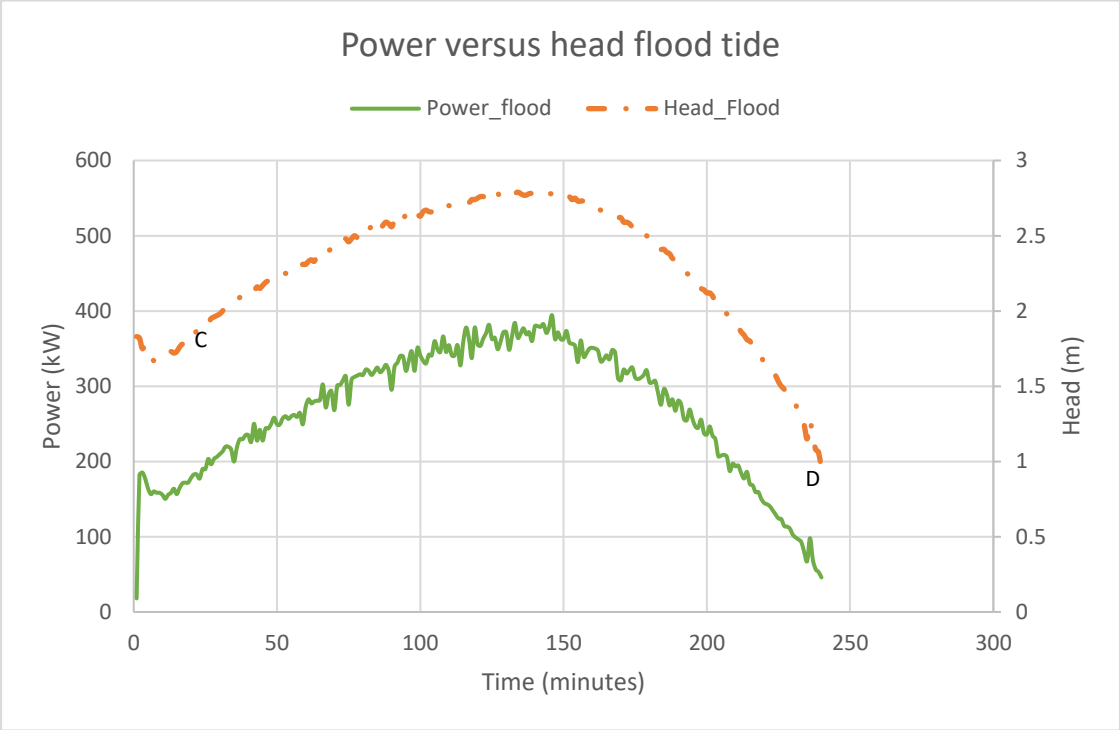

Figure 5-13 Flood generation power versus head

For the flood tide, an example is shown in Figure 5-13, with C marks the start of the generation and D marks the end. From the examples shown in Figures 5-12 & 5-13, for different tidal conditions, even under the same head, there were differences in power generation. According to these results, for a head of 2 m, for an ebb tide, 400 kW power was generated, but only 208 kW was generated for the flood tide. The ebb tide generated approximately 100% more energy than the flood tide, under this head.

After the data was analysed, the relationship between the head and power outputs for the different tides are shown in Figure 5-14 and 5-15, respectively.

From both figures, the curves representing the head and power for both ebb and flood were close to linearity. Additionally, it was clear that for the ebb generation, for the same head, the power output was higher than the flood generation. As a result, a function of the power output and the head difference for Jiangxia Tidal Power Station can be calculated using tidal levels and power data.

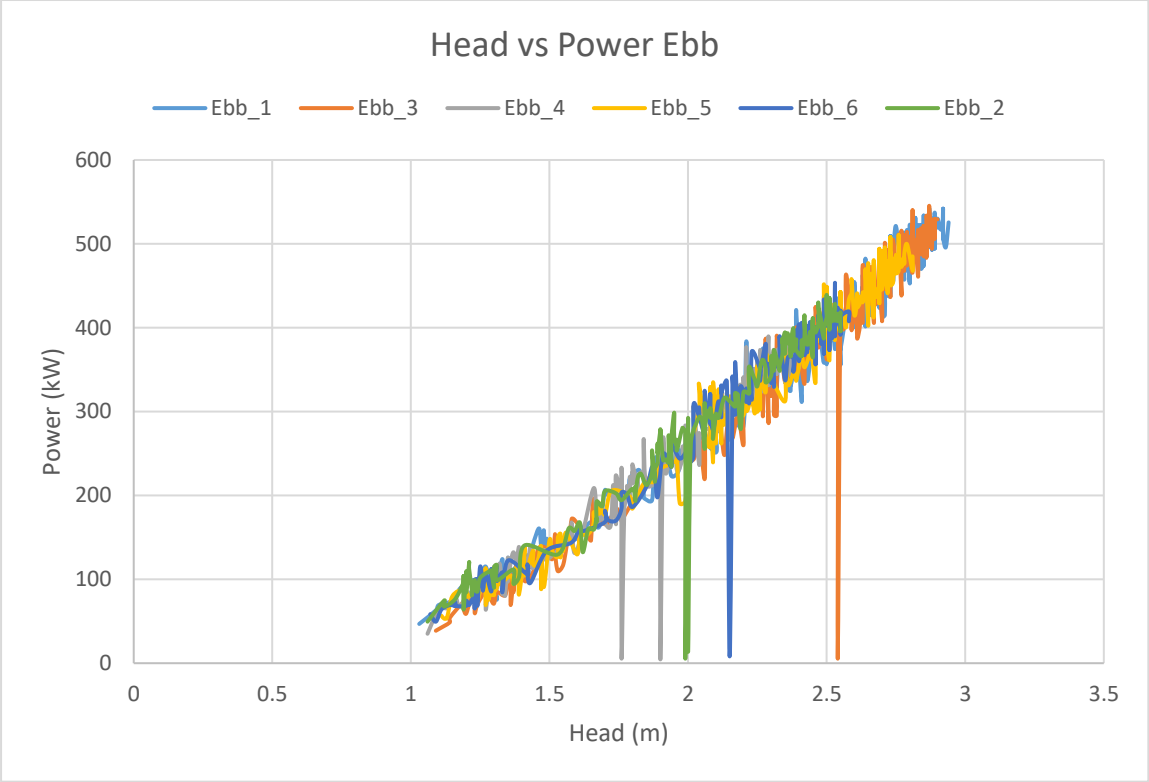

Figure 5-14 Tidal data from the 1st week of August 2011 for ebb generation

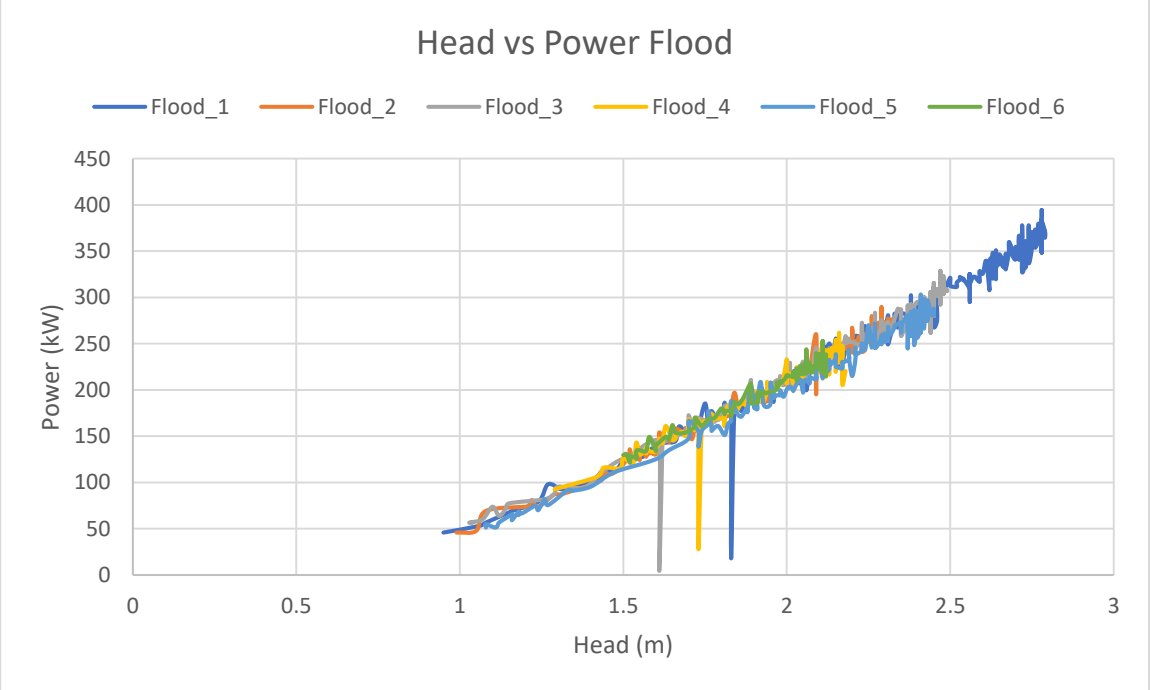

Figure 5-15 Tidal data from the 1st week of August 2011 for flood generation

From the results from Figure 5-14 & 15, the power output under the same head was

different under ebb and flood tides, with more power generated under ebb tides. There are two assumptions made to explain this situation:

1. Efficiency difference:

   The turbine efficiency varies in different tidal scenarios, because the water would hit the turbine from different directions, which would have a result in efficiency difference.

2. Flowrate control:

   The tidal station controls the amount of water goes into the reservoir during the flood tide because it has an upper reservoir level. In order to keep the reservoir level below that limit, the inlet flowrate during the flood tide was controlled. During the ebb tide, the reservoir won't be flooded because the water is existing, the controlled flowrate would be higher than flood tide.

However, these two assumptions were not be confirmed by the officials from the station.

5.3.2 Validation of the power data

From the results in Chapter 5.2 and 5.3.1, Figure 5-16 shows an updated numerical model for Jiangxia Tidal Power Station, validated by inputting the tidal data only.

Figure 5-16 Power data comparison: Example 1

The orange curve represented results from the numerical model given the same tidal level input. From Figure 5-16, the results from the numerical model matched the real data at the start and ending points. For the maximum power outputs, the patterns generally matched. However, in the latter part of the 2nd ebb generation, there was a mismatched area, where the difference between the two results was significant. This was due to the fluctuation of the original recorded data, discussed in a previous section (Chapter 5.2.1), which could provide incorrect values. Moreover, for the last generation, the two results were not matched perfectly, the predicted maximum power was reduced by 15%, about 50 kW.

A different set of data which was selected randomly was input in the model, the original and simulated results are shown in Figure 5-17.

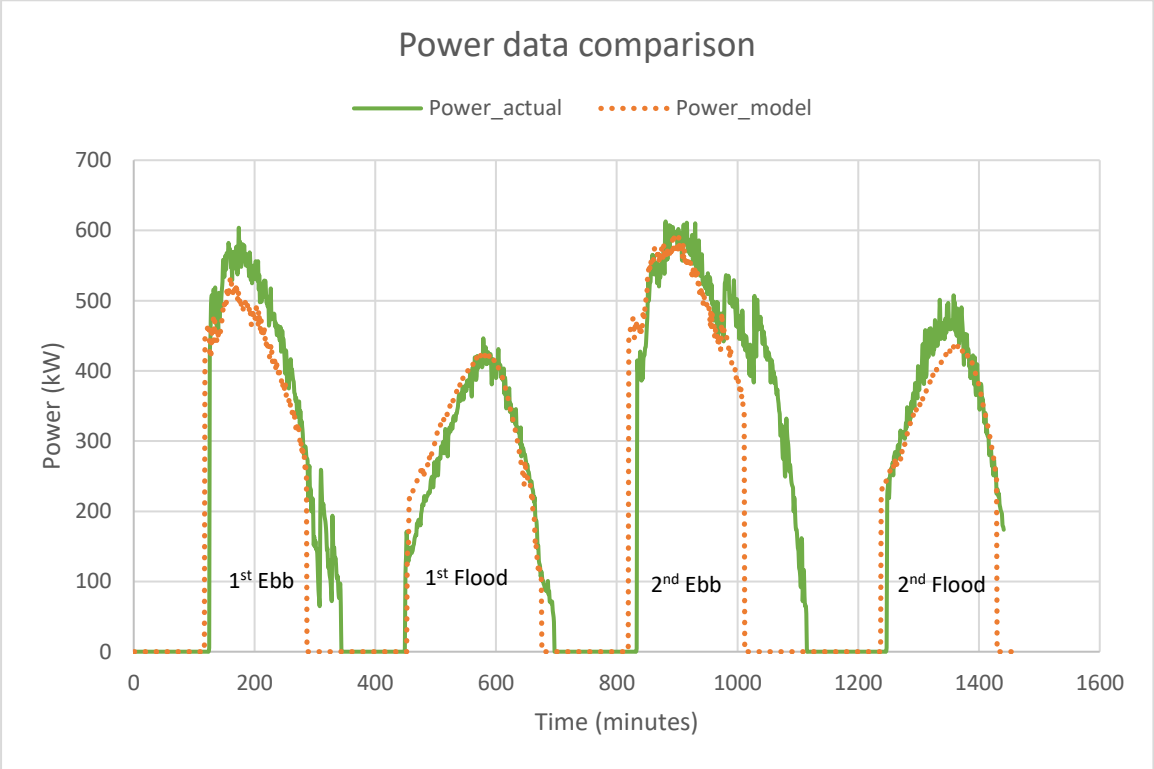

Figure 5-17 Power data comparison: Example 2

From Figure 5-17, the power results from the numerical model generally follows the same trend as the recorded data. The numerical model predicted less peak power in 1st ebb and 2nd flood generation, also during the end of both ebb generations, there were fluctuations that recorded in the real data, which the numerical model did not show this scenario. However, for generations do not have fluctuations, such as 1st flood and 2nd ebb generations, the results from the model generally matched the recorded data, have similar peak power, and matching the starting and ending time.

5.3.3 Discussion

By using this method, a relationship between the power and head was analysed using power and level data. Comparing the level results between the numerical model and the actual data, overall, both results matched. With the recorded values, there were fluctuations, which is to be expected as the water was constantly moving. Also, the

location of sensors could be a factor accounting for fluctuations. For the power data, the overall patterns were matched, but in some areas, there were still differences. However, the method used for the numerical model was based on assumptions from an analysis. With the help of data from Jiangxia Tidal Power Station, many assumed variables used in the numerical model were replaced with actual values. But some values could not be confirmed, including an efficiency profile for the system. Moreover, with the correct reservoir level prediction, if an efficiency profile were provided, then the numerical model would be more accurate for power prediction. Furthermore, it was confirmed by their engineer that sometime, the station would alter the setting for the initiation of power generation, which means it could start at different head, but the conditions that determine the end of generation would remain unchanged.

The software would be able to predict the potential power output at any location if the detailed information is provided.

5.4 Development of a data analysing software

5.4.1 Introduction

The data acquired from Jiangxia Tidal Power Station was comprehensive. The data included:

1. Power data for all six turbines,
2. Level data for reservoir and tides,
3. Guide vane angles for all six turbines,
4. RPM for six generators,
5. Output frequencies from six generators.

These data were recorded daily on an Excel spreadsheet. Moreover, one data point

was logged every minute, e.g. the power data for a day consisted of six turbines over 1,440 minutes, totalling 8,640 values under one category. It was found it is very hard to pin the key moments in the data, with only values and times were recorded. To analyse the data quickly, a tool was required to sort the data, pick out key points and distil the most important information to the user.

5.4.2 Logic of the program

A Matlab program was created to analyses the raw data. The reason why Matlab was used is because that the program has the ability to calculate large amounts of numerical data quickly. The program analysed the power data along with the tidal and reservoir levels. However, the program was flexible as more elements could be added if required.

Two categories of excel data were inputted into the sorting program, tidal levels and power data. This program would analyse the two data sets and provide results for:

1. Peak power for power generation along with tidal levels;
2. Average generation power;
3. Total generation time; and
4. Total energy generated.

5.4.3 Determining peak power

To determine the peak power, the program had to determine how many generation cycles were occurring during that day. For a standard day, there would be four cycles. However, tides were consistently shifting, and also the power station was not guaranteed to run a full energy production. Sometimes the power station ran a reduced service, where there were 1, 2, 3 or no generations at all.

There were two scenarios:

1. The day begins with on-going generations.

2. The day begins with no generations.

For option 1, the first value of the power data would be greater than 1, because it was part of the generation which started the day before and carried on for the next day. Option 2 is for the first value of zero, meaning there would be a generation later that day.

There are 5 examples will be discussed.

5.4.3.1 Example A: First power value is greater than zero:

If the first value was greater than zero, this meant the generation was started the day before the recording. For this scenario, the system would decide whether peak power had passed or was yet to come. In Figure 5-18, the first value is greater than zero. The program would detect the ending point of this on-going generation, then calculate the elapsed time, starting from 00:00. If the elapsed time between the first data point and the first zero was greater than 100 minutes (the average generating time for ebb was 230 minutes and for the flood was 150 minutes), then the first peak value would be chosen between this period. Otherwise, this generation period would be neglected, as the peak value may have passed.

The system would then pick up the 2nd non-zero value, and the first zero value after the non-zero value to determine the 2nd generation period, and on to find the maximum value of that period.

For the last generation of the day, if there were no zero value by the end of the data set, the program would calculate how long the system had generated before the end of the day. If the time was greater than 100 minutes, then it would pick up the peak value, otherwise it would neglect this generation.

For each peak value, the program finds the allocated position of this value in the data

set and uses that position in the tidal data to find the corresponding tidal level.

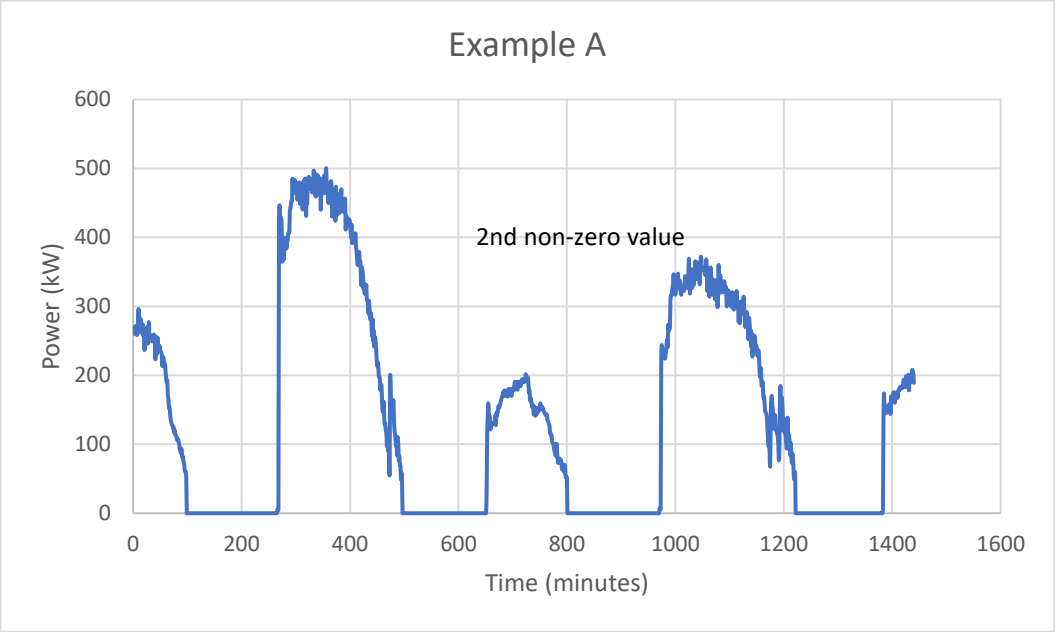

Figure 5-18 Example A: If the first power data value is non-zero

5.4.3.2 Example B: First power value is zero:

If the first power data value is zero, as shown in Figure 5-19, the first generation would be the first one of the day.

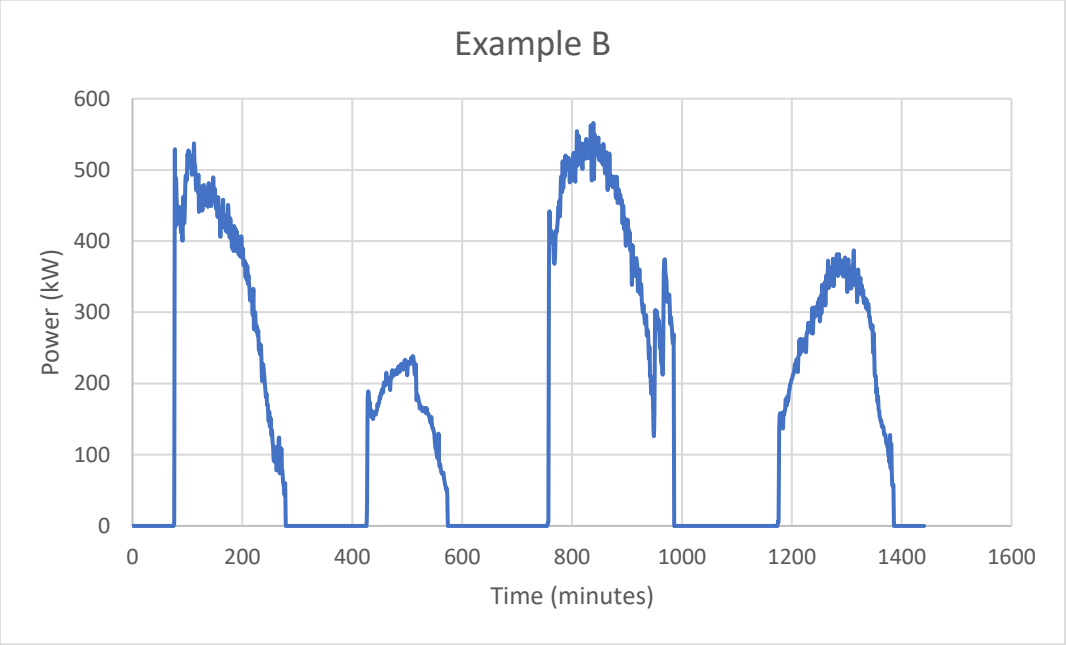

Figure 5-19 Example B: The first power data value is zero.

In this case, the program picks up the first non-zero value. This marks the starting point of the first generation. The first zero value after that marks the end of the first generation, then it picks up the maximum value between these periods. This is followed by the same method for the rest of the generation.

5.4.3.3 Example C & D: Reduced generation cycles

Figure 5-20 and 5-22 show examples of reduced generation service from the Jiangxia Tidal Power station. The most extreme case is represented in Figure 5-20, where there were no generations at all for the day, where the recorded power values were zeroes. However, from the tidal and reservoir level on that day which is shown as an example in Figure 5-21, it shows that water still travels between the dam. There was no official explanation for this situation, but technical maintenance was suspected.

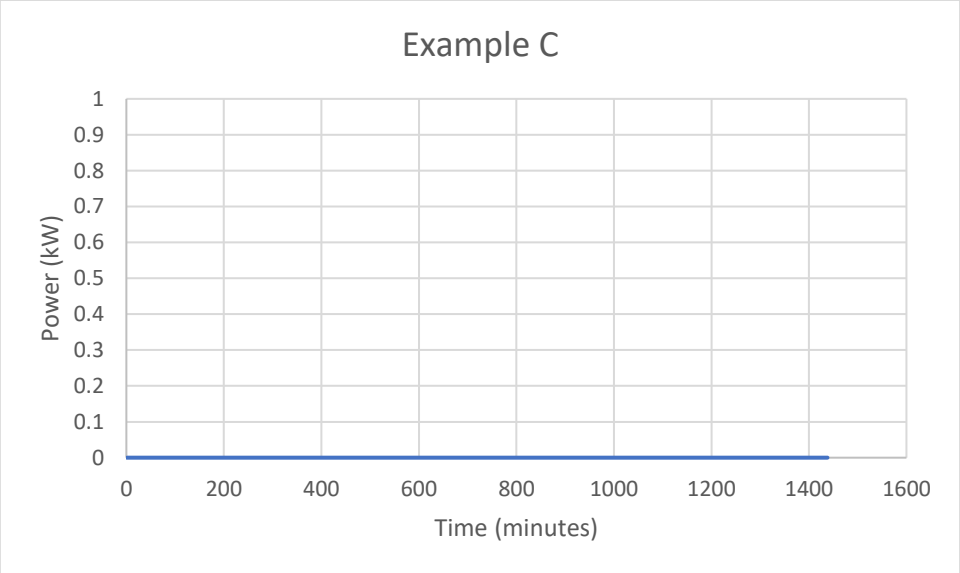

Figure 5-20 Example C: Zero values recorded in power data

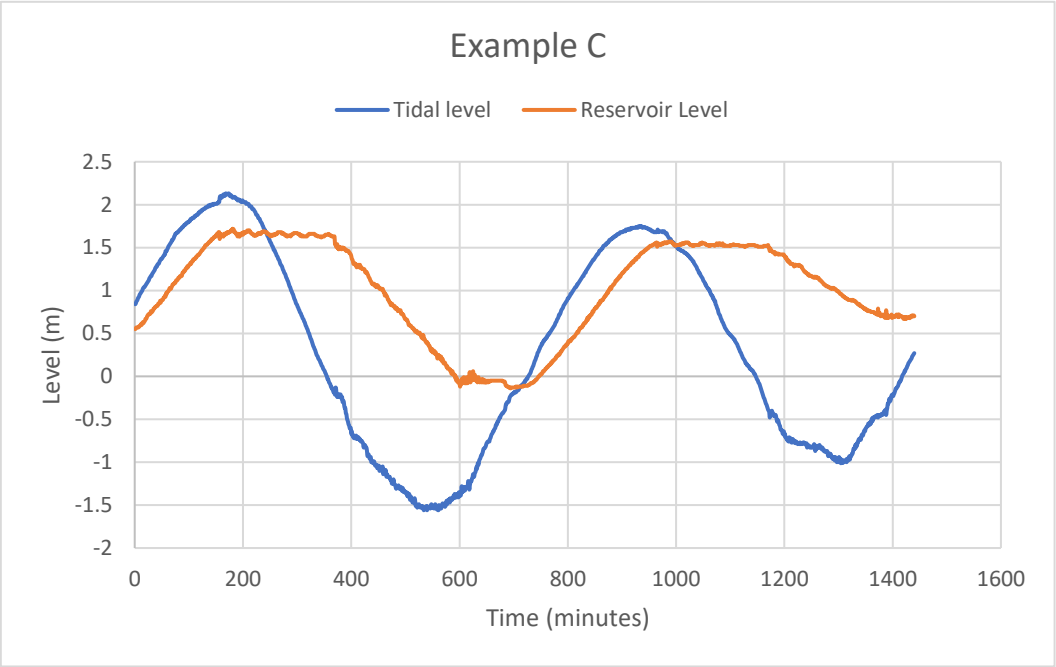

Figure 5-21 Example C: Recorded tidal and reservoir level

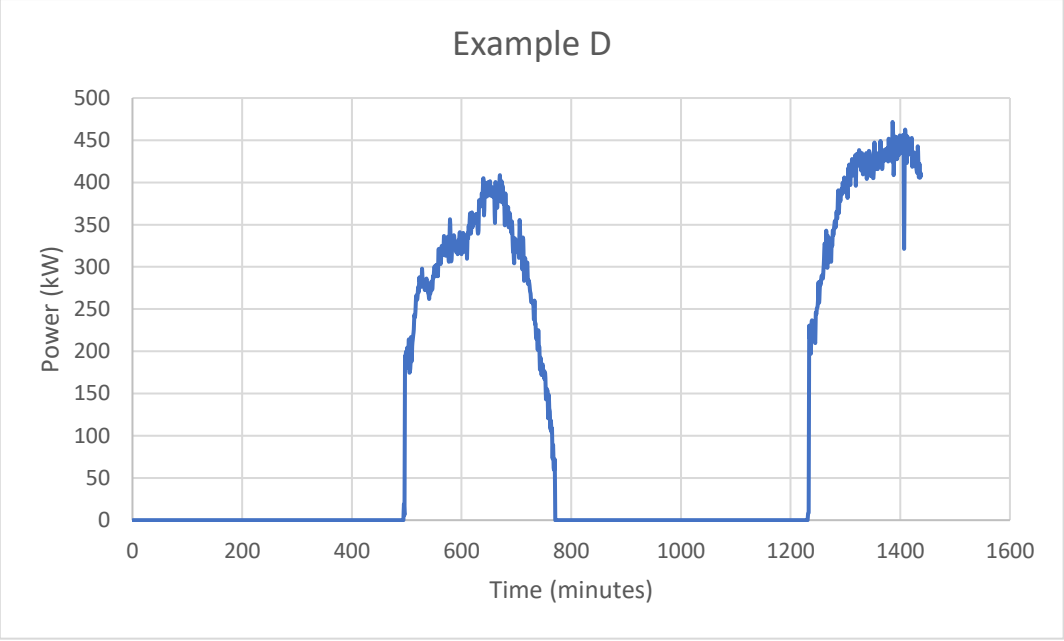

Figure 5-22 Example D: Reduced generations

Figure 5-22 indicates that the tidal station only ran two generations rather than the standard four. Again, there was no official explanation for this.

This sorting software will detect these scenarios if no generation occurred during the

tide, then that value will be recorded as zero in the software. If the elapsed time between generations were greater than 300 minutes (average time between generations was 150 minutes), then the program would declare that the maximum power for that period was zero because there was no generation. It would move onto the next period. Moreover, if the data were like that represented in Figure 5-15, then, for that day there would be no generation, the peak power results for that day would be four zeros.

5.4.3.4 Example E: Bad recording

By looking into the data, sometimes, a bad recording was stored in the Excel data sheet which is shown in Figure 5-23. From this figure, at the start of the 4th generation, there was a negative power value. After consulting with the engineer, the explanation was a bad data point due to a technical issue, which could be ignored.

The sorting software treated every negative power value as zero, as bad data did not represent the real situation.

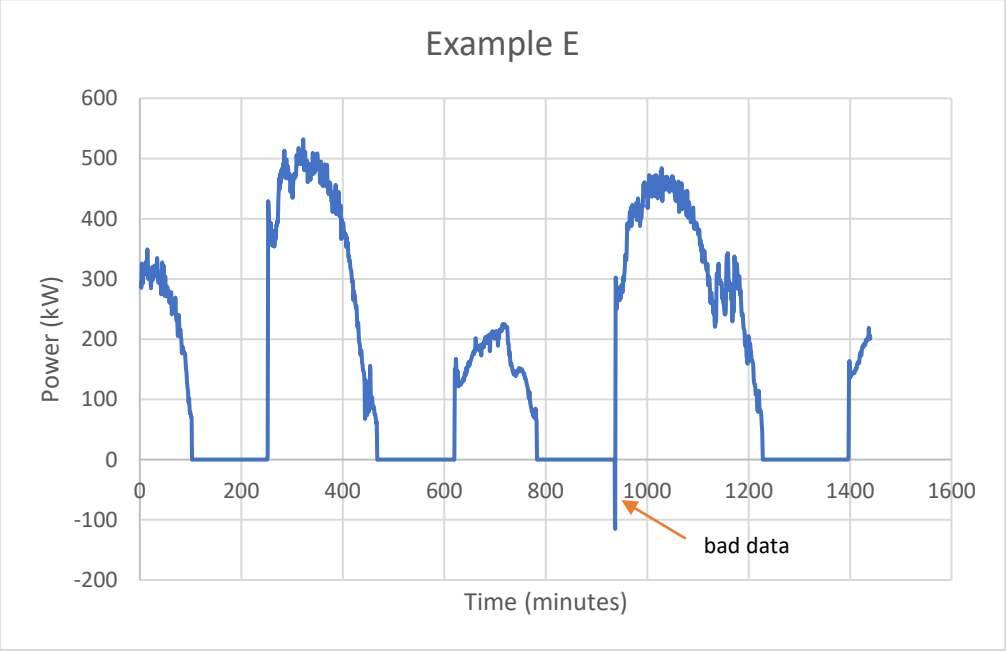

Figure 5-23 Example E: Bad data recording

5.4.3.4. The four-month peak power versus tidal level data

By using this sorting software, the raw recorded data can be analysed quickly, with the key point highlighted, Figure 5-24 to 5-27 show examples shown the result of the software by analysing input the 4-month data.

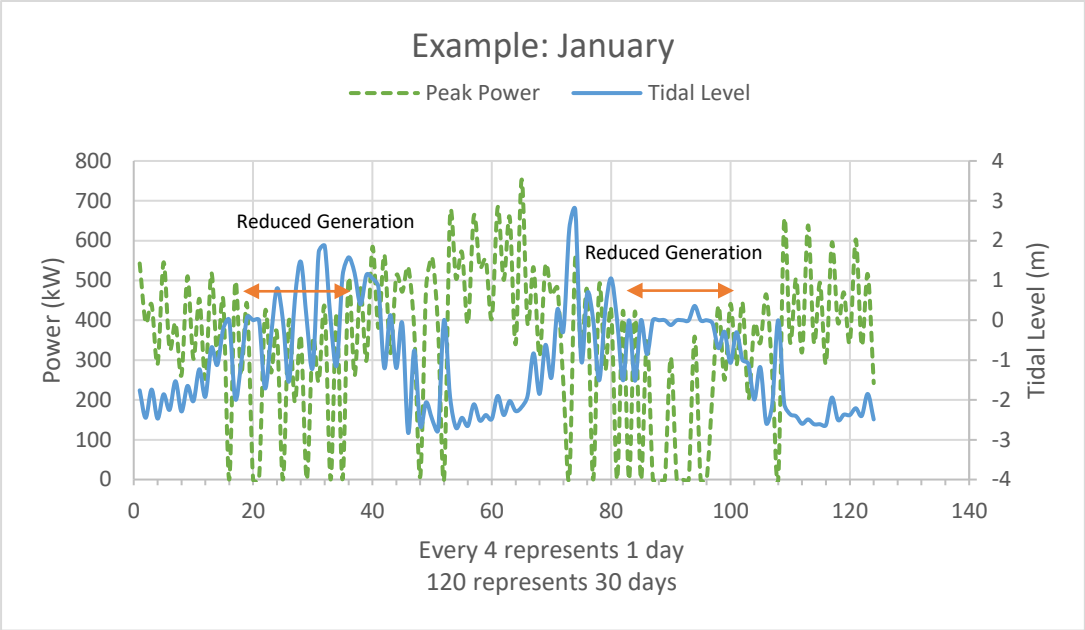

Figure 5-24 Data from January

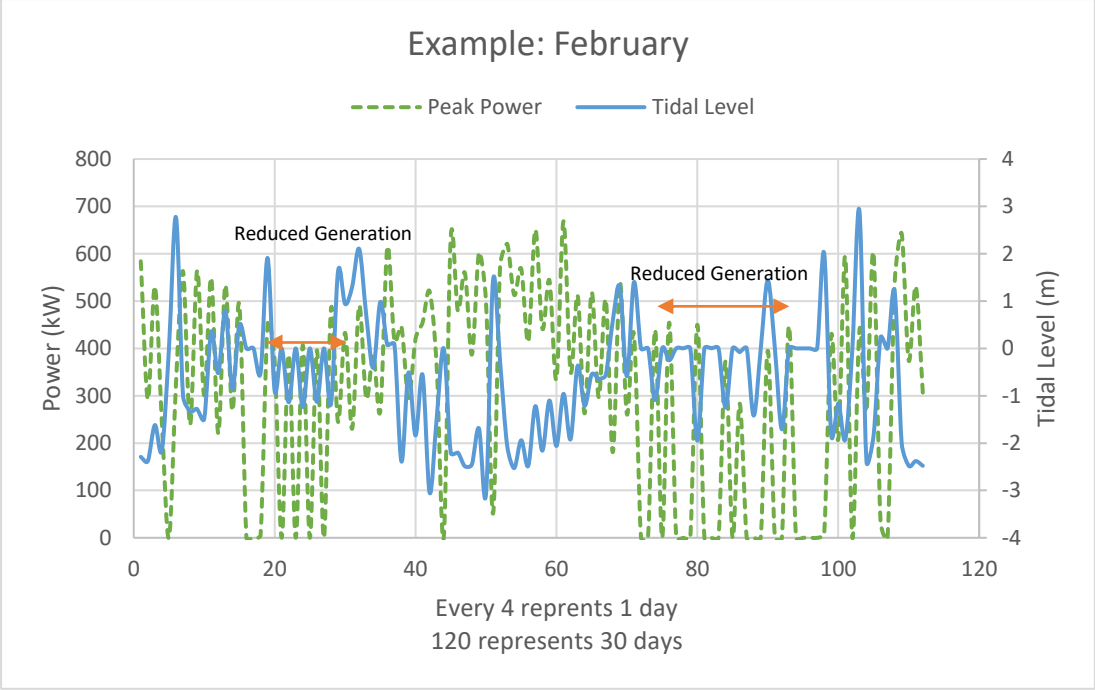

Figure 5-25 Data from February

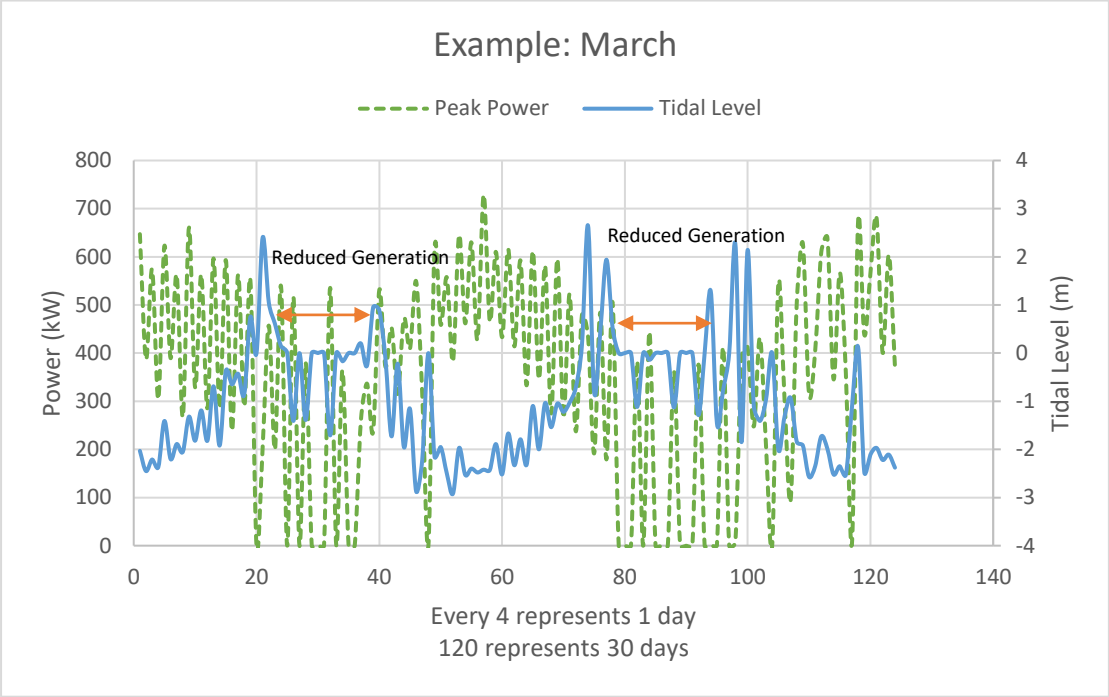

Figure 5-26 Data from March

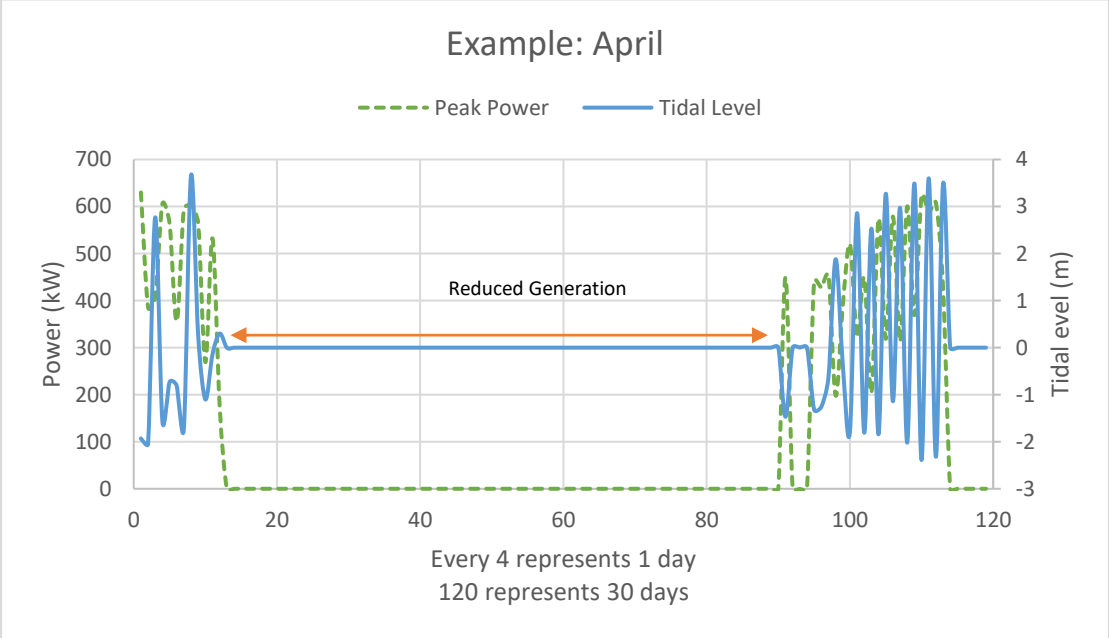

Figure 5-27 Data from April

Figures 5-24 to 5-27 show the three-month peak power versus tidal level analyses using the sorting program. The left Y-axis is the power (dashed green line), the right Y

-axis is the tidal level (solid blue line). The X axis is the number of data, the programme select four peak values from each generation cycle for each day, therefore, every four data represents one day, 120 represents 30 days.

From these data between January to March, between 80-100 (Day 20 to Day 25) and 20-28 (Day 5 to Day 7), all three sets of data show reduced generation cycles; Figure 5-27 shows in April, when the majority of the time, the system did not produce any power. The reason for this behaviour was unclear, there was no official explanation, it was assumed that planned maintenance was carried out during these periods, but this could not be confirmed.

5.4.4 Average power

After inputting the recorded power data, the sorting software outputted the average power during a day's generation. The software detected and calculated the number of all non-zero values and calculated the average power for a day's generation. An example is shown in Figure 5-28, which shows the results for January.

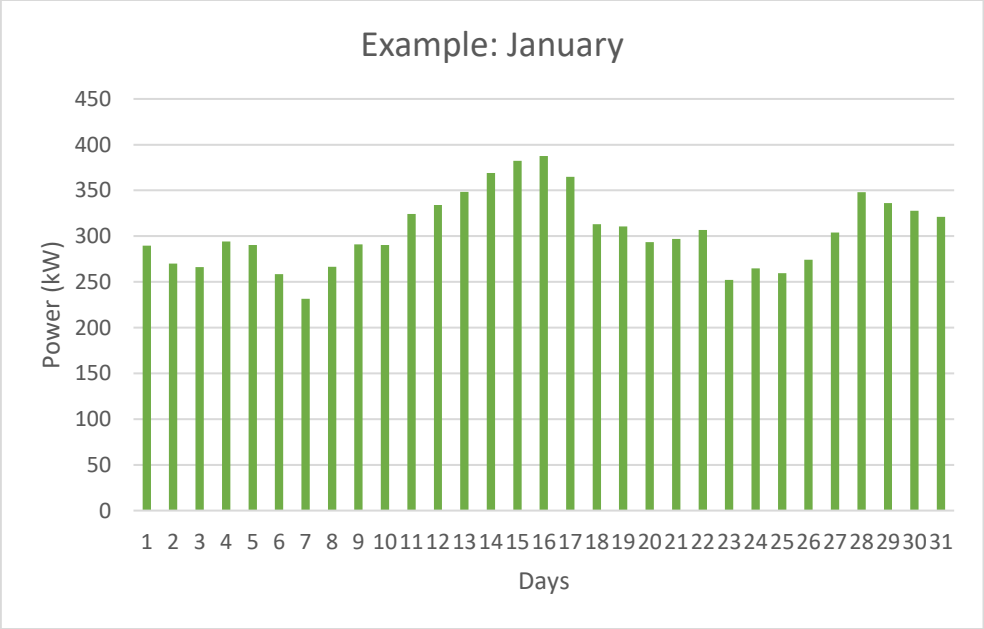

Figure 5-28 Average generation power for January

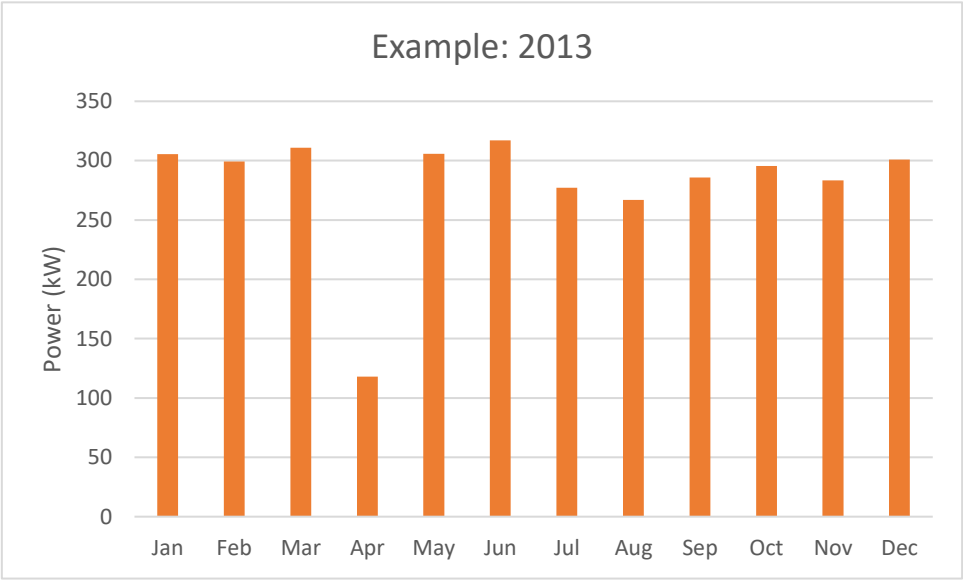

Figure 5-29 Monthly average generation power

The monthly average generation power is shown in Figure 5-29, where each month's value was an average taken from each day within the month. Similarly, according to Figure 5-29, the average power output was close to 300 kW for every month, except April. For this month, there was a large deficit, more than 50% under than the average value.

5.4.5 **Total generation time**

By sorting the power data, the software counted how many non-zero values would provide information on total generation time, given a value was recorded every minute which this information is shown in Figure 5-30.

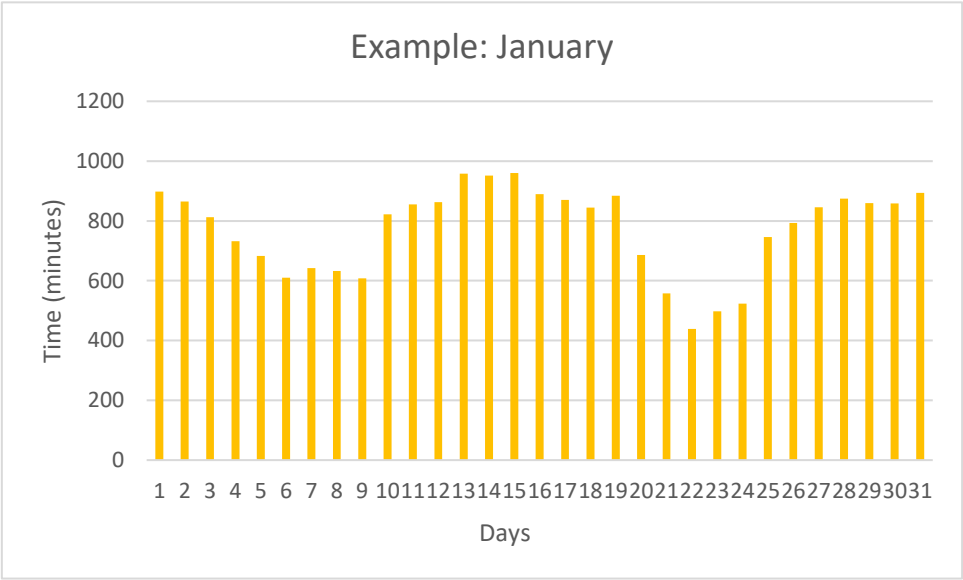

Figure 5-30 Generation time: January

From Figure 5-30, the daily generation time for January was not constant. The generation time was fluctuating. The year's data is shown in Figure 5-31.

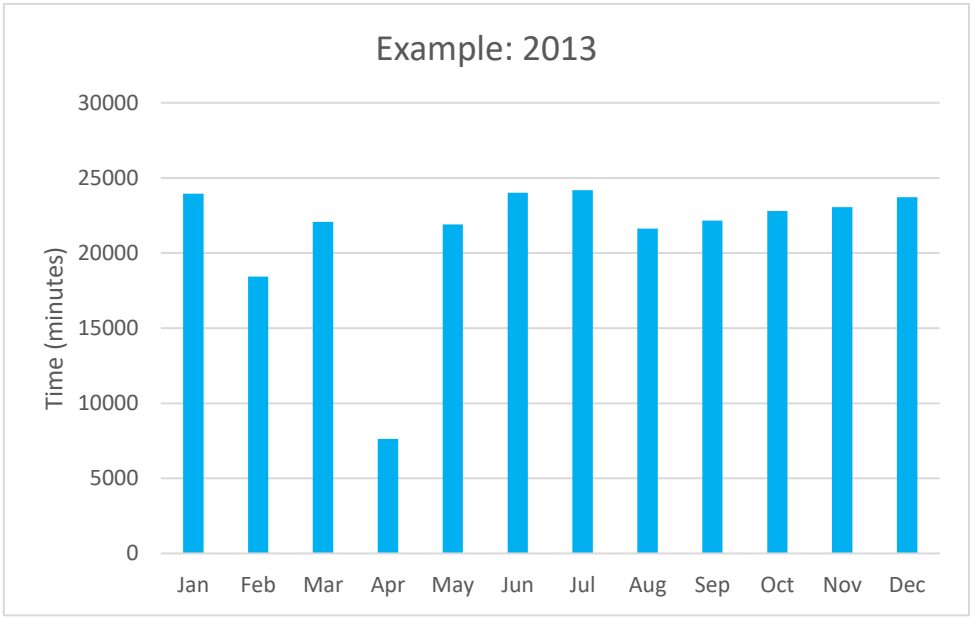

Figure 5-31 Monthly average generation time

From Figure 5-31, there was no significant difference between total generation times for each month, except April. In the previous, the average generation power was low.

It was also worth noting that the generation time for February was lower than average, due to fewer days in that month.

5.4.6 Total energy generated

With the given power data, Figure 5-32 shows the total generated energy was calculated.

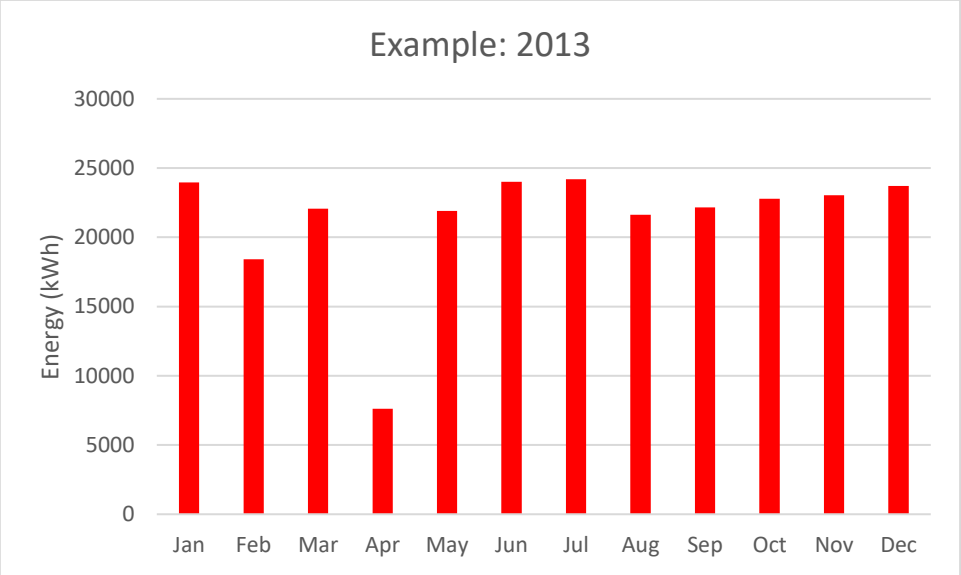

Figure 5-32 Monthly generated energy

From Figure 5-32, as expected, the total energy generated in April was the lowest. This was due to lower average generation power and generation time. February was also lower due to fewer days in that month.

5.5 Chapter Summary

The numerical model of the proposed system was created, and by comparing the results for the hybrid and conventional tidal system, the hybrid system generated more energy and had a higher peak power when compared to conventional systems, using the same conditions. With the hybrid system's ability to use the 2nd dock as a back- up the reservoir and additional turbine units to adjust water levels, this system

could generate energy conventionally, and could also generate energy if demand required it, regardless of tidal conditions.

The core part of the numerical model, which accounts for conventional energy generation was validated using real data from Jiangxia Tidal Power Station. The results show that the system predicts a correct reservoir level with the given information. The results could be used to predict the correct power value if more information was provided.

This data sorting program allows users to derive overviews of the most important factors from a massive data set. However, this programme has not had a user interface yet to allow the adjustment to be changed quickly. The program picks up key points which can be customised by the user. In this case, the software outputted peak power versus tidal levels, the average generation power, generation times and total energy generated, all based on the provided data. Additionally, the results showed that in April, the tidal station was on a different procedure, when compared to other months, with less energy generation.

Overall, this hybrid system could estimate how much energy would be generated at a particular site. Additionally, the model also provides an economic revenue value for power generation, if a figure for cost per kWh was given, therefore an economical balance point could be determined.

6. Case study: Converting active docks to a hybrid tidal system

The numerical model from Chapter 5 has been validated and updated to make it more user-friendly and realistic. However, Newport Docks used in the original model were based on a concept whereby the docks would be solely used for power generation purposes only. Docks with good local tidal ranges would be ideal for power generation. However not all docks could give up their main purpose of shipping, for power generation.

In this chapter, a case study was conducted at two sites; Cardiff Docks and Avonmouth Docks, to ascertain how different sites would react to power generation, under different scenarios. These sites were chosen because:

1. They both are located in the Bristol Channel and both have similar tidal levels.
2. Avonmouth Docks is much busier site in terms of shipping than Cardiff Docks, (Marinetraffic.com. 2017)
3. Both sites consist of multiple docks.

Bristol Channel has the world's second largest tidal range (Green, 2009), which makes Avonmouth Dock a desirable site to generate power by using tidal energy. However, with the minimum stream speed of 1 m/s required for a large tidal stream turbine design like SeaGen, the tidal stream speed in the Severn Estuary is too low to effectively drive the large-scale tidal stream turbine used in the model. As concluded in Chapter 4.3.2. Around 39% of the time, the tidal stream speed will not meet the minimum 1 m/s. Therefore, the Severn Estuary is not ideally practical and economical for the hybrid system to by applied at Avonmouth Dock. Therefore, in this chapter, the control system used does not feature the turbine-pump unit which in the hybrid system which introduced in Chapter 4.

6.1 Dock Comparison

A detailed comparison between the two sites (Avonmouth & Cardiff) was using a random pick data from 25/03/2017 to 09/04/2017 (total: 16 days).

6.1.1 Local tidal levels

To convert potential tidal energy into electricity, tidal ranges for the sites were required. This data would determine the maximum potential in terms of power generation.

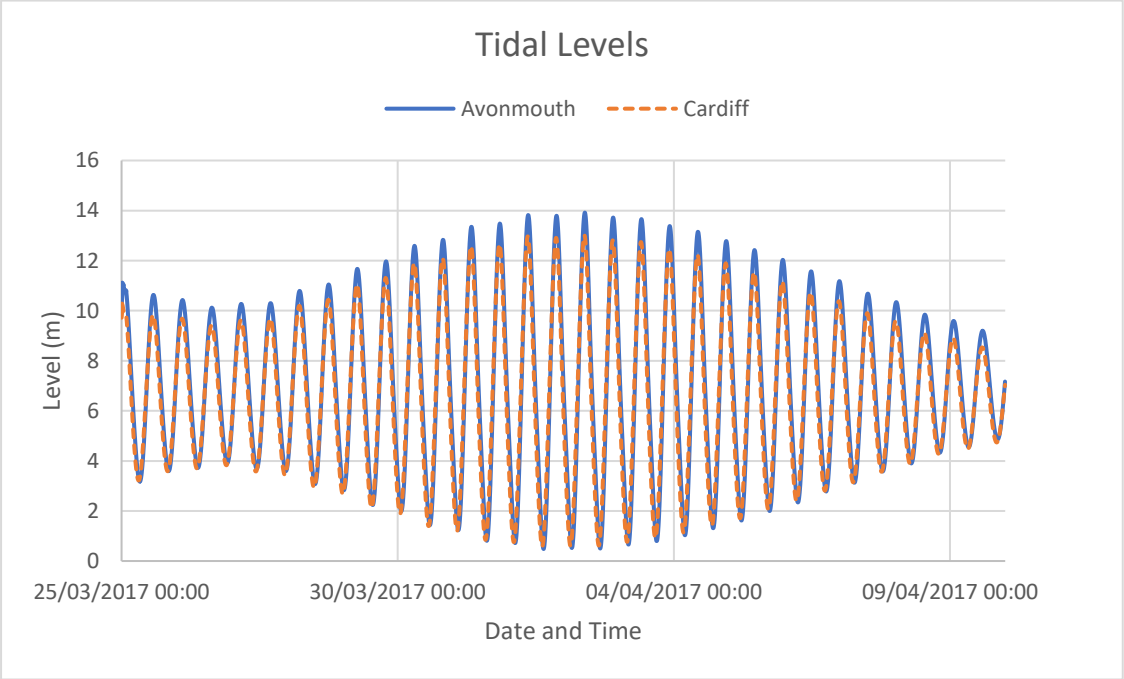

Figure 6-1 Tidal level comparisons, Cardiff & Avonmouth

As shown in Figure 6-1, the tidal levels for both sites indicate that Avonmouth had a slight advantage in tidal ranges; approximately 0.8 m during lower range days and about 1 m during higher range days, equating to 10% and 8% more than Cardiff, respectively. Additionally, although the two sites were located in the Bristol Channel, Avonmouth was further inland, therefore peak levels for both sites did not occur at the same time. For these 16 days, during lower range days, the peak levels for Cardiff

occurred about 30 mins earlier than Avonmouth. However, during high range days, both sites recorded the highest levels at about the 20 mins apart.

6.1.2 Site size

Cardiff Docks consists of two docks, Queen Alexandra Dock and Roath Dock. Avonmouth Docks consisted of two docks, the larger, Dock 1 and the smaller, Dock 2. Table 6-1 shows detailed information on each dock.

Table 6-1 Details of dock dimensions

	Base area of Dock (m^2)	**Depth of Dock (m)**	**Volume (m^3)**
Cardiff Queen Alexandra Dock	188,811	10	1,888,110
Cardiff Roath Dock	133,042	10	1,330,420
Total Cardiff:	321,853		3,218,530
Avonmouth Dock 1	274,862	14.5	3,985,499
Avonmouth Dock 2	77,427	14.5	1,122,691.5
Total Avonmouth	352,289		5,108,190.5

The geometry information of Cardiff Docks was acquired from ABP South Wales (ABPport.co.uk. 2017). For Avonmouth Docks; only the depths were published by The Bristol Port company (Bristolport.co.uk. 2017). To get a surface area for Avonmouth

Docks, measurements from Google Earth were used. To validate the results from Google Earth, it was essential to measure Cardiff Docks. Figure 6-2 shows results from Google Earth, measuring the area of Cardiff Docks. Figure 6-3 shows the published data from ABP South Wales.

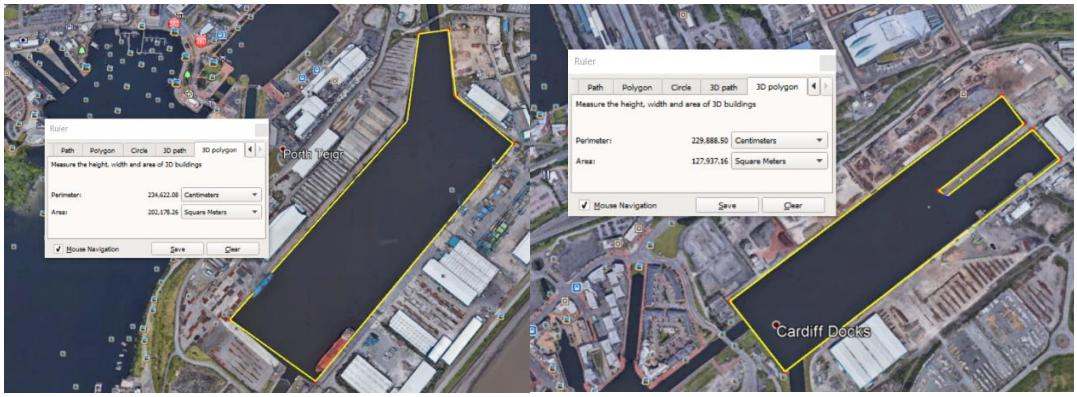

Figure 6-2 Aerial view of Cardiff Docks (image source: Google Earth)

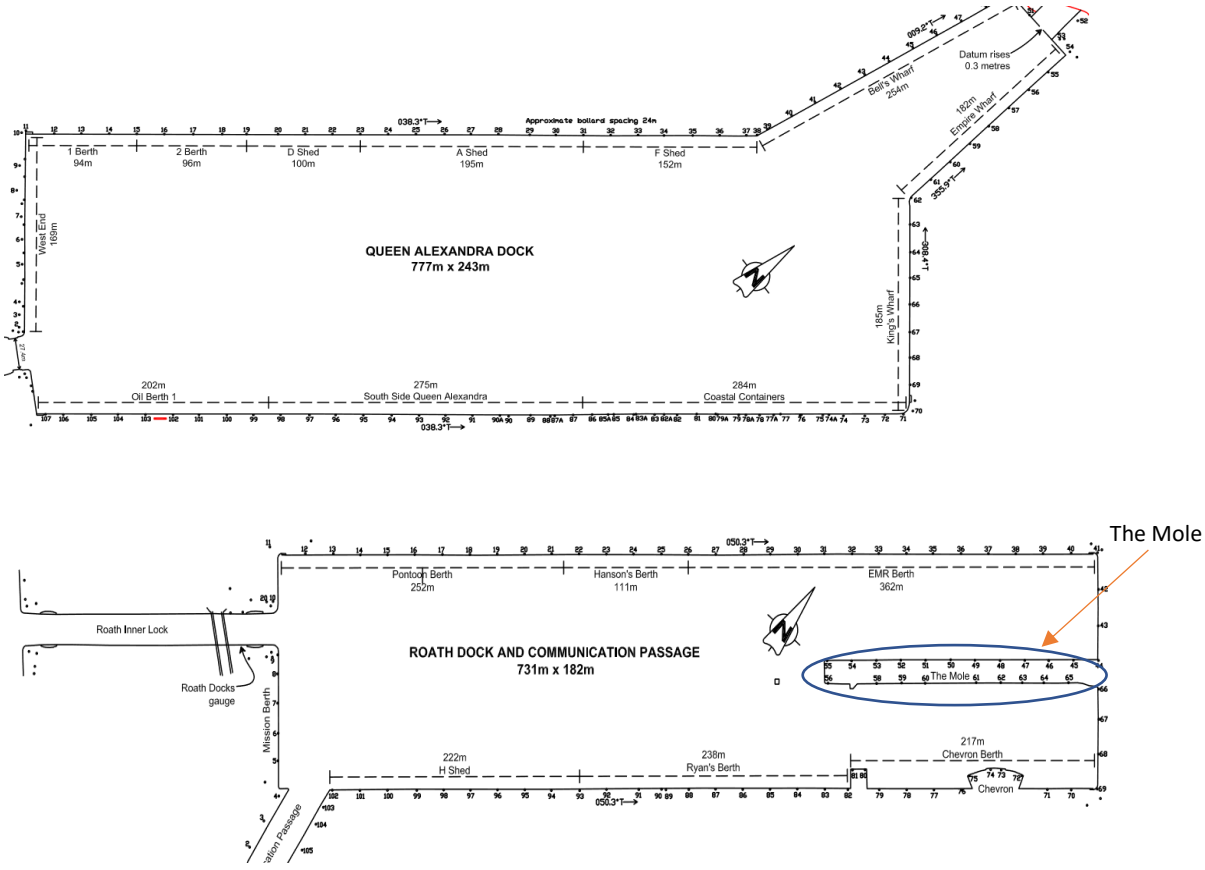

Figure 6-3 Layout of Cardiff Docks (ABPport.co.uk. 2017)

From Figure 6-2, the measurements for Queen Alexandra Dock was 202,178.26 m^2, and for Roath Dock it was 127,937.16 m^2. When compared with values from ABP South Wales, our data was 7% more for Queen Alexandra Dock and it was 4% less for Roath Dock. For Queen Alexandra Dock, the data given by ABP South Wales were estimated values, which was focused on a rectangular shape, not including the north east corner of the dock as shown Figure 6-3. However, for Google Earth, this additional area was included, hence it was bigger.

For Roath Dock, again the values given by ABP South Wales were estimates for the rectangular shape, which includes the mole which is highlighted in Figure 6-3. Therefore, explains the differences between the values given by ABP and Google Earth.

Using Google Earth, complex areas can be measured and by comparing the results with Cardiff Docks, it provided good accuracy.

6.1.3 Dock shipping traffic

Shipping traffic data was acquired from MarineTraffic.com [Marinetraffic.com, 2016], which is a website providing shipping information including current vessels in port, expected arrivals and recent departures. The website provides only live data, which means previous data cannot be accessed. Additionally, the website provided daily departure data for the docks, but the information was only available for already departed ships, not planned departures. Therefore, data for both sites were taken around 20:00 PM on the day. Table 6-2 lists the elements recorded from MarineTraffic.com. All data was recorded with tidal levels at the same time.

Table 6-2 Elements recorded from MarineTraffic.com

Elements
Current No. of ships in dock
The designed draught of ships in the dock
Arrival times for ships
Departure times for ships
The designed draught of departed ships
The planned arrival times of incoming ships and draught

Figure 6-4 shows the number of ships sitting in both docks during data recording. The figure represents the shipping activities at both docks.

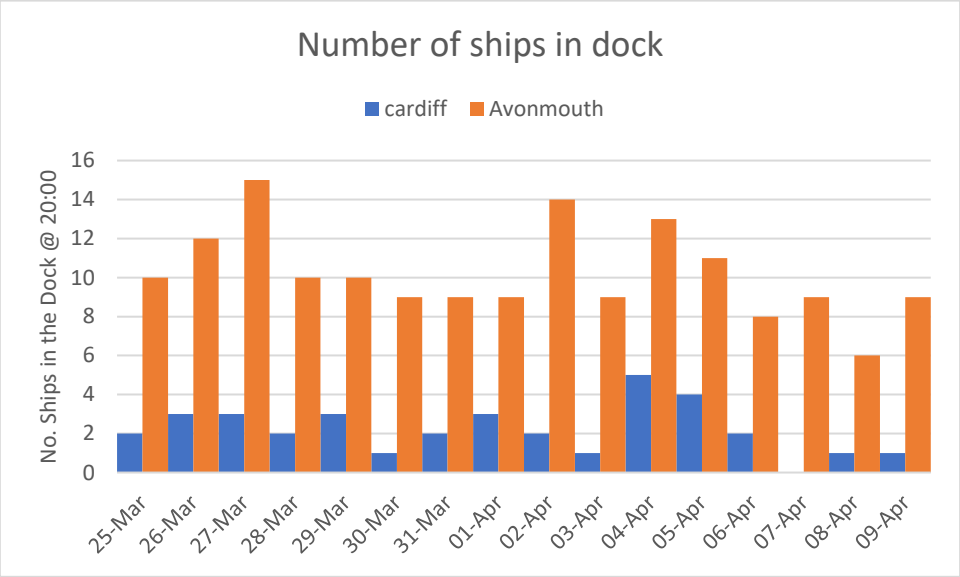

Figure 6-4 Number of ships in dock, Cardiff & Avonmouth

From Figure 6-4, Avonmouth Docks was much busier than Cardiff Docks. At this port, an average of 10.18 ships were sitting in the dock, whereas at Cardiff, this was 2.18 ships, nearly five times less than Avonmouth.

6.2 Case Study

To determine how these two sites would perform, a case study was conducted. For this case study, two concepts were used. Concept 1 focused on power generation, where the dock prioritised power generation, and how shipping would be affected. On the other hand, Concept 2 focused on shipping, where and how power generation would be affected by shipping.

6.2.1 Concepts

Two concepts were used for the case study, Concept 1 and 2. Concept 1 focused on power generation under the same conditions, meaning the components used would be assumed to be the same. Hence, there would be no difference in efficiency, minimum generation head requirement etc. The only difference would be local tidal ranges and the size of the docks.

Concept 2, unlike Concept 1, focused on the shipping activity. Shipping information would be taken from the recorded data of MarineTraffic.com, discussed in previous sections. Minimum water levels in the dock would be determined by the deepest draught of the ship, inside the dock for safety reasons. Therefore, the dock would not use the full potential range for power generation.

6.2.2 Cardiff Docks

During the 16-day testing period, examples, representative of the scenarios are discussed. There are five examples which are discussed in this section, the dock levels and power output will be compared between both concepts.

6.2.2.1 Example 1

The results for Cardiff Docks are shown in Figure 6-5. For the first day 25/03/2017,

starting water levels in the dock was set to 10 m, the maximum design level.

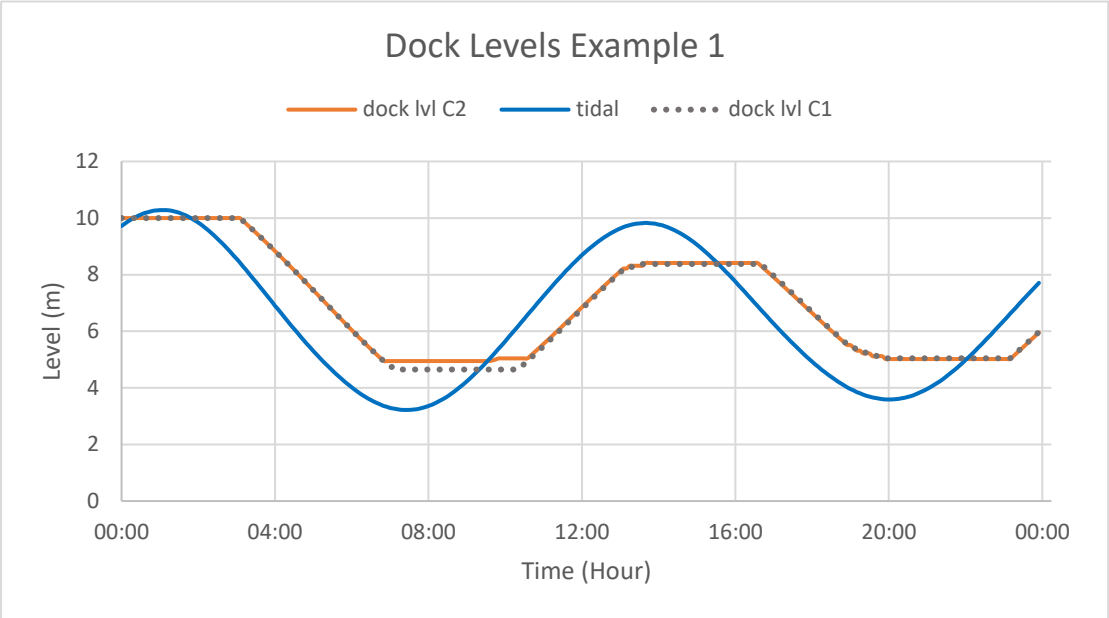

Figure 6-5 Cardiff: Dock level comparisons on Day 1

25/03/2017 was the first day of this case study. After the first ebb tide, there was a difference between the two dock levels. Concept 1 had a lower level. According to shipping data, there was a ship with a 4.5 m draught docked in Cardiff Docks at that time. Here, the minimum dock water level was 5 m.

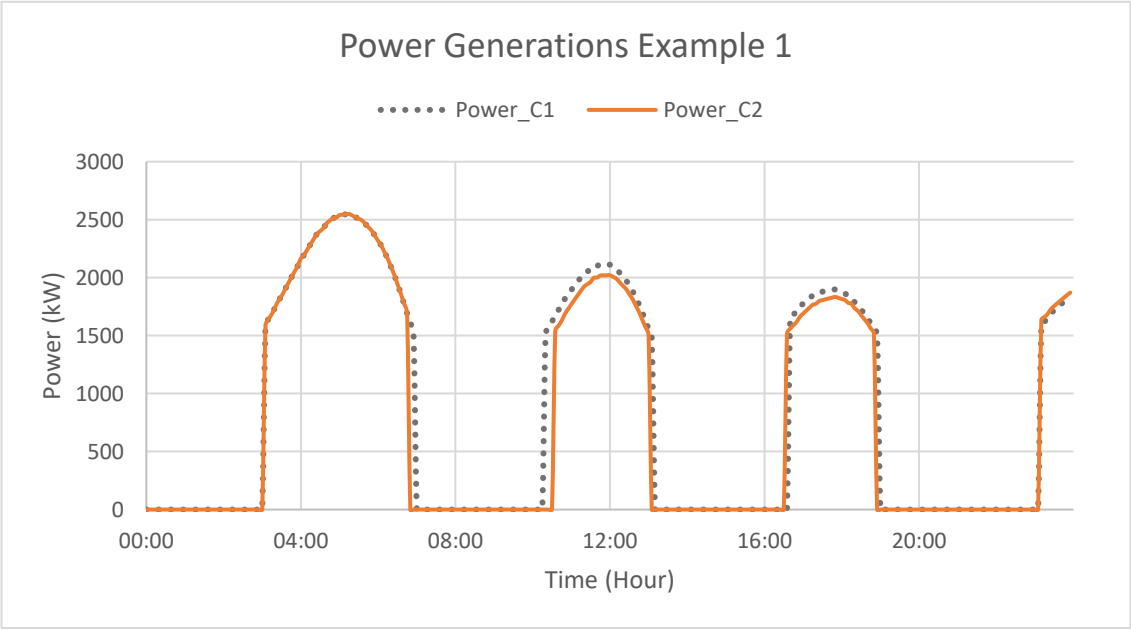

Figure 6-6 Cardiff: Power generation comparison on Day 1

The predicted power curves are shown in Figure 6-6. Concept 1 had advantages in generation times in the first two cycles and for the 2nd and 3rd generation, provided 5% more than Concept 2. The power output was higher than Concept 1 due to larger head. However, the difference in head ranges for the two methods were small, hence a big difference in power generation was not recorded.

6.2.2.2 Example 2

Figure 6-7 shows results from the second day, where a ship of 6.8 m draught docked at 2:09. As shown in Figure 6-7, to have enough water in the dock, water must enter to raise water levels during the flood tide to accommodate shipping. From Figure 6-7, the dock lets in water during the first flood tide for incoming ships, but for Concept 2, the system was still waiting for the ideal head for power generation.

After the ship was docked, minimum water levels were determined by the biggest ship in the dock, which in this case was a 6.8 m draught ship. Therefore a 7 m limit was used, where during the first ebb, the dock level would not go below the 7 m limit to ensure the ship would remain floating. However, for Concept 1, as power generation was the priority, the dock level would go much lower, for a longer time generation.

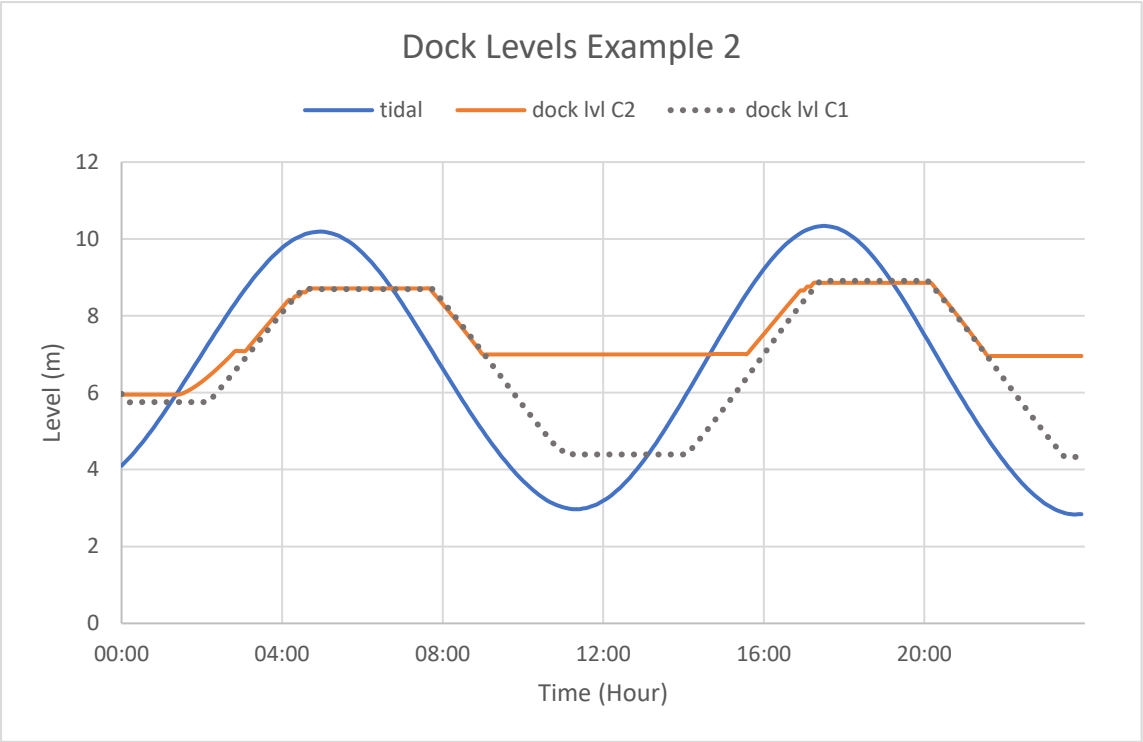

Figure 6-7 Cardiff: Dock level comparison on Day 2

The power data is shown in Figure 6-8. The results show how the two systems react once shipping becomes involved. For the first generation cycle under the flood tide, the power curve for Concept 1 started generation when the head reached 1.5 m. But for Concept 2, because a ship was docked at 2:09, the system had to let water in, to raise dock levels. During the process, the head value between the dock and tide was less than the 1.5 m for power generation. Hence, Concept 2 ran a reduced generation when compared to Concept 1.

Because of the big ship in the dock, the potential head range was reduced. This was why the 2nd generation did not last in Concept 1, during the ebb tide, because the dock level could not go below the designed draught of the ship. Consequently, the next Flood generation would be affected, due to higher dock levels.

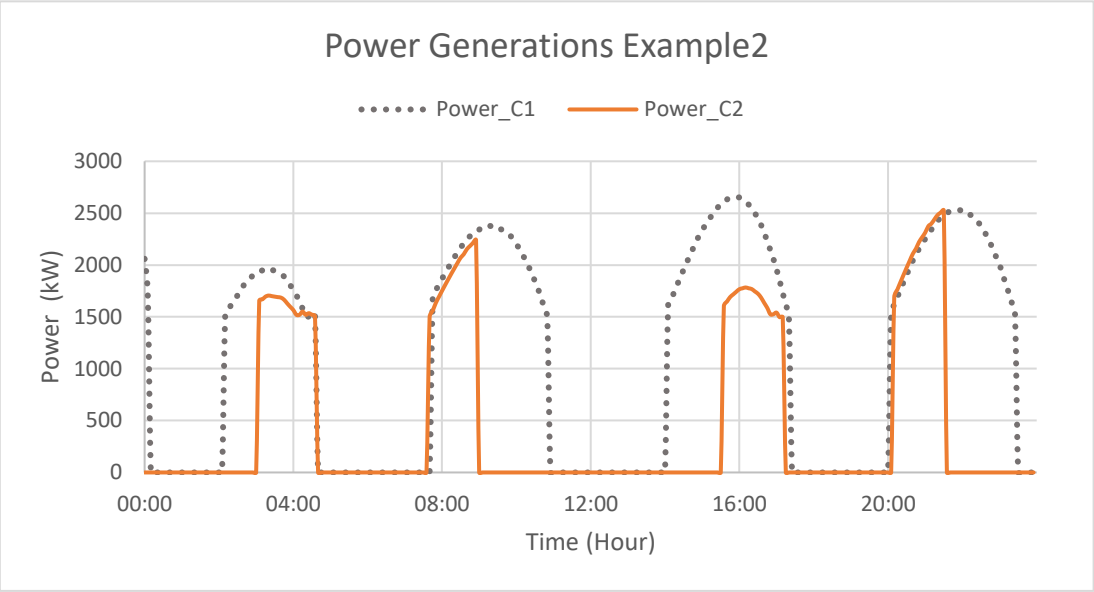

Figure 6-8 Cardiff: Power generation comparison Day 2

6.2.2.3 Example 3

For day 3, the results are shown in Figure 6-9. Day 3 was similar to day 2, as minimum dock levels were limited by the largest ship in the dock. The top level of the dock was determined by the tide if the level was below the designed maximum value.

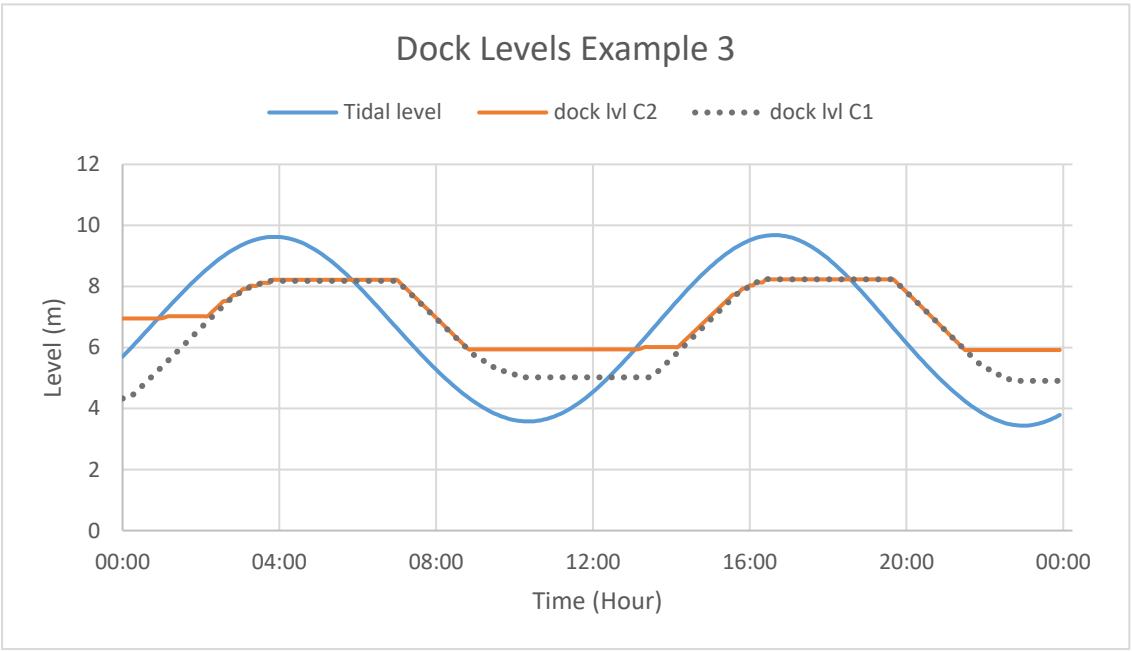

Figure 6-9 Cardiff: Dock level comparisons Day 3

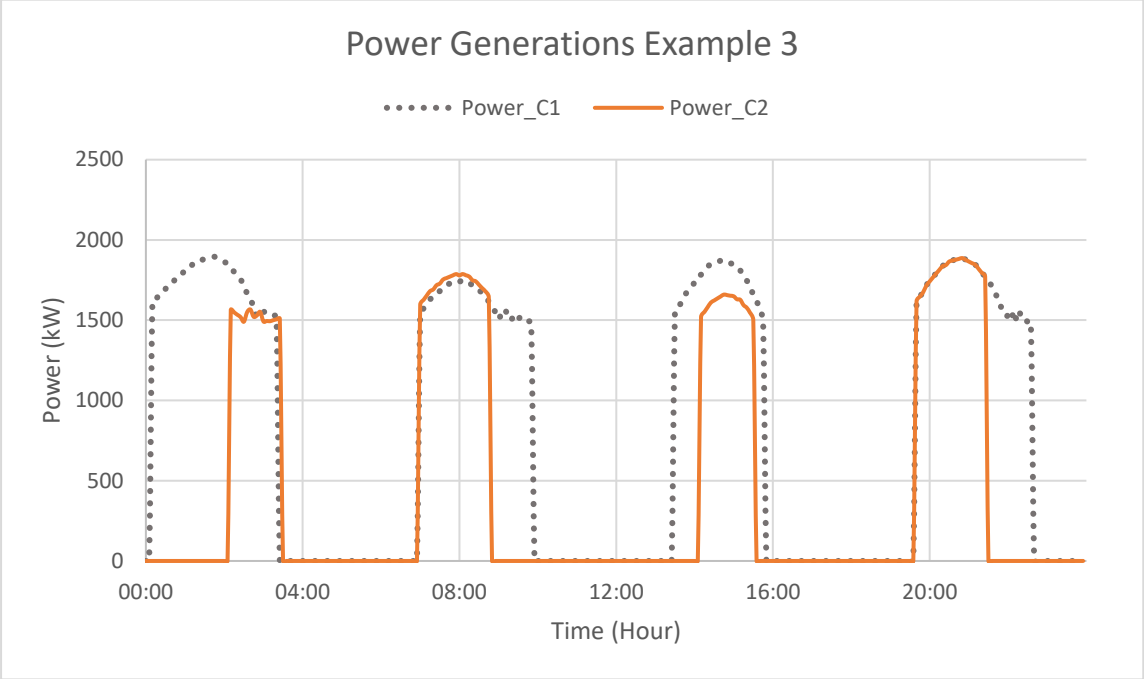

Figure 6-10 Cardiff: Power generation comparisons Day 3

From Figure 6-10, the power curves in Example 3 reflected the dock levels in Figure 6-9, with the Concept 1 out performed Concept 2 in both generation time and peak power generated.

6.2.2.4 Example 4

Another example from Day 9 is shown in Figure 6-11. The tidal range on that day was at the highest during the testing period. However, due to ships with big draughts sitting in the dock for Concept 2, the system could not use the full potential head for power generation. The available range was 4 m, when compared with 9 m for Concept 1. In this case, it could be a worst-case scenario for power generation for Concept 2, as the available head was limited by the docked ships. The predicted electricity generated by these two concepts were: 1,061,442 kWh for Concept 1 and 626,903 kWh for Concept 2. Results from Concept 1 were 70% more than results from Concept 2, under the same tidal conditions.

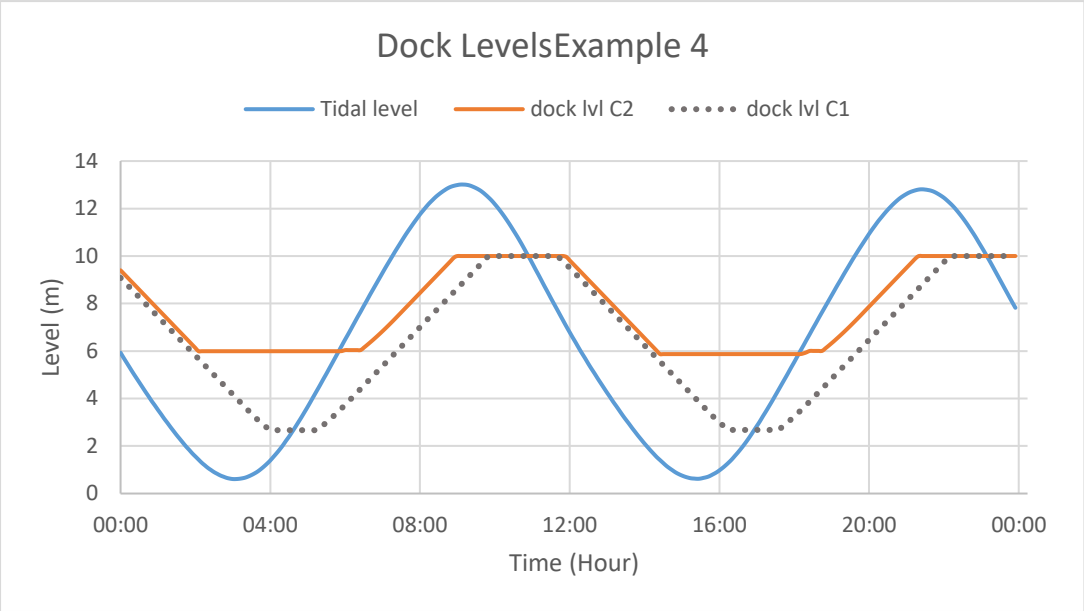

Figure 6-11 Cardiff: Level comparisons Day 9

The power data is shown in Figure 6-12. From Concept 2, the generation time during the flood tide was cut off during the highest power output. This was as a result of higher dock values, as water reached the dock limit and could no longer be used for generation. For ebb tide generation, the power data from Concept 2 was less than Concept 1, which was also a result of the available head being limited.

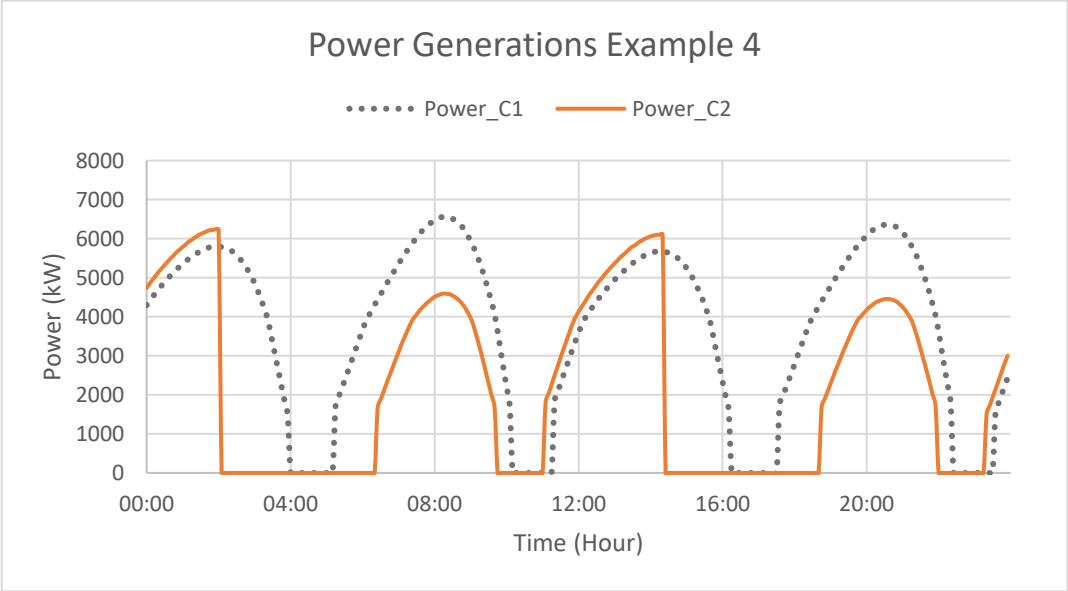

Figure 6-12 Cardiff: Power generation comparison Day 9

6.2.2.5 Example 5

The final example data is shown in Figure 6-13 and features results from Day 14. According to dock records, a ship with an 8.2 m draught docked on Day 12. Therefore, the lower limits of water levels for Concept 2 were set at 9 m. With this limit, the dock had only 1 m head for a generation, but in this case, the system required at least 1.5 m head to start generation. From Figure 6-13, for the first two tides, there were no changes in dock levels as the ship was still docked. However, that ship left the dock at 12:55, removing the minimum water requirements. For the next tide, both concepts used the full potential head for power generation.

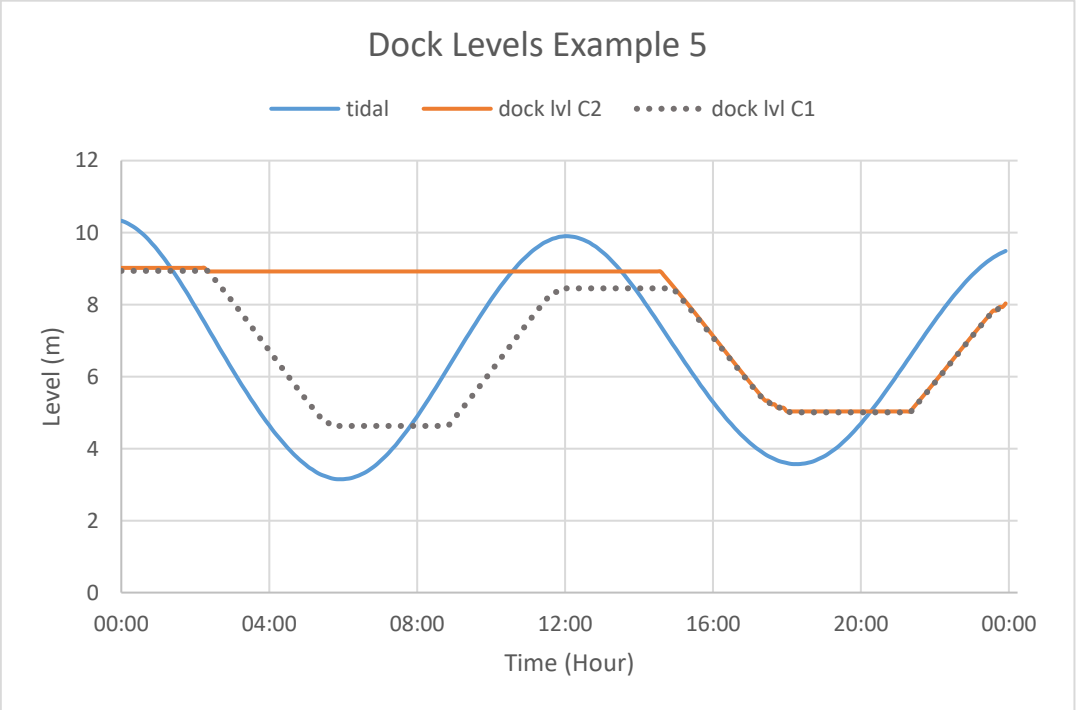

Figure 6-13 Cardiff: Dock level comparison Day 14

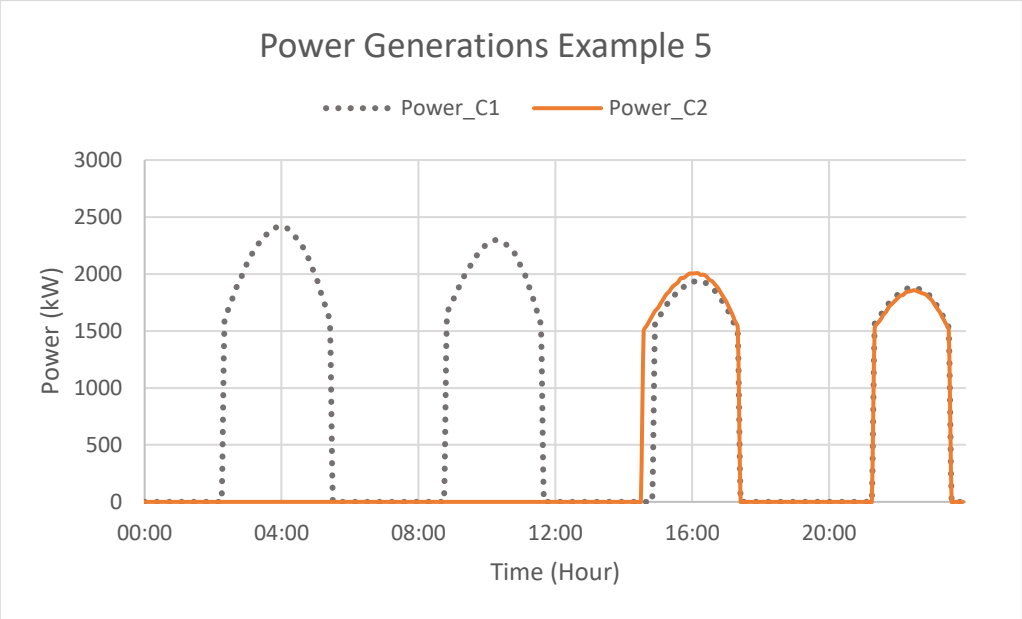

Figure 6-14 Cardiff: Power generation comparison Day 14

In this case which is shown in Figure 6-14, there was no power output for Concept 2, which is a result of the large ship staying in the dock. There was not enough head range for power generation before the vessel which has a deep draught left the dock, which for Concept 2, at the first two tide cycles, there was zero energy output. Once that vessel left the dock, limitations on dock levels were removed, and for the two concepts, there was little difference in the predicted power outputs.

6.2.3 Avonmouth Docks

A few examples will be discussed during the testing period which was believed to be representative.

6.2.3.1 Example 1

Figure 6-15 shows the first example shows results from Day 1. The starting dock levels for both concepts were set to the design maximum, 14.5 m. According to dock data, a ship with a 6.8 m draught was staying at the dock; this was why the limit for concept

2 was set to 7 m. Moreover, that ship departed Avonmouth Docks at 13:18, and after that, the 7 m limit was changed to 6 m, as the largest vessel in the dock had a draught of 5.6 m. For Concept 1, the system behaved as expected, dock levels dropped during the ebb tide, and increased during the flood tide, using the maximum potential range for power generation.

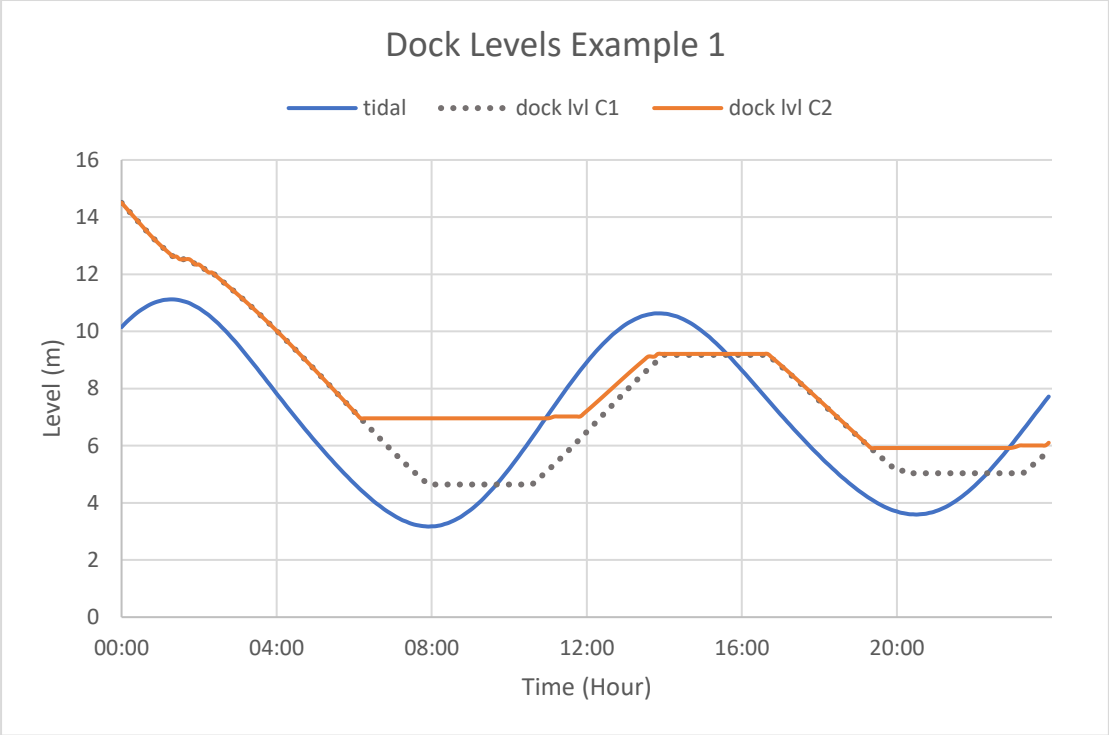

Figure 6-15 Avonmouth: Dock level comparison, Day 1

Power data was calculated using the level results (Figure 6-16). From Figure 6-16, the two concepts provided the same results before 6:00, as dock levels were the same before that time. Next, for Concept 2, the dock reached the lower limit. Therefore, power generation was stopped due to no available head. For Concept 1, it continued to produce power until the head was below the required value.

For the second generation under the flood tide, results showed that Concept 2 was generating less power and less generation time when compared to Concept 1. This was expected as the available head was limited for Concept 2, for this generation.

Moreover, as the 7 m dock level limit was removed from Concept 2, once the big ship left the dock, for both systems the predicted power was similar for the 3rd generation under the ebb tide. At the start of the generation, both systems had the same dock level and starting time; but Concept 1 had an advantage on the generation time of 30 minutes more than Concept 2, as there was another level limit of 6 m for Concept 2.

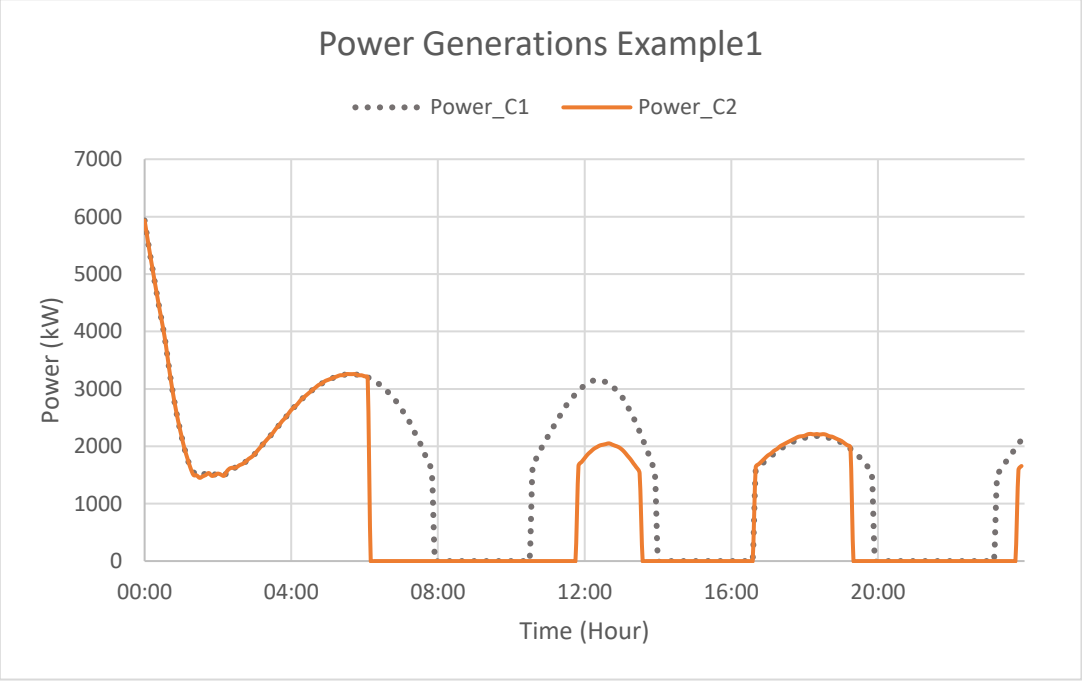

Figure 6-16 Avonmouth: Power level comparison, Day 1

6.2.3.2 Example 2

Figure 6-17 shows Example 2 shows the results from the 2nd day of the 16-day testing.

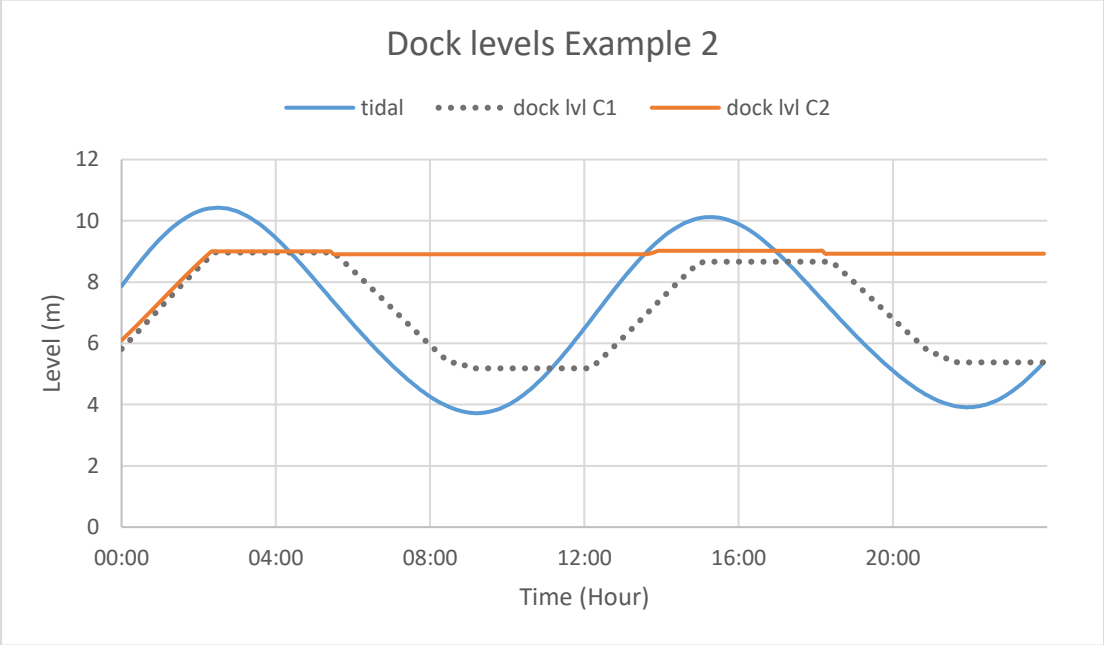

Figure 6-17 Avonmouth: Dock level comparison, Day 2

In this example, Avonmouth Docks had a ship docked at 2:46 with an 8.6 m draught. For Concept 2, the system needed to prepare the dock for sufficient water to accommodate the vessel. From Figure 6-17, during the first flood tide, the dock reached 9 m at 2:40. This was enough for the 8.6 m depth ship to dock. However, once docked, the head range for power generation was greatly reduced for Concept 2, as from Figure 6-17, the dock stayed at that limit for the rest of the day. Additionally, Concept 1 was generating for every tide, given the head range was not affected by docked ships.

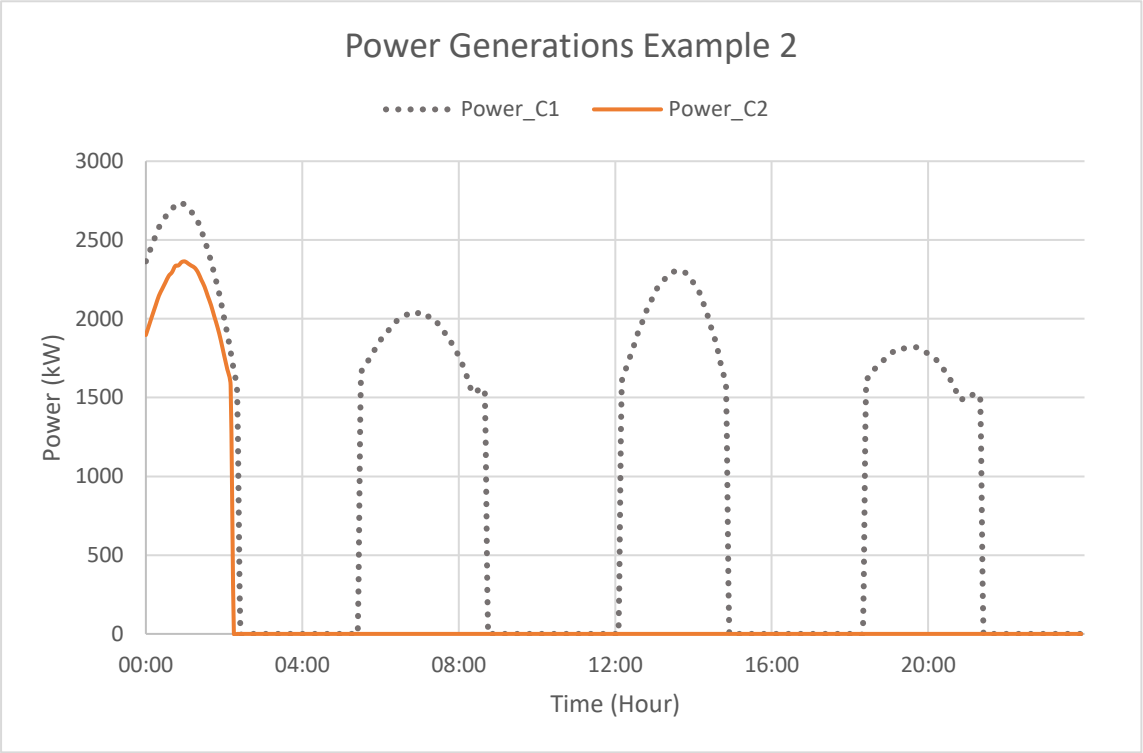

Figure 6-18 Avonmouth: Power level comparison, Day 2

Figure 6-18 shows the power level for example 1. As expected, Concept 1 produced four power generation cycles under the tidal conditions. Due to the shipping, Concept 2 generated one power generation during the first flood tide.

6.2.3.3 Example 3

The data and results for Day 8 for the Example 3 can be seen in Figure 6-19. As the 8.6 m draught ship arrived on day 2, the lower limit remained at 9 m for Concept 2. However, on this day, the tidal range was much higher than the previous two examples, reaching 14 m and 0.5 m low. Given the range of 13.5 m, when compared to 6 m from Examples 1 and 2, unfortunately for Concept 2, the system could not benefit from this tidal range, due to limitations of dock levels.

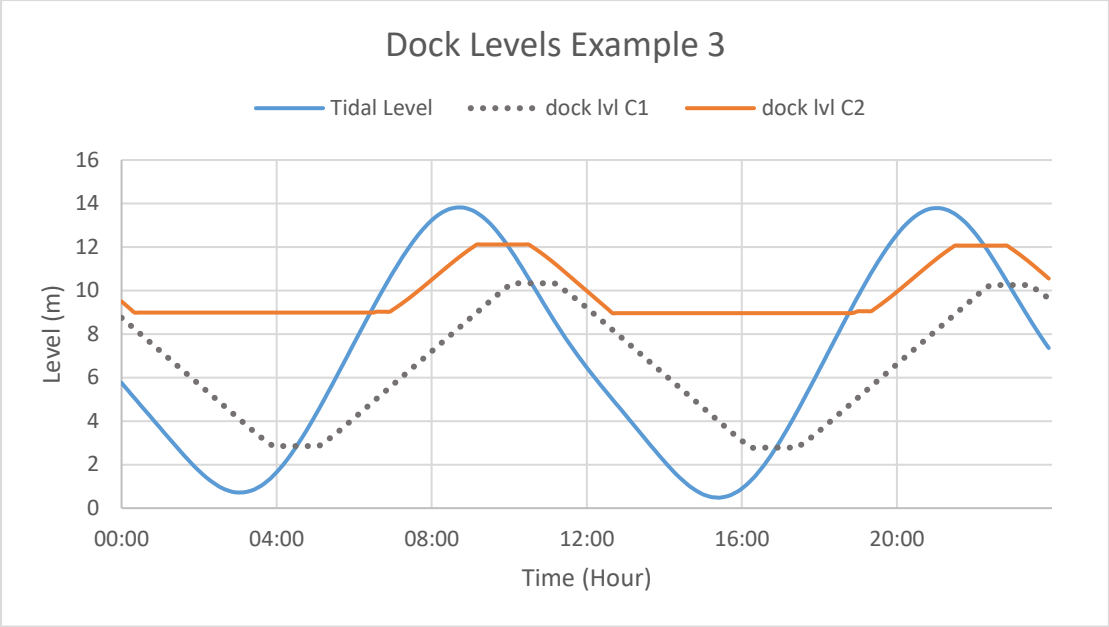

Figure 6-19 Avonmouth: Dock level comparison, Day 8

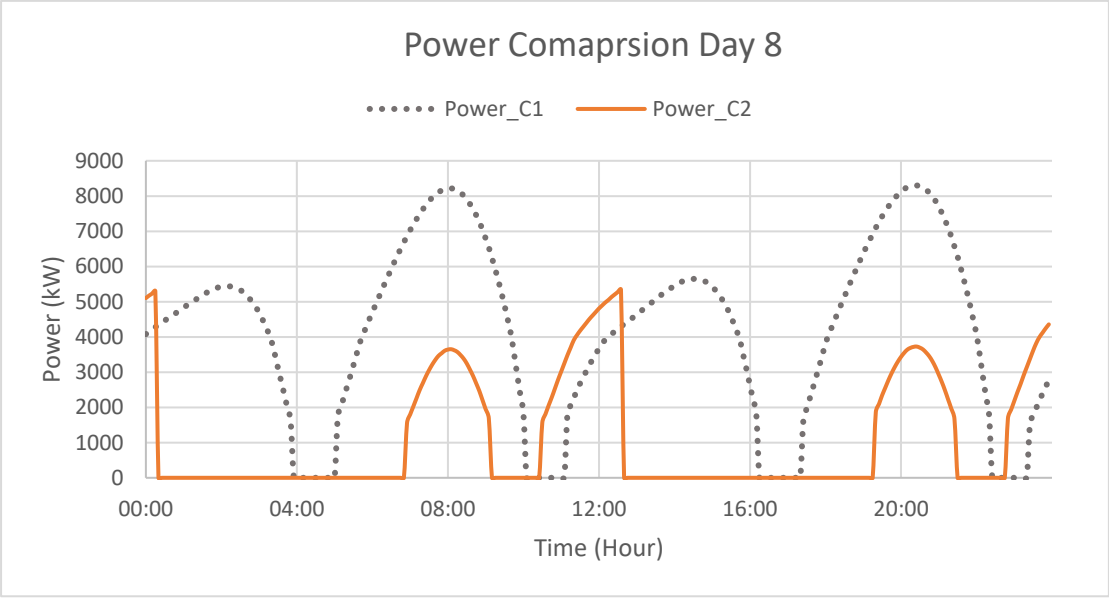

Figure 6-20 Avonmouth: Power comparison, Day 8

Figure 6-20 shows the power data from this example. The results were expected; under the big tidal range, Concept 1 out-performed Concept 2 in terms of power generation. For the first generation of the ebb tide, for Concept 2, dock levels could be no lower than the set limit of 9 m, which resulted in minimum power generation.

Following the flood tide generation, as the dock level reached 10 m, due to high tide, this increased the head range under the limitation, leading to an earlier generation time for the 3rd tide of the day, in comparison to concept 1. Overall, for day 8, because its full potential was limited by docked ships, the power generation was significantly affected.

6.2.3.4 Example 4

Figure 6-21 shows data and results from day 12. A ship with an 8.6 m draught arrived on day 2 and departed later this day at 12:53.

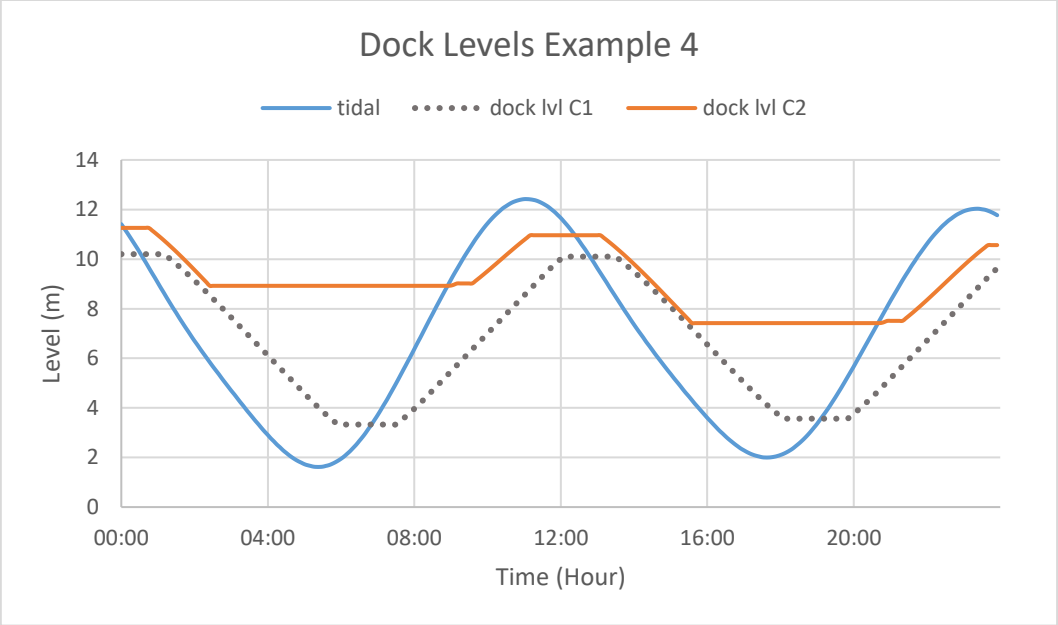

Figure 6-21 Avonmouth: Dock level comparison, Day 12

Before departure at 12:53, the dock for Concept 2 was still at the 9 m minimum dock level setting. Once this ship left, the lower limit was set by the next largest ship in the dock. This was an oil tanker of 7 m draught. The 9 m limit was changed to 7.5 m, resulting in an increase in head range for power generation. For the 2nd ebb generation, dock levels for Concept 2 were lower than levels in the first ebb generation.

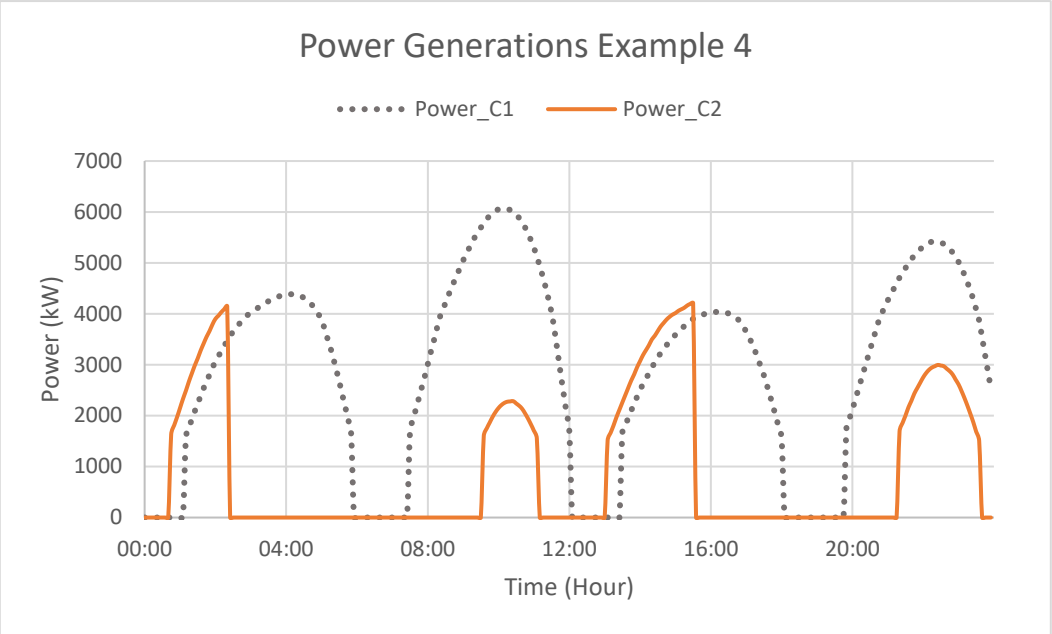

Figure 6-22 Avonmouth: Power comparison, Day 12

For power results which can be seen in Figure 6-22, as expected the first two generation for Concept 2 was limited. With the dock lower limit changed after 12:53, the generation time was extended for the 3rd and 4th generation, as more range was released. However, for power output, Concept 1 had clear advantages over Concept 2; in all four generations, the generation times for Concept 1 were 200% more than Concept 2. This was due to no limitations on dock lower levels.

6.2.3.5 Example 5

Example 5 was taken from Day 16. Level data is shown in Figure 6-23.

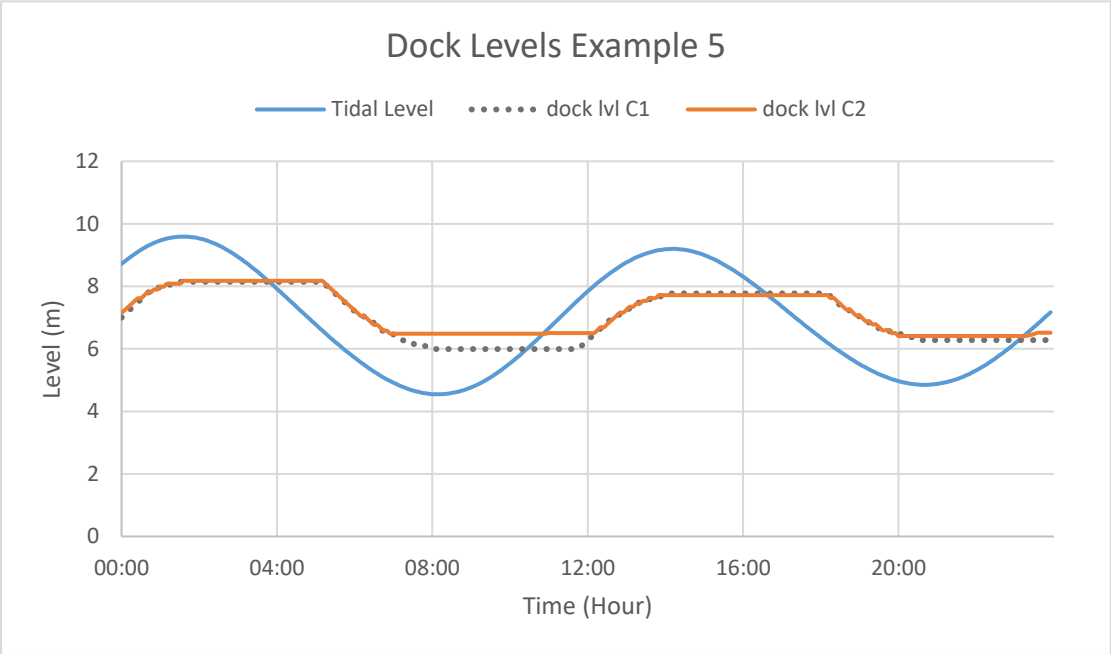

Figure 6-23 Avonmouth: Dock level comparison, Day 16

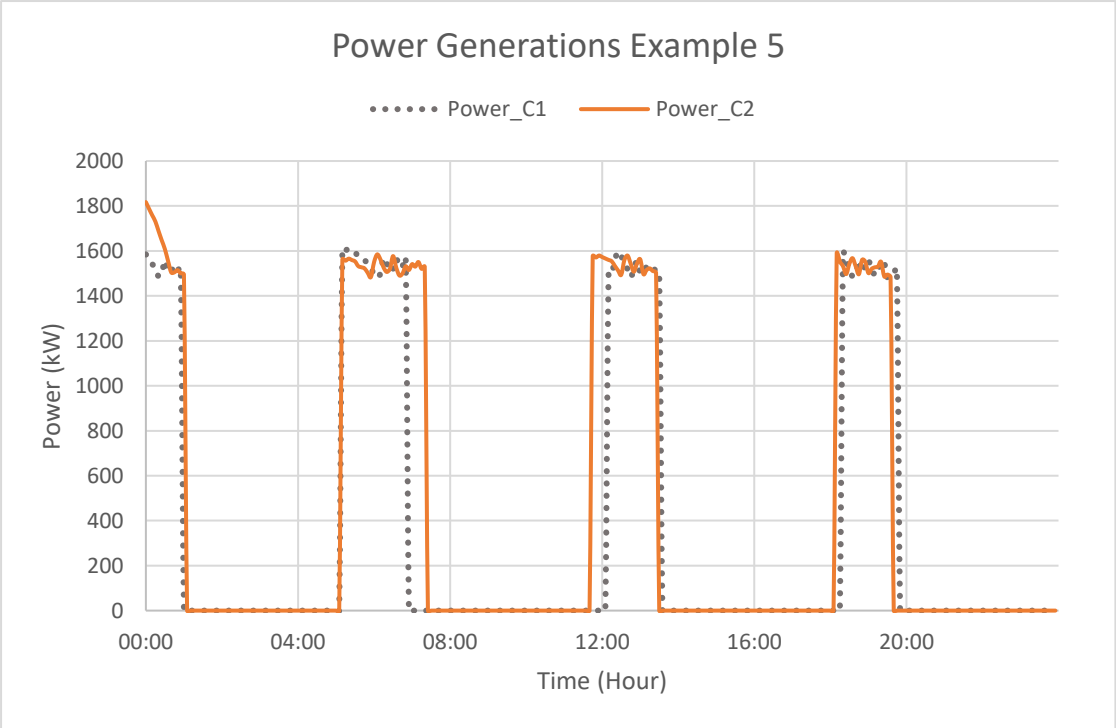

Figure 6-24 Avonmouth: Power comparison, Day 16

From Figure 6-23, the tidal range on day 16 was less than days 8 and 12, as the lower tidal range also reduced the ranges for both concepts for power generation. A 6.5 m limit was set for Concept 2, as a ship of 6 m draught was docked. However, due to lower tidal ranges, both systems could not use the full potential of the dock. As for Concept 1, which reached 6 m for the first ebb generation, (compared to the 6.5 m setting for Concept 2), the difference was not significant. For the following two tides, both results for both systems were nearly identical, which again could be a result of lower tidal ranges.

The predicted power curves in Figure 6-24 were expected. Concept 1 had an advantage in generation time for the 2nd and 3rd generation cycles, but Concept 2 matched the maximum power generation of Concept 1. Overall, Concept 1 did not have a great advantage over Concept 2.

6.2.4 Overall results

The predicted generated energy for all four cases over the 16 days is shown in Figure 6-25.

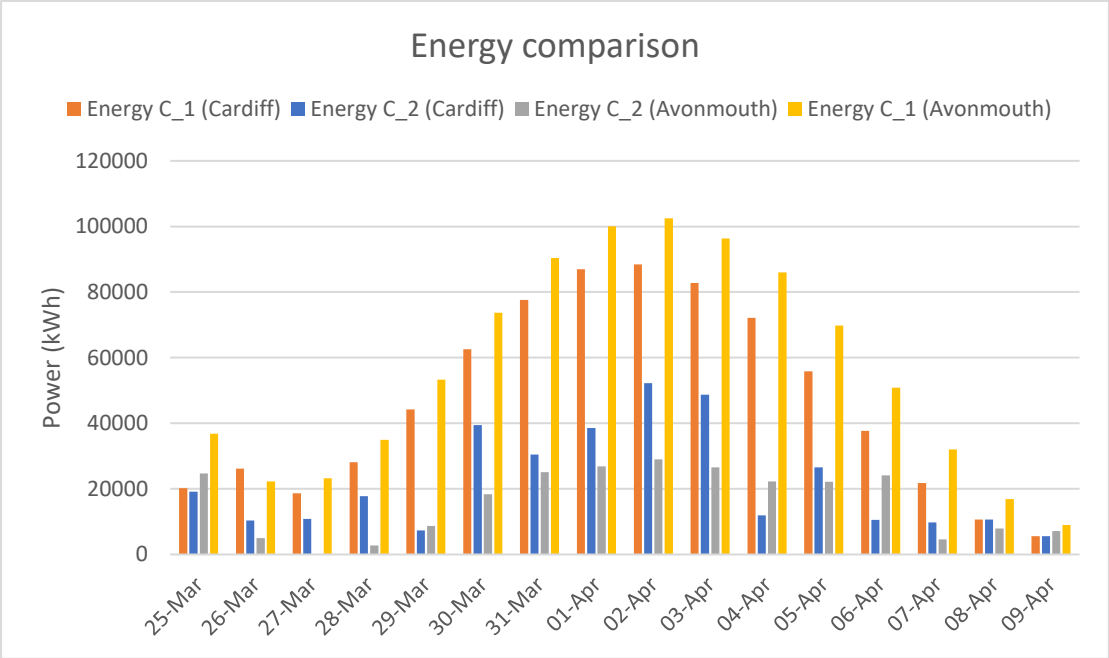

Figure 6-25 Energy data comparison, all four cases

For Concept 1, under the same tidal conditions, when the docks were converted into a tidal energy station which did not consider shipping, Avonmouth Docks had the advantage over Cardiff Docks every day during the testing period. This was due to size differences. However, despite having 60% more volume than Cardiff Docks, the energy produced by Avonmouth Docks was 21% more than Cardiff Docks. This figure could reflect the fact that both systems were run at the same settings, for power generation, for easier comparisons. However, a tidal power station with a larger reservoir uses different settings than a smaller reservoir. The model showed that in the 16 days testing period, Avonmouth Docks could generate 898,251 kWh, and for Cardiff Docks, the total energy generated was 739,390 kWh.

For Concept 2, shipping was a priority for both docks. Despite the larger size of the Avonmouth Docks, the data indicated that Cardiff Docks generated more energy during this period. The main reason was Avonmouth's busy shipping; a large ship of 8.6 m draught docked for 10 days, thereby significantly reducing the available head range. The results from Concept 2 showed that for Avonmouth, 255,330 kWh energy could be generated, and 350,035 kWh for Cardiff Docks, approximately 37 % more than Avonmouth.

6.2.5 Discussion

For Cardiff Docks, the main purpose of Concept 1 was power generation. Therefore, the dock would generate energy under local tides, regardless of shipping. Dock levels are determined by the tides, as long as the highest level remained under the maximum.

For Concept 2, limits were first determined by the largest ship inside the dock. To ensure ships could float inside the dock, there would need to be sufficient water to meet these requirements. The dock would also need to be preparing to accommodate incoming ships in the nearest flood tide before the scheduled arrivals, which could compromise power generation. Once the ship was in the dock, the available head range for power generation was reduced. The longer the ship stayed in dock, the greater the impact on power generation, especially when there was a good tidal range.

For Avonmouth Docks, under the same settings, the power prediction for Concept 1 over Cardiff Docks was not as big as the difference in volume over two docks. This was due to the two systems using the same conditions for power generation. This included a maximum flow rate allowances for the tidal system. Using the same maximum flow rates, the larger dock could not empty or fill fast enough, but by running the same conditions this would make the comparison more readable; such settings could be

changed to suit different needs.

The biggest problem for Concept 2 at Avonmouth Docks was stationary ships, in particular those ships with large draughts. From the recorded shipping data, the ship with an 8.6 m draught stayed in the dock for 10 days. For a normal dock, this would have been fine, but if the dock were a tidal station, the available head range would be massively reduced. During these 10 days, there were some significant tidal range available, but the dock was unable to benefit from its full potential, for power generation. This was a significant loss in power production. However, for lower tidal range days, there were no big differences between the two concepts nor for the two docks, because lower potential energy was offering in the tidal range.

6.3 Case study 2

From case study 1, it was noted that shipping was the priority. The docked ship was the biggest factor in power generation; once the ship was docked, the potential head for energy generation was reduced. Importantly, this amount was related to the ship's draught. This case study used the information from the previous case study. The results were compared with the previous case study.

6.3.1 Concept 3

The new concept allowed the dock to operate ordinary shipping while minimising the effects of shipping which would affect power generation. For the two sites; Cardiff Docks and Avonmouth Docks, both had multiple docks. Concept 3 proposed the smaller dock be used to accommodate docked ships, allowing the larger dock to operate mainly as a power generation. The smaller dock would take the biggest allowable ship; in this case, both for Cardiff Docks and Avonmouth Docks, the smaller dock has the same depth as the larger one.

Furthermore, to access the smaller dock, vessels had to travel through the bigger dock, which was linked to the sea lock. The numerical model would make sure there would be enough water in the big dock to ensure vessels could travel freely. But according to the data, all vessels had a deep draught (> 6 m), the arrival times were all in the high tide during flood tide, when in theory, there would be enough water in the dock, but the numerical model would make sure of that.

Several conditions were set for this concept. The minimum water level for the main dock was set to 4 m, ensuring unscheduled smaller ships could use the dock. For water transfer between docks, a minimum head difference of 1 m was required, which would avoid constant opening and closing sea locks. This condition was not used if the docks were preparing for incoming traffic. In that case, the smaller dock would be filled by the bigger dock, if there was a positive head difference.

6.3.2 Examples and results: Avonmouth Docks

Data for Avonmouth Docks used in the previous case studies were used for Concept 3. There are five examples are discussed below, with the power results compared with the Concept 1 & 2.

6.3.2.1 Example 1

The first example used data and results from Day 1 which is shown in Figure 6-26. From this figure, starting levels for dock 1 and dock 2 were the same, where dock 1 is the largest dock of the two. According to the shipping data, before 13:18, the largest vessel in the dock had a maximum draught of 6.8 m, this would be kept in the smaller dock 2. The lower limit for dock 2 was 8 m. For the first ebb tide, dock 1 went lower than dock 2, as dock 2 had to maintain a minimum amount of water. After that vessel left the dock, the lower limit for dock 2 was set to 7 m, to accommodate the next largest ship, which had a draught of 5.6 m. Moreover, water could be transferred

between these two docks, if conditions were met for the ebb tide. If dock 2 had sufficient water, it would allow water flow into dock 1. For the flood tide, it would accept water from dock 1. However, if dock 2 was below the minimum requirement level, and dock 1 was higher than dock 2, then dock 1 would top up dock 2, to ensure requirements were met.

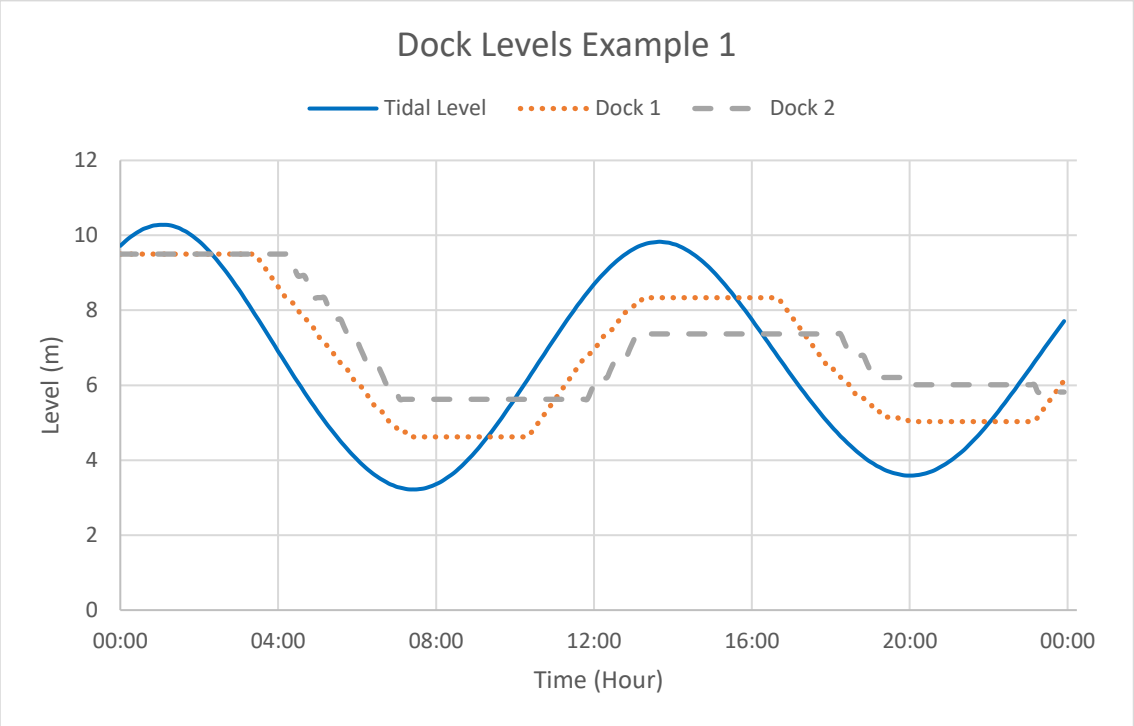

Figure 6-26 Avonmouth: Dock levels

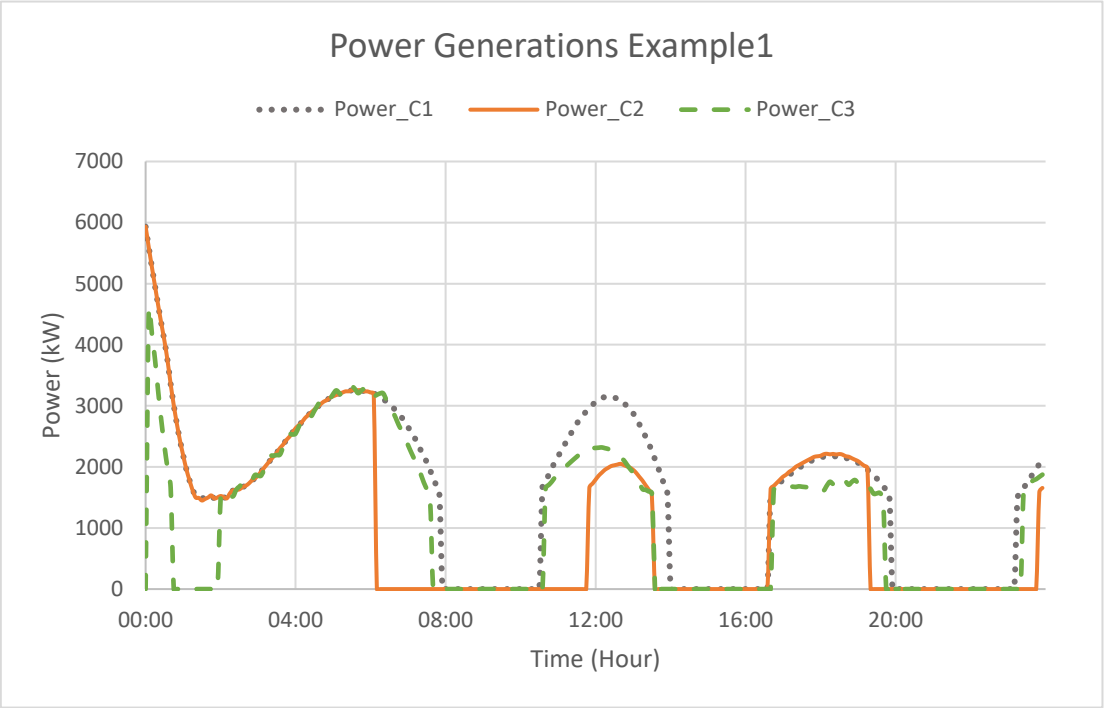

Figure 6-27 Avonmouth: Power level comparison, Day 1

By comparing the estimated power data with the other two Concept 2, it was noted that for the first power cycle, Concept 3 matched the result from Concept 1, for the 2nd power cycle. Concept 3 had a good generation time, compared with the other two concepts, about 40% more than Concept 2, but the peak power was below Concept 1. All three concepts were very close, but Concept 2 had a shorter generation time.

6.3.2.2 Example 2

On day 2, a ship of 8.6 m draught docked at 2:46, and stayed until day 12. In previous cases, this had a significant impact on power production for Concept 2. The level results for concept 3 are shown in Figure 6-28.

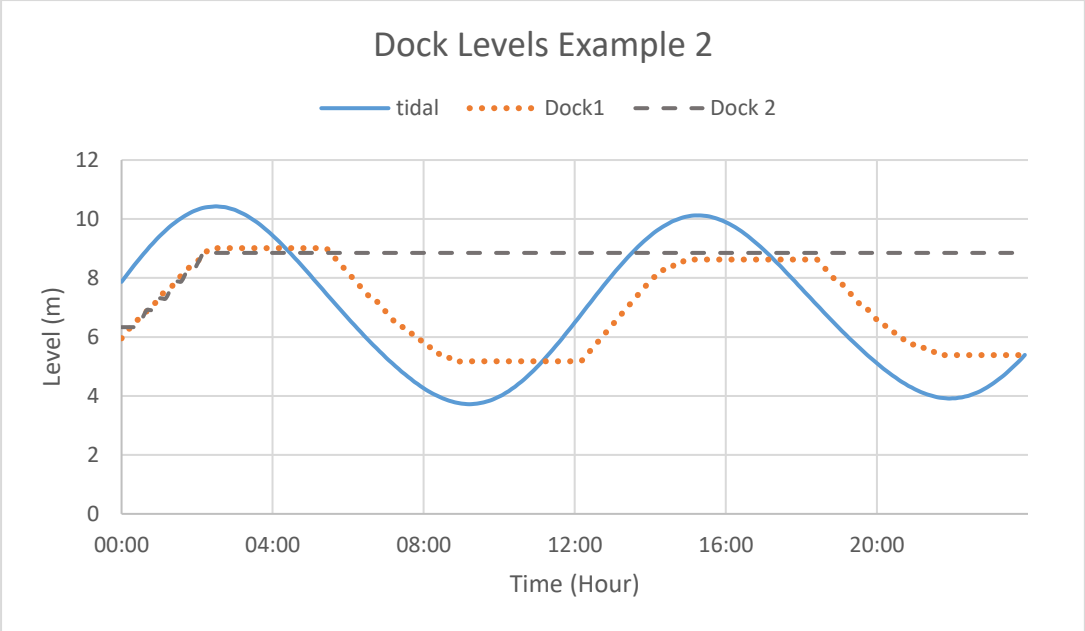

Figure 6-28 Avonmouth: Dock level comparison, Day 2

As required, the ship had to pass through dock 1 to get to dock 2. Therefore, both docks were required to have minimum water levels for incoming ships. In this example, a larger ship was scheduled to arrive at 2:46, and from Figure 18, both docks were prepared before that time. Moreover, once the ship was docked, the level requirements for dock 2 would change to suit the vessel. Dock 1 would be used as a generation reservoir and water levels for dock 2 would remain unchanged for the rest of the day once the ship was docked.

Figure 6-29 shows the estimated power result for all three concepts. Concept 3 and Concept 1 were the only concepts to generate during the four tides. This had a huge advantage over Concept 2. However, Concept 1 still produced most of the power out of the three, but Concept 3 matched the operation time of Concept 1.

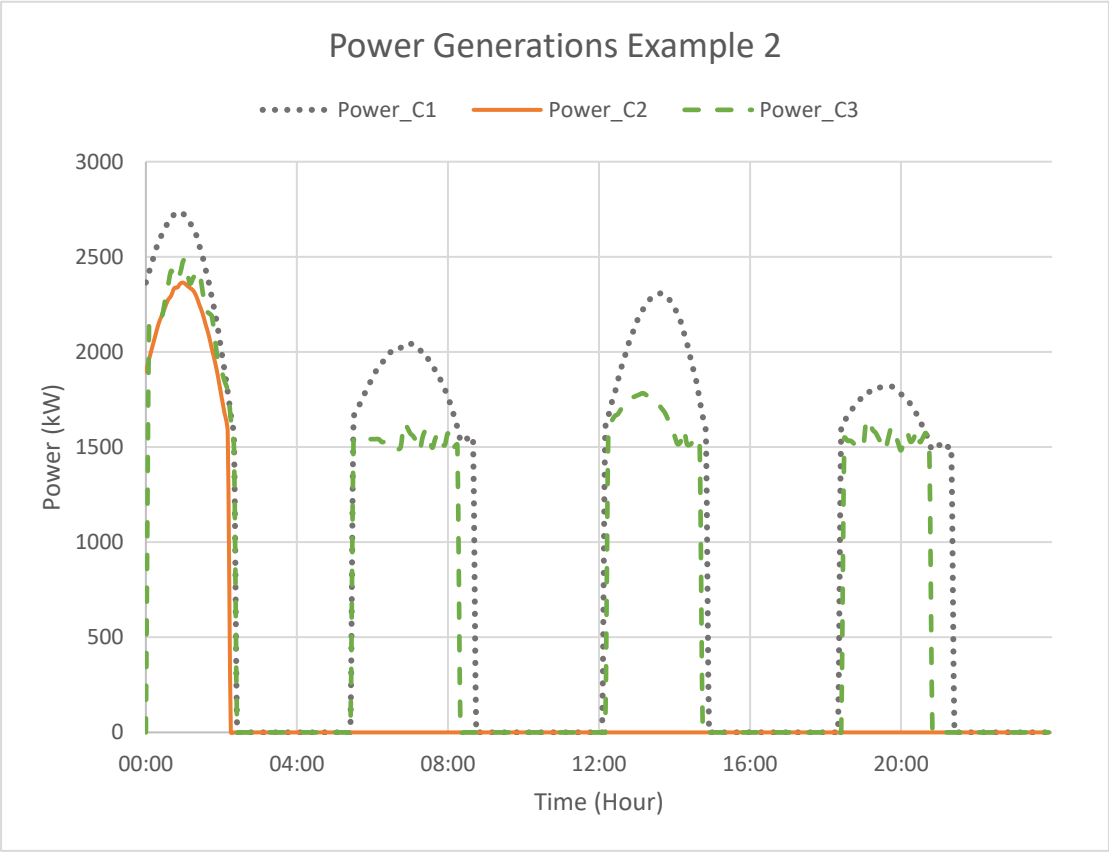

Figure 6-29 Avonmouth: Power level comparison, Day 2

6.3.2.3 Example 3

Figure 6-30 shows that Day 8 had the biggest tidal range during the testing period.

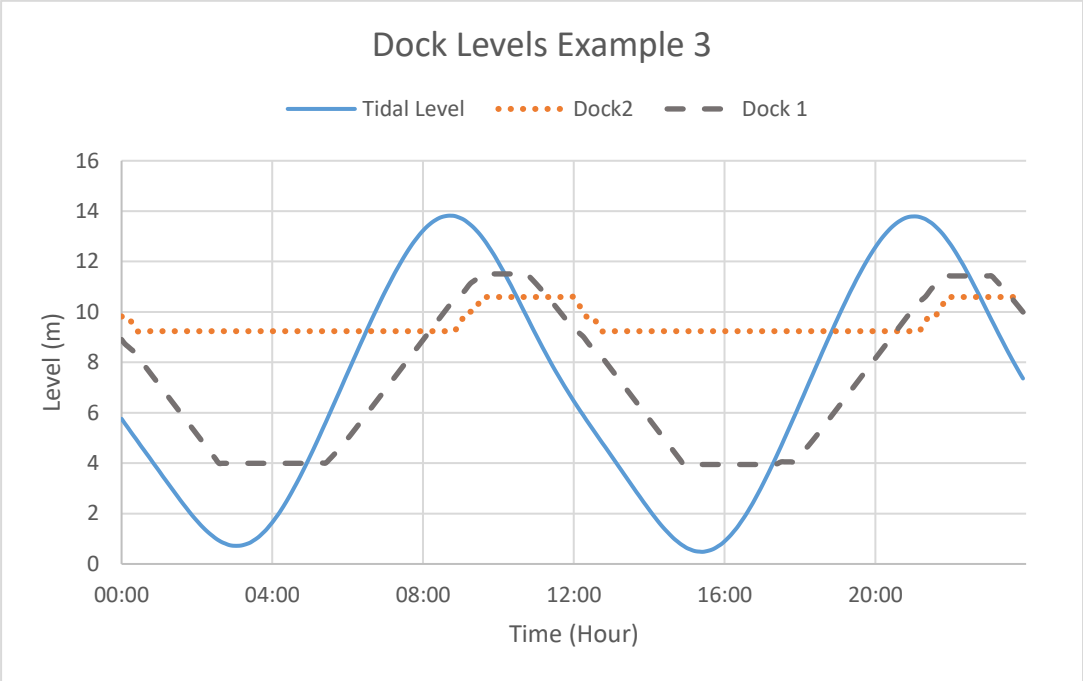

Figure 6-30 Avonmouth: Dock level comparison, Day 8

From Figure 6-30, before 8:00, when dock 2 was higher than dock 1, dock 2 did not transfer water to dock 1 as long as levels were close to the required value. However, if dock 1 were higher than dock 2, it would top up dock 2 only if dock 2 was below the maximum value, which in this case was 14.5 m. Once dock 2 had a head range above the minimum requirement, it could be used to top up dock 1 during the ebb tide, but it could not drop below the required level.

Under the big tidal range, from the power data in Figure 6-31, as Concept 1 remained the favourite option if the power generation was the priority, in both maximum power and generation time, it was the top of the three. However, Concept 3 was the 2nd in these two areas, for the 1st and 3rd generation, the maximum power was 15 % less than concept 1, and 39% less in the 2nd and 4th cycle, where the generation times were about 1 hour less than concept 1 in the 1st and 3rd, and 30 minutes in the 2nd and 4th.

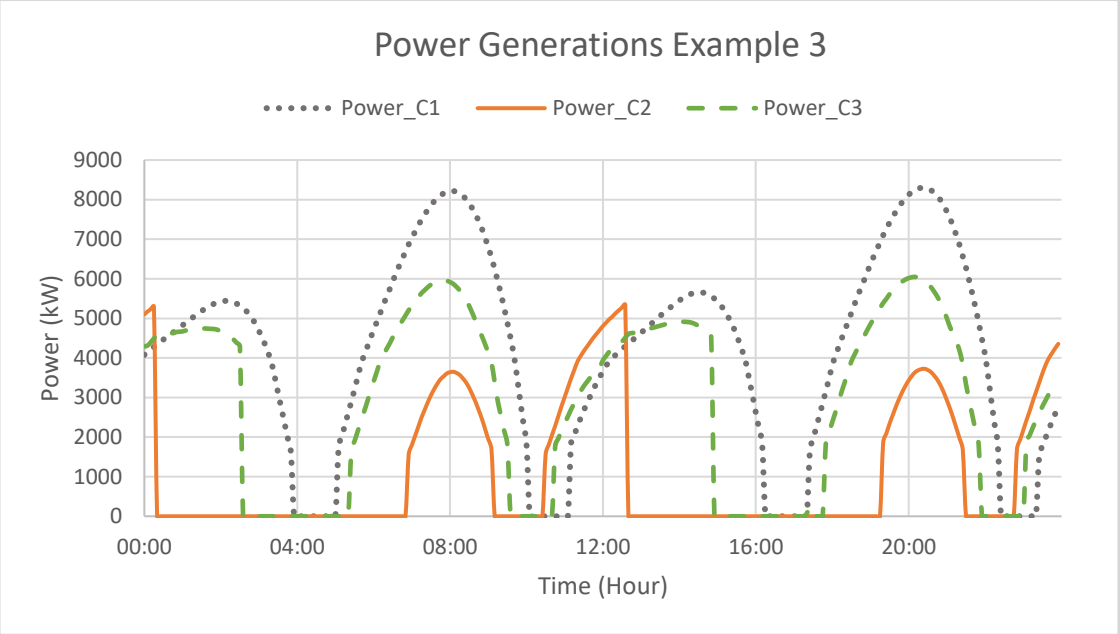

Figure 6-31 Avonmouth: Power comparison, Day 8

6.3.2.4 Example 4

On day 12, the largest ship left Avonmouth Docks at 12:53. To ensure that the ship safely entered the sea, both dock 1 and dock 2 needed to have a water depth to accommodate this ship. According to the results in Figure 6-32, there was enough water for both docks, allowing the ship to pass safely. Once departed, the minimum water depth value was changed accordingly.

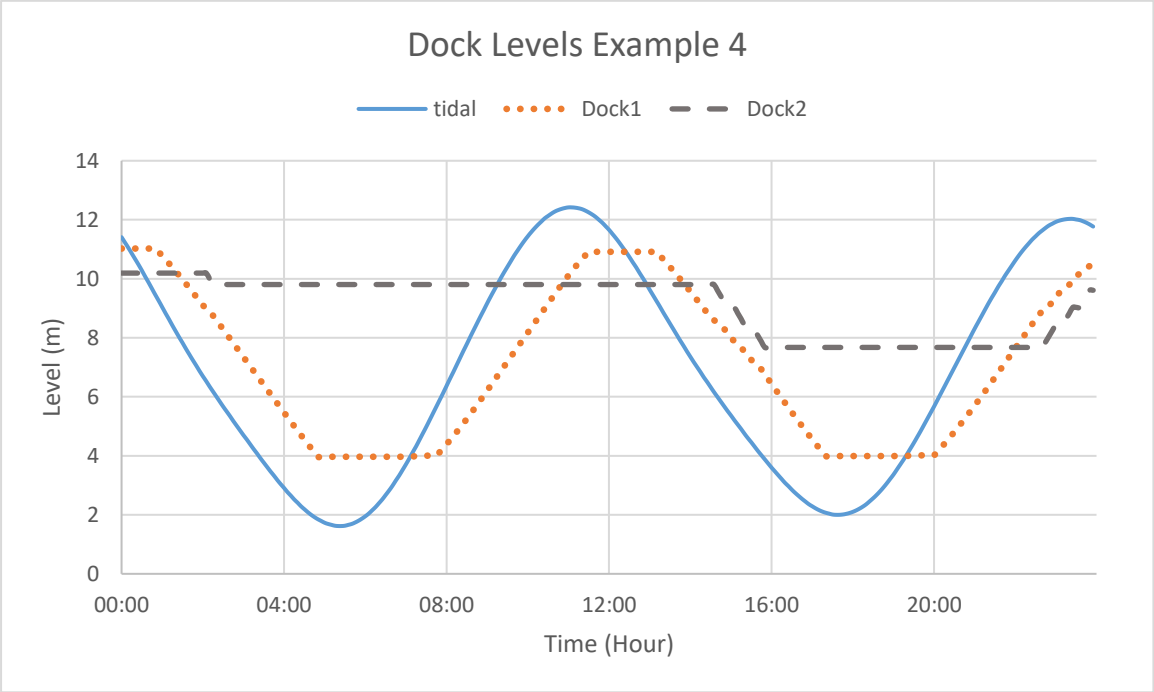

Figure 6-32 Avonmouth: Dock level comparison, Day 12

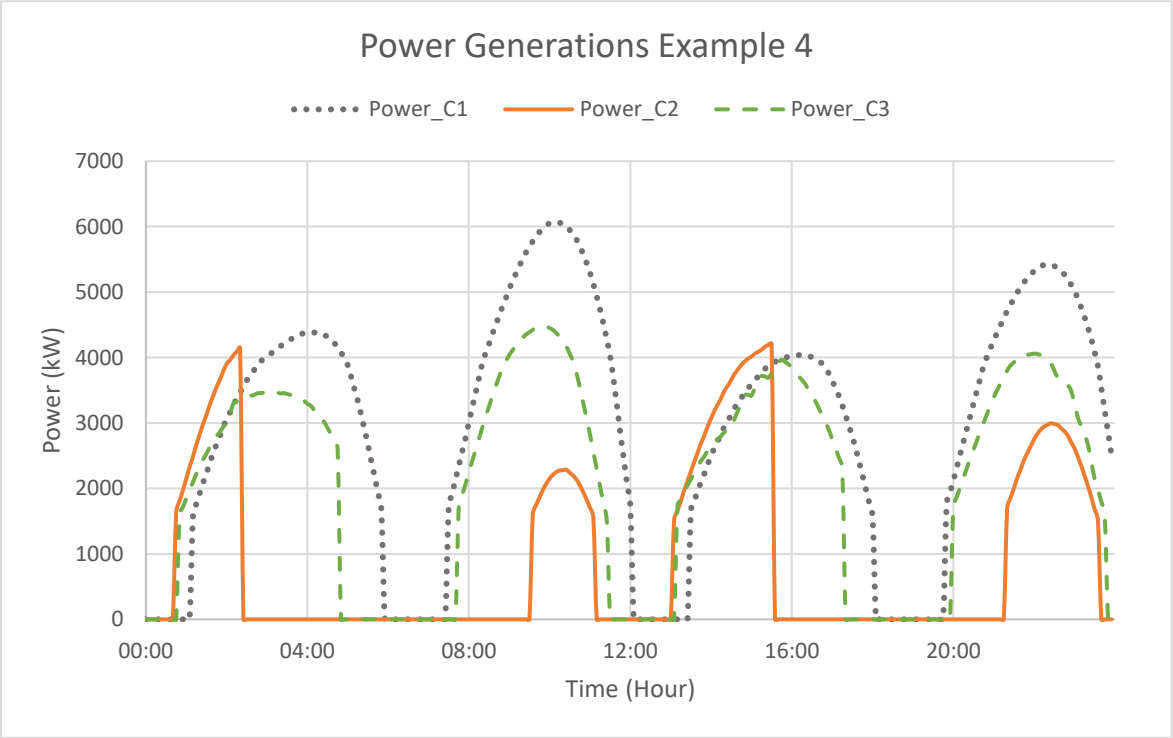

Figure 6-33 Avonmouth: Power comparison, Day 12

As shown in Figure 6-33, with the departure of the big ships, Concept 3 nearly matched

Concept 1 in the 3rd generation, whereas in the 1st cycle, the peak power for Concept 3 was 30% less than Concept 1. Moreover, Concept 3 out-performed Concept 2 in both peak power generation and generation time, whilst maintaining shipping abilities.

6.3.2.5 Example 5

Figure 6-25 shows that Example 5 features results and data from the final day of this period.

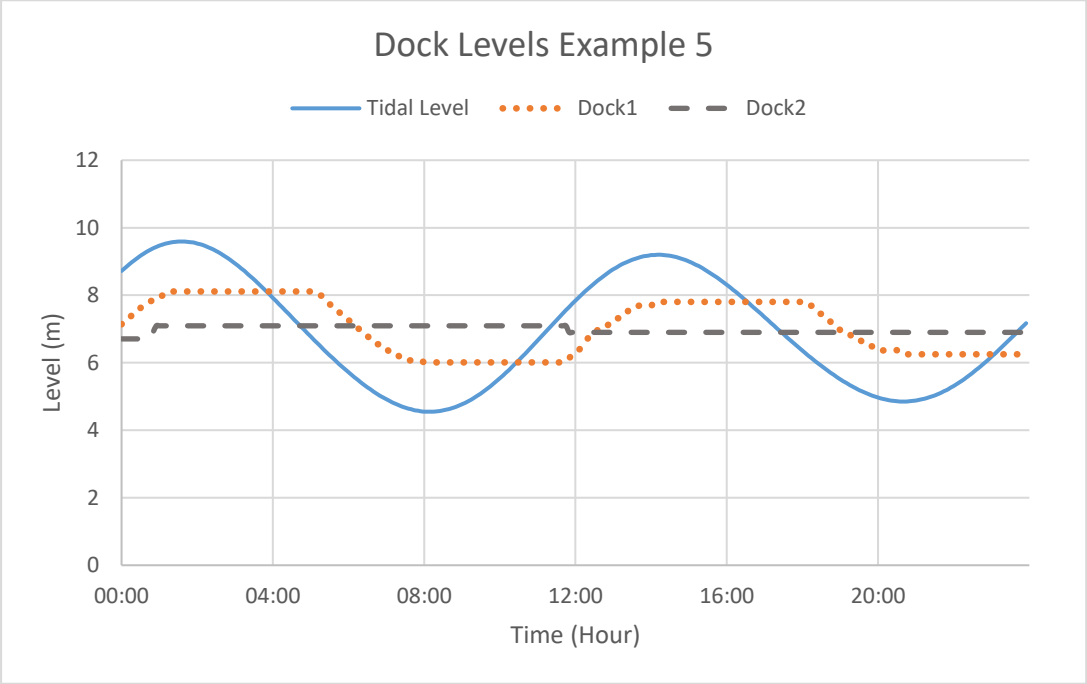

Figure 6-34 Avonmouth: Dock level comparison, Day 16

From Figure 6-34, the tidal range of day 16 was lower than in previous examples. For this concept, the head range for power generation was also affected by the tidal range. Moreover, as the biggest ship in the dock had a draught of 6 m on this day, the required depth for dock 2 was set to 7 m.

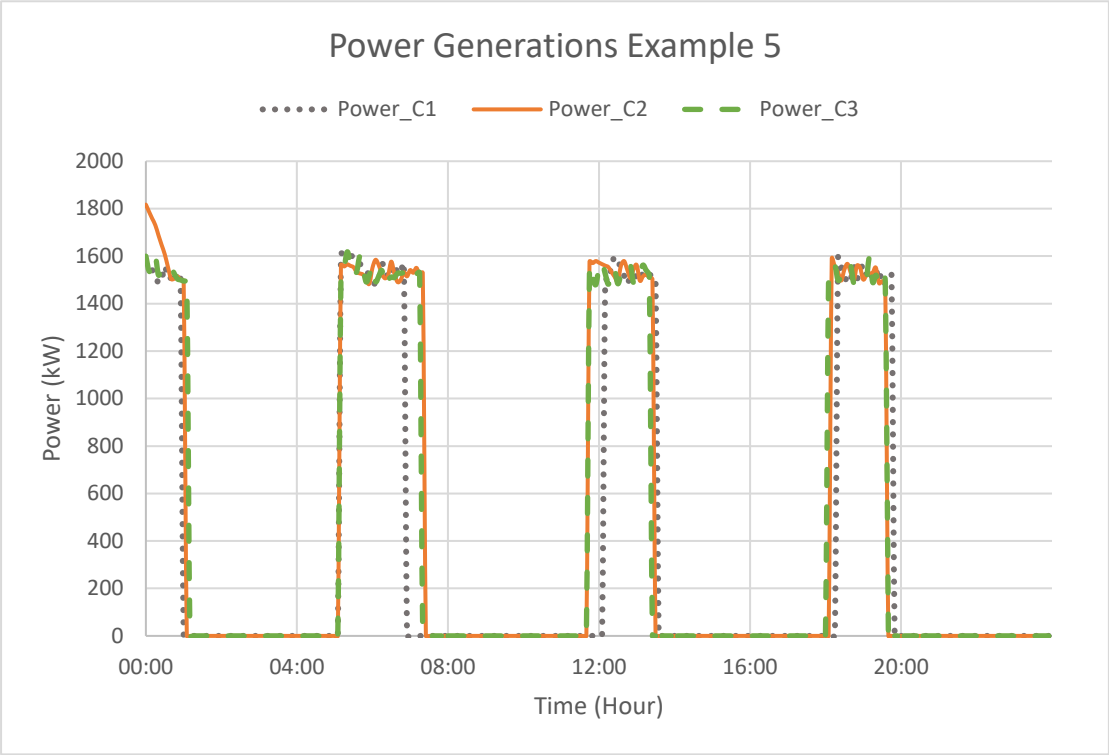

Figure 6-35 Avonmouth: Power comparison, Day 16

The estimated power data for all three concepts were very similar for day 16. It was believed the low tidal range would lower the potential energy, affecting the head range inside the dock. Hence, the head ranges for all three systems were very similar at this stage.

6.3.2.6 Power results

The power results for the 16 days are shown in Figure 6-36, with the results from a previous case study for Avonmouth Docks used as a reference.

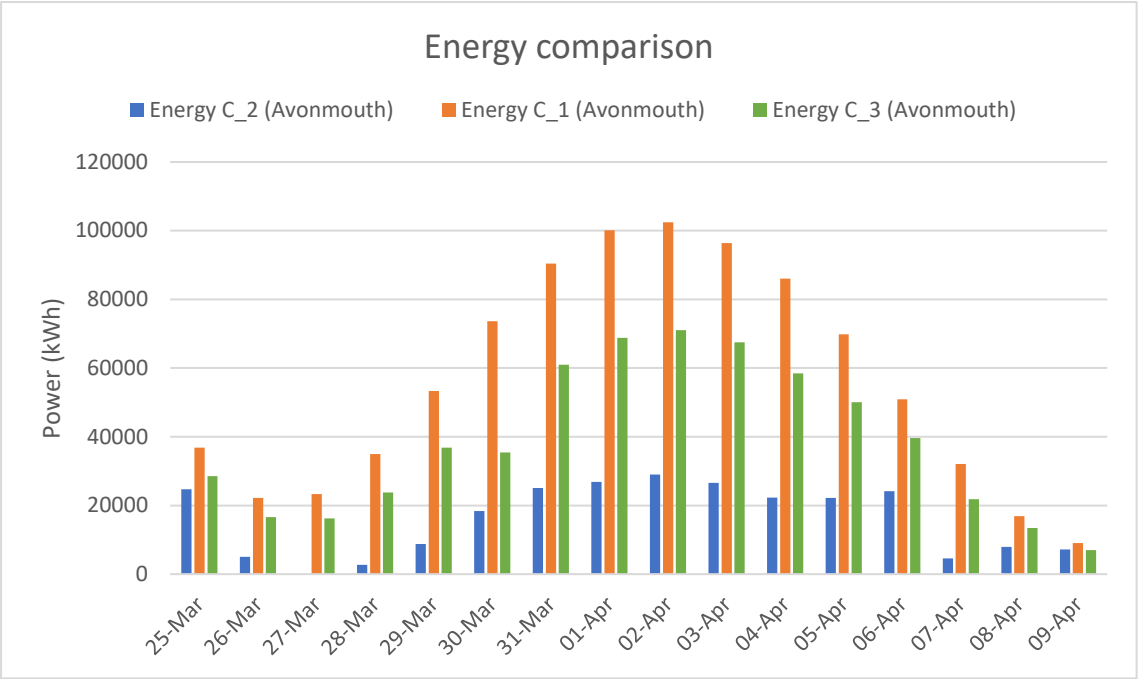

Figure 6-36 Avonmouth: Energy data comparison, all 3 concepts

From Figure 6-36, the estimated power produced by Concept 3 was higher than Concept 2, in all cases. Concept 3 has the potential to generate 615,804 kWh energy, which is 100 % more energy than Concept 2 (255,330 kWh), and approximately 60% more energy than Concept 1 (898,251 kWh), where the sole task was power generation. For lower tidal range days, differences between all three concepts were reduced, as the total potential energy was low.

6.3.3 Examples and results: Cardiff Docks

Concept 3 used the same information as previous cases for Cardiff Docks. Results and examples were shown below. There are three examples will be discussed in this section, and the power results from all three concepts will be compared.

6.3.3.1 Example 1

The first example shows the level results from day 1 which is shown in Figure 6-37, where the largest ship in Cardiff Docks had a maximum draught of 4.5 m. As instructed,

dock 2 would not go below 5.5 m. The level of dock 1 was not affected by the ships inside the dock. During the flood tide, dock 2 was filled up by dock 1, which in theory would give dock 1 a better head generation. That extra head was returned to dock 1 during the ebb tide, but the water level for dock 2 did drop below the requirement.

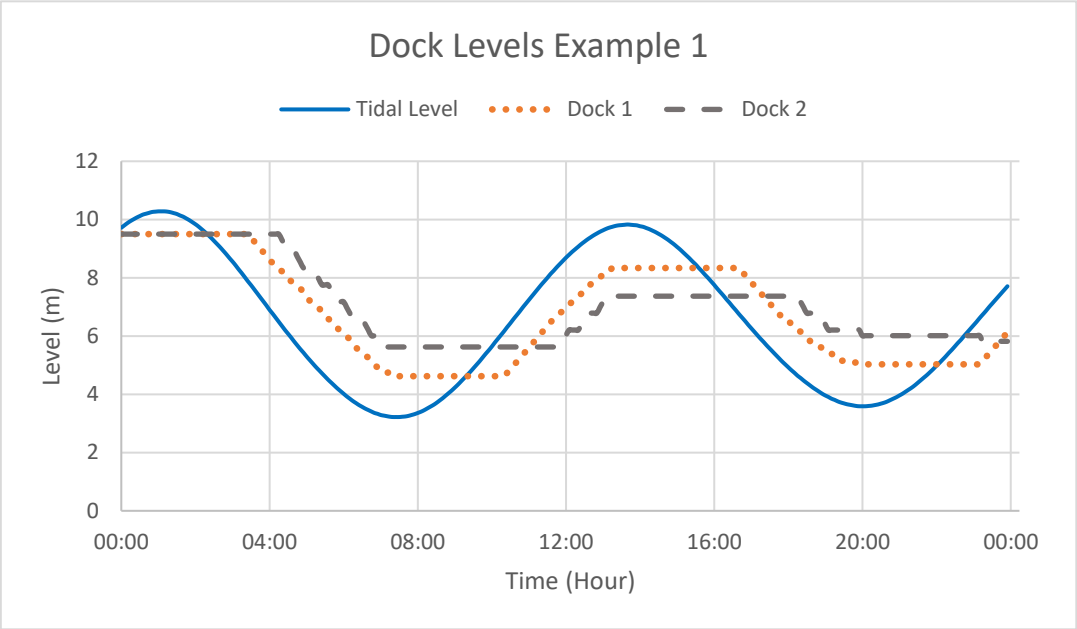

Figure 6-37 Cardiff: Dock levels comparison on Day 1

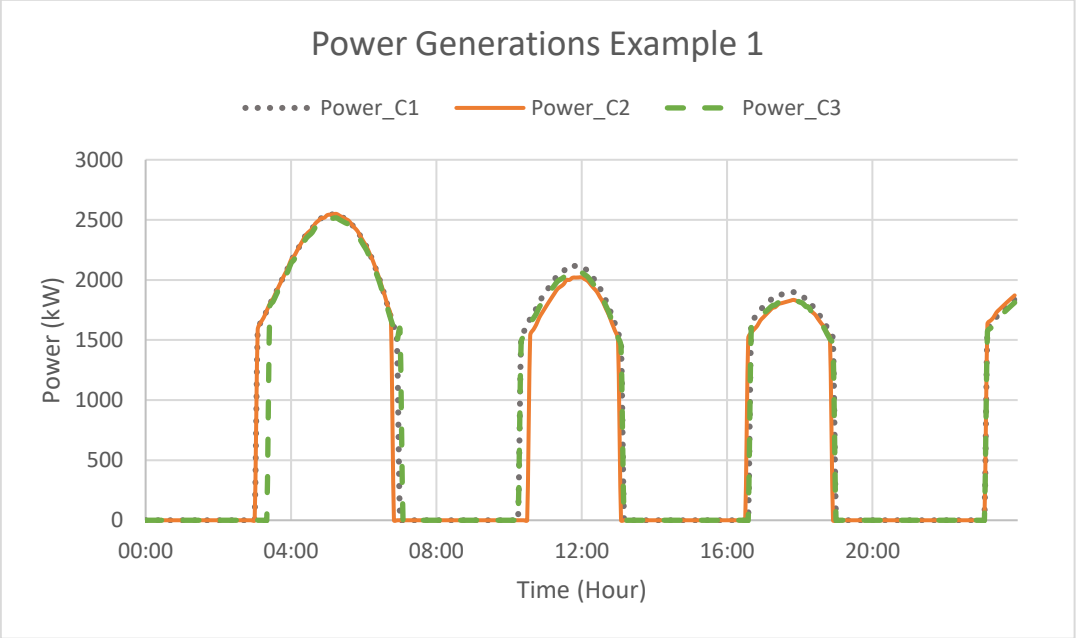

Figure 6-38 Cardiff: Power generation comparison on 25/03/18, all 3 concepts

Figure 6-38 shows the power results for all three concepts. In this case, there was no big difference between the three concepts. This was due to dock levels being similar to the shipping on that day.

6.3.3.2 Example 2

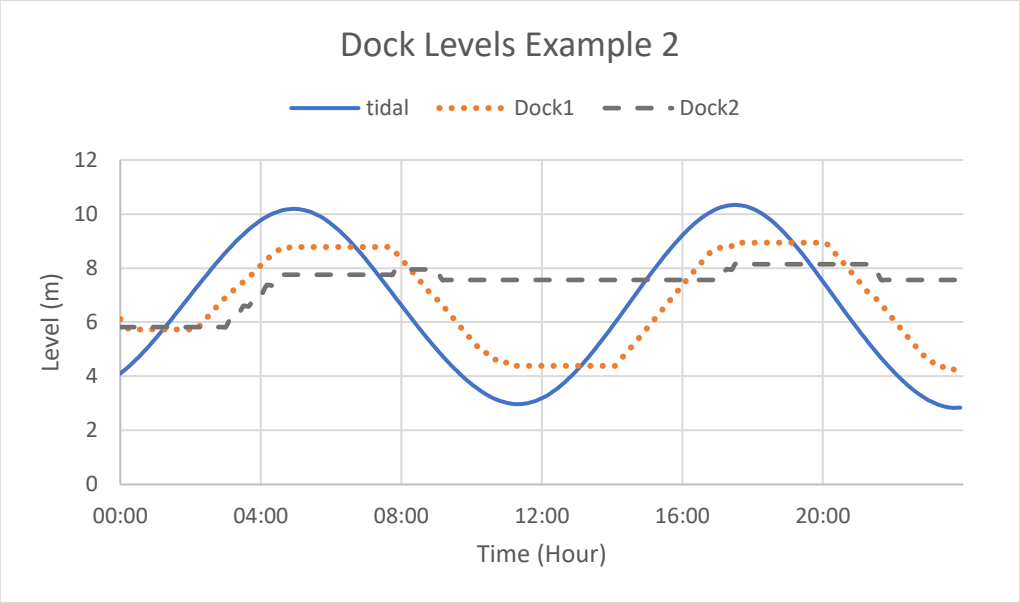

Figure 6-39 Cardiff: Dock level comparison, Day 2

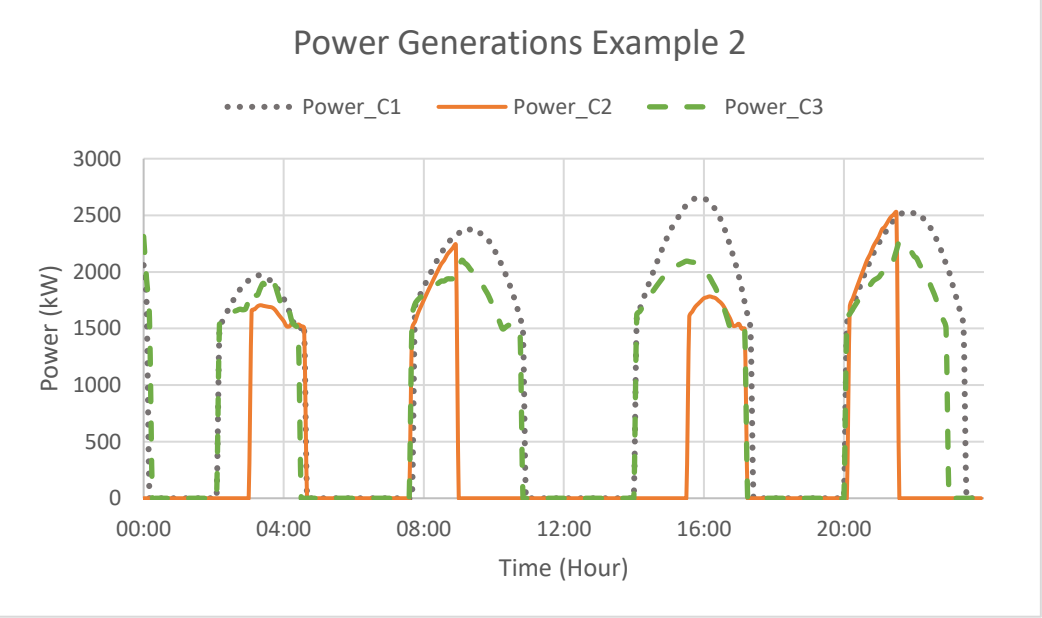

Figure 6-40 Cardiff: Power generation comparison, Day 2

Both Figures 6-39 & 6-40 show the results from day 2. On this day a ship with a 6.8 m draught docked at 4:09. Dock 2 had to be prepared to accommodate this vessel. Once docked, there would be a minimum water level for dock 2, which according to Figure 6-30, dock 2 was not below 7.5 m after the arrival the ships. Moreover, with the ship in dock 2, dock 1 was still active for power generation, as Figure 6-31 suggests. The estimated power production for Concept 3 can generate all four tides. It matched the generation time of Concept 1, but with a reduced power, which resulted from a lower level limit of 4 m.

6.3.3.3 Example 3

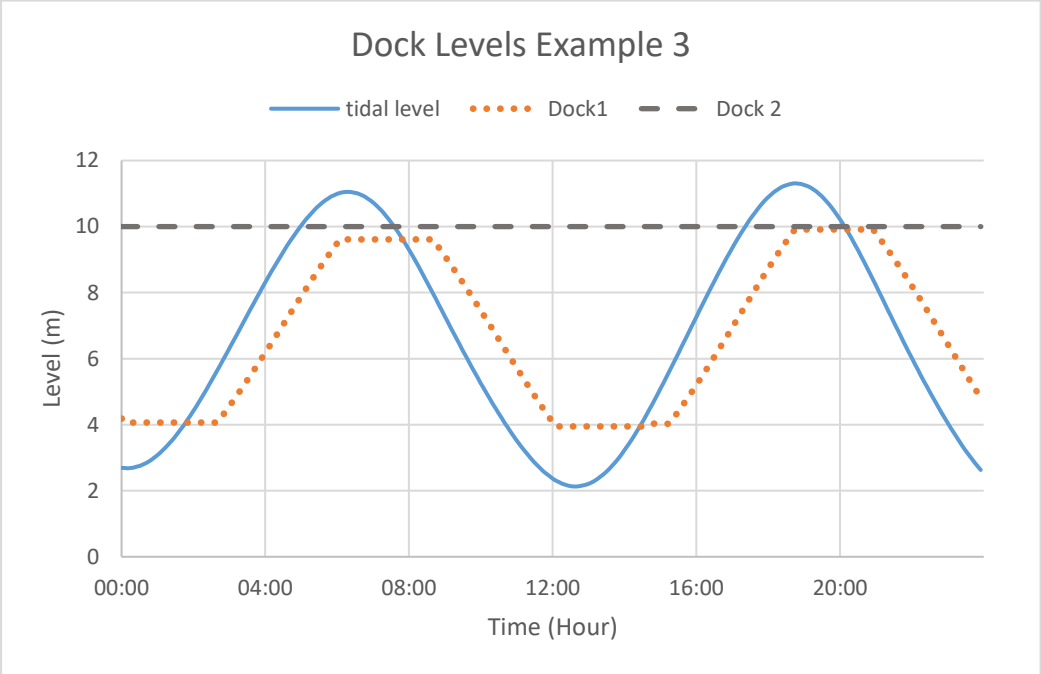

Figure 6-41 Cardiff: Dock level comparison on Day 5

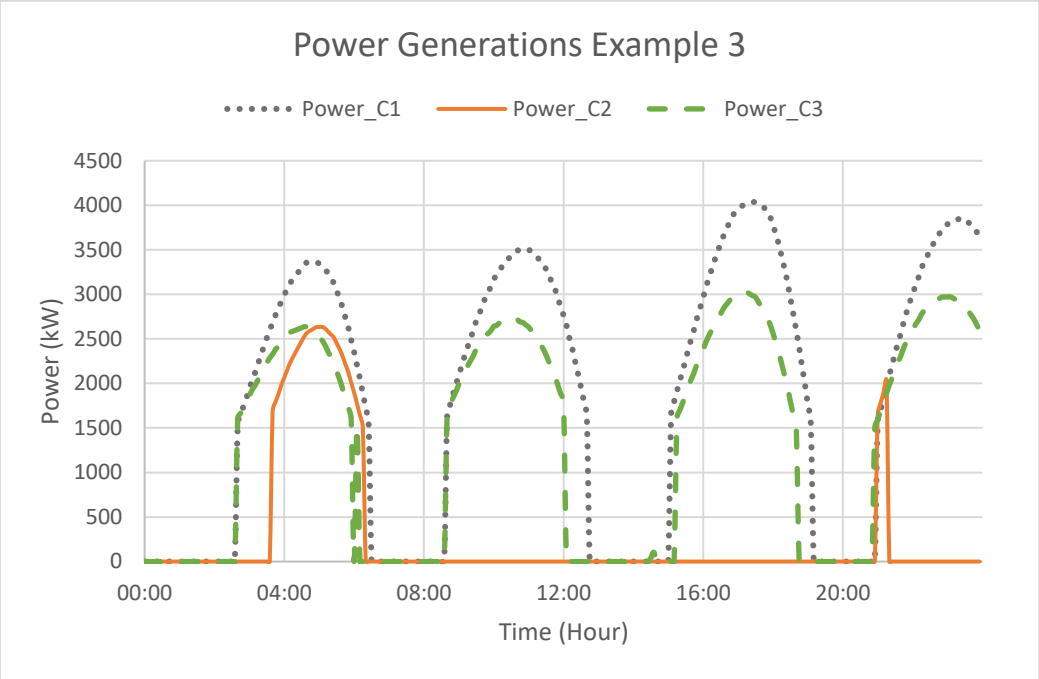

Figure 6-42 Cardiff: Dock level comparison on 29/03/18

Example 3 shows data and results from Day 5. A ship with an 8.7 m draught arrived at 7:57. However, another ship with an 8.8 m draught was already in the dock. There was no need to change the limits for dock 2. In this example, the level for dock 2 remained at 10 m for both ships.

The power results shown in Figure 6-42 indicated that Concept 1 and 3 were the only concepts capable of producing four power cycles, while there was only one power cycle by using Concept 2. For Concept 3, the maximum power was approximately 28% less than Concept 1, but generation times were close, about 40 minutes less in every cycle.

6.3.3.4 Power results

The energy generation results for Cardiff Docks, for all three concepts can be seen in Figure 6-43.

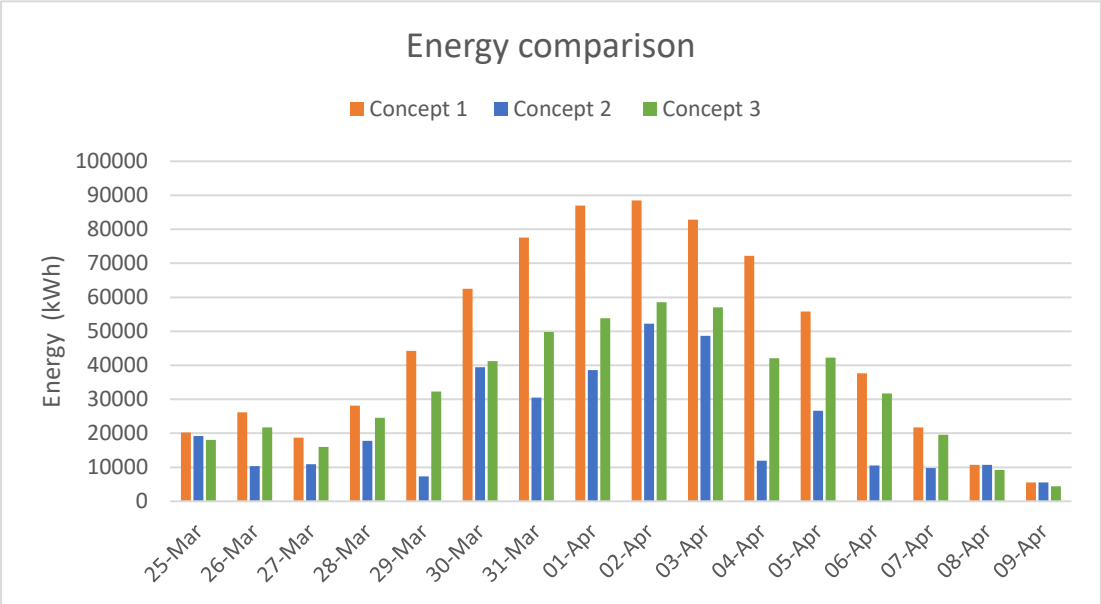

Figure 6-43 Cardiff: Energy data comparison, all 3 concepts

From Figure 6-43, Concept 3 did not have any advantages in terms of power generation over concept 2, for all testing days. For lower tidal ranges, light shipping traffic days, the results from Concept 2 and 3 were very close. Concept 2 had slight advantages; the reasons for this was the new 4 m lower limit for the main dock introduced for Concept 3. This had the effect of reducing the potential head in the dock for power generation. Moreover, for high tidal range days, the estimated power produced by concept 3 was higher than Concept 2 for Cardiff Docks, because shipping traffic was light during the high tidal range period, although there was little differences between Concepts 2 and 3. However, for Concept 2 on day 5 (29/03/17), because of two large vessels, the power generation was very low compared to the other two concepts. This scenario was again repeated on 04/04/17.

According to the results that shown in Figure 6-43, the total energy estimated at Cardiff Docks for Concept 3 is 522,338 kWh, comparing with 350,035 kWh for Concept 2 and 739,390 kWh for Concept 1. It is a more balanced option of the three with the undisturbed shipping schedule.

6.4 Discussion

From the results of this case study, for both sites and three different methods, there are many factors affecting power production if a dock was converted into a tidal station, while maintaining shipping capabilities.

Depending on priorities, if shipping was not a major business of these sites, then under the same tidal ranges, for the same mechanical conditions, the larger the reservoir, the better the power generation. Larger reservoirs store more potential energy. For Concept 1 that discussed in Chapter 6.2.4, which focused on power generation only, over the 16-day testing period, Avonmouth Docks estimated energy production was 15% higher than Cardiff Docks which is shown in Figure 6-44. However, given Avonmouth Docks is 58% larger in volume than Cardiff Docks, the advantage in terms of energy generation at Avonmouth is insignificant. The main reason for this result was the relative positions of the bottom of the dock and sea level were not available. For this, an assumption was made that both sites share the same position. This affected the potential head for the system, but this information can be changed when correct values are given.

It was also found that the shipping has a significant influence on the power generation. By altering the schedule, which allows the large ships to arrive and departure during the flood tide. Which less time could be consumed when preparing the dock level, as the water is entering in the dock during the flood tides. Therefore, the system could potentially generate more energy. However, sometime there are always a change in the schedule due to varies reasons, such as bad weather and navigation, which would add complications to the rescheduling.

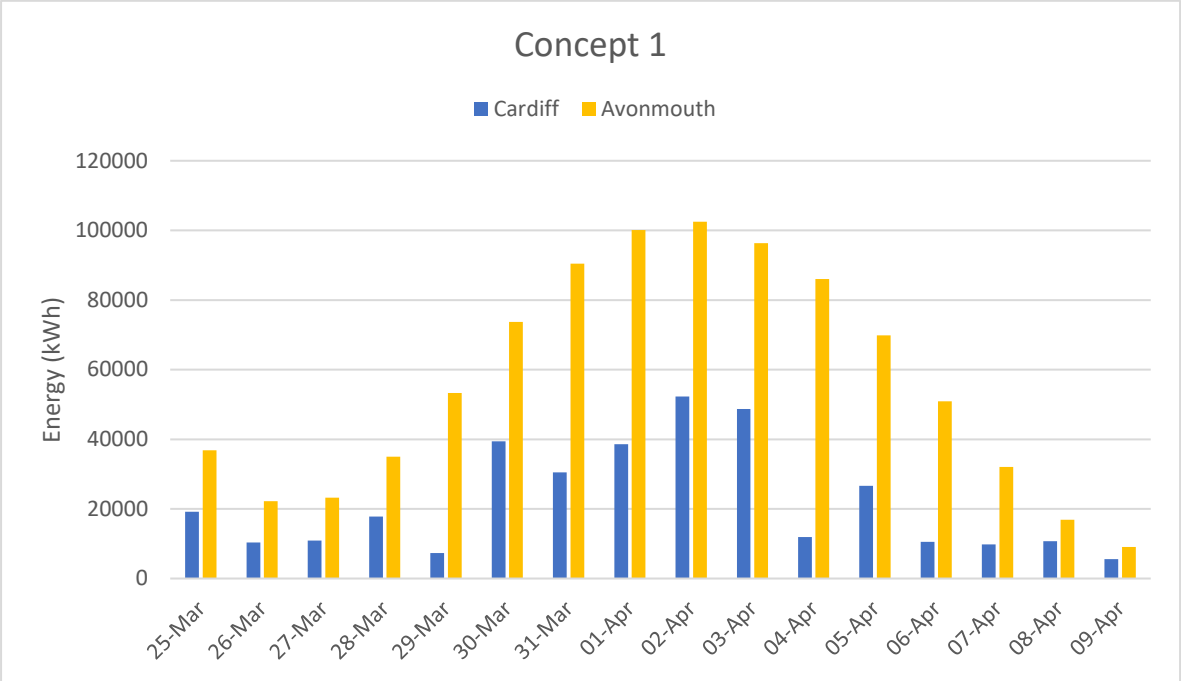

Figure 6-44 Energy data comparison (Concept 1), Cardiff & Avonmouth

If shipping was the priority, then Concept 1 was not appropriate for the task. From Concept 2, an interesting finding noted that if shipping was the priority, then the size differences of the dock was not as significant as how busy the dock was with shipping. Figure 6-45 shows the power difference for Concept 2.

Unlike Concept 1, Cardiff Docks could generate more energy than Avonmouth. On the 3rd of April, more than 100% more energy was generated, when tidal ranges were high. From this result, the biggest impact of energy generation is shipping. The ship with a deep draught staying in the dock for a long time, and in that case, the available head for generation would be limited.

Both Concepts 1 and 2 had strengths and weakness. For Concept 1 the strength was the maximum power generation, but shipping would be affected. On the other hand, Concept 2 maintained a normal shipping business, while generating power, but generation was dependent on the ships. Therefore, a balanced third option Concept 3 was proposed, by using the smaller dock to accommodate large incoming vessels,

while the bigger dock could generate power, with a limited impact from shipping. The results were as expected, the estimated power from Concept 3 could not match Concept 1, but it met all shipping requirements within Concept 2, where Concept 1 could not.

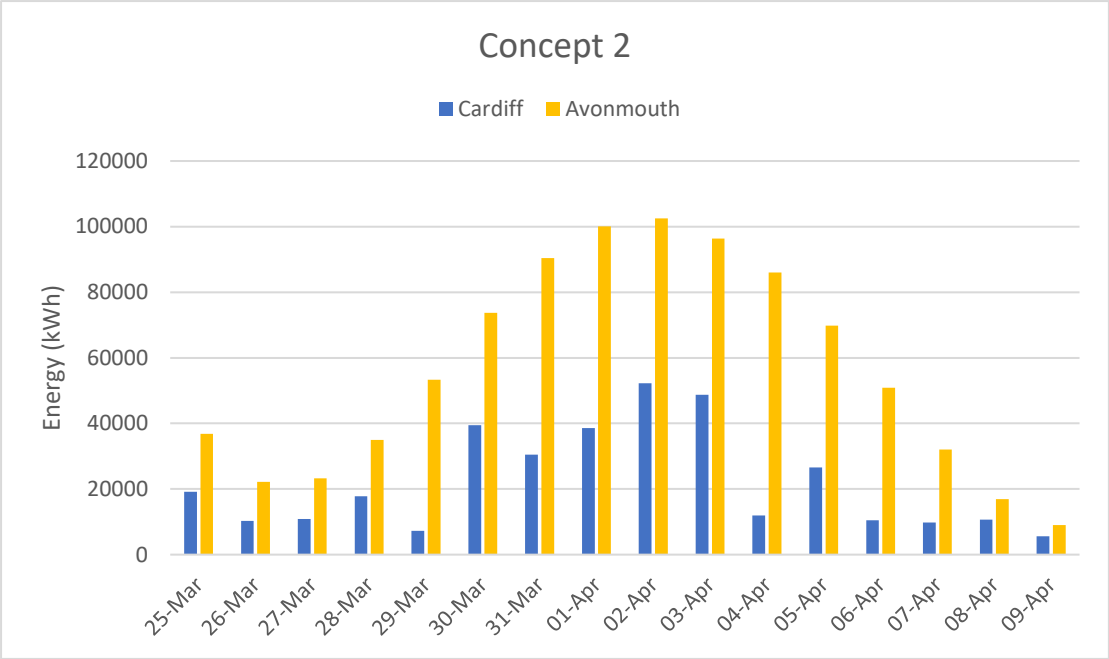

Figure 6-45 Energy data comparison (Concept 2), Cardiff & Avonmouth

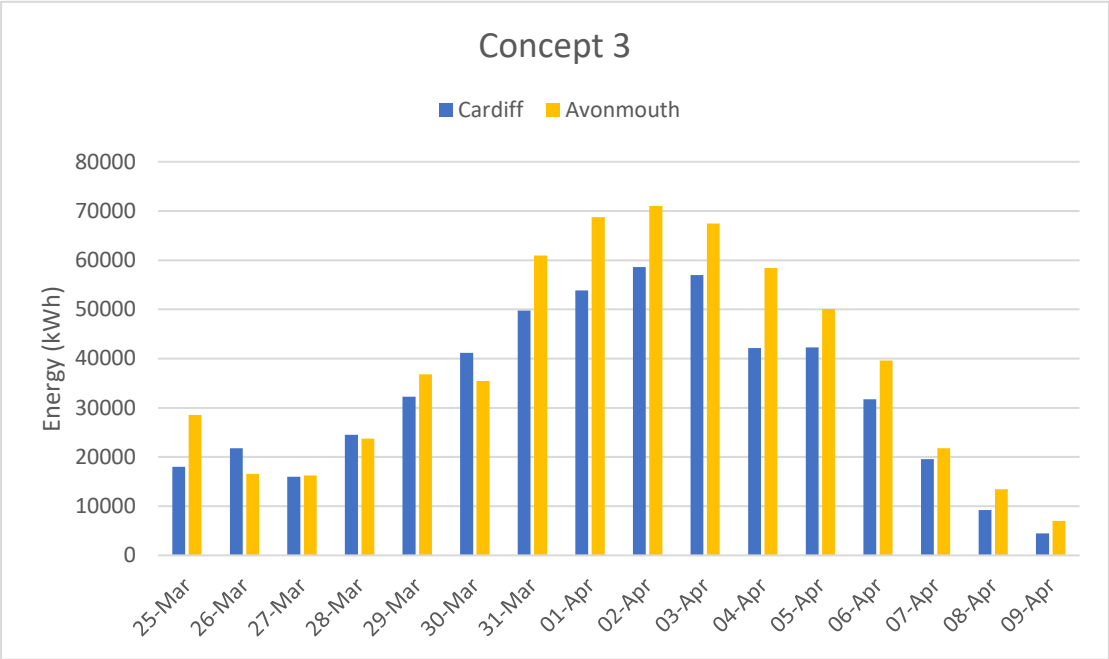

Figure 6-46 Energy data comparison (Concept 3), Cardiff & Avonmouth

From Figure 6-46, for Concept 3, the results indicated that the larger dock was advantageous in terms of power generation, over the smaller dock. In this case, Avonmouth's busy shipping traffic was not affected. However, for lower tidal range days, difference was not as big as for high tidal range days.

From the results for both sites, for all three concepts, concept 3 provided the most balanced choice; it could power while maintaining regular shipping. Concept 1 had the ability to produce maximum power, but shipping had to be changed. Lastly, Concept 2 seemed the worst option, the estimated energy production was poor, when compared to the other concepts.

6.5 Chapter Summary

From the results, under similar tidal ranges and mechanical conditions, Concept 1 produced the most energy, but regular shipping would be delayed. In the worst case situation, ships would not be permitted to dock due to low water levels, insufficient

to accommodate the ship's draught.

Concept 3 proved that the system could maintain a power generation, without sacrificing regular shipping. By comparing energy generation over the testing period, differences between Concept 3 and Concept 1 were much smaller than Concept 1 and 2. Additionally, if shipping was not considered as the priority, the docks with larger volumes would be advantageous in terms of power generation. However, once shipping was introduced, energy production was affected by docked ships. From the case study results, Avonmouth Docks is 58% bigger than Cardiff Docks, but with busy shipping traffic, it would generate much less energy than Cardiff Docks, if Concept 2 was used. Finally, under the lower tidal ranges, the potential energy generated by the tide was low, resulting in lower energy production for all three concepts.

To conclude, Concept 1 was the best option for sites with light shipping traffic. To accommodate smaller ships. From the results of Concept 1, the dock level would not be empty, For Cardiff Docks, a minimum 3 m depth was maintained through the 16-day testing period, which for a ship with a small draught, so that the dock would still be useable.

For docks like Avonmouth Docks, where heavy shipping was required, then Concept 3 proved a good option. Although this option does not produce the most energy, it would allow the dock to maintain regular shipping, allowing ships with big draughts to dock in the smaller docks and thereby using the bigger dock to generate energy. In doing so, the head range for power generation would not be reduced by large ships staying in dock.

Furthermore, this numerical model can be changed to allow users to input cost-profiles for energy generation and shipping, generating economic profiles. Users could use this information to improve onsite systems for better energy generation.

7. Discussion and Conclusion

This chapter discusses the results of the following chapters of this thesis. The tidal energy related technologies were reviewed in Chapter 2. A hydraulic driven tidal turbine system is introduced in Chapter 3. Chapter 4 introduces the pumped tidal lagoon system that uses the docks as the reservoir. Chapter 5 analyses the recorded data from Jiangxia Tidal Power Station, with the numerical model is validated with such data. Chapter 6 investigates of conversion of the active docks into a tidal lagoon, whilst kept the scheduled shipping.

7.1 Renewable technologies review (Chapter 2)

The ocean provides the opportunity for a significant source of energy, and there are many technologies available to generate renewable energy. In Chapter 2, several systems were discussed, which included wave energy devices, tidal stream turbine systems, a tidal lagoon, hydroelectric, and pumped hydroelectric systems. Generally, the tidal lagoon, hydroelectric and pumped hydroelectric systems can provide large amounts of power due to their size, which is significantly larger than the other systems that were discussed. Furthermore, the lifespan of these systems is long, for example, La Rance Tidal Power Station has been generating energy since 1966 and Jiangxia Tidal Power Station started to deliver energy to the grid in 1980, and they are still in operation in 2018. The pumped hydroelectric storage system is a system typically used for load balancing, which generates power from potential energy stored in the reservoir located above the generator. During the peak demand period, water is released to produce power, and when the demand is low, water is pumped back into the reservoir using surplus electricity. Although this pumping method consumes electricity, the system would increase revenue by selling energy during peak demand, when the price is higher. However, these systems have a significant construction cost,

for example, La Rance cost £500 million to build (priced in 2009), and £160 million for the proposed Glyn Rhonwy pumped hydroelectric storage which will begin construction in 2019.

However, the wave and tidal stream systems discussed are much smaller in size compared with a system like La Rance, as they are only rated at a power output between 250 – 2,000 kW, with estimated energy costs below £0.35 compared with £0.02 for La Rance, per kWh. Although the wave and tidal stream systems discussed are not yet fully commercially operated, it is believed that once these systems are fully deployed, the costs could be even lower.

One of the potential issues of these wave and tidal stream systems is the accessibility, as many of these systems are fully submerged in the water, which it harder to access, unlike the hydro and tidal lagoon systems. The design of SeaGen is an exception of this case, as the turbines can be raised above water for maintenance and inspection.

Visits to Xiaolangdi Hydro Power Station, Jiangxia Tidal Power Station and Dahang Wind Farm, provided a unique opportunity to experience real commercial facilities and to discuss the operations with on-site engineers. The visit to Jiangxia Tidal Power Station proved to be particularly useful as it resulted in an agreement to provide a year's worth of recorded operating data which was used in this research to help with the development of the simulation model.

7.2 Hydraulic driven tidal turbines (Chapter 3)

The current tidal stream turbine systems share similar mechanical designs to current wind turbines, and as such, they suffer from similar operational problems. According to the research reviewed, the failure rate of the wind turbines between 2008-2012, showed that the gearbox failure contributed the longest downtime. Because of shared technology, the current tidal stream turbine systems also enclose the gearbox inside

the nacelle, but access for maintenance and inspection is made far more difficult due to the underwater working environment.

To make the tidal stream turbine system more maintainable, a hydraulic system was proposed in Chapter 3. By using hydraulic transmission, the problem of poor accessibility of the conventional design, could be improved by locating the hydraulic motor, electrical generator, and oil reservoir on shore. Additionally, to address the gearbox issue which contributed the longest downtime in the wind turbine system, this hydraulic system would not use a gearbox but a gear pump that could efficiently operate at turbine speed, such as a swash-plate pump. The proposed closed-loop hydraulic system, features a turbine driven pump, which generates the high pressure hydraulic flow, which drives a land-based hydraulic motor, which drives an electrical generator - underwater hydraulic pipes connect the hydraulic pump and motor assemblies.

Additionally, it was proposed that multiple turbine/hydraulic systems could be connected to a single motor-generator unit. A hypothetical system was proposed and modelled, which consisted of a twin-rotor design, and an on-shore generator located 200 m away. The results show that this design has a hydraulic efficiency of 97.6%, and an overall efficiency of 82.57%.

An attempt was made at estimating the potential cost of this system, which was found to be approximately £2 million, excluding the cost of the hydraulic fluid, oil reservoir and other components such as the control systems. Compared to SeaGen, which was installed at a cost of £3 million (priced in 2008), the hydraulic turbine system would cost even more when fully operational.

Finally, one of the biggest hazards of using a subsea hydraulic system, is the risk of the leakage of the hydraulic fluid. The results showed that in order to generate 1,250 kW from the hydraulic motor, it would require 0.04 m^3/s (2,431 l/min) at 340 bar (4,932

psi), with a total mass of oil of approximately 8 tonnes. If there was a leakage in the system, with the large flowrate and high pressure, the result would be a significant environmental disaster.

As a result of the high installation cost and the potential for oil leakage, it was concluded that the proposal is impractical and too risky from an environmental point of view.

7.3 Hybrid tidal energy system (Chapter 4)

To address the issues discussed in Chapters 2 and 3, a new system is proposed. This new system consists of a pumped storage tidal lagoon, which utilises architected docks as the reservoir, and a tidal stream driven pump to augment the water level inside the dock. This could help to mitigate the high construction costs typically associated with tidal barrage, and large scale pumped storage hydro systems.

The numerical model of the proposed hybrid pumped storage system, is based on a conceptual dock which is geometrically similar to Newport Docks. By comparing the results from the hybrid system with the conventional tidal lagoon system, the hybrid system showed that it could generate 2% more energy under the same tidal conditions.

Additionally, a new control method is introduced which can be applied to multiple docks, which uses the largest dock as the main reservoir for power generation, and the smaller dock as a storage. When the head is less than optimum, the smaller dock will top up the larger dock, in order to reduce the rate of the head difference between the larger dock and the tidal range. Results show that by using this control method, the system can generate 20% more energy compared with the original hybrid system where the two docks operate as one reservoir.

7.4 Data analysis for Jiangxia Tidal Power Station and further development of the numerical model (Chapter 5).

Granular data, recorded between 2011-2012, was provided by Jiangxia Tidal Power Station. These data, recorded power generated, water levels, guide vane angles, and generator speed.

This data was too comprehensive to analyse manually therefore a Matlab code was developed identify and tag key stages in the power generation, and to summarise the power data. This programme identifies peak power within each generation cycle and its corresponding tidal level. Additionally, the programme can also calculate the total energy generated (kWh), the average generation power (W) and generation time (minutes). It was found that there were a number of erroneous power data recordings with negative values, which the programme was developed to identify and subsequently ignore, as advised to do so by the site engineer.

By analysing this data, it was possible to understand how Jiangxia Tidal Power Station was operated. It was found that there were two elements that determine the end of the generation cycle. The first element is the reservoir level, above and below a reference point. For flood tides, the generation is stopped once the reservoir level has reached 1.7 m. For ebb tides the generation is stopped once the reservoir level has reached -0.6 m. The second element is the head value, where the generation is stopped when value is less than 1 m. The head value is the only element that would determine the start of the generation, with a minimum requirement of 2 m for the flood tides, and 2.5 m for the ebb tides.

The overall efficiency of Jiangxia Tidal Power Station is confidential, therefore it was necessary to calculate it. The potential energy from the head difference was calculated because the level data for both tide and the reservoir, along with the actual power output from the generator, were recorded. In some cases, it was observed that under

the same head, the power generated during the ebb tide was 100% higher than that generated during the flood tide. Jiangxia Tidal Power Station did not explain this anomaly but one hypothesis is that a control method is used to regulate the flowrate for different tides, and therefore reduce flood risk to the surrounding residential area.

The conventional tidal lagoon part of hybrid system simulation was refined and then validated using the Jiangxia Tidal Power Station data from a different time of the year.

7.5 Conversion of active docks to a hybrid tidal system (Chapter 6)

The hybrid system is applied to two commercially active docks, Avonmouth and Cardiff Docks, which are located in the Bristol Channel. These were chosen as they provide significant potential to generate tidal energy, due to the tidal range.

The results from the simulation showed that for 39% of the time, the required 1 m/s tidal stream speed for the large-scale tidal stream turbine used in the numerical model, is not met. Therefore, it was concluded that these docks were not suitable for a full hybrid system. Moreover, it was noted that the effect of the arrival and departure of the ships will compromise the power generation strategy, by dictating when the dock gates have to be open and closed. The model was used to simulate the effect of the tidal range and the recorded shipping schedules for a chosen period, on power generation. Information regarding inflow from any water feeders into the docks was unavailable, therefore not included.

7.6 Conclusion

- This thesis has reviewed existing tidal and wave energy devices, including wave energy generators, tidal stream turbines, hydroelectric, pumped storage and tidal range. The strengths and weaknesses of each of these systems were discussed.
- Since the units are fully submerged, one of the potential problems for tidal stream turbines is accessibility, which significantly complicates installation, maintenance and repair. A conceptual design for a hydraulic tidal turbine system was proposed and analysed. The results showed that the system had an overall efficiency of 87%, but it was concluded to be infeasible due to the high installation cost, and the concern of environmental hazards due to the potential for catastrophic oil leaks.
- A hybrid pumped/storage system was proposed, featuring the use of existing docks as a reservoir, to generate power locally. A detailed Matlab simulation model was developed which showed that there is an improvement in both peak power generation, and generation time, when compared with the conventional storage-only design. The simulation model was refined and validated using recorded data from the Jiangxia Tidal Power Station. A Matlab programme was developed to help analyse the extensive Jiangxia data. This investigation showed that a 2% increase in power generated could be achieved when using the hybrid system versus the storage-only system, for the same operating conditions.
- The simulation model was then applied to Avonmouth, and Cardiff Docks to simulate their potential for power generation. Unfortunately, due to the low tidal stream velocity of the Bristol Channel, the pumping facility of the hybrid model was not implemented, so the simulation was limited to treating the docks as simple tidal lagoons. The results showed that these two sites could

generate 899,000 and 740,000 kWh respectively for Avonmouth, and Cardiff Docks during the 16 days testing period.

- The simulation of Avonmouth, and Cardiff Docks was modified to take account of scheduled ships entering and leaving the docks. Two scenarios were investigated. The first scenario assumed that the water level in the largest dock had to be maintained at the maximum height to accommodate the ship with the largest draught. The second scenario allowed the water level to be lowered in the largest dock, by assuming the largest ship could be moored in the smallest dock. This allowed the full, larger dock to be used for power generation. The results of these simulations showed that the second scenario provided a practical compromise between power generation and operating a commercially viable dock, with 616,000 and 522,000 kWh for Avonmouth, and Cardiff Docks respectively in the same 16 days testing period.
- It was proposed that the simulation could be eventually developed into a programme which could be used to schedule the arrival and departure of ships, alongside desired future periods of power generation, in order to maximise the revenue generated by the overall dock system.

7.7 Future work

- The simulation model was developed for the author to use. It should now be modified to be user-friendly, thereby enabling it to be used by other interested parties.

- As mentioned in the conclusions, the simulation model should be further developed into a scheduling algorithm to obtain the optimum combination between power generation and the required shipping schedule.

- The size and number of tidal stream turbines required for pumping in a hybrid configuration needs to be identified. This requires a detailed bathymetric and flow velocity study of a proposed site.
- The above should be expanded to include a levelised cost of energy study (LCOE) for an actual proposed site, and to include a comparison with established renewable technologies, such as wind.

References

Abports.co.uk. [Online] Available at: http://www.abports.co.uk/Our_Locations/South_Wales/Cardiff/ [October 2017]

Abuelsamid, S., (2007). *1.2 MW Tidal Turbine to be installed off Northern Ireland. Autobloggreen*. [Online] Available at: http://www.autobloggreen.com/2007/06/16/1-2-mw-tidal-turbine-to-be- installed-off-northem-ireland/ [April 2009]

Ashton, T. S., (1998) *The Industrial Revolution*, 1760-1830. London.

Atwater, J.F., Lawrence, G.A., (2008) *Limitations on tidal power generation in a channel*. Proc. World Renewable Energy Congress (WRECX). pp. 947-952.

Baker, C., Walbancke, J., Leach, P. (2006) *Tidal Lagoon Power Generation Scheme in Swansea Bay. A report on behalf of the Department of Trade and Industry and the Welsh Development Agency*. AEA Technology Contract numbers: 14709570 and 14709574. URN number: 06/1051.

Black. (2004) *Phase II, UK Tidal stream energy resource assessment*. Marine energy challenge. Carbon Trust.

Black. (2005) *Tidal Stream Energy Resource and Technology Summary Report*. Carbon Trust.

Bristolport.co.uk. [Online] Available at: http://uk-ports.org/the-bristol-port-company/ [October 2017]

Boschrexroth.com. (2011) *Hägglunds CBP* [Online] Available at: http://www.hydba.com/es/wp-content/uploads/2017/01/Manual-CBP-Ingl%C3%A9s.pdf [November 2014]

Bosserelle, C., Kruger, J., Reddy, S. K. (2015) *Cost analysis of wave energy in the pacific.*

Bryden, I.G., Couch, S.J. (2007) *How much energy can be extracted from moving water with a free surface: A question of importance in the field of tidal current energy?* Renewable Energy 32

Cameron. L, Doherty. R., Henry. A. (2010) *Design of the Next Generation of the Oyster Wave Energy Converter*. 3rd international conference on Ocean Energy. 2010

Carbon Trust. (2006) *Future Marine Energy. Results of the Marine Energy Challenge: Cost competitiveness and growth of wave and tidal stream energy.*

Casey, B. *Use more than data to determine your hydraulic pump life*. (2014)

[Online] Available at: https://www.hydraulicspneumatics.com/hydraulic-pumps-motors/use-more-data-determine-your-hydraulic-pump-life [July 2017]

Chartsandtides.co.uk [Online] Available at: http://www.chartsandtides.co.uk/tideplotter [October 2018]

Drtina, P., Sallaberger, M. (1999) *Hydraulic turbines-basic principles and state-of-the-art computational fluid dynamics applications. Sulzer Hydro AG, Zurich, Switzerland*.

DTI. (2006) *SEAFLOW Marine Current Turbine*. Project Summary No. PS244.

EDF.fr. *TIDAL POWER: EDF A PRECURSOR* [Online] Available at: https://www.edf.fr/en/the-edf-group/industrial-provider/renewable-energies/marine-energy/tidal-power [November 2018]

El-Zahaby, A. M., El-Nady, A. O. (2017) *FAULT ANALYSIS OF THE "A4VSO" AXIAL PISTON PUMP*

Emec.org.uk. *Pelamis wave power* [Online] available at: http://www.emec.org.uk/about-us/wave-clients/pelamis-wave-power/ [November 2018]

En.wikiversity.org [Online] Available at: https://en.wikiversity.org/wiki/Power_Generation/Hydro_Power#/media/File:Hydroelectric_dam.svg [June 2016]

Evans, D. J., Carpenter, G., Farr. G. (2018) *Mechanical Systems for Energy Storage-Scale and Environmental Issues. Pumped Hydroelectric and Compressed Air Energy Storage.* Environmental Science and Technology No. 46

Fraenkel, P. L. (2004) *Marine Current Turbines: An emerging technology, Hydraulic aspects of renewable energy*, 16th Annual Seminar, Scottish Hydraulics Study Group, Glasgow, March

Fraenkel, P. L. (2007) *Marine Current Turbines: pioneering the development of zero-head hydro*. BHA Annual Conference

G.B. National Grid Status. [Online]. Available: http://www.gridwatch.templar.co.uk/ [November 2018]

Gent, E. (2014) *Tidal Lagoon Power Scheme Plans Submitted* [Online]. Available at: http://eandt.theiet.org/news/2014/feb/tidal-lagoon.cfm [February 2015]

Green, Joe. (2009). *the Severn Estuary and Bristol Channel - Wildlife and Countryside Link* [Online]. Available: https://www.wcl.org.uk/docs/2009/Joint_Links_AcrosstheWaters_SevernEstuary_BristolChannel_Dec09.pdf [June 2016]

Greenmatch.co.uk. (2017). *Tidal Energy and Wind Power as Renewable Energy Sources in the UK* [Online] Available at: https://www.greenmatch.co.uk/blog/2016/10/tidal-and-wind-energy-in-the-uk [December 2018]

Greenpeace UK. (2009). *Nuclear power*. http://www.greenpeace.org.uk/nuclear [June 2015]

Hagerman, G., Polagye, B., Bedard, R., Previsic, M. (2006) *Methodology for estimating tidal current energy resources and power production by Tidal In-Stream Energy Conversion (TISEC) devices*. EPRI-TP-001 NA Rev 2.

Hamilton, M. (2012) *Introduction to the Scotrenewables Tidal Turbine* [Online]. Available at: http://www.all-energy.co.uk/__novadocuments/14981 [March 2016]

Hansen, H. H., Kramer, M. M., Vidal, E. (2013) *Discrete Displacement Hydraulic Power Take-Off System for the Wavestar Wave Energy Converter* energies

Hau, E. (2006) *Wind turbines: fundamentals, technologies, application, economics*. Edition 2. ISBN .3540242406, 9783540242406

Henderson, R. (2006) *Design, simulation, and testing of a novel hydraulic power take-off system for the Pelamis wave energy converter*. Renewable Energy, Volume 31, Issue2, Pages 271-283.

Hossain, J. (2015) *Possibility and Methodology Investigation of Ocean Wave Power Generation*. Thesis for: B.Sc. in Electrical and Electronic Engineering

House of Lords. (2008). *The EU's target for renewable energy: 20% by 2020. Volume I: Report. 27th report of session 2007-08*. Pub. House of Lords. [Online] Available at: http://www.publications.parliament.Uk/pa/ld200708/ldselect/ldeucom/l 75/175 .pdf [June2015]

Inhabitat.com (2010) *New Oyster 2 Wave Power Generator Unveiled This Morning*. [Online] Available at: https://inhabitat.com/the-oyster-wave-generator-2-buoyant-wave-power-without-the-turbine/?variation=b [November 2018]

Insider.co.uk (2017) *Tidal energy developer Atlantis Resources reports £7.3m pre-tax loss* [Online] Available at: https://www.insider.co.uk/company-results-forecasts/tidal-energy-developer-atlantis-resources-10532674 [November 2018]

Jo, C.H. (2008) *Recent development of ocean energy in Korea. Proc. World Renewable Energy Congress (WRECX)*. pp. 911-916.

Johnson, G. (2016) *Decommissioning of the SeaGen tidal turbine in Strangford Lough*, Northern Ireland: Environmental Statement

Jones, J A. (2012) *Tidal energy system for on-shore power generation*. [Online] Available at: https://www.osti.gov/servlets/purl/1046042 [April 2014]

Marquis, L., Kramer, M., Frigaard, P. (2010) *First Power Production Results from the Wave Star Roshage Wave Energy Converter.* 3rd International Conference on Ocean Energy

Massey, B.S., (1989). *Mechanics of Fluids, 6th ed*. Chapman and Hall, London. ISBN 0-412-34280-4

MCT. (2008) *Marine Current Turbines outline plans for SeaGen's installation in Strangford Lough* [Online] Available at: http://www.seageneration.co.uk/media/080207%20MCT%20Press%20Release%207%20Fe b%202008.pdf [January 2014]

Merritt Herbert (1967) *Hydraulic Control Systems.* Page 3 John Wiley & Sons

Niauk.org (2017*). Official statistics confirm nuclear largest source of low carbon power in UK – contributing 21% of all electricity in 2017* [Online] Available at: https://www.niauk.org/media-centre/press-releases/official-statistics-confirm-nuclear-largest-source-low-carbon-power-uk-contributing-21-electricity-2017/ [December 2018]

Oceanpowertechnolegies.com *Products: PB3.* [Online] Available at: https://www.oceanpowertechnologies.com/pb3 [March 2016]

Orme, J.A.C., Masters, I. (2004) *Design and testing of a direct drive tidal stream generator*. Proc. MAREC (Institute of Marine Engineering, Science and Technology)

Parliament.uk (2018) *Energy Prices 2018* [Online] Available at: researchbriefings.files.parliament.uk/documents/SN04153/SN04153.pdf [December 2018]

Pelamis Wave Power. Pelamis Wave Power [Online]. Available at: http://ctp.lns.mit.edu/energy/files/pelamisbrochure.pdf. March 2016

Plunkett, R. *Marine Current Turbines & SeaGen in the news*. [ONLINE] Available at http://www.smruconsulting.com/marine-current-turbines-seagen-in-the-news/. [Accessed 5 September 2016].

Quaarybattery.com. *A changing energy landscape* [Online] Available at: https://www.quarrybattery.com/ [December 2018]

Renew.biz (2016) *Scotrenewables bags EU cash* [Online] Available at: https://renews.biz/43928/scotrenewables-bags-eu-cash/ [October 2018]

Reuk.co.uk (2016). *La Rance Tidal Power Plant.* [Online] Available at: http://www.reuk.co.uk/wordpress/tidal/la-rance-tidal-power-plant/ [November 2018]

Rodrigues, Leao. (2018) *Wave power conversion systems for electrical energy production.*

Rolandez, G., Abgottspon, A., Staubli, **T**. (2014) *Discharge Measurements at la rance Tidal Power Plant Using Current Meters Method*. 10th International Conference on Innovation in Hydraulic Efficiency Measurements

Ruol, P., Zanuttigh, B., Martinelli, L., Kofoed, P., Frigaard, P. (2010). *Near-shore Floating Wave Energy Converters: Applications for Coastal Protection*. ICCE 2010 Shanghai.

Salter, S.H. (2007) *DTI Energy Review Question 2. Possible under-estimation of the UK tidal resource*.

Shi, W.C., Atlar M., Rosli, R., Norman, R. (2016) *Cavitation observations and noise measurements of horizontal axis tidal turbines with biomimetic blade leading-edge designs.* Ocean Engineering 121:143-155

SDC (2007). *Tidal Technologies Research Report 2., Tidal Power in the UK*. [Online] Available at: http://www.sd-commission.org.uk/pages/tidal-power.html [May 2016]

Sheng, S. (2013) *Report on Wind Turbine Subsystem Reliability- A Survey of Various Databases*. National Renewable Energy Laboratory.

Smith, C.E. (2016) *Natural gas pipeline profits, construction both up 2016* [Online] Available at: https://www.ogj.com/articles/print/volume-114/issue-9/special-report-pipeline-economics/natural-gas-pipeline-profits-construction-both-up.html [November 2018]

Snowdoniapumpedhydro.com *Snowdonia pumped hydro* [Online] Available at: https://www.snowdoniapumpedhydro.com/ [November 2018]

Soares, C. (2007) *Tidal Power: the next wave of electricity*. Pollution Engineering. [May 2015]

Subseaprotectionsystems.co.uk [Online] Available at: http://www.subseaprotectionsystems.co.uk/concrete-mattresses [May 2016]

Tethys.pnnl.gov (2009) *La Rance Tidal Power Plant 40-year operation feedback – Lessons learnt* [Online] Available at: https://tethys.pnnl.gov/sites/default/files/publications/La_Rance_Tidal_Power_Plant_40_year_operation_feedback.pdf [September 2016]

Theengineer.co.uk (2017) *How pumped hydro storage can help save the planet* [Online] Available at: https://www.theengineer.co.uk/pumped-hydro-storage/ [December 2018]

Valerio. D., Beirao. P., Sa da Costa. J. (2007) *Reactive control and phase and amplitude control applied to the Archimedes Wave Swing*

Wavestar (2011) *Performance Evaluation of the Wavestar Prototype* [Online] Available at: http://wavestarenergy.com/sites/default/files/EWTEC2011_2011-09-06.pdf

White, F.M. (1999) *Fluid Dynamics*, McGraw-Hill, New York, ISBN 0-07-116848-6

Wind-turbine-model.com *Vergnet GEV HP 1MW*. [Online] Available at: https://en.wind-turbine-models.com/turbines/435-vergnet-gev-hp-1mw [November 2018]

Xu, F., Ouyang, X.P., Yang, H.Y. (2018) *Investigation into the Effects of the Variable Displacement Mechanism on Swash Plate Oscillation in High-Speed Piston Pump.*

Zhang, C. (2013) *Report of the Research application of the wind farm in Datang, Henan.* Page 1_1-1_3 Huadong Engineering Corporation. (2013)

Zhou, X. J. (2013) *New Record for Wenxia Jiangling Tidal Power Station: 3,800,000 kW·h* [Online]. Available at: http://html.wlin.net/2013/07/24/BGbsjVwlMm2d3tBijmVBg.html [February 2015]

Appendix

Appendix I: Calculations for Chapter 3

3.4.1.1 Pressure loss in pipes & hoses:

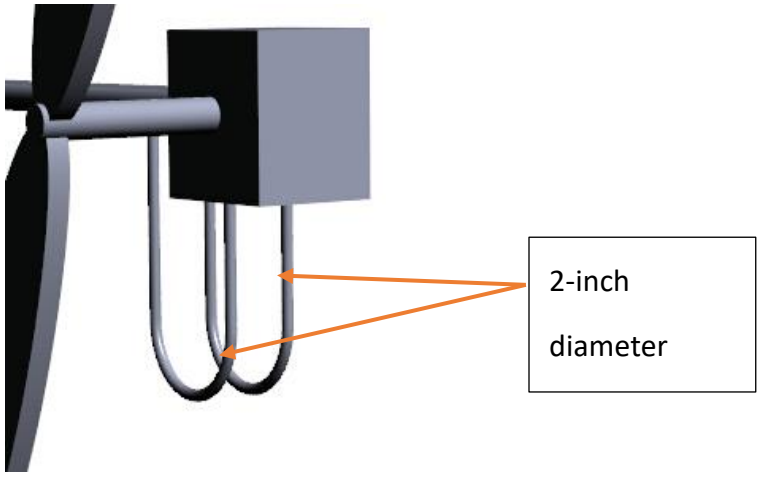

Figure 3-2 2-inch flexible hose used to connect pumps

A 2 inch (50.8 mm) flexible hose connected the pump and the main pipe in the crossbeam. The flow rate in this hose was calculated as:

$$u_h = \frac{q}{A_h} = \frac{0.02}{0.0508^2 \cdot \pi/4} = 9.87\ m/s$$

Where u_h the flow velocity in the hose and A_h is the cross-area section of the flexible hose. The Reynolds number of this flexible hose is:

$$Re = \frac{u_h d}{v} = \frac{9.87 \times 0.0508}{40 \times 10^{-6}} = 12535$$

Where Re is the Reynolds number, d is the hose diameter and v is the fluid viscosity.

For general wire reinforced rubber flexible hoses, the roughness value is k = 0.3 mm

For this hose, k/d = 0.006

From Moody's diagram, the friction factor 4f for this case is 0.038

Hence the head loss (h_{loss}) in the hose is calculated as:

$$h_{loss} = 4f\frac{l{u_h}^2}{2gd} = 0.038\frac{2 \times 9.87^2}{2 \times 9.81 \times 0.0508} = 7.43\ m$$

Pressure loss (p_{loss}) due to friction:

$$p_{loss} = \rho gh = 870 \times 9.81 \times 7.43 = 5830\ pa = 0.058\ bar$$

The hose is then to be connected to the larger diameter pipe measuring 4.87 inches (124.38 mm) located on the crossbeam. The flow characteristic in the pipe:

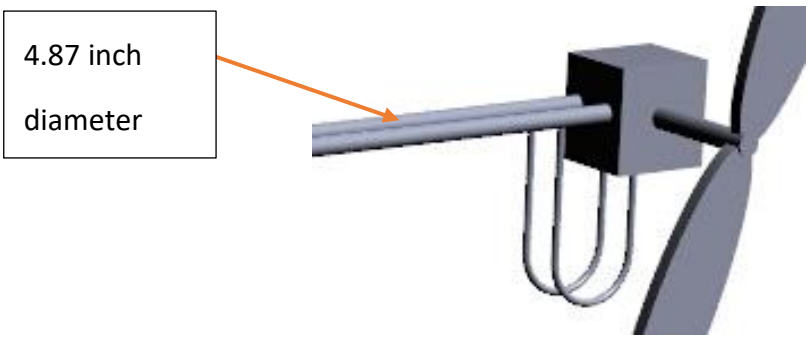

Figure 3-3 4.87 inch (124.38 mm) diameter pipe at crossbeam

Flow velocity (u_{cb}):

$$u_{cb} = \frac{q}{A_{cb}} = \frac{0.02}{0.12438^2\pi/4} = 1.65\ m/s$$

Reynolds number of the pipe:

$$Re = \frac{ud}{v} = \frac{1.65 \times 0.12438}{40 \times 10^{-6}} = 5130$$

The pipe roughness of the stainless steel pipe is 5.5 micro meters (µm), the k/d value

is 4.33 x 10^{-5} and from the Moody's diagram, the friction factor 4f is 0.037

The head loss in the pipe is:

$$h_{loss} = 4f\frac{lu^2}{2gd} = 0.037\frac{10 \times 1.65^2}{2 \times 9.81 \times 0.12438} = 0.41\ m$$

Pressure loss in the pipe is

$$p_{loss} = \rho gh = 870 \times 9.81 \times 0.41 = 3522\ pa = 0.035\ bar$$

After two flows from each turbine are combined, the flow is then headed to a larger flexible hose located in the tower central pillar. Therefore, the total flow rate in this case is 2 x 0.02 m^3 = 0.04 m^3

Flow characteristics:

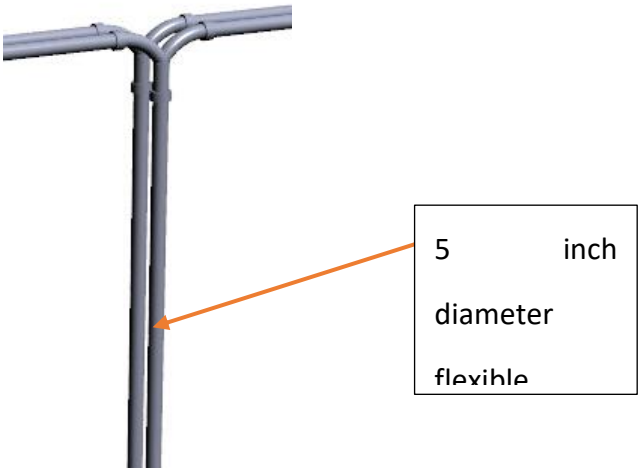

Figure 3-4 Central pillar 5-inch diameter flexible hose

Flow speed (u_{ch}):

$$u_{ch} = \frac{q}{A_{ch}} = \frac{0.04}{0.127^2\pi/4} = 3.16\ m/s$$

Reynolds number:

$$Re = \frac{ud}{v} = \frac{3.16 \times 0.127}{40 \times 10^{-6}} = 10033$$

Hose roughness k=0.3 mm, k/d = 2.36x10^{-3}, friction factor 4f= 0.034

Head loss:

$$h_{loss} = 4f\frac{lu^2}{2gd} = 0.034\frac{40 \times 3.16^2}{2 \times 9.81 \times 0.127} = 5.45\ m$$

Pressure loss:

$$p_{loss} = \rho gh = 5.45 \times 9.81 \times 870 = 46515\ pa = 0.465\ bar$$

A 200 m underwater stainless steel pipe line of diameter of 4.87 inches (124.38 mm) is used as a connection from the tower structure to the on-shore unit.

Figure 3-5 Subsea pipeline turbine end

Flow characteristics:

Flow speed u_p:

$$u_p = \frac{q}{A_p} = \frac{0.04}{0.12438^2\pi/4} = 3.29\ m/s$$

Reynolds number:

$$Re = \frac{ud}{v} = \frac{3.29 \times 0.12438}{40 \times 10^{-6}} = 10230$$

Take the same k/d value from the previous calculation, 4f factor in this case is 0.33.

Therefore the head loss in the pipeline is:

$$h_{loss} = 4f\frac{lu^2}{2gd} = 0.033\frac{200 \times 3.29^2}{2 \times 9.81 \times 0.12438} = 29.27\ m$$

Pressure loss:

$$p_{loss} = \rho gh = 29.27 \times 870 \times 9.81 = 250000\ pa = 2.5\ bar$$

The flow needs to be delivered to the power units which are located 50 m above the sea bed.

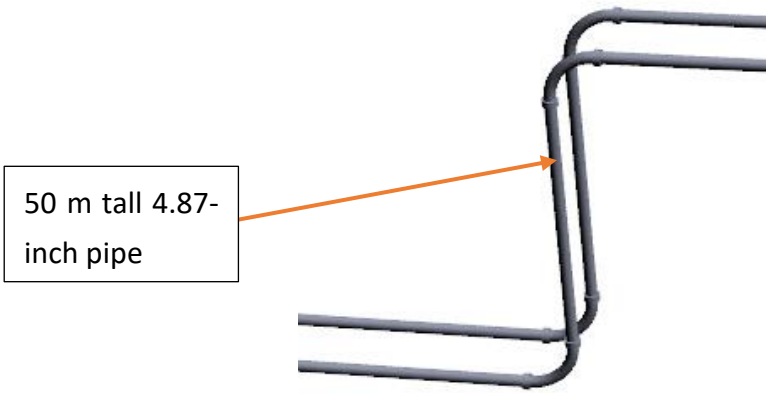

Figure 3-6 7 Subsea pipeline shore end

Pressure loss due to gravity (pressure line):

$$p_{loss} = \rho g h = 50 \times 9.81 \times 870 = 426735\, pa = 4.27\, bar$$

For the return flow, the tower structure is 40 m high, therefore the pressure loss due to gravity (return line) is:

$$p_{loss} = \rho g h = 40 \times 9.81 \times 870 = 341388\, pa = 3.41\, bar$$

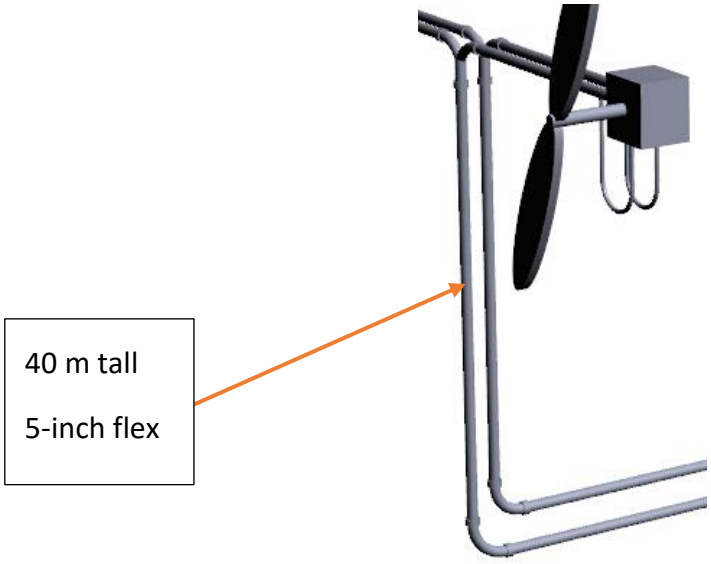

Figure 3-7 Tower structure of the turbine system

The on-shore unit is located 20 m from the coast.

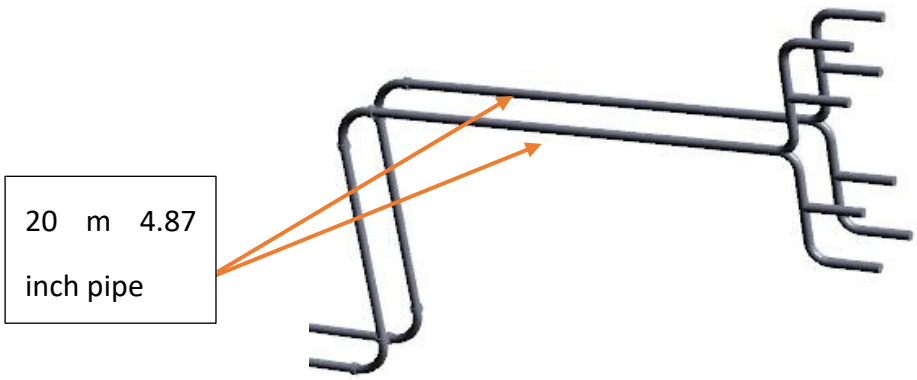

Figure 3-8 Additional 20 m length for onshore pipeline

$$h_{loss} = 4f\frac{lu^2}{2gd} = 0.034\frac{20 \times 3.29^2}{2 \times 9.81 \times 0.12438} = 3.02\ m$$

Pressure loss:

$$p_{loss} = \rho gh = 3.02 \times 9.81 \times 870 = 25741 = 0.257\ bar$$

The hydraulic motor required four inlet ports and four outlet ports, therefore the pipe must be split into four smaller hoses of 2-inch diameter for the connection. Therefore, the flow rate in each of these hoses is 0.01 m^3.

Flow characteristics:

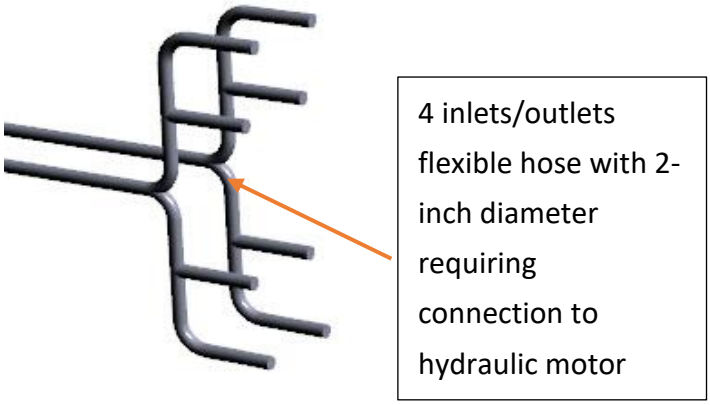

Figure 3-9 Splitter fittings for motor connection

Flow speed (u_h):

$$u_h = \frac{q}{A_h} = \frac{0.01}{0.0508^2 \cdot \frac{\pi}{4}} = 4.933\ m/s$$

Reynolds number:

$$Re = \frac{ud}{v} = \frac{4.933 \times 0.0508}{40 \times 10^{-6}} = 6266$$

From the previous calculation, the k/d value for the flexible hose with 2 inch diameter is 0.006, therefore the friction factor is 0.043

Head loss:

$$h_{loss} = 4f\frac{lu^2}{2gd} = 0.043\frac{2 \times 4.933^2}{2 \times 9.81 \times 0.0508} = 2.1\ m$$

Pressure loss:

$$p_{loss} = \rho gh = 2.1 \times 870 \times 9.81 = 17920\ pa = 0.179\ bar$$

3.4.1.2 Pressure loss in fittings & bends:

Fittings:

In many hydraulic system designs, the pressure loss in fittings is normally neglected. It was argued that losses are relatively small compared to other components in the circuit. However, due to the large flow rates and high pressures in the circuit, it is essential to account for all losses in the system.

To determine pressure loss in the fittings, a method called equivalent length is used.

The equivalent length L_e allows the calculation of pressure loss through a fitting, as a length of straight pipe. Table 3-2 shows the equivalent length of the pipe fittings.

Table 3-2 Equivalent lengths for pipe fittings. (Source: The Engineering Tool Box, 2014)

Fitting Type	L_e/D
Gate valve, full open	8
Ball valve, full bore	3
Ball valve, reduced bore	25
Globe valve, full open	320
90° screwed elbow	30
90° long radius bend	13
45° screwed elbow	16
45° long radius bend	10
Welded Tee, thru-run	10
Welded Tee, thru-branch	60

To calculate the equivalent length (L_e) for different fittings:

$$L_e = \frac{L_e}{D} \cdot D$$

Where D is the pipe diameter. Using the Darcy-Weisbach and pressure equation to calculate pressure loss;

$$h_{loss} = 4f \frac{L_e u^2}{2gd}$$

$$p_{loss} = \rho g h_{loss}$$

Where u is the flow velocity in the fittings (m/s).

In this case, a 90° screwed elbow, a 90° long radius bend and welded tee, thru-branch are used.

Figure 3-10 45° bend fitting

For a 90° 2 inch diameter bend used on the pump, the pressure loss is 0.44 bar. The same bend for the motor application is 0.11 bar. The 90° bend for the 4.87 inch bend has a pressure loss of 0.018 bar.

The tee joint for the tower structure has a pressure loss of 0.085 bar.

Bends:

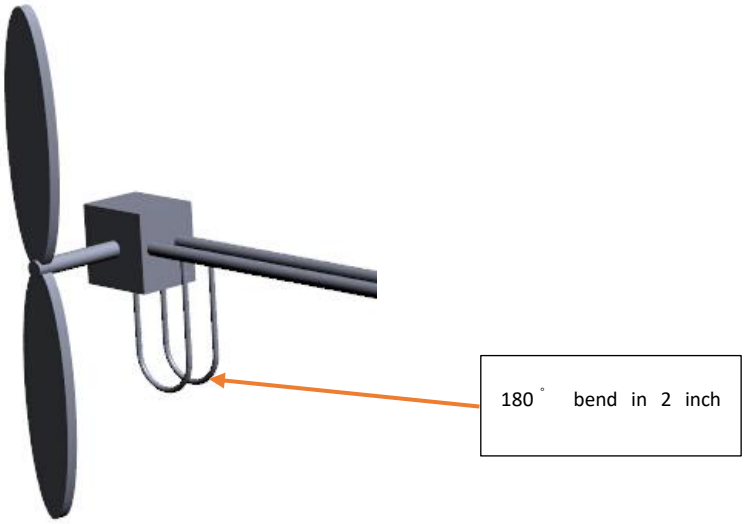

Figure 3-11 180° bend in 2-inch flexible hose

For the flexible hose used in this design, there will be a pressure loss when the fluid passes the bend. This is calculated as:

$$p_{bend} = \frac{1}{2} 4 f \rho u^2 \frac{\pi R_b}{d} \frac{\theta}{180^0} + \frac{1}{2} k_b \rho u^2$$

Where R_b is the bend radius,

θ is the bend angle,

k_b is the bend loss coefficient.

According to the design drawing, the bend radius is 1 m, the bend angle is 180° and the k_b is 0.3.

The pressure loss in this bend is:

$$p_{bend} = \frac{1}{2} \times 0.038 \times 870 \times 9.87^2 \frac{\pi}{0.0508} \frac{180^0}{180^0} + \frac{1}{2} \times 0.3 \times 870 \times 9.87^2$$

$$= 99584.86 + 968.22 = 100553 pa = 1\ bar$$

3.4.1.3 Pressure loss in couplings:

For flexible hose connections, the coupling must be installed at both ends of the hose. The coupling is streamlined to eliminate pressure loss when fluid is passing, however, by inspecting the sample coupling, it was noticed that the size of the coupling is the inner diameter, so for the hose connection, there is no change in the section area, which will not cause the disturbance in the fluid. However, when the coupling is screwed into an adapter, it was noticed that in the connection, there was a small gap. Such a gap will cause turbulence in the system. Unfortunately, no equations or calculation methods have been devised to account for this problem.

Pressure loss due to area changes:

When a flow is passing through an altered diameter (contraction and expansion), there will be disturbances in the pipe, therefore fluid pressure loss will occur. Figure 3-17 shows flow disturbances when passing an altered cross-section area.

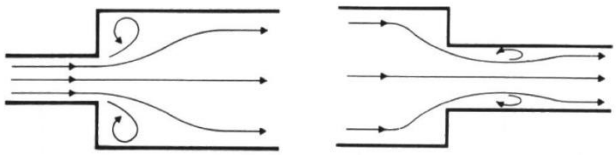

Figure 3-12 Flow disturbance in an altered area

To calculate this pressure loss, the following equation is used:

$$H = K_2 \frac{u^2}{2g}$$

Where H is the head loss, K_2 is the loss coefficient and u_2 is the exit flow velocity.

By using this formula, the pressure losses due to area changes are:

Contraction:

5 inches to 4.87 inches: 0.001 bar

4.87 inches to 2 inches: 1.56 bar (pump end return line)

Expansion:

2 inches to 4.87 inches: 0.29 bar (pump end pressure line)

4.87 inches to 5 inches: 0

Pressure gain by gravity:

For the pressure line, because fluid is to be transmitted vertically downwards in the 40 m tower structure, therefore the pressure gained from gravity (p_{gain_pline}) is:

$$p_{gain\_pline} = \rho gh = 40 \times 9.81 \times 870 = 341388\ pa = 3.41\ bar$$

For the return line, fluid must pumped up a 50 m vertical pipe, therefore the gain is (p_{gain_rline})

$$p_{gain\_rline} = \rho gh = 50 \times 9.81 \times 870 = 426735\ pa = 4.27\ bar$$

3.4.1.4 Pressure loss in the hydraulic motor:

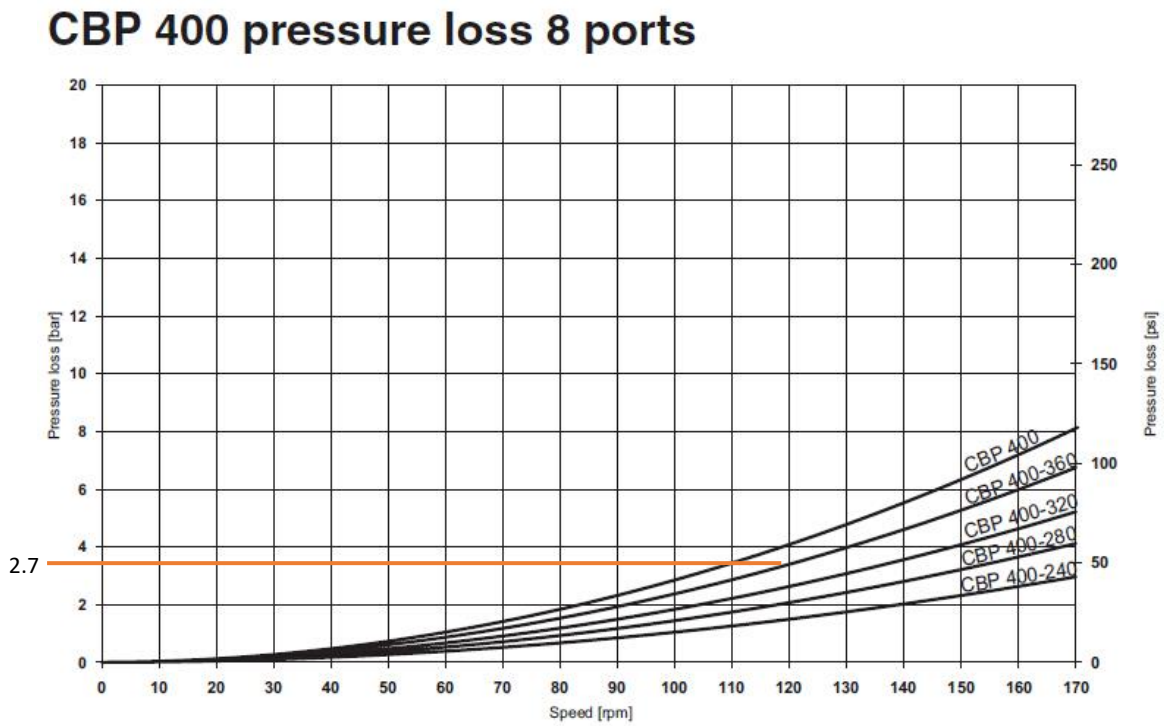

Figure 3-13 Pressure loss profile for the hydraulic motor (boschrexroth.com, 2014)

According to Figure 3-18, for a motor speed of 120 rpm, the pressure loss for the motor CBP 400-320 is approximately 2.7 bar.

Appendix II: Publication

Introduction of a hybrid tidal energy system

Sheng Deng[1], Carl Byrne[2], Allan Mason-Jones[3]

Cardiff Marine Energy Research Group (CMERG), Cardiff School of Engineering
Cardiff University, Wales.

[1]dengs2@cardiff.ac.uk

[2]byrne@cardiff.ac.uk

[3]mason-jonesa@cardiff.ac.uk

Abstract— **Tidal range energy is not a new concept and has been used over the centuries to generate energy locally. For example, tidal mills. Like the barrage, the tidal lagoon has the potential to generate power on both ebb and flood tides, which has the advantage of temporal predictability. Technologies from tidal range systems have been applied to the concept of the tidal lagoon which has the potential to reduce the environmental impact by limiting the effect of a barrage system.**

This paper proposes a solution to convert Newport Docks, Wales, UK into a tidal lagoon system. The proposed hybrid system features a pumping system which is powered by a tidal turbine, allowing the control of the head difference between the dock and the local tide. A Matlab programme is used to simulate the tidal barrage system, results are compared with the standard barrage system. By shifting the generation time, the results show there is an increase in power production generation time when using the hybrid system. Moreover, another advantage of the hybrid system is that it can be used as a power storage for peak demand. This methodology as the potential to enable other tidal energy sites, to supply energy to the grid.

Keywords— **Tidal energy, Tidal Turbine, Pumping storage, Control**

I. INTRODUCTION

Tidal range energy is generated by using the level difference between the two water surfaces, when water passing between the barrage between the two surfaces, it drives the water turbine, and hence generate electric energy. However, the generation is entirely depends on the tidal condition, one of the big advantages of the tidal energy system is the tide is highly predictable, so the energy output can also be predicted, but the tidal cycle is different each day, so that means the generation time can also varies each day, as shown in Figure 1 below, the tidal profile was from Newport, and the power demand was from National Grid [1], it can be seen the demand curves from two figures are very similar in the same time slot, but the tide is changing, which at the same location but different time, the tidal range varies, which would affect the tidal energy system, for example, greater the tidal range would lead to a greater power generation, and vice versa. Therefore, to maximum the potential of the current standard tidal system, a new design was proposed, the idea was to use the current tidal energy plant structure as a base model, which alone can be used as a power source, but this base model is connected with another technology, which is marine current turbine. But unlike the many tidal turbine designs, in this project, there is a pump to replace the generator, the pump is used to control the water in the reservoir to get the optimum head.

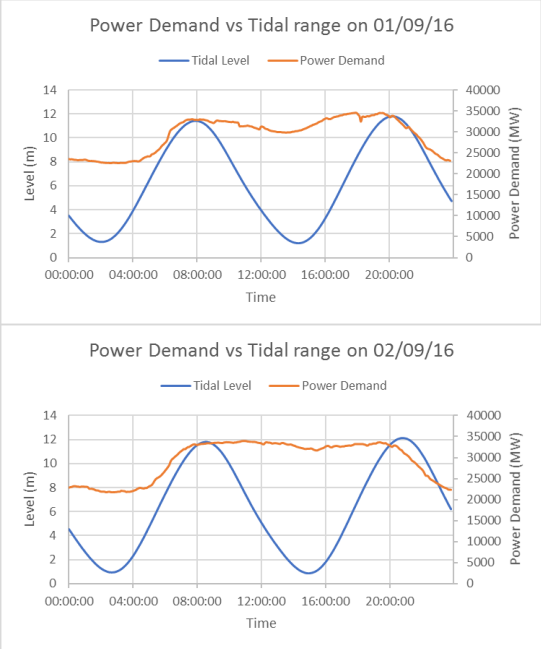

Figure 1 Tidal range vs UK national Power demand from two different dates

II. DESIGN

This project is aiming to use current available technologies which used in the renewable energy and general industries to create a new solution for providing energy to the surrounding area.

Tidal energy plants proved reliable and predictable power, the Rance power station features 24 water turbines and can produce a peak power of 240 MW and an average of 57 MW with a cost per kilo-watt about £0.1[2], it has been used since 1966 and it is still operational which given an advantage in the lifespan. One of the major disadvantage of this type of system is the construction cost, which requires huge initial invest and long

long period for construction time, the Rance power station cost about 620 million French francs (about £80 million) at time, [3] it required 20 years for the station to recover the cost, but given it is still running after 50 years, it is arguably cost effective.

From success of wind farms, in recent year, there has been a huge development for the tidal turbine, SeaGen is one of the famous one which built by MCT [4]. Compare to its close relative wind turbine technologies, tidal turbines are normally smaller in size, which due to the density advantage of sea water compares to the air, it does not need enormous size to harvest similar energy, and it does not have the huge visual impact as wind turbine. However, due to shears similar technologies with the wind turbines, some drawback of the wind turbines could become the potential problems for tidal turbines, one of them is the maintenance, it is arguably that doing maintenance on the sea is harder than on the land, and perhaps in some circumstances, some of the works would be carried out underwater with increase the risk of health and safety.

This paper proposes a system for the marine renewable energy, it would use the reliable technologies from both of the tidal-electric system and tidal turbine system.

One of the biggest disadvantage of the tidal station is the initial cost is high, to counter this, the idea was to convert the docks into a small tidal system, which to provide energy to the surrounding area. However, by introducing this design, there was another question, how to maximum the power generation from a relatively small reservoir (docks) compare to the one used in the tidal system. In hydroelectric, power is related to effective head and flowrate passing the turbine, by increasing the head or the flowrate is related to an increased power, but a higher flowrate could fill or empty the reservoir quickly, and the system could generate less power in the long term, which increase head while maintain flowrate can increase the power and longer the generation time. To achieve this concept, another feature was introduced into the system, which involves a tidal turbine driven pump, to connected to the dock, using the power from moving water to adjust the water level inside the reservoir to get an optimum head, the reason why the tidal turbine is not directly driven a generator to produce power directly, it was believed that it is more economical to run the pump compare to the generator, and maintenance wise more reliable.

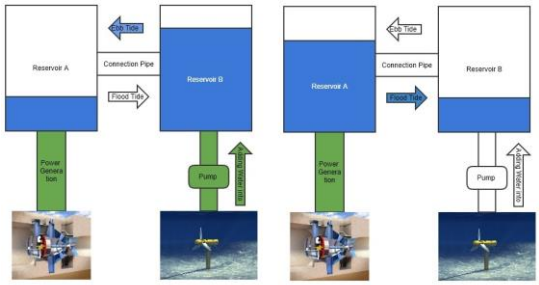

Figure 2 System Diagram

Many sites have more than one docks, and the docks are located closely to each other. According to the system diagram (Figure 2), this design features two reservoirs, Reservoir A is directly used for power generation, and the Reservoir B will be using for adjusting water level for the Reservoir A. During the ebb tide, the water would exit from the reservoir into the open water via water turbines for power generation, and when the head difference between the reservoir and the tide is too small, this process would be stopped due to the insufficient head. By introducing the second reservoir, it could be using to top up the main reservoir once its level is below the optimum, to extend the generation time and maximum power; for the flood tide generation, the water level for the Reservoir B would be low from the ebb generation, and would accept water from Reservoir A when its water level is above the optimum.

I. METHODOLOGY

A. *Hydro*

The hydraulic power can be calculated by using the equation (1)

$$P = \eta \rho g H Q \qquad (1)$$

Where P is the total theoretical power output, η is the efficiency of the turbine system; ρ is the density of the; g is the gravitational acceleration, H is the effective head in m and Q is the inlet flow rate of the water turbine.

Where the effective head H can be calculated by:

$$H = H_{tide} - H_r \quad (flood) \qquad (2)$$

$$H = H_r - H_{tide} \quad (ebb) \qquad (3)$$

H_{tide} is the head of the tide, and H_r is the head of the reservoir. The inlet flowrate Q can be calculated by:

$$Q = A_{turbine} \cdot V \qquad (4)$$

$A_{turbine}$ is the water turbine swept area, and V is the flow velocity given by:

$$V = C_d \sqrt{2gH} \qquad (5)$$

Cd is the discharge coefficient.

To reassembly the equations above, the new equation to calculated power is given:

$$P = \eta \rho g H A_{turbine} C_d \sqrt{2gh} \qquad (6)$$

A. Marine Current Turbine:

The power output of tidal turbine is given:

$$P_{tidal\ turbine} = Cp_t \frac{1}{2} \rho A_{current\_turbine} V_c^3 \qquad (7)$$

Where $P_{\text{tidal turbine}}$ is the power output by tidal turbine, Cp_t is the coefficient, ρ is the density of the fluid; $A_{current\_turbine}$ is the swept area of the turbine and V is the speed of the current.

B. Pump

The pump is driven by the tidal turbine and the equation is given:

$$P_{tidal\ turbine} = P_{pump} = Q_{pump} \cdot H_{pump} \cdot \rho \cdot g \qquad (8)$$

Q_{pump} is the pumping flowrate, and H_{pump} is the pumping head. By changing orders:

$$Q_{pump} = \frac{P_{pump}}{H_{pump} \cdot \rho \cdot g} \qquad (9)$$

I. Numerical Modelling

The project is about to convert Newport dock into a hybrid tidal system, a Matlab programme was created to simulate how much power would this site generated.

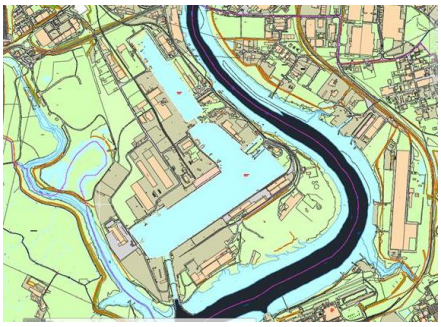

Figure 3 Newport dock layout.

There are numbers of parameters need to be justified, for water turbine:

TABLE I
PARAMETERS

Name	Value
Turbine Diameter	3 m
Minimum Head for generation	2 m
Discharge coefficient	0.9
Coefficient of turbine	0.40
Area of tidal turbine	201 m^2
Head of Pump	10 m
No. of pump turbine	10
No. of water turbine	1
Maximum reservoir level	8 m
Minimum reservoir level	3 m
Area of reservoir	532,967 m^2

All the parameters in Table 1 are assumed value, which can be changed if more suitable ones are available.

A. Modelling the standard tidal system

The standard tidal system would be the base line of this project, Figure 4 shows the bi-directional generation process for the Rance tidal power station in France.

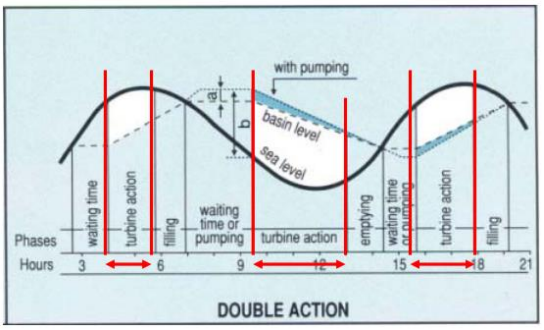

Figure 2 level comparison for standard tidal system [5]

From Figure 2, the result shows how would the standard tidal system work, when the head is less than the optimum value, the system would stop and wait for that head to come (for Range tidal station, the minimum head is 1.7 m). Another feature for this tidal station is the bulb turbines installed are

capable to pump water from the sea into the reservoir, by doing that is because the additional energy it would generated during the ebb tide would cover the energy consumed by pumping.

Based on this standard tidal system, a Matlab programme was created to simulate the generation process, by input the tidal data profile into this programme, it would provide how much power the site would potentially generation with providing the information that listed in Tible I.

A set of 3-day tidal data was input into the computing model, with the basic parameters from Table I. Unlike the Rance tidal station, the Matlab programme was only simulating the bi-directional power generation without the reverse pumping of the turbine. Figure 3 below shows the how would the reservoir level changes with the tidal level for Newport.

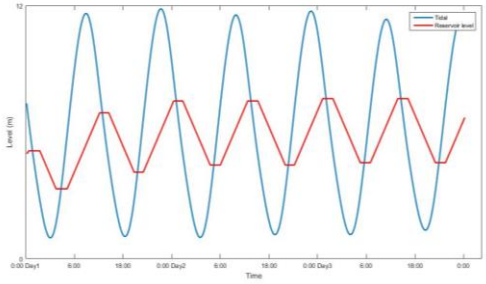

Figure 3 3day Level comparison for a standard system

From Figure 3 above, by given a starting reservoir level, after the initiating stage (first 6 hours), the result shows that under similar tidal cycles, the pattern for change of the reservoir level is small.

With the reservoir level successfully simulated, the next step was to use the model to predict the power output.

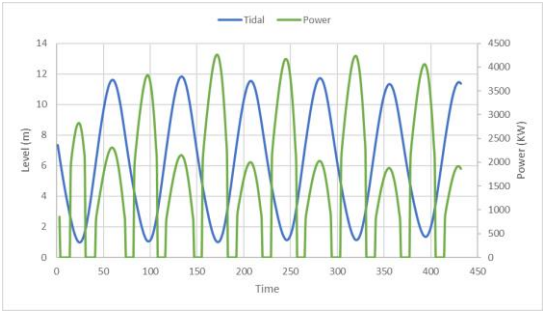

Figure 4 power curve of a standard tidal system

According to Figure 4, it can be seen how power output related to the tidal condition. However, this model did not include the water turbine efficiency profile, which the power output value was not realistic, but it is an indication that how would the standard tidal system perform.

A. Hybrid tidal system modelling

To increase the power production, in both maximum power and total power, a hybrid design was proposed. This design features two major parts.

Newport dock has two docks, the large South dock and the smaller North dock, the design is to use one of the docks as the main reservoir for generate, and the other one as the backup reservoir. When the effective head is below the optimum value, the water gate between the two docks open, allowing water to releasing water to flow in or from the back up reservoir which depends on the tidal condition. Which theoretically, would increase the effective head during the generation period.

The second implement is to use an additional pumping system, which is connected to the backup reservoir to adjusting the water level within, the pumping system in this project was a proposed tidal turbine driven pump, which uses the flow current to drive a tidal turbine to power the pump.

For this concept, because it would have at least two reservoirs, which it is important to choose which reservoir would be the best option for direct power generation. The Newport dock has two docks which can be used as Reservoir A and B, but the question would be which option is better to achieve the maximum potential.

There are two options of the modelling, the first option was to use the smaller North dock as the main generation site, and the large one as the back-up reservoir, with the turbine-pump unit connected to the North dock as the change of the head would be more effective on the smaller area. The second option was to use the large South dock as the main generation reservoir and North dock as the back-up reservoir with the turbine-pump unit still attach to the smaller dock. The maximum flowrate passing the two docks was limited to as 100 m3/s, The larger South dock has a full capacity of 4,546,195 m3 compare with the smaller North dock's 928,587 m3.

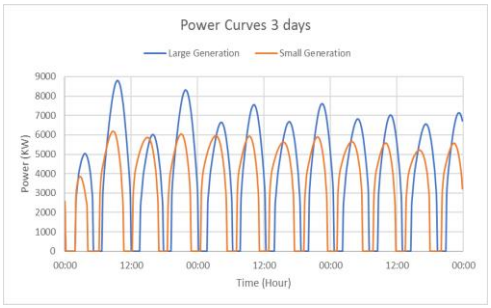

Figure 5 power comparison for the hybrid tidal system

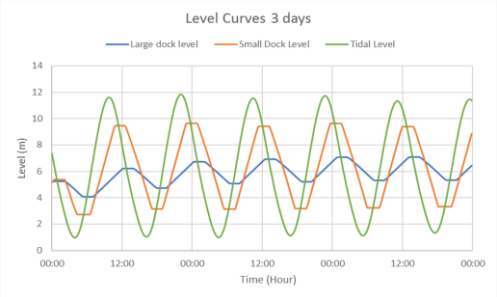

Figure 6 Level comparison between option1 & 2 for the hybrid tidal system

Figure 7 Power data of three systems

From Figure 6, under the same tidal condition, the performance by using the large dock as the main reservoir is As shown in Figure 5. Under the same starting water level, the initial power output produced by both docks were identical. However, from 2:00, the large dock had an advantage in both maximum power and the generation time. According to Figure 6. It could be seen that from 2:00, the water level in the smaller tank dropped much quicker than the larger dock, the reason for this was because the area of the North dock is much smaller than the South one, and therefore under same amount of the flowrate change, the smaller dock would have a much dramatic effect. As shown in Figure 6, the gradient of the level curve for small dock was similar to the tide, and which means the head difference would not increase much when tide comes in or goes out, and the large dock has a lower slow curve compares to the tidal one, and when the tide rises or drops, the head difference was increased, hence more power was produced.

During the second-generation period, the smaller dock started the generation earlier than the large one due to the lower level, but again from Figure 6, the smaller dock was filled up within about 5-hours, and the level for the large dock has increased by 2 m, which gave the large dock 1.5 hours more generation time than the smaller dock, and with the maximum power reaching nearly 9000 KW compares the smaller's 6000 KW, which was a 50% increase.
The third power period, which the two docks matching each other on the maximum power, which was about 6000 KW, the smaller dock generated for about 5 hours vs 4 hours 30 mins for the large dock.
For the final generation period of the day, it was still the large dock had the advantage in the maximum power, which was more than 8000 KW compares to the 6000 KW of the other dock.
The larger dock's area is nearly 5 times of the smaller dock, and has large capacity for water, which gave it an advantage in the generation period, and hence the maximum power, but the large size would take longer time to prepare to the optimum level.

The large dock still has advantages in power output over the smaller dock, and the power generated during the ebb was generally greater than the flood generations, it is noticed that the power generation by the small dock was consistent in the maximum power, and the generation time under flood tide was a little bit more than the ebb period, the average time within 24 hours for both options is shown in Table 2.

Table 2 Average generation time for two options

Main Reservoir	Avg Ebb Generation Time	Avg Flood Generation Time
Small dock	4H 40 min	4H 10 min
Big dock	5H 20 min	4 H 30 min

From Table 2, by optioning the Big dock as the main reservoir would provide a 40 mins more generation time than the Small dock during the Ebb generation for 24 hours, which is a 14.29% increase, and also a 20 mins increase for Flood generation, which is an 8% increase.
The gain in both maximum power output and time was significant between this concept and the standard one under the same circumstances, it is believed when more realistic factors were included i.e. losses of the mechanical components, losses in the flow etc. These numbers would be less.

I. PUMPING STORAGE

The results in this section show that the hybrid system could improve the energy generation in both peak power and average power. Power generation is still depending on the tidal condition, which brings a question, what if a power generation is required, but the tidal condition does not meet the requirement?
As the tidal condition can be accurately predicted, and with the tidal pump system, the system has the ability to prepare the reservoir into an optimum level, and when the generation begins, it would perform better than the standard system.

However, the trade-off is the system needs time to prepare the reservoir, and whether it is economical to do so, it is depends on the energy price difference.

For example, according to the National Grid [5], the energy usage for a typical week in the UK in both winter and summer is shown in Figure 8 below,

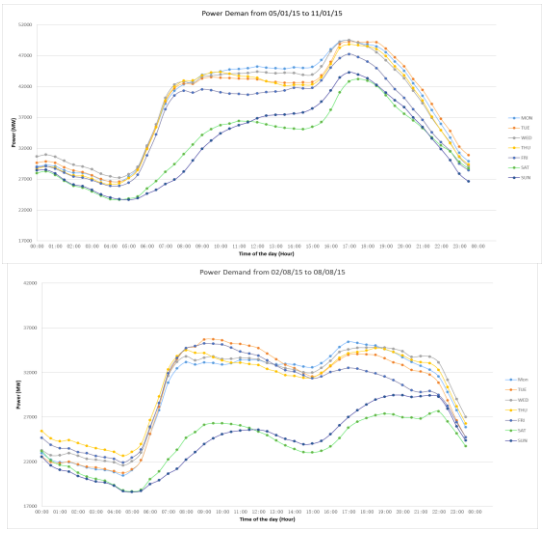

Figure 8 Energy demand for a week in the UK (Winter and Summer)

From Figure 8, it is noticeable that for weekdays, the demand patterns are very similar in both figures, but the demand number in the winter is much higher, with average hourly power demand for winter weekdays (Monday to Friday) was 38436.2 MW, comparing with the average power demand for summer weekdays' 29941 MW, which was about 28.38% more, for the weekends, the hourly average demand for winter was 32834 MW, equalling 85% of the weekday's demand, but it was higher than summer weekday's value, the summer weekend demand had an hourly average value of 24087 MW, which was about 80% of the summer weekday's value.
From Figure 8, the power demand patterns were similar for weekdays apart from Friday afternoon, and for the weekend, the demand patterns follow a similar trend but with reduced number. For week days, the demands are stable 8:00 to 20:00. To find out what is the best case for a system to generate between this period, a series of analysis was carried out.

The tides will be divided into four different scenarios at the starting point at 8:00, 1. In the middle of Ebb tide; 2. At the starting point of Ebb tide; 3. In the middle of Flood tide; 4. At the starting point of the Flood tide. These four tidal scenarios represent a tidal cycle, and for each tidal scenario, there would be three simulations based on that tidal profile. The system was to set to hold the water in the reservoir before the start of the peak window, and would not operate before that time. There were three settings of the initial water level of within the reservoir, 1. Full tank, where the reservoir level is at the maximum (10.8 m); 2. Half tank, where the reservoir level is at the half of the maximum (5.4 m); 3. Min tank, where the reservoir level is at the minimum (2 m).
The Matlab programe would calculate the generated power by providing the tidal profile, and it would be compared with the local power demand to provide an analysis.

A. Case 1 Ebb

The providing tidal data is shown in Figure 9, at the beginning of the peak window (around 8:00), the tidal condition was Ebb, and the advantage of this scenario is the stream speed was much faster than when the tidal level is at highest or lowest. Therefore, the tidal turbine-pump unit would generate more power due to the fast flow speed, and hence more water would be pumped into the reservoir and provide a longer generation window with a higher head difference.

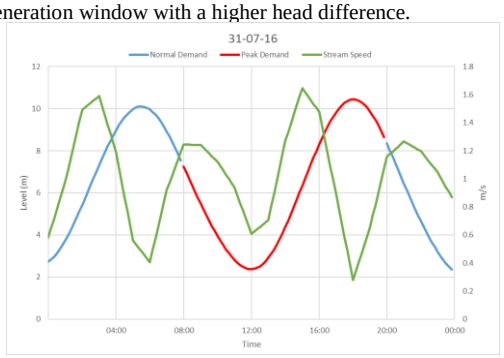

Figure 9 Tidal data from Newport on 31/07/16

After compare the results from the numerical simulation, the best case to generate within peak window under this tidal condition is when the starting level of the reservoir is at full level, as the results shown in Figure 10 below.

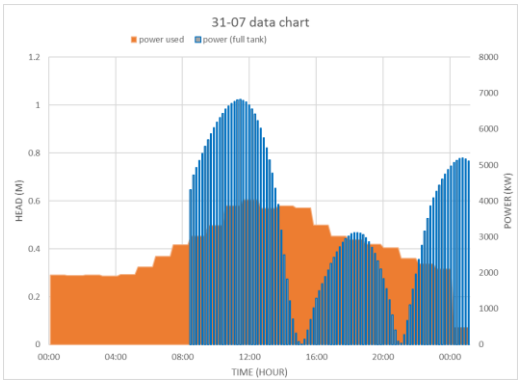

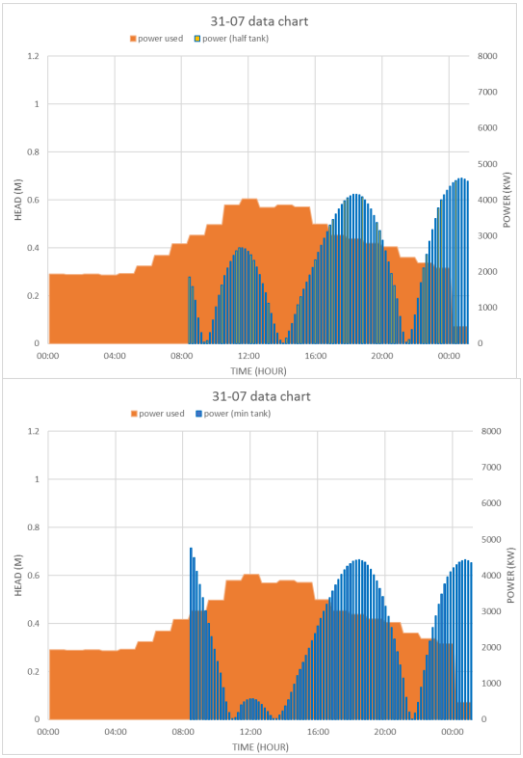

Figure 10 Results for Case A

From the results, the Min tank option under this tidal scenario was not ideal, it had the longest gap when the demand was at the highest, and has a short coverage window (4 hour).
The Half tank option also did not meet the expectation, the demand was not meet until 17:00, and the coverage window was the shortest, around 3 hours, which indicates this option was not optimal.
The Full tank option under this tidal condition had the best power output. It had the longest coverage window (around 7 hours), had the shortest gap (around 2 hours), and for 8:00 to 14:00, the system generated much more energy than the demand. Therefore, this was the best option out of the three that could be optimized.

A. Ebb start

In this case, the tidal scenario at the beginning of the peak window was the early stage of the Ebb tide, where the tidal level reached the highest and about to drop. However, due to the characteristics of the tide, the stream speed was low at the starting point as shown in Figure 11, therefore the power output for the tidal turbine-pump unit was low, and the amount of the water that pumped into the reservoir was less.

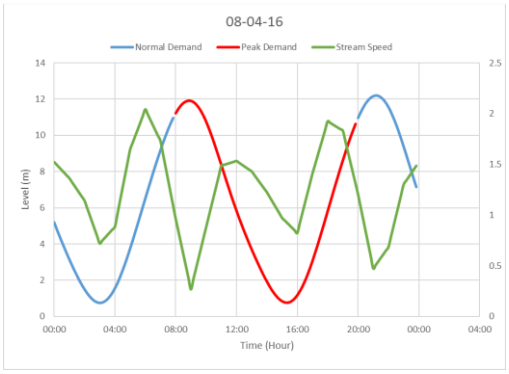

Figure 11 Tidal data from Newport on 08/04/16

The results from three different reservoir settings are shown in the Figure 12 below.

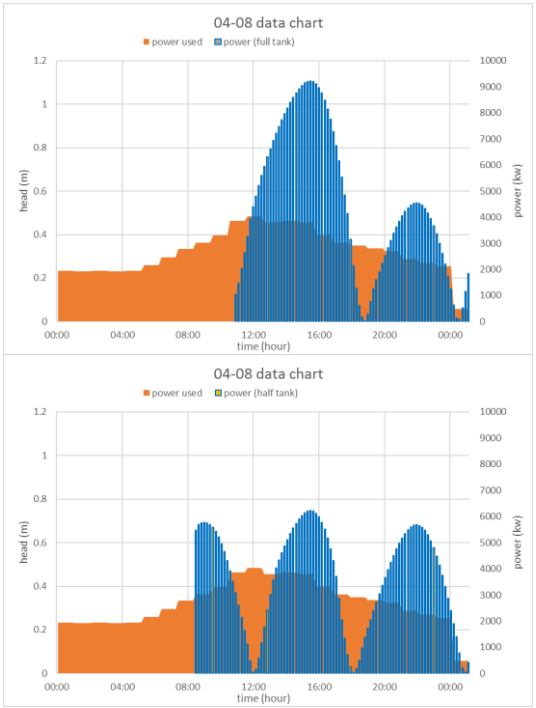

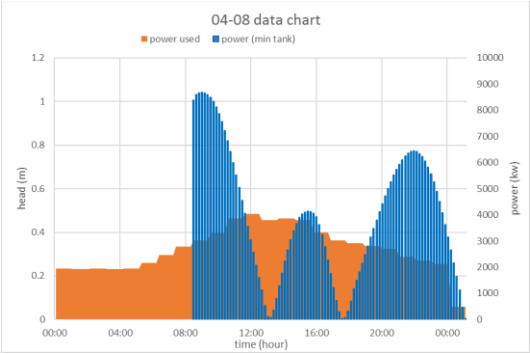

Figure 12 Results for case B

Generally, all three cases had reasonable power output during the peak demand window. However, the first case, where the reservoir was full, there was a 4-hour gap at the start, but the energy produced covered the demand for the most of the remaining time; the second case, where the reservoir was half full, this was regarded as the best option out of three, the peak power performances were almost the same, the coverage time was good, the underperforming time was about 5 hours, by comparing more than 6 hours in the other two cases; the third case, where the reservoir was at minimum level, energy generation was good at the first 4 hours at the start, but followed by the same unsatisfied demand.
The conclusion was the half tank option was ideal for the optimization under this tidal condition.

A. Flood

The starting tide in this case is during the flood, from data in Figure 13, it is noticed that the stream speed was fastest between 8:00 – 10:00, as the tide reaches the highest level at around 12:00, the stream speed falls back to a low value.

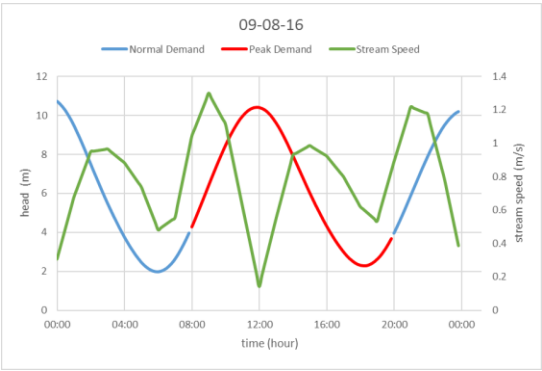

Figure 13, Tidal data from Newport on 09/08/2016

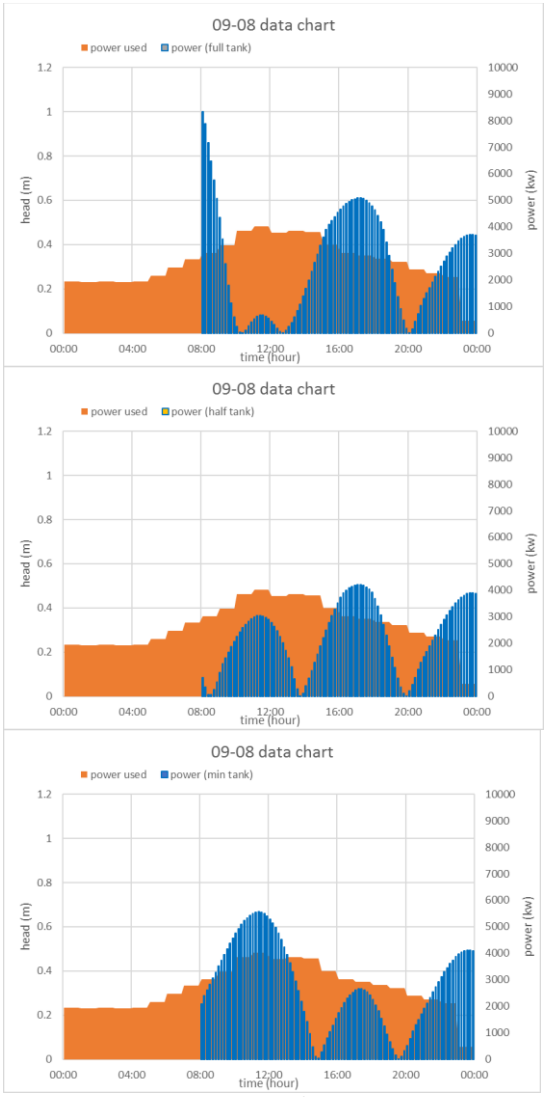

Figure 14 Results from Case C

From all the results shown in Figure 14, the full tank option has a big head advantage at the start as the tide was rising from a low level, however, as the water exiting from the reservoir and tidal level continue rising, the initial head advantage could not last long, and for a long time between 10:00 to 14:00, this option left a big gap within the peak demand window. The half tank option did not have a power surge which happened in the full tank option, it provided a relative steady power output, having one gap around 13:00. There was no power surge in the min tank option either, and the power output was better than the half tank option. The

first-generation cycle has well covered the demand for about first 6 hours since the start. The power generation begun to drop after 14:00 due to the tidal characteristics, which means for the rest of the time, the system would not provide enough power to feed the demand.

A. Flood start

The last tidal scenario was the at the beginning of the peak window, the tidal condition at the beginning of the peak demand window was about to switch to flood tide. Under this condition, the starting tidal level was at the lowest, and as shown in Figure 15, the stream speed was at minimum as well. The tidal level reached highest at time around 16:00 and then the Ebb begun, which just about to reaches the end of the ebb at the end of the peak demand window at time of 20:00.

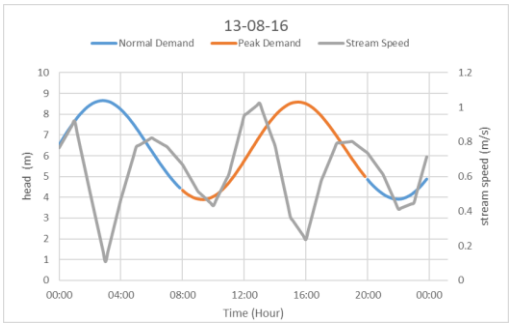

Figure 15 Tidal data from Newport on 13/08/2016

And the results are shown in Figure 16 below

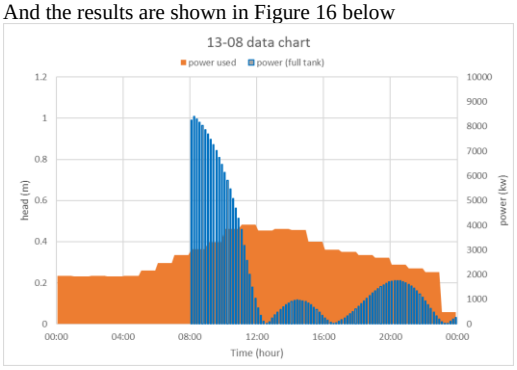

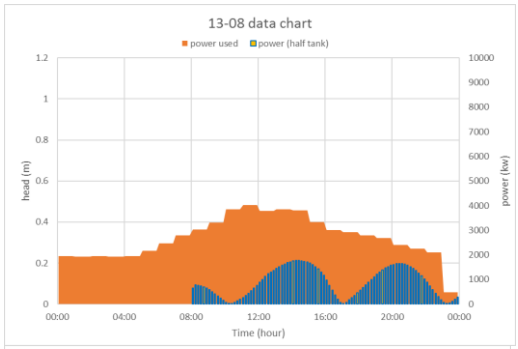

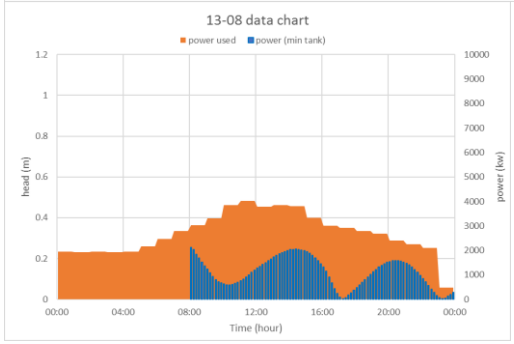

Figure 16 Results from Case D

The tidal condition in this case was not ideal, it was different when comparing the ones in the previous simulations, the difference between the highest and lowest position was small, was about 5 m (the same value for previous case was 9 m). Therefore, the available energy between the tides were smaller, which results in the generally lower power production in all three options.

The full tank option has a power surge at the start, which was due to the lower tidal level provided a big head difference, and the consequence was the power output for the rest of the time within the window was less ideal, the rest two options provided similar pattern, which both were steadier than the full tank one, but the min tank option has a better power generation of all three.

I. FUTURE WORKS

The Matlab programme would be tested for the accuracy by using a set of recorded data from a tidal station, but by doing such test, given the tidal station uses conventional system rather than this hybrid, the Matlab programme would be tested as if it can predict the power accurately by feeding the same tidal data.

A scale physical test is arranged in the later this year to conduct another test for the accuracy of the hybrid system, as the main target is to find out if this system could predict the head correctly.

I. DISCUSSION

By intruding this type of system, from the numerical model, it shows that there is an improvement in both peak power and average power. However, the margin is depending on the power of the tidal turbine, and the layout of the reservoir, this system could under perform at some areas where the tidal condition is poor, and it is also limited by geographic reasons, in some area there could be no ideal place to locate the additional turbine-pump unit. It is also would be determined by the cost factor of each components used by given profit from the electricity generation, although a cost study in the future for a specific site would find the balance point for the implement of this system.

This system does not require significant initial investment to build a brand new tidal electric station, but to convert some current reservoir into one, which could save money and time, also to use the current dock as the power station could supply energy to surrounding area better as the requirement of electric cable could be shorten, and by introducing the pumping storage gives the system ability to generate power when required regardless of the tidal condition, although the system would need to generate less energy than it would normally do, and again it would require a cost effective study to find the balance point.

Furthermore, the current tidal station would also be benefited if this system could be implemented, given the long-life span of the current tidal system, even the small improvement from power production would be magnifies in a longer term.

II. CONCLUSION

From the numerical results, there is an advantage to use this hybrid system by comparing with the current conventional tidal ones, but this system's performance is limited to geographic conditions, as in some area, it is difficult to put tidal turbine in the surrounding water or the stream energy is too low and the tidal turbines would not perform in an optimum condition. Furthermore, another key factor to determine the number of the additional tidal-turbine pump unit would be the cost factor, there is no cost study in this project as the cost for different components varies.

To conclude, this project proposes a concept which could be used as a development for the current tidal system to increase the power without making a huge change, also can convert the local reservoirs into a tidal energy system which to supply to the surrounding areas, also this system enables the system to have the potential to generate energy when the tidal condition is not ideal.

Acknowledgment

This work uses the available data from the ongoing research and studies from Cardiff Marine Energy Research Group.

REFERENCES

[1] G.B. National Grid Status. [Online]. Available: http://www.gridwatch.templar.co.uk/

[2] Tidal Power Case Studies. [Online]. Available: http://www.esru.strath.ac.uk/EandE/Web_sites/01-02/RE_info/tidal1.htm

[3] Tidal Giants- the World's Five Biggest Tidal Power Plants. [Online]. Available: http://www.power-technology.com/features/featuretidal-giants---the-worlds-five-biggest-tidal-power-plants-4211218/

[4] P. Fraenkel. "Marine Current Turbines: pioneering the development of zero-head hydro," BHA Annual Conference, 2007

[5] V.Laleu. "La Rance Tidal Power Plant 40-year operation feedback-Lessons learnt" BHA Annual Conference, 2009